

Biochemical Study of Rapid Discolouration Mechanisms in Bison Meat

By

Md Mahmudul Hasan

A Thesis Submitted to the Faculty of Graduate Studies of
The University of Manitoba

In Partial Fulfillment of the Requirements of the Degree of

DOCTOR OF PHILOSOPHY

Department of Food and Human Nutritional Sciences

University of Manitoba

Winnipeg, MB R3T 2N2, Canada



Copyright © 2021 by Md Mahmudul Hasan

ABSTRACT

Studies were conducted i) to examine lipid [malondialdehyde (MDA), 4-hydroxy-2-nonenal (HNE)] and protein [(carbonyl content (CAR)] oxidation products affecting colour stability in bison muscles, *longissimus lumborum* (LL) and *psoas major* (PM), ii) to investigate the potential of visible-near infrared (Vis-NIR) and short-wave infrared (SWIR) spectroscopy to segregate LL and PM based on muscle type, retail display and ageing time, and iii) to examine the proteome changes in LL and PM muscles to characterize muscle-specific colour stability during ageing. LL muscles exhibited higher redness (a^* value; $P = 0.04$), lower surface discolouration ($P < 0.01$) including lower MDA, HNE, and CAR compared with PM ($P < 0.05$). In both muscles, MDA demonstrated the strongest correlation to a^* ($r = -0.78$; $P < 0.01$) and discolouration ($r_s = 0.82$; $P < 0.01$) scores, especially in PM. Furthermore, principal component analysis (PCA) results revealed four clusters of colour deterioration within day 4 displayed steaks. On the other hand, Vis-NIR range segregated muscles based on ageing time, whereas SWIR region discriminated better based on muscle type. Furthermore, partial least squares (PLS) discriminant analysis models accurately classified muscles based on muscle type and ageing periods in Vis-NIR range. Finally, the PLS-regression models successfully predicted a^* value with an R^2 of 0.88 (RMSEC: 1.57) for calibration, 0.84 (RMSECV: 1.88) for cross-validation, and 0.90 (RMSEP: 1.41) for prediction. Similarly, effective predictions were achieved for colour score (CS) with an R^2 of 0.96 (0.25), 0.95 (0.27), and 0.92 (0.32), and discolouration score (DS) with an R^2 of 0.96 (0.47), 0.93 (0.63), and 0.93 (0.56). In proteomic analysis, 97 differential abundant proteins ($P < 0.05$, fold change > 1.5) were identified when compared between muscles during ageing. In PM, proteins from oxidative phosphorylation, TCA cycle, lipid oxidation, ATP and oxygen transport, and muscle contraction exhibited increased expression during ageing than in LL. Therefore, in bison, oxidation products and Vis-NIR spectroscopy could be utilized for colour stability assessment and for ageing-based segregation, and predictions of redness, CS and DS, respectively. Furthermore, oxidation related enzymes/proteins could be used as biomarkers for characterizing colour stability in bison LL and PM muscles.

ACKNOWLEDGEMENTS

First of all, I am greatly thankful to the Almighty Allah for giving me the proper strength and patience to complete my dream journey successfully.

I am highly grateful from the core of my heart and want to express my sincere gratitude to my advisor Dr. Argenis Rodas-Gonzalez for his continuous cordial guidance, supports and inspirations in every possible way. I would like to say that I am one of the luckiest persons to work under the supervision of such a good-hearted and knowledgeable advisor.

My most heartfelt gratitude goes to Dr. Surendranath P. Suman from University of Kentucky for providing his best possible continuous supports as a committee member and mentor. I am also grateful to Dr. Jitendra Paliwal for allowing me to work in his near-infrared spectroscopy (NIRS) laboratory with logistics supports as well as cordial help and inspirations. I am equally grateful to Dr. Helene Perreault and Dr. Manuel Juarez for their kind suggestions for continuing my Ph. D research works properly. In addition, I would like to thank Dr. Chyngyz Erkinbaev for training me how to operate NIRS instruments.

I am also thankful to Dr. Muhammad Mudassir Arif Chaudhry for helping me in NIRS data analysis. I would like to thank to my meat science lab mates: Vipasha Sood, Dipana Maharjan and Marion Mogire for their helps during my sample processing. I am thankful to the students from Food Science and Animal Science who participated on conducting the sensory colour evaluation. I am also grateful to all staff members of Food and Human Nutritional Sciences for always supporting me by providing necessary laboratory trainings and helping in official works.

I would like to express my gratefulness to the Faculty of Graduate Studies, University of Manitoba for selecting me for the University of Manitoba Graduate Fellowship (UMGF). It was quite impossible even to think about starting my Ph. D study here without this funding support for four years. At the same time, I am also highly thankful to the Natural Sciences and Engineering Research Council (NSERC Discovery Grants Program # RGPIN-2016-06006) for providing funding support for conducting this Ph. D research project.

Lastly, I am immensely grateful to my family members, my mother, father and two brothers for supporting me constantly from my home country Bangladesh. Last but not least, my heartfelt gratitude goes to my friend and beloved wife Afroza Parvin for tolerating and supporting me continuously in every aspect of this long journey.

DEDICATION

This thesis is dedicated to my mother, Taslima Begum and father, Md Abdus Sattar, and my wife Afroza Parvin for always supporting me in every possible way.

“The people, who satisfied in little, are not abolished”.

THESIS ORGANIZATION

This thesis is a grouped manuscript (sandwich) thesis and comprises six chapters where chapter 3 to 5 were each formatted as a research manuscript.

Chapter one contains the general introduction, followed by **chapter two**, which comprises literature review, containing thorough review of necessary literature relevant to fulfill all the study objectives.

Chapter three is the manuscript titled “Principal component analysis of lipid and protein oxidation products and their impact on colour stability in bison *longissimus lumborum* and *psaos major* muscles” which has been published as: Hasan, M. M., Sood, V., Erkinbaev, C., Paliwal, J., Suman, S., & Rodas-Gonzalez, A. (2021). *Meat Science*, 178: 108523. <https://doi.org/10.1016/j.meatsci.2021.108523>

Chapter four contains the manuscript focused on the investigation of the “Application of Vis-NIR and SWIR spectroscopy for the segregation of bison muscles based on their colour stability”. This manuscript was submitted in *Meat Science* and has been published as: Hasan, M. M., Chaudhry, M. M. A., Erkinbaev, C., Paliwal, J., Suman, S. P., & Rodas-Gonzalez, A. (2022). *Meat Science*, 188: 108774. <https://doi.org/10.1016/j.meatsci.2022.108774>

Chapter five is another manuscript prepared by focusing the research works on the “Tandem mass tag labeling-based analysis to characterize muscle-specific proteome changes during postmortem ageing of bison *longissimus lumborum* and *psaos major* muscles. The above-mentioned manuscript was prepared as per the *Meat and Muscle Biology* journal guidelines and has been published as: Hasan, M. M., Rashid, M., Suman, S. P., Perreault, H., Paliwal, J. & Rodas-Gonzalez, A. (2022). *Meat and Muscle Biology*, 6(1): 13055, 1-23. <https://doi.org/10.22175/mmb.13055>

Chapter six contains the general conclusions of the entire thesis.

Other research activity which was performed and published but not included in my Ph. D. thesis:

- Chaudhry, M. A., Hasan M. M., Erkinbaev, C., Paliwal, J., Suman, S., & Rodas-Gonzalez A. (2021). Bison muscle discrimination and colour stability prediction using near-infrared hyperspectral imaging. *Biosystems Engineering*, 209, 1-13.

CONTRIBUTIONS OF AUTHORS

The contributions of authors in different manuscripts are shown below:

Manuscript No. 1: Principal component analysis of lipid and protein oxidation products and their impact on colour stability in bison *longissimus lumborum* and *psaos major* muscles. *Meat Science*.

Author's contributions: **M. M. Hasan:** investigation, formal analysis, writing (original draft). V. Sood: formal analysis and writing (reviewing & editing). C. Erkinbaev and J. Paliwal: methodology & investigation and writing (reviewing & editing). S. P. Suman: conceptualization, investigation, formal analysis, writing (reviewing & editing). A. Rodas-González: Funding acquisition, conceptualization, methodology, project administration, supervision, investigation, formal analysis, writing (reviewing & editing).

Manuscript No. 2: Application of Vis-NIR and SWIR spectroscopy for the segregation of bison muscles based on their colour stability. *Meat Science*.

Author's contributions: **M. M. Hasan:** investigation, formal analysis, writing (original draft). M. M. A. Chaudhry: formal analysis and writing (reviewing & editing). C. Erkinbaev: methodology & investigation and writing (reviewing & editing). J. Paliwal: methodology & investigation and writing (reviewing & editing). S. P. Suman: conceptualization, investigation, formal analysis, writing (reviewing & editing). A. Rodas-González: Funding acquisition, conceptualization, methodology, project administration, supervision, investigation, formal analysis, writing (reviewing & editing).

Manuscript No. 3: Tandem mass tag labeling-based analysis to characterize muscle-specific proteome changes during postmortem ageing of bison *longissimus lumborum* and *psaos major* muscles. *Meat and Muscle Biology*.

Author's contributions: **M. M. Hasan:** investigation, formal analysis, writing (original draft). Mahamud-ur Rashid: formal analysis and writing (reviewing & editing). S. P. Suman: conceptualization, investigation, formal analysis, writing (reviewing & editing). Helene Perreault: methodology & investigation and writing (reviewing & editing). J. Paliwal: methodology & investigation and writing (reviewing & editing). A. Rodas-González: Funding acquisition, conceptualization, methodology, project administration, supervision, investigation, formal analysis, writing (reviewing & editing).

TABLE OF CONTENTS

Contents	Page No.
ABSTRACT	ii
ACKNOWLEDGEMENTS	iii
DEDICATION	iv
THESIS ORGANIZATION	v
CONTRIBUTIONS OF AUTHORS	vi
TABLE OF CONTENTS	vii
LIST OF TABLES	x
LIST OF FIGURES	xi
ABBREVIATIONS USED	xiv
SYMBOLS USED	xvii
CHAPTER 1: GENERAL INTRODUCTION	1
CHAPTER 2: LITERATURE REVIEW	6
2.1 Meat colour	6
2.1.1 Myoglobin structure	6
2.1.2 Myoglobin chemistry in fresh meat	8
2.1.3 Factors affecting fresh meat colour	10
2.1.3.1 General factors	10
2.1.3.2 Other biochemical factors	13
2.2 Oxidation products in meat	16
2.2.1 Lipid oxidation	16
2.2.1.1 Malondialdehyde	16
2.2.1.2 4-Hydroxy-2-nonenal	18
2.2.2 Protein oxidation	20
2.2.3 Interactions between lipid and myoglobin oxidation	22
2.3 Near infrared spectroscopy and its application in meat studies	23
2.4 Sarcoplasmic proteome and fresh meat colour	26
2.5 Overview of bison	28
2.5.1 Possible reasons for darker and unstable colour in bison meat	29
2.5.2 Postharvest techniques to improve colour in bison	31

2.5.2.1 Carcass chilling techniques	31
2.5.2.2 Injection enhancement combined with carcass chilling	32
2.5.2.3 Injection combined with packaging and storage temperature	33
2.5.2.4 Electrical stimulation	34
2.5.2.5 Rinse and chill method	35
2.5.2.6 Nitrite film packaging	36

CHAPTER 3

MANUSCRIPT NO. 1: Principal component analysis of lipid and protein oxidation products and their impact on colour stability in bison <i>longissimus lumborum</i> and <i>psoas major</i> muscles	38
--	----

3.1 Abstract	38
3.2 Introduction	38
3.3 Material and methods	40
3.4 Results	47
3.5 Discussion	55
3.6 Conclusions	59

CHAPTER 4

MANUSCRIPT NO. 2: Application of Vis-NIR and SWIR spectroscopy for the segregation of bison muscles based on their colour stability	60
--	----

4.1 Abstract	60
4.2 Introduction	60
4.3 Material and methods	62
4.4 Results and discussion	68
4.5 Conclusions	86

CHAPTER 5

MANUSCRIPT NO. 3: Tandem mass tag labeling-based analysis to characterize muscle-specific proteome changes during postmortem ageing of bison <i>longissimus lumborum</i> and <i>psoas major</i> muscles	87
--	----

5.1 Abstract	87
5.2 Introduction	88
5.3 Material and methods	89

5.4 Results	94
5.5 Discussion	114
5.6 Conclusions	118
CHAPTER 6: GENERAL CONCLUSIONS	119
LITERATURE CITED	122
APPENDICES	160

LIST OF TABLES

Table No.	Title	Page No.
Table 3.1	Correlation between oxidation products and colour evaluation traits from <i>longissimus lumborum</i> and <i>psoas major</i> steaks.	51
Table 3.2	Regression analysis for predicting colour traits with oxidation products for <i>longissimus lumborum</i> steaks.	51
Table 3.3	Regression analysis for predicting colour traits with oxidation products for <i>psoas major</i> steaks.	52
Table 3.4	Principal component loadings (74.85%).	53
Table 4.1	Confusion matrix for the classification of <i>longissimus lumborum</i> and <i>psoas major</i> muscle samples in the Vis-NIR range.	78
Table 4.2	Confusion matrix with best calibration model for the classification of <i>longissimus lumborum</i> and <i>psoas major</i> muscle samples based on ageing and retail display periods.	79
Table 4.3	Calibration and prediction statistics for a^* value, and colour and discolouration score.	81
Table 5.1	Differentially abundant proteins between bison <i>longissimus lumborum</i> and <i>psoas major</i> muscles at 2 d, 7 d and 14 d postmortem (fold change > 1.5; $P < 0.05$) ageing periods.	97

LIST OF FIGURES

Figure No.	Title	Page No.
Figure 2.1	Mb structures. a) 3-D structure of Mb and b) Simplified Mb structure.	7
Figure 2.2	Interconversions of Mb redox states in fresh meats.	8
Figure 2.3	Diagram of 4-hydroxy-2-nonenal	19
Figure 2.4	Summary of interactions between Mb and lipid oxidation.	23
Figure 3.1	Effects of interaction of muscle × retail display on redness (a^*), discolouration score and on carbonyl content ¹ .	48
Figure 3.2	Effects of interaction of ageing × retail display on objective colour evaluation.	48
Figure 3.3	Effects of interaction of muscle × postmortem ageing × days of retail display on colour score and malondialdehyde ¹ .	49
Figure 3.4	(a) Plotting principal component (PC1 × PC2) analysis for bison muscles under ageing and retail display conditions, (b) Plotting principal component (PC1 × PC3) analysis for bison muscles under ageing and retail display conditions.	55
Figure 4.1	Overview of spectra in the Vis-NIR range. a) Spectra based on muscles types (LL and PM), b) Averaged spectra based on muscles types (LL and PM), c) Spectra based on ageing periods, and d) Averaged spectra based on ageing periods.	69
Figure 4.2	Overview of spectra in the SWIR range. a) Spectra based on muscles types (LL and PM), b) Averaged spectra based on muscles types (LL	

	and PM), c) Spectra based on ageing periods, and d) Averaged spectra based on ageing periods.	70
Figure 4.3	PCA based classification in the Vis-NIR range. a) Scores plot for PC1 and PC2 (coloured by ageing and retail display period), b) Scores plot for PC1 and PC3 (coloured by muscle type), c) Loadings plot for PC1, d) Loadings plot for PC2 and e) Loadings plot for PC3.	71
Figure 4.4	PCA based classification in the SWIR range. a) Scores plot of PC1 and PC2 (coloured by ageing and retail display period), b) Scores plot of PC1 and PC3 (coloured by muscle type), c) Loadings plot of PC1, d) Loadings plot of PC2, and d) Loadings plot of PC3.	72
Figure 4.5	a) PLS-DA scores plot for the classification of <i>longissimus lumborum</i> and <i>psaos major</i> muscle samples, and b) Loadings plots for LV1, LV2 and LV3.	79
Figure 4.6	a) Calibration plot for the prediction of a^* value, and b) loadings plot for first 3 LVs.	82
Figure 4.7	a) Calibration plot for the prediction of colour score, and b) loadings plot for first 2 LVs.	82
Figure 4.8	a) Calibration plot for the prediction of discolouration score, and b) loadings plot for first 2 LVs.	83
Figure 5.1	Heatmap showing overall expression of differential proteins ($P < 0.05$, > 1.5 -fold change) in bison <i>longissimus lumborum</i> and <i>psaos major</i> muscles from different ageing periods.	102
Figure 5.2	Distribution of differentially abundant proteins between bison <i>longissimus lumborum</i> and <i>psaos major</i> muscles at 2 d, 7 d and 14 d postmortem ageing.	103

Figure 5.3	Protein-protein interaction networks of differential proteins between bison <i>longissimus lumborum</i> and <i>psoas major</i> muscles at (3a) 2 d postmortem, (3b) 7 d postmortem and (3c) 14 d postmortem ageing.	104
Figure 5.4	Distribution of the functional clusters of differential proteins between bison <i>longissimus lumborum</i> and <i>psoas major</i> muscles at 2 d, 7 d and 14 d postmortem ageing.	107
Figure 5.5	Complexes of ETC pathway affected during comparisons of bison <i>psoas major</i> vs <i>longissimus lumborum</i> muscle at 2 d, 7 d and 14 d postmortem ageing.	109
Figure 5.6	Major protein-protein interaction networks during comparisons of bison <i>psoas major</i> vs <i>longissimus lumborum</i> muscle at 2 d, 7 d and 14 d postmortem identified using Ingenuity pathway analysis.	110

ABBREVIATIONS USED

ADP	Adenosine diphosphate
AMP	Adenosine monophosphate
AMSA	American Meat Science Association
ATP	Adenosine triphosphate
BC	Blast chilling
BCA	Bicinchoninic acid
CAR	Carbonyl content
CBA	Canadian Bison Association
CC	Conventional chilling
CO	Carbon monoxide
COMb	Carboxymyoglobin
CS	Colour score
DFD	Dark, firm, and dry
DM	<i>Diaphragma medialis</i>
DMb	Deoxymyoglobin
DNA	Deoxyribonucleic acid
DNPH	2, 4-dinitrophenylhydrazine
DS	Discolouration score
EDTA	Ethylenediaminetetraacetic acid
ELISA	Enzyme linked immunosorbent assay
ERK	Extracellular signal-regulated kinase
ES	Electrical stimulation
ETC	Electron transport chain
FAD	Flavin adenine dinucleotide
GM	<i>Gluteus medius</i>
GTP	Guanosine triphosphate
Hb	Haemoglobin
HI	Heme iron
HNE	4-hydroxy-2-nonenal
HSI	Hyperspectral image

HSP	Heat shock protein
HVES	High voltage electrical stimulation
IMP	Inosine monophosphate
IPA	Ingenuity pathway analysis
iPLS	Interval partial least squares regression
LC-MS	Liquid chromatography mass spectrometry
LD	<i>Longissimus dorsi</i>
LL	<i>Longissimus lumborum</i>
LMW	Low molecular weight
LSD	Least significant difference
LV	Latent variable
LVES	Low voltage electrical stimulation
MAP	Modified atmosphere packaging
MAPK	Mitogen activated protein kinase
Mb	Myoglobin
MCL	Markov clustering
MDA	Malondialdehyde
MMb	Metmyoglobin
MRA	Metmyoglobin reducing activity
NAD	Nicotinamide adenine dinucleotide
NADP	Nicotinamide adenine dinucleotide phosphate
NBA	National Bison Association
NFP	Nitrate film packaging
NHI	Non-heme iron
NIRS	Near infrared spectroscopy
NO	Nitric oxide
NOMb	Nitrosomyoglobin
OCR	Oxygen consumption rate
OM	Outer membrane
OMb	Oxymyoglobin
PC	Principal component

PCA	Principal component analysis
PLS-DA	Partial least squares discriminant analysis
PLSR	Partial least squares regression
PM	<i>Psoas major</i>
PMSF	Phenylmethylsulfonyl fluoride
PSE	Pale, soft, and exudative
PVC	Polyvinyl chloride
PUFA	Polyunsaturated fatty acid
RC	Rinse and chill
RD	Retail display
RH	<i>Rhomboideus</i>
RMSE	Root mean square errors
RMSEC	Root mean square errors of calibration
RMSECV	Root mean square errors of cross-validation
RMSEP	Root mean square errors of prediction
SM	<i>Semimembranosus</i>
SWIR	Short wave infrared spectroscopy
TB	<i>Triceps brachii</i>
TBARS	Thiobarbituric acid reactive substances
TCA	Tricarboxylic acid cycle
TFL	<i>Tensor fasciae latae</i>
TMT	Tandem mass tag
upH	Ultimate pH
UV	Ultraviolet
VIP	Variable importance in projection
Vis-NIR	Visible near infrared spectroscopy
WHC	Water holding capacity

SYMBOLS USED

Cm	Centimeter
d	Day
Fig.	Figure
g	Gram
h	Hour
Hg	Mercury
Kg	Kilogram
kDa	Kilodalton
kV	Kilovolt
log(e)	Natural logarithm
log ₂	2 base logarithm
m	Metre
mg	Milligram
min	Minute
ml	Millilitre
mM	Millimolar
ms	Millisecond
m/z	Mass/charge
nm	Nanometre
nmoles	Nano moles
rpm	Revolutions per minute
s	Second
V	Volt
v/v	Volume/volume
W	Watt
μg	Microgram
μL	Microlitre
nL	Nanolitre
μM	Micromolar
=	Equal

<	Less than
>	Greater than
~	Approximately
α	Alpha
β	Beta
ω	Omega
%	Percentage
°	Degree
°C	Degree Celsius

CHAPTER 1: GENERAL INTRODUCTION

Bison meat could be a great alternative protein source to the diet and health-conscious consumers who are looking for protein diets with higher nutritional value (CBA, 2021a). Bison meat is well-known as a nutrient-rich food with high lean protein (Galbraith et al., 2006; Marchello et al., 1998; Marchello & Driskell, 2001) and low-fat contents (Koch et al., 1995; McDaniel et al., 2013). Additionally, bison meat is also a great source of essential fatty acids, iron, zinc, phosphorous, selenium, vitamin B6, vitamin B12 and niacin (CBA, 2021a). As a result, the demand for bison meat in the red meat market is rapidly increasing (Galbraith et al., 2014; Steiner et al., 2010).

Fresh meat colour is the most important sensory attribute which influences the consumers' purchase decision and is an indication of retail meat's freshness and wholesomeness (Mancini & Hunt, 2005). However, its colour stability is a dominant drawback factor for the availability of fresh bison meat in retail stores (Hasan et al., 2021). Bison meat is visually darker (Koch et al., 1995), and its colour deterioration (from cherry-red to brown) occurs promptly in aerobically packaged conditions compared to beef (Narváez-Bravo et al., 2017; Pietrasik et al., 2006). This colour instability of meat and meat products results in a loss in annual revenue of \$1 billion (Nair et al., 2017, 2018; Smith et al., 2000; Suman & Nair, 2017). Therefore, there is a need to consider this discolouration or early browning problems during the marketing of fresh bison meat (Dhanda et al., 2002; Galbraith et al., 2014).

The rapid pigment oxidation and surface discolouration mechanisms of red meats are not well understood. Structurally, a study comparing the Mb proteins of bison and beef demonstrated that the amino acid sequences, oxidation kinetics, and thermostability are similar in both types of meat (Joseph et al., 2010). On the other hand, bison muscle fibres differ from those of beef (Koch et al., 1995), resulting in higher concentrations of pigment (Galbraith et al., 2014; Galbraith et al., 2016) and iron (Galbraith et al., 2006; Marchello & Driskell, 2001). Polyunsaturated fatty acids (PUFA) of phospholipid cell membranes are present in range-fed and feedlot-fed bison in more significant amounts than in range- and feedlot-fed cattle (Rule et al., 2002). Thus, a higher concentration of total PUFA and iron may cause a rapid deterioration of bison muscle colour quality. Higher PUFA concentrations are prone to suffer oxidative damage (Wood et al., 2008) and can generate highly reactive secondary lipid oxidation products (e.g., α , β -unsaturated

aldehydes) such as malondialdehyde (MDA) and 4-hydroxy-2-nonenal (HNE). Moreover, HNE can initiate oxidation of oxymyoglobin (OMb) to metmyoglobin (MMb) (Alderton et al., 2003; Joseph et al., 2010; Lee et al., 2003; Schneider et al., 2001; Suman et al., 2006) resulting in meat discolouration (Alderton et al., 2003). 4-hydroxy-2-nonenal is also responsible for the declines in both electron transport mediated and NADH-dependent MMb reduction. Thus, discolouration may occur partly due to the HNE and mitochondria interactions (Ramanathan et al., 2012). However, the effect of HNE in the colour stability of bison meat has yet to be determined.

Protein oxidation in muscle tissues can alter different critical functional attributes of proteins such as viscosity, emulsification, gelation, hydration, and solubility (Wang et al., 1997; Wang & Xiong, 1998). At the same time, due to the protein oxidation in refrigerated storage, heme and free (non-heme) iron are released and can subsequently increase the oxidative damages in meat protein (Estévez et al., 2006; Estévez & Cava, 2004). Furthermore, lipid and Mb oxidations can be enhanced by each other (Faustman et al., 2010). Due to the initiation of lipid oxidation in an earlier stage, it has been proposed that primary lipid oxidation products, such as peroxide radicals, may promote protein oxidation (Aalhus & Dugan, 2014). Furthermore, the products of lipid peroxidation can attack the reactive side chains of different amino acids. Stadtman and Levine (2003) and Lund et al. (2011) reported that free radicals' reactions with protein molecules result in cross-linking and fragmentation of proteins and/or amino acid side chain modifications. Therefore, carbonyl compounds (CAR) are formed when oxidation occurs in the amino acids' side chains within the protein skeleton (Lund et al., 2011; Stadtman & Levine, 2003; Xiong, 2018). The critical amino acids which participate in the CAR formation are arginine, lysine, proline and threonine (Soladoye et al., 2015).

Sarcoplasmic proteomes contain different types of proteins. Therefore, in the meat system, lipid oxidation and meat discolouration can be initiated when the ratio of those proteins, particularly antioxidant/pro-oxidant, is imbalanced (Joseph et al., 2010; Ramanathan et al., 2009). Furthermore, the sarcoplasmic proteins in beef muscles contribute to muscle-specific colour attributes (Suman et al., 2014). In colour stable beef muscles (e.g., *longissimus lumborum*, LL), the proteome contains higher amounts of soluble antioxidants such as peptide methionine sulfoxide reductase, thioredoxin, and peroxiredoxin-2 and chaperone (e.g., heat shock protein-27 kDa) proteins in comparison with colour labile muscles (e.g., *psaos major*, PM) (Joseph et al., 2012). Furthermore, colour-stable beef muscles showed positive correlation with redness (e.g., creatine

kinase, aldose reductase, and β -enolase) and colour stability [e.g., peroxiredoxin-2, and heat shock protein (HSP) 27 kDa]. In addition, the increased expression of glycolytic enzymes (e.g., phosphoglucomutase-1) in colour-stable LL steaks likely contributes to better colour stability in postmortem muscles via NADH regeneration (Canto et al., 2015).

Colour stability, on the other hand, is a strikingly muscle-specific quality attribute due to the particular anatomical locations and physiological roles of each muscle in living animals, leading in differences in postmortem biochemistry and colour stability (King et al., 2011; Suman et al., 2014). Consequently, to establish a specific mitigation strategy based on the muscle's colour stability, it is necessary to apply a reliable sorting tool that identifies muscles according to their colour stability. Non-destructive and rapid assessment techniques, such as near infrared spectroscopy (NIRS) provide information on the molecular bonds of organic chemicals and tissue ultrastructure in a scanned sample (Downey & Hildrum, 2015), making it a perfect tool for studying meat properties. Indeed, NIRS has been implemented successfully to predict chemical constituents of meat, especially fatty acids (Prieto et al., 2011, 2014). The near infrared spectrum comprises physical and chemical information about the meat samples under examination. The spectrum information is derived from the many vibrational modes of the molecules induced by their interaction with electromagnetic light absorbed at wavelengths ranging from 750 to 2500 nm. The application of chemometrics with multivariate calibration algorithms and statistical approaches enable the extraction of important information from NIR spectra to construct calibration models that allow the prediction of the composition of material comprising the samples (Font et al., 2007).

Although both bison and beef cattle are ruminants, there may be species-specific variations in meat lipid and protein oxidation, as well as sarcoplasmic proteins, which have not yet been studied in bison. Furthermore, in this project the immunochemical determination of HNE using enzyme linked immunosorbent assay (ELISA) for the quantitative detection of lipid peroxidation was performed, which is the first attempt to determine HNE from bison meat samples directly. Moreover, the application of NIRS for the segregation of bison muscles has not been studied yet. This NIRS study will open a new window for the online prediction of meat colour parameters in bison meat during ageing and retail display periods as well as the segregation of two bison muscles with inherent colour stability based on muscle types, ageing, and retail display periods. Additionally, most of the studies conducted to investigate sarcoplasmic proteomes and protein

profiles are mainly gel-based approaches using gel electrophoresis method in combination with liquid chromatography-mass spectrometry (LC-MS/MS). However, gel-based proteomic analysis approaches have some limitations for the identification of various number of proteins from a single gel run. Recently, tandem mass tags (TMT) based gel-free proteome analysis in combination with LC-MS/MS has been the most advanced technique for identifying sarcoplasmic proteins with better understanding.

The current thesis work was designed to study rapid discolouration mechanisms in bison muscles (LL and PM) by examining the biochemical parameters (e.g., lipid and protein oxidation products), potential of application of NIRS and sarcoplasmic proteomes, and how these experimental outcomes can differentiate those muscles with muscle-specific inherent colour stability. Therefore, based on the obtained results from this study, it would be possible to develop and apply different muscle-specific post-harvest strategies and technologies for the mitigation of discolouration problems in bison industry.

Hypotheses:

The overall hypotheses of this current thesis were:

1. High levels of malondialdehyde (MDA), 4-hydroxy-2-nonenal (HNE) and carbonyl contents (CAR) vary between muscles, and HNE and CAR have higher influence than MDA in increasing the discolouration of bison meat.
2. Near infrared reflectance spectroscopy (NIRS) predicts colour parameters, and segregate stable vs. unstable colour bison muscles.
3. The over-abundance of the sarcoplasmic proteins (antioxidants, chaperones and glycolytic enzymes), contributing to improvements in redness and colour stability.

Objectives:

Therefore, the objectives of the present thesis works were:

1. To examine and compare the effect of lipid [malondialdehyde (MDA); 4-hydroxy-2-nonenal (HNE) and protein (carbonyl contents (CAR)] oxidation products and their impact on colour stability in bison *longissimus lumborum* (LL) and *psoas major* (PM) muscles during ageing and retail display periods.

2. To test the potentiality of NIRS [both visible near infrared spectroscopy (Vis-NIR); and short wave near infrared spectroscopy (SWIR)] for the segregation of bison portions based on muscle type [*longissimus lumborum* (LL; colour-stable) and *psaos major* (PM; colour-labile)], ageing and retail display periods, and to predict the colour parameters.
3. To examine the variations in sarcoplasmic proteome in bison *longissimus lumborum* (LL) and *psaos major* (PM) muscles during postmortem ageing periods using tandem mass tag (TMT) labeling coupled with liquid chromatography mass spectrometry (LC-MS/MS) for the categorization of muscles based on muscle-specific inherent colour stability.

CHAPTER 2: LITERATURE REVIEW

2.1 Meat colour

Meat colour and its visual appearance in retail display are the major driving forces that influence consumers' purchasing decision (Carpenter et al., 2001; Djenane et al., 2001). Thus, providers must generate and apply specific strategies to maintain the desired meat colour attributes. As most consumers use meat colour as a sign of its wholesomeness and freshness (Mancini & Hunt, 2005), a deviation of colour stability is considered an indicator of poor functionality and possible spoilage, causing financial losses to retailers (Nair et al., 2018). Any deviation from the cherry red colour of fresh meat results in product discount prices, and in case of extensive discolouration, products are discarded (Canto et al., 2015; Suman et al., 2014). Smith et al. (2000) reported an estimated \$1 billion revenue loss in the U.S. meat industry due to the discolouration of fresh meat. Moreover, meat discolouration can significantly limit the growth of national and international fresh meat marketing (Galbraith et al., 2006).

The colour of muscle foods is primary due to the red pigment in meat known as myoglobin (Mb). Myoglobin is a heme containing sarcoplasmic protein that is responsible for the representative red colour of meats. Generally, the colour in raw meat is attributed from 90 to 95% to Mb (Aberle et al., 2001; Jeong et al., 2009) and around 2-5% to hemoglobin (Hb) (Feiner, 2006). However, Hb and other heme protein, namely cytochrome C, minimally affect the fresh meat colour (Mancini & Hunt, 2005). The pigment/colour compounds (hemoglobin, cytochromes and various catalase enzymes) other than Mb protein are more associated with the visible colour in poultry, game meats, and fish than well-bled livestock species such as beef, pork, and lamb (Suman & Joseph, 2013, 2014). Generally, Mb concentration remains the same during ageing, and retail display periods; however, the formation of different redox states of Mb and their proportions ultimately influences the meat colour.

2.1.1 Myoglobin structure

Myoglobin is a water-soluble sarcoplasmic protein with a molecular weight of 17 000 Da. Structurally, Mb is a hemoprotein (**Figure 2.1**) comprised of 153 amino acids (Suman et al., 2007), with a flat porphyrin ring exhibiting a central iron atom (AMSA, 2012). Myoglobin protein moiety consists of 8 α -helices (A-H) with a prosthetic heme group, and a centrally positioned iron atom

in the hydrophobic core of protein (Suman & Joseph, 2013). The iron atom can exist either in Fe^{2+} (ferrous) or in Fe^{3+} (ferric) state, reduced and oxidized forms of Mb; respectively. Structurally, six binding sites are associated with this central iron atom, of which the heme ring is connected with four nitrogen atom pyrrole groups within the porphyrin structure. The 5th bond is attached to a proximal histidine-93, which is connected to the globin protein structure. An additional histidine residue known as distal histidine-64 is also found in the surroundings of heme, but is not involved in the bond formation with heme (Suman & Joseph, 2013). Finally, the 6th site is available for the reversible binding to the ligands, including carbon monoxide (CO), diatomic oxygen (O_2), water (H_2O), and nitric oxide (NO) molecules (AMSA, 2012). However, the spatial arrangement of heme and Mb's distal histidine-64 residue regulates the size and shape of ligands binding on the 6th coordinate position in primary Mb, as well as the interactions of heme with large molecules (Cornforth & Jayasingh, 2004; Govari & Pexara, 2015), which influences colour dynamics (Mancini & Hunt, 2005). Finally, the changes in the valence of iron (+2 or +3) and the presence of a particular ligand on the 6th binding site determine the perception of visual meat colour of muscle foods.

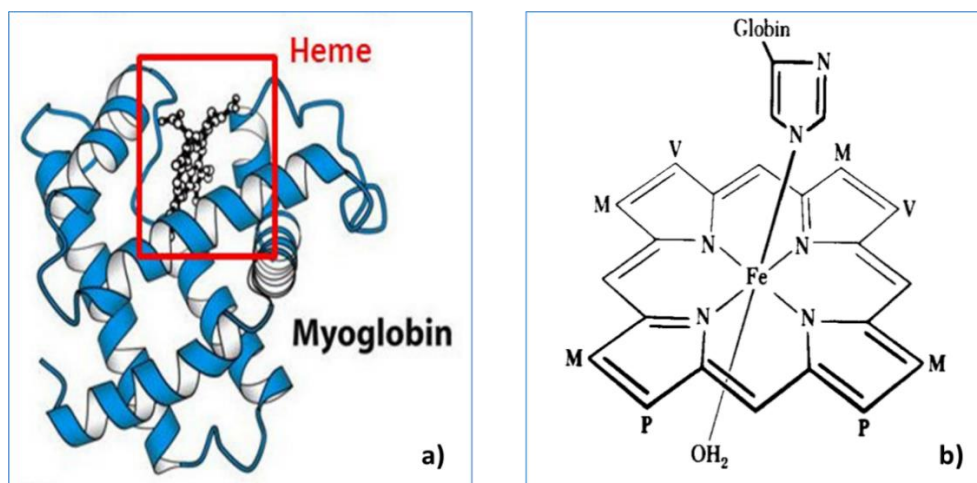


Figure 2.1. Mb structures. a) 3-D structure of Mb (Berg et al., 2012), and b) Simplified Mb structure (Seideman et al., 1984)

Structurally, beef Mb contains both helical and non-helical sections in the structure (Suman & Joseph, 2013). Together, the Mb moiety and the porphyrin ring structure form the final Mb protein structure. The conjugated double bonds (with resonance properties) present in the Mb

structure are mainly responsible for absorbing light and providing muscle pigmentation (Suman & Joseph, 2013). Additionally, the presence of 8 α -helices surrounding the central heme core can function as a protective shield against oxidative and other stresses. Joseph et al. (2010) studied extensively to characterize bison Mb structure and revealed that both bison and beef are 100% similar in the number and sequence of amino acids. They also reported that structurally bison and yak Mb are almost identical.

2.1.2 Myoglobin chemistry in fresh meat

In fresh meat, there are four different reported chemical states of Mb, including deoxymyoglobin (DMb), oxymyoglobin (OMb), metmyoglobin (MMb), and carboxymyoglobin (COMb) (Suman & Joseph, 2013). Basically, these are the four different redox forms of Mb, formed during reduction-oxidation (redox) reactions of the iron atom. The visual interconversion pathways of different redox states of Mb in fresh meat are presented in **Figure 2.2**.

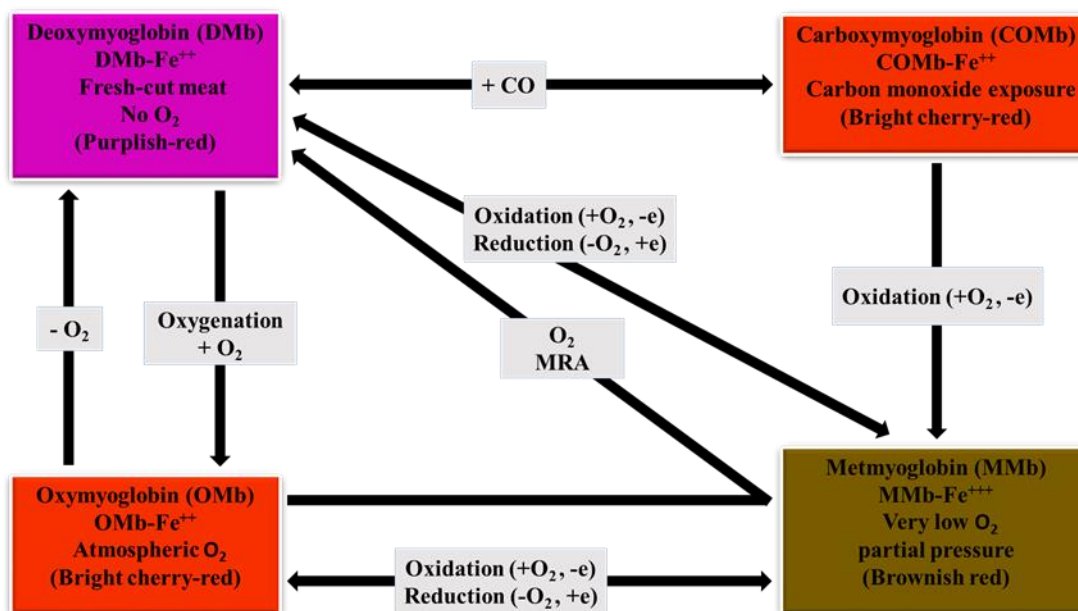


Figure 2.2. Interconversions of Mb redox states in fresh meats [Adopted and modified from (Mancini & Hunt, 2005; Suman & Joseph, 2013)]

In freshly cut meat, DMb is the native form of Mb that contains the heme iron in its reduced ferrous state (Fe²⁺) and depicts the purplish-red or purplish-pink colour of meat. The DMb state is obtained at low oxygen pressure (<1.4 mm of Hg) in the vacuum packaged environment (Mancini

& Hunt, 2005). After the exposure of oxygen to Mb, oxygenation occurs, resulting in OMb formation with bright cherry-red colour (bloomed), and still, the iron is in its reduced state (ferrous/ Fe^{2+}). In the DMb form, the 6th coordination position in Mb structure is empty, whereas in the OMb form, O_2 is attached to that coordination site (Lindahl, 2005). In addition, when Mb is exposed to CO in a modified atmosphere packaging (MAP), COMb is formed with a more stable bright cherry-red colour, and it has been reported that CO has more binding affinity to Mb than oxygen (Mancini & Hunt, 2005; Suman & Joseph, 2013). However, it is still uncertain which Mb form is converted to COMb. On the other hand, MMb, tan to brownish red in colour, results from the oxidation of either of ferrous (Fe^{2+}) states to a ferric (Fe^{3+}) state (Suman et al., 2007). Recently, it was demonstrated that oxidation of OMb to brown MMb causes meat discolouration (Roberts et al., 2017). Typically, MMb develops readily at low oxygen concentrations (< 7 mm of Hg or about 1 to 2% oxygen) and H_2O is attached as a ligand at the 6th position of this Mb state (AMSA, 2012). Generally, in fresh meat, the main three forms of Mb (DMb, OMb and MMb) occur simultaneously and MMb is introduced between the OMb (outer) and DMb (inner) layers. The MMb form thickens progressively, shifts close to the outer surface, and consequently covers the surface, resulting in meat discolouration. Colour deterioration or discolouration is not observable until the meat surface is covered by 30% of MMb, and when MMb formation exceeds 60%, the meat colour is considered as undesirable (Seideman et al., 1984).

All Mb forms are water-soluble and dissolve immediately in buffer solutions with low ionic strength. They exhibit light absorption properties within the spectral range of 500-600 nm wavelength, and it is quite difficult to measure using spectrophotometers due to the narrow spectral range (Suman & Joseph, 2013; Tang et al., 2004). In a study, Tang et al. (2004) reported that DMb and MMb show maximum absorption peaks at 557 nm and 503 nm wavelength, respectively, whereas OMb portrayed two large peaks at 542 nm and 582 nm. Furthermore, COMb has been reported to exhibit twin peaks (543 and 581 nm) which are interestingly almost identical to those of OMb. The highest magnitudes of peaks for OMb and COMb have been detected at 580 and 540 nm, respectively (Suman et al., 2006). However, the total Mb concentration from fresh meats is estimated at 525 nm wavelength as this is the isobestic point for all four Mb redox forms (Tang et al., 2004).

2.1.3 Factors affecting fresh meat colour

There are many intrinsic and extrinsic factors that can consequently affect meat colour (Neethling et al., 2017). These factors can influence meat discolouration individually or in combination. There is a need to study and to understand these factors in detail for developing necessary effective strategies to mitigate the discolouration of meat (Suman et al., 2014; Suman & Joseph, 2013).

2.1.3.1 General factors

The intrinsic factors are species, sex, breed, age, animal genetics, management of dietary supplement, inter and intramuscular effects, muscle type, and pH; whereas extrinsic factors include various postmortem conditions (immobilization method, parameters of cooler influencing chilling rate, scalding, spacing and alignment of carcasses, criteria for electrical stimulation and addition of antimicrobials), temperatures and time of postmortem storage, as well as a number of other factors during processing, packaging, display and lighting variables, and particularly postmortem ageing periods (AMSA, 2012; Jeong et al., 2009). It has also been shown that the difference in colour and/or colour stability traits could be due to a few other crucial intrinsic factors such as species-specific variations in the distributions of red and white muscle fibres, as well as Mb chemistry (Faustman & Cassens, 1990; Joseph et al., 2010).

Species-specific variations (Faustman & Suman, 2017; Hunt & Hedrick, 1977b, 1977a) in meat colour are already established, where beef and lamb have a greater content of Mb compared to pork, veal, poultry and fish. Myoglobin concentration increases with the age; thus, meat from older animals is reported as having darker red colour (Aberle et al., 2001). For example, veal meat with pale muscles indicates the presence of lower content of Mb, whereas mature animals with dark red colour demonstrate a higher Mb concentration when compared to each other. Sex also influences Mb concentration such as bulls (intact males) were reported to have higher Mb concentrations than steers (castrated) or female animals (Aberle et al., 2001).

Genetics is another pre-harvest factor that has detrimental effect on meat colour, especially in pork. Furthermore, the pre-harvest factors that affect pork colour are genetics, diets, and glycolytic potential. Genes such as halothane, ryanodine, and Rendement Napole have effects on pork colour. Lighter pork colour was noticed for the presence of the halothane allele (Fàbrega et

al., 2002; Moelich et al., 2003; Velarde et al., 2001) which can lead to pale, soft, and exudative (PSE) pork (Mancini & Hunt, 2005) whereas cooked colour was not affected (Moelich et al., 2003). It was reported by Fisher et al. (2000) that halothane negative (NN) pigs exhibit greater pH up to 24 h and a reduced occurrence of PSE (8%) than with halothane positive (nn) genotypes (100% PSE). In a study, Bertram et al. (2000) reported that the presence of ryanodine RN-genotype improved the redness in *longissimus*, probably due to increased content of pigment. Pork from napole gene containing animals yield acidic meat with very low pH and WHC, and finally light colour meat. In addition, loci positions for lightness, redness, and pigment content have already been identified (Mancini & Hunt, 2005).

Diet is one of the crucial pre-harvest factors, which can affect meat colour. Generally, forage-based diets enhance oxidative metabolism and restrict glycogen storage resulting in darker muscle than *ad libitum* concentrate diets due to higher postmortem pH (Vestergaard et al., 2000). Additionally, muscle from grain-finished steers has been found redder and less dark than pastured steers, due to the presence of high subcutaneous fat levels, and slower chilling, and low pH (Bruce et al., 2004). In another study, Realini et al. (2004) reported that the $L^*a^*b^*$ values of *longissimus* muscles were higher for pasture-finished cattle compared to concentrate-finished during display period of 21 days. In addition, over-wintered heifers contain higher α -tocopherol resulting in increased lipid stability, and subsequent colour improvement compared with pastured heifers (Lynch et al., 2002). Dietary supplements also can affect pork colour. In growing-finishing pigs, when provided dietary supplement with a manganese and amino acid mixture, consistent pork colour was observed (Apple et al., 2004). Similarly, feeding magnesium mica to a similar group of pigs has improved pork redness, chroma, and sensory (visual) assessment (Apple et al., 2000).

Both post-harvest pH drop rate and muscle's ultimate pH (upH) in the post-rigor stage can play a significant role in affecting the stability of meat colour. Generally, in postmortem muscles, acidification occurs due to the formation of lactic acid from the breakdown of muscle glycogen. As a result, the upH range in post-rigour muscle is 5.4 to 5.8. An unusual rate of pH fluctuations can cause two major colour defects in postmortem muscle during muscle to meat conversion, PSE and DFD (dark, firm, and dry). In general, PSE condition is developed in all species and depends mainly on the pre-slaughter handling. PSE is linked with the postmortem pH of meat at a specific time and this occurred at 45 minutes after slaughtering when the meat pH < 6 (5.0-5.2). Different types of stress (acute or short term) that can lead to PSE including the use of electric prods, fighting

among animals before slaughtering and overcrowding of animals in the lairage (Adzitey & Nurul, 2011). In PSE meats, the acidification rate is faster resulting in lower pH in meat when the carcass temperature is still high. The combined effects of low pH and high temperature result in some muscle proteins denaturation and finally lead to the reduction in WHC of muscle (Warriss, 2000). Due to the lower pH, muscle proteins cannot retain protein-bound water. In addition, poor WHC is reflected by the exudation of a large amount of fluid in PSE meats. As a result, the refractive indices change due to the presence of released fluid in myofibrils. Warriss (2000) also mentioned that, in sarcoplasm and myofibrils, due to the differences in refractive indices, light is scattered. When these differences are larger, the light scattering is higher resulting in paler meat appearance. Due to higher scattering, the light absorption is lower, and thus selectively green light is absorbed by the haem pigments; therefore, normal red colour is reduced. As a result, PSE meat looks less red and more yellow. Moreover, the low pH in PSE accelerates the oxidation of haem from OMB (red) to MMB (brown) as the myofibril structure is in a more relaxed state and haem iron is exposed (Seideman et al., 1984) for interacting with other compounds. Generally, PSE conditions occur in pork; however, then may also appear in different meat species for example beef, lamb, and poultry. The other colour defect condition appearing at high upH in beef and pork, is known as DFD (Seideman et al., 1984). The DFD condition or dark cutting appears when the upH is reached ≥ 6 (6.2) after 12-48 h postmortem. According to Adzitey and Nurul (2011), the major reason for occurring DFD is the exposure of animals to long-term or chronic stresses (e. g., long-distance transportation, long-time food deprivation, and overcrowded lairage) prior to slaughtering. The chronic stress before slaughtering is ultimately responsible for the depletion in muscle glycogen storage. Therefore, in postmortem muscle, less amount of stored glycogen is available to complete the regular acidification (lactate formation) process, resulting in high upH of meat. Moreover, the high upH in DFD meat results in relatively less protein denaturation and higher content of protein-bound water. As a result, there is no shrinkage of the myofilament lattice resulting in the less differences in myofibrillar and sarcoplasmic refractive indices and finally the meat appearance is darker due to the light absorbed by the muscles (Warriss, 2000).

Temperature plays detrimental roles in the stability of meat colour. Higher temperatures exert effects on meat discolouration by accelerating oxygen consumption rate (OCR), and microbial growth, and generating lipid oxidation products. In contrast, temperature decline can delay the process of discolouration by decreasing Mb oxygenation (Seideman et al., 1984). The

underlying reason is that low temperature enhances oxygen penetration through the meat surface by increasing oxygen solubility, resulting in stable OMB (Renner, 2000). It has been reported that meat discoloration is 2-5 times greater at 10 °C storage temperature compared with 0 °C at the end of four days of storage (Hood & Riordan, 1973). Therefore, lower temperatures are suitable for the storage of meat with desirable bright cherry red colour (bloom) for longer times.

Differences in meat colour can also be observed due to the presence of distinct muscle types and fibre distribution (Hunt & Hedrick, 1977b). During postmortem storage and retail display, some muscles show greater colour stability compared with other types. In general, muscles involved in locomotion contain higher Mb than other muscles (support) since they need more oxygen to produce energy (Seideman et al., 1984). Generally, Mb and hemoglobin (Hb) are the two major proteins involved in the oxygen storage and transportation in tissues (Sammel et al., 2002). In addition, high red fibres containing muscles exhibit a dark red colour appearance (Aberle et al., 2001). The mechanisms lie in the metabolic activities of different types of muscles. Red fibre-containing muscles are predominant in aerobic metabolism, whereas white fibre-containing muscles are related to anaerobic metabolism (Seideman et al., 1984). Therefore, the oxidative muscles with higher Mb concentration and more oxidative stress exhibit a darker red colour than glycolytic muscles (Seideman et al., 1984).

Antimicrobials are applied in meat and meat products to improve shelf life and to control pathogenic growth but their effects on meat colour have caught less attention. The application of antimicrobials in meat and meat products has both positive and negative impacts on colour (Mancini & Hunt, 2005). For example, addition and mixing of 5% acetic acid as a solution in *E. coli* and *Salmonella* incubated trimmings into a meat tumbler seems to have negative effects on the colour of ground beef, resulting in less surface OMB and redness due to lowering of pH (Stivarius et al., 2002). In contrast, beef trimming samples mixed with 0.50% cetylpyridinium chloride, followed by 10% trisodium phosphate (1250 ml solution of each) into a meat tumbler improved ground beef's retail display OMB stability (Jimenez-Villarreal et al., 2003).

2.1.3.2 Other biochemical factors

There are mainly two mechanisms that regulate meat colour, oxygen-utilizing catalytic enzyme system and enzymatic reduction of MMb. The biochemical mechanisms of meat colour are already known and depend mainly on the changes in the redox forms of Mb, Hb and

cytochromes (cyt) in the meat system (Bekhit & Faustman, 2005). Metmyoglobin can be reduced to ferrous OMb by MMB reductase enzyme with the availability of cofactors and substrates, and this process is known as MMB reducing activity (MRA). The catalytic mechanism is decreased quickly in postmortem muscle, and thus the reducing system (MRA) is responsible primarily for the colour stability of meat. Colour stability varies among different beef muscles and is characterized as LL and *tensor fasciae latae* (TFL) as most stable, *semimembranosus* (SM) as stable, *gluteus medius* (GM) as unstable, and PM and *diaphragma medialis* (DM) as least colour-stable muscles (Hood, 1980; Ledward, 1970; O’Keeffe & Hood, 1981, 1982; Renner & Labas, 1987). Among those muscles, PM has higher accumulation of MMB, lower MRA, and higher OCR compared with LL muscle. These increased OCR (respiration), oxidative processes are responsible for reducing MMB reduction and meat discolouration during ageing (Madhavi & Carpenter, 1993).

The well-characterized NADH reduction system for the oxidized Fe-containing proteins (Mb and Hb) involves NADH-cyt *b5* MMB reductase enzyme (Bekhit & Faustman, 2005). The major components of this enzyme are NADH-cyt *b5* MMB reductase, cyt *b5*, and NADH as a cofactor. This enzyme is involved in NADH-dependent catalytic reduction of cyt *b5* and can reduce various electron acceptors as well as methylene blue and ferricyanide. Initially, NADH-cyt *b5* reductase transfers two electrons from NADH to two molecules of cyt *b5*, and then the reduced cyt *b5* transfers the electrons to various electron acceptors, including MHb or MMB (Bekhit & Faustman, 2005; Shirabe et al., 1993). This enzyme can be classified into soluble and membrane-bound forms. Typically, the soluble form is found in erythrocytes, while the membrane-bound form is found in mitochondria’s outer membrane (OM) (Enoch et al., 1977). Moreover, OM cyt *b* and cyt *b5* have been identified in liver mitochondrial, and microsomal fractions, respectively, and can reduce MMB to Mb (Arihara et al., 1995, 1997; Bekhit & Faustman, 2005).

There are various factors involved with MRA in meat. Both assay and storage temperatures can influence MRA in a species-specific manner (Bekhit & Faustman, 2005). For example, the optimum temperatures for MRA are 37 °C and 37.5 °C in bovine cardiac (Hagler et al., 1979), and bovine skeletal (Echevarne et al., 1990a) muscles respectively. Meat is typically stored and displayed at < 10 °C and this temperature has no actual role on MRA for meat colour stability (Echevarne et al., 1990a). Furthermore, MRA levels in beef liver elevate, when the temperature rises to 30 °C (Mikkelsen & Skibsted, 1992). In another study on porcine LD tissue, Mikkelsen et al. (1999) reported that MRA is not affected by the storage temperature of -80 °C, while a 14%

decrease was observed after two weeks at the same temperature. In general, MRA increases with elevated pH and depends on reducing activity sources and assay conditions. For example, Hagler et al. (1979) showed that bovine cardiac muscles exhibit maximum MRA at pH 6.5 (5.7-7.3). Additionally, MRA in bovine LD muscle is maximum at pH 6.4 (Reddy & Carpenter, 1991). The storage time and oxygen have shown inconsistent effects on MRA. For example, Zhu and Brewer (1998) and Madhavi and Carpenter (1993) reported that muscle MRA decreased during 7 and 21 days of storage period, respectively. In other study, scientists (Bekhit et al., 2001; Echevarne et al., 1990a; Feldhusen et al., 1995) found an increase in MRA during 14, 7, and 13 days of storage time, respectively. On the other hand, Echevarne et al. (1990) exhibited that aerobic and anaerobic MRA did not differ significantly in beef muscles. The NADH, generated from glycolytic intermediates has an increasing effect on MMb reduction. Higher levels of NADH, lower levels of NAD, and oxygen uptake can increase MMb reduction and maintain desirable meat colour. Furthermore, NAD concentration in Holstein breed animals was found significantly negatively correlated with MMb accumulation, whereas no correlations were noticed in crossbreeds (Faustman & Cassens, 1991). In different meat producing species, MRA follows the sequence- bovine > ovine > porcine based on the MRA determinations performed in different animals and on muscles within same animals (Bekhit & Faustman, 2005). In addition, Kendrick and Watts (1969) reported that the glycolytic intermediate compounds related to the NAD-dehydrogenase systems in meat have MMb reduction activity. Furthermore, NADH, ascorbate, vitamin E and some microorganisms can reduce MMb non-enzymatically (Bekhit & Faustman, 2005).

The mitochondrion is one of the most important cellular organelles that has a significant influence on muscle colour stability. As a result, the involvement of mitochondria in meat colour has received considerable interest, and the processes by which mitochondria regulate Mb redox stability have previously been intensively investigated. The effects of lipid oxidation, vitamin E (Tang et al., 2005), OCR (Mohan et al., 2010), and metabolites (Ramanathan et al., 2009) on the interactions between mitochondria and Mb in postmortem muscles have revealed that both the electron transport chain (ETC) and reductase enzymes in the mitochondrial outer membrane can reduce the accumulation of MMb, which in turn, can affect colour stability. Mitochondria participate in MMb reduction by scavenging the residual oxygen and providing NADH through reversal of electron transport (Ramanathan et al., 2012).

On the other hand, the mitochondrial respiratory activity by utilizing available oxygen in meat system is known as OCR (Ramanathan & Mancini, 2018). The OCR is affected by several important factors such as pH (English et al., 2016; Tang et al., 2005b), temperature (Phung et al., 2011; Tang et al., 2005b), species (Atkinson & Follett, 1973), breed (Lanari & Cassens, 1991), muscle effect (Abraham et al., 2017; Ke et al., 2017; McKenna et al., 2005; M. Seyfert et al., 2007), muscle location (Nair et al., 2017), postmortem ageing (King et al., 2011; Mancini & Ramanathan, 2014), substrates applied during meat processing (Ramanathan et al., 2009; Jiali Tang et al., 2005a), packaging conditions (Seyfert et al., 2007), lipid oxidation (Ramanathan et al., 2012; Seyfert et al., 2007) and meat processing (Madhavi & Carpenter, 1993; Tang et al., 2006).

Therefore, MRA and OCR are two crucial factors affecting fresh meat colour stability, and these factors should be considered into account during meat discolouration studies.

2.2 Oxidation products in meat

2.2.1 Lipid oxidation

There are two crucial lipid oxidation products produced in meat with detrimental effects on quality attributes, MDA and HNE (Hasan et al., 2021). Significantly, these oxidation compounds can deteriorate the meat colour either alone or in combination with protein oxidation products (Faustman et al., 2010). Both MDA and HNE are secondary lipid oxidation products and are aldehydes in nature (Larsson et al., 2016).

2.2.1.1 Malondialdehyde

In the lipid oxidation process, a variety of highly reactive free radicals, for examples, alkyl ($R\cdot\dot{C}H_2$), alkoxy ($R\dot{O}$) and peroxy ($RO\dot{O}$), can be generated and promptly extract protons (H^+) from the surrounding available molecules (Domínguez et al., 2019). The primarily produced lipid oxidation products are peroxides (\dot{O}_2^{-2}) and these can be further converted into other secondary lipid oxidation products along with aldehydes, ketones, and epoxides (Sakai et al., 1995, 1998; Sakai & Kuwazuru, 1995; Siu & Draper, 1978). Among those produced aldehyde compounds in meat and meat products, MDA is one of the most abundant secondary products in lipid peroxidation (Okolie & Okugbo, 2013).

Malondialdehyde is a highly reactive organic compound and its molecular formula is $CH_2(CHO)_2$. It is a colourless liquid and exists in enol form where a hydroxyl group is attached to

the end of the alkene double bond (Nair et al., 2008). The other names of MDA are malonaldehyde, malonodialdehyde, malonyldialdehyde, malonic aldehyde, propanedial, 1, 3-propanedial (NCBI, 2021a). Malondialdehyde is produced from the oxidations of both ω -3 and ω -6 PUFA, and it can play potential cytotoxic and mutagenic roles (Larsson et al., 2016). It is an electrophilic reactive molecule and partial positively charged compound with electron deficiency. As a result, it accepts electrons from surrounding fatty acid molecules, resulting in the conversion into free radicals. Lipid oxidation is consequently continued as free radical induced chain reactions. Furthermore, MDA can react with surrounding proteins and DNA molecules (Larsson et al., 2016). Malondialdehyde is considered as a potent biomarker for measuring the oxidative stress induced damage of cells and foods including meat (NCBI, 2021a).

Malondialdehyde is measured as thiobarbituric acid (TBA) reactive substances (TBARS) in muscle foods to determine lipid peroxidation (Ganhão et al., 2011). Malondialdehyde is produced during lipid peroxidation due to the decomposition of primary oxidation product (e.g., hydroperoxide). During MDA determination, TBA interacts with MDA to develop a pink colour complex, which is measured using a spectrophotometer at 532 nm wavelength. The production of MDA is a muscle-specific property and varies between muscles based on muscle types which have been presented in various research works (Jeong et al., 2009; Joseph et al., 2012; McKenna et al., 2005). It was reported that TBARS are accumulated more in PM muscles than in LL. Joseph et al. (2012) conducted a study on beef muscles and reported that LL exhibited lower lipid oxidation as TBARS ($P < 0.05$) and greater colour stability ($P < 0.05$), than PM muscles. In another study, McKenna et al. (2005) showed that TBARS was lower in colour stable muscles (e.g., LL muscles) than colour labile PM muscles, when comparing meat discolouration factors in 19 bovine muscles. In contrast, Jeong et al. (2009) found no differences in TBARS values between three different muscles from Korean Hanwoo cattle. Furthermore, production of MDA is significantly influenced by both ageing and retail display times. The findings from some researchers (Legako et al., 2018; Mancini et al., 2018; Wang et al., 2018, 2021) demonstrated that MDA increases gradually during ageing and retail display periods. In a study on longissimus muscles, Galbraith et al. (2016) reported that bison has significantly greater TBARS contents ($P < 0.01$) compared to beef when 6 d ageing samples displayed for 3 d. However, lipid oxidation studies are not available comparing bison LL and PM muscles and therefore, there is a need to examine MDAs' (measured as TBARS) effects on bison meat colour.

Lipid oxidation can be caused in meat systems with the aid of a variety of factors. Lipid oxidation and/or peroxidation is a non-microbial cause of quality degradation in muscle foods that has been widely researched (Decker & Xu, 1998; Faustman et al., 2010; Monahan, 2000). Unsaturated fatty acids (UFA), oxygen, and oxidative agents such as iron where heme iron (HI) from meat pigments and non-heme iron (NHI) play active roles on lipid oxidation (Kanner et al., 1988). Higher proportions of UFAs are present in the meat from non-ruminants (Enser et al., 1996), making it more prone to quick lipid oxidation compared with ruminants (Tichivangana & Morrissey, 1985). Likewise, muscles with a high red fibre content are more vulnerable to lipid oxidation due to the presence of greater contents of iron and phospholipid compared to white fibres (Wood et al., 2004). Due to the increased available surface area in ground beef, this meat is exposed to more oxygen and oxidative compounds resulting in higher lipid oxidation than whole cuts (Gray et al., 1996).

Among the other factors, NHI and its role in lipid oxidation has been studied in red meat (Rhee et al., 1987). Although there are several common forms of NHI, ferritin, lactoferrin, iron-dependent enzymes (cytosolic), and low molecular weight (LMW) chelatable iron ions accelerate lipid oxidation in meat (Halliwell & Gutteridge, 1986). It has been shown that LMW (Kanner & Doll, 1991) and ferritin (Miller et al., 1994; Seman et al., 1991) are two most important initiators of lipid peroxidation in meats. However, it has also been demonstrated that NHI is the major catalyst for the accumulation of lipid oxidation compounds in cooked meat (Igene et al., 1979). Additionally, Liu and Watts (1970) reported that HI has more influence on lipid peroxidation in fresh meat than heme iron.

2.2.1.2 4-Hydroxy-2-nonenal

The molecular formula of 4-hydroxy-2-nonenal (HNE) is $C_6H_{16}O_2$ and it is also known as 4-hydroxy non-2-enal, 4-hydroxynonenal and 4-HNE. It is a hydroxyalkenal compound containing three reactive groups such as an aldehyde (α , β -unsaturated), one double bond at C-2 and one hydroxyl group at C-4 (**Figure 2.3**; NCBI, 2021b). HNE is a highly toxic lipid oxidation product, generated by the oxidation of ω -6 PUFA (Larsson et al., 2016).

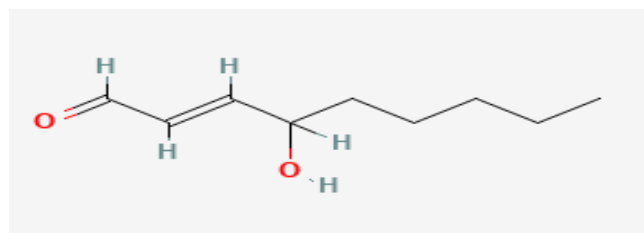


Figure 2.3. Diagram of 4-hydroxy-2-nonenal (NCBI, 2021b)

More precisely, HNE is formed from the linoleic and arachidonic acids positioned within the intramuscular fat molecules and mitochondria's membranes (Ramanathan et al., 2014). This compound is found throughout the animal tissues and produced in higher amounts during oxidative stress in cellular systems including meat (Suman et al., 2006). This aldehyde compound is very stable and reactive, and can readily react with cellular macromolecules like lipids, proteins, and DNA (Witz, 1989). HNE shows high reactivity to thiol and amino groups of proteins (Suman et al., 2006). Moreover, it can react with histidine, cysteine and lysine amino acid residues, causing alterations of protein structures, as well as in inactivation of enzymes (Ramanathan et al., 2012). Some researchers (Alderton et al., 2003; Ramanathan et al., 2012; Suman et al., 2007) reported that HNE can covalently binds with the histidine residues in Mb structure, consequently decreasing the colour stability of meat. Furthermore, HNE can exert effects on the functions of various enzymes including glucose-6-phosphate dehydrogenase, lactate dehydrogenase, pyruvate dehydrogenase, cytochrome c oxidase, glutathione transferase and glutathione reductase (Ramanathan et al., 2014).

In humans, when HNE is present at levels higher than physiological concentration, it can severely affect health. The readily available physiological concentration of HNE in human tissue and serum is below 0.1 μM , which is important for biological activities like the stimulation of oriented migration of neutrophils (Curzio et al., 1990), and the modulation of adenylate cyclase activity (Dianzani et al., 1989; Rossi et al., 1990). However, a greater quantity of HNE (1-20 μM), can impair the synthesis of DNA and protein (Sharaf el Din et al., 1989). Concentrations exceeding 100 μM elicit cytotoxic effects that are both acute and unspecific, resulting in rapid cell death. Subsequently, HNE can contribute to the development of atherosclerotic plaques via formation of oxidized human low-density lipoproteins (Requena et al., 1997).

In the last decade, few studies attempted to detect HNE levels in meat products, all from incubated or spiked meat, not from fresh meat. For example, a solid phase extraction and HPLC-MS/MS-based method was demonstrated for measuring HNE in pork meat products where the detection limit was 0.043 mg/kg, with good recovery (approximately 60% depending on the concentration) and assay linearity and reproducibility (Zanardi et al., 2002). For conducting this experiment, 10 g of spiked pork samples were prepared as 0.1, 0.5, 1.0 and 10 mg/kg with the incubation of required standard HNE concentrations and the amounts of HNE in spiked samples were confirmed by solid phase extraction and HPLC-MS/MS.

Suman et al. (2006) conducted a study in bovine and porcine Mb to investigate the effect of HNE incubation on MMb formation, where Mb was isolated and purified from heart samples. Oxymyoglobin was then prepared by reduction of Mb with hydrosulfite. The study findings exhibited that following 48 h of incubation at 4 °C and pH 5.6, MMb formation was greater in bovine compared to porcine Mb. This study result suggests that at typical storage conditions of meat, Mb from bovine is more vulnerable to lipid oxidation-induced oxidation compared to porcine Mb. 4-hydroxy-2-nonenal has been shown to alter both electron transport-mediated MMb reduction and NADH-dependent MRA. Furthermore, HNE can exert its action by interacting with mitochondria in addition to covalently binding to Mb (Ramanathan et al., 2012). Nevertheless, HNE has not been tested yet to see how it affects the colour stability of bison meat.

2.2.2 Protein oxidation

Protein oxidation produces quality deterioration in meats. Several studies have been conducted to examine the effects of protein oxidation in meat, despite the fact that oxidative changes in meat and meat products can alter the various functional attributes (Estévez & Xiong, 2021; Lund et al., 2011; Soladoye et al., 2015; Wang et al., 1997; Wang & Xiong, 1998; Xiong & Guo, 2020; Zhang et al., 2013). Oxidative instability increases in meat when iron, as a prooxidant (Lund et al., 2011), is released after the breakdown of porphyrin ring structure in Mb during refrigerated storage (Estévez et al., 2006; Estévez & Cava, 2004). Carbonyl compounds are produced as protein oxidation products and can be used as important biomarkers for meat quality evaluation (Lund et al., 2011).

Carbonyl compounds are a class of organic compounds containing one carbonyl group in their structures. The carbonyl group is a functional group found in organic compounds that consists

of a carbon atom connected to an oxygen atom through a double bond (C=O). Furthermore, CAR can be classified as aldehydes (RCHO), ketones (RCOR'), carboxylic acids (RCOOH), carboxylate esters (RCOOR'), and amides (RCOR'R'). These compounds are electrophilic in nature and can readily interact with cellular macromolecules. Carbonyl groups such as aldehydes and ketones are formed during protein oxidation due to oxidative stress in cells which produces reactive oxygen species (ROS), and this process is well known as protein carbonylation (Colombo et al., 2016; Estévez et al., 2021; Stadtman & Levine, 2003). These carbonyl groups containing CARs are generated in cells when the side chain amino acids (proline, arginine, lysine and threonine) in protein structures are modified by oxidation processes (Dalle-Donne et al., 2003). Generally, CARs are produced due to the direct oxidation of the above mentioned amino acids by reactive hydroxyl radicals (HO•) formed in cellular oxidative processes (Colombo et al., 2016). CARs can also be generated by the reactions of protein's cysteine, histidine, and lysine residues with the major aldehyde compounds (MDA and HNE) produced during lipid oxidation, and the underlying chemical reactions are known as Michael additions (Butterfield et al., 2006; Dalle-Donne et al., 2003). Other vulnerable amino acids for protein oxidation are cysteine and methionine and these can be affected by the ROS resulting in cross-linking structure of proteins and sulfur-containing end products (Lund et al., 2011).

Myoglobin oxidation can further affect lipid oxidation, and these processes can accelerate each other (Faustman et al., 2010). The other impacts include oxidative stress's ability to alter the side chains of amino acids in muscle proteins, resulting in accumulation of CAR as protein oxidation products (Stadtman & Levine, 2003; Xiong, 2018). Furthermore, the generation of different intermediate products during the conversions of various redox states of Mb can also enhance protein and lipid oxidation in meat. As a result, the protein oxidation products may have detrimental impacts on the colour of fresh meat.

Muscle-specific variations in protein oxidation has been documented by Estévez et al. (2011), who reported that the production of CAR was higher in pork PM than LL and it progressed with increasing retail display times. During refrigerated storage, CAR contents have been found to increase gradually in both muscles (Cho et al., 2015; Popova et al., 2009).

2.2.3 Interactions between lipid and myoglobin oxidation

Lipid and Mb oxidation products can further accelerate the oxidation processes in an interactive fashion (Faustman et al., 2010). Previously, it was observed that an antioxidant such as α -tocopherol, can delay the discolouration process in beef by decreasing lipid oxidation (Faustman, 2007).

The oxidation of OMb to MMb produces reactive intermediate molecules that accelerate the oxidation of OMb and/or UFAs. More precisely, superoxide anions (Gotoh & Shikama, 1976) are produced and readily converted to hydrogen peroxides (H_2O_2). Both MMb- H_2O_2 (Harel & Kanner, 1985; Kanner & Harel, 1985) and ferryl Mb (Baron & Andersen, 2002) have been reported as potential factors governing lipid oxidation in meat.

The main responsible agents for OMb oxidation are secondary lipid oxidation products (Arnold et al., 1993; Faustman, Cassens, Schaefer, Buege, & Scheller, 1989; Faustman, Cassens, Schaefer, Buege, Williams, et al., 1989). Secondary lipid oxidation products such as α , β -unsaturated aldehydes (e.g., MDA and HNE) are potent initiators of OMb redox instability. Among those, monounsaturated aldehydes promote OMb to MMb formation more rapidly than their saturated counterparts. Moreover, HNE stimulates the oxidation of OMb by interacting with specific histidine residues in Mb and this interaction was studied in different species such as bovine (Alderton et al., 2003; Ramanathan et al., 2012; Suman et al., 2007), porcine (Suman et al., 2006), chicken and turkey (Maheswarappa et al., 2009; Naveena et al., 2010).

The interactions among Mb and lipid oxidation products are presented in **Figure 2.4**. Firstly, the PUFAs are oxidized to primary lipid oxidation products such as peroxy radicals which are known as reactive oxidizing compounds. Then those primary oxidation products are converted to secondary lipid oxidation products (e.g., HNE and MDA). Secondly, among those secondary oxidation compounds, HNE can interact with oxidized Mb (MMb) and form MMb-HNE complex. At the same time, MMb and H_2O_2 can be produced as Mb oxidation products. At the end of this interaction processes, Mb oxidation compounds can further accelerate the generation of primary and secondary lipid oxidation products.

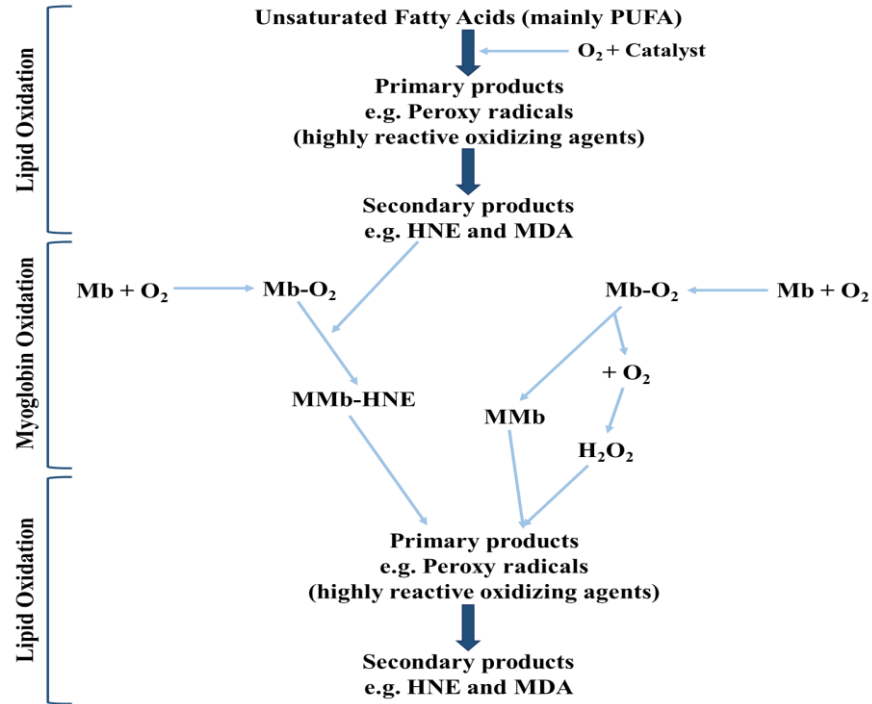


Figure 2.4. Summary of interactions between Mb and lipid oxidation (Faustman et al., 2010)

PUFA = polyunsaturated fatty acid, HNE = 4-hydroxy-2-nonenal, MDA = malondialdehyde, Mb = myoglobin, MMb = metmyoglobin

All possible factors related to oxidative processes in meat need to be considered when evaluating lipid and Mb oxidation, as well as their interactions. These may include monitoring the consumption of oxygen by all potential candidates such as mitochondrial activities, microbial metabolisms and lipid oxidation, and highly reactive lipid oxidation species generated by Omb oxidation.

2.3 Near infrared spectroscopy and its application in meat studies

Most laboratory-based analyses for meat quality assessment are time-consuming, expensive, and produce environmentally harmful chemical wastes (Prieto et al., 2009; Weeranantanaphan et al., 2011). Therefore, as an alternative online technique, NIRS can be implemented to examine meat quality parameters, including colour.

Near infrared spectroscopy is an objective and non-destructive method that can be performed rapidly without reagent requirements and minimal sample preparation (Osborne et al., 1993; Prieto et al., 2009). Moreover, NIRS provides valuable information regarding the molecular

bonds of the organic compounds and ultrastructure of tissue in a scanned sample (Downey & Hildrum, 2004; Prieto et al., 2009), making it a cost-effective (Prieto et al., 2017), and it is an ideal tool for investigating colour attributes and biochemical characteristics of meat muscle samples. The spectral information has its origin in the different vibrational modes of the organic molecules (water, protein, and fat) caused by their interactions with the electromagnetic radiation absorbed at wavelength range from 400 to 2500 nm. NIRS can be categorized into two major types; where the first type is visible-near infrared (Vis-NIR) spectroscopy which covers the wavelength range of 400-1000 nm, whereas the other one with 1000-2500 nm wavelength range is known as short-wave infrared (SWIR). The measured absorptions by NIRS correspond predominantly to the vibrational modes and combinations of overtones related to O-H, C-H and N-H chemical bonds (Osborne et al., 1993). Thus, the collected NIR spectrum contains data regarding physical and chemical characteristics of organic molecules on the sample being analyzed and, consequently, vital information on sample composition. NIRS has been implemented successfully to predict chemical compositions of meat such as different types of fatty acids (Prieto et al., 2011, 2014), myoglobin (Prieto et al., 2006; Ripoll et al., 2008), protein (Chan et al., 2002; Cozzolino et al., 2000; De Marchi et al., 2007; Gaitán-Jurado et al., 2008; McDevitt et al., 2005; Prieto et al., 2014; Prieto et al., 2006; Sanderson et al., 1997; Tøgersen et al., 1999, 2003), intramuscular fat (Alomar et al., 2003; Andrés et al., 2007; Balage et al., 2015; Chan et al., 2002; Cozzolino & Murray, 2002; Cozzolino et al., 2000; Prieto et al., 2011, 2014; Prieto et al., 2006; Ripoll et al., 2008; Sanderson et al., 1997; Tøgersen et al., 1999, 2003), ash (Abeni & Bergoglio, 2001; Alomar et al., 2003; McDevitt et al., 2005; Prieto et al., 2006; Sanderson et al., 1997), moisture (Abeni & Bergoglio, 2001; Andrés et al., 2007; Cozzolino & Murray, 2002; Cozzolino et al., 2000; Prieto et al., 2014; Ripoll et al., 2008; Tøgersen et al., 1999, 2003), dry matter (Alomar et al., 2003; Berzaghi et al., 2005; Prieto et al., 2006) and energy (Prieto et al., 2006). In a very recent study, Fe and Cu contents were also successfully predicted using NIRS in beef samples (Goi et al., 2021). In addition, colour attributes can be assessed using NIR spectral features (Damez & Clerjon, 2008; Hildrum et al., 1994; Prieto et al., 2008). The predictions of meat colour parameters using NIRS in different meat samples were performed including $L^*a^*b^*$ values in pork (Balage et al., 2015; Čandek-Potokar et al., 2006; Cozzolino et al., 2003; Kapper et al., 2012; Meulemans et al., 2003; Savenije et al., 2006), beef (Andrés et al., 2008; De Marchi, 2013; Hoving-Bolink et al., 2005; Leroy et al., 2004; Liu et al., 2003; Prieto et al., 2008, 2014) and poultry (De Marchi et al., 2011; Liu et al., 2004).

Among others, functional parameters were also predicted in meat samples such as pH (Andersen et al., 1999; Andrés et al., 2008; Balage et al., 2015; Čandek-Potokar et al., 2006; Chan et al., 2002; Cozzolino & Murray, 2002; De Marchi et al., 2011; Liu et al., 2003; McDaniel et al., 2013; Meulemans et al., 2003; Prieto et al., 2014, 2008; Savenije et al., 2006), WHC (Andrés et al., 2008; Chan et al., 2002; Hoving-Bolink et al., 2005; Leroy et al., 2004; Meulemans et al., 2003; Prieto et al., 2008; Ripoll et al., 2008; Savenije et al., 2006), and shear force (Balage et al., 2015; Chan et al., 2002; De Marchi et al., 2013; Leroy et al., 2004; Liu et al., 2003; Prieto et al., 2008, 2014; Ripoll et al., 2008). Some researchers also conducted studies for the prediction of sensory parameters including flavour (Andrés et al., 2007; Brøndum et al., 2000; Byrne et al., 1998; Liu et al., 2004; Venel et al., 2001), tenderness (Byrne et al., 1998; Liu et al., 2004; Ripoll et al., 2008; Venel et al., 2001), juiciness (Andrés et al., 2007; Liu et al., 2004; Ripoll et al., 2008; Venel et al., 2001) and acceptability (Byrne et al., 1998; Venel et al., 2001). Furthermore, Moran et al. (2018) reported that NIRS has the capability to segregate muscles and ageing periods based on muscle colour changes.

In general, hyperspectral imaging acquired from NIRS are processed in different steps such as image correction by removing the backgrounds, segmentation of images, extraction of spectral data and preprocessing. Data obtained are then analyzed for supervised and unsupervised classification approaches. Principal component analysis (PCA) is a statistical approach for analyzing multivariate data, and practiced in unsupervised classification where raw spectral data are used to visualize and investigate data pattern, structure, and grouping among the data, if any, without human interference. On the other hand, the partial least squares discriminant analysis (PLS-DA) method is utilized for supervised classification by selecting the wavelength representing the parameters of interest. In PLS-DA analysis, calibration models are developed for the prediction of classes of meat based on different criteria such as muscle type, ageing and retail display periods. Finally, partial least squares regression (PLSR) analysis is performed by developing calibrations models, including selected data points from a specific wavelength range and components of interest as variables for the prediction of parameters of interest in meat quality such as colour and chemical compositions. Therefore, the use of NIRS in combination with multivariate data analysis techniques for calibration and statistical approaches allows the important features contained in the NIR spectra to be extracted for developing calibration models that allow the predictions of the constituents in unknown samples (Font et al., 2007).

Near infrared spectroscopy has previously been applied to segregate beef and pork muscles based on their inherent muscle-specific colour stability and to predict various meat quality attributes. However, there is a need to research the potentiality of NIRS in the study of bison muscles to see if it can successfully discriminate bison muscles based on muscle types, ageing and retail display, predict meat quality attributes including colour.

2.4 Sarcoplasmic proteome and fresh meat colour

Muscle proteins are classified into three types based on their solubility properties: sarcoplasmic, myofibrillar and stromal proteins. These proteins constitute around 3,560 proteins among the 1000 muscle proteins estimated by proteomic analysis and cover 15% of proteins in the muscle tissue (Lametsch & Bendixen, 2001). Sarcoplasmic proteins are soluble in water and salt solutions and comprise a minimum of 500 individual proteins; many of those are metabolic enzymes (Wood, 1990). Their globular structure is the main feature of most sarcoplasmic proteins, and their side chains contain a high density of polar and charged groups. Myoglobin, a 17 kDa protein, is a familiar member of the sarcoplasmic protein superfamily, responsible for the colour formation in fresh meat. The proteins found in sarcoplasmic proteome of muscle tissue have very important roles in water binding capacity, fat emulsification and muscle colour (Xiong, 2018).

The variations in meat colour stability, based on muscle-specific trait, are influenced by the sarcoplasmic proteins, and the presence of the proteins in beef sarcoplasm is affected by the postmortem ageing periods. The biochemical mechanisms that regulate the quality parameters of meat undergo changes during post-harvest ageing periods (Nair et al., 2018). Muscles are generally classified as colour-stable (e.g., LL) or colour-labile (e.g., PM) based on their colour stability in beef during retail display. Therefore, for the investigation of colour stability based on changes in proteomic profile, colour stable LL and colour labile PM muscles can be utilized as valuable models (Seyfert et al., 2007).

According to Sayd et al. (2006), darker pig meat exhibited 22 proteins with differential expression in the sarcoplasmic fraction of pig muscle, where oxidative metabolism proteins were more abundant such as mitochondrial respiratory chain enzymes, haemoglobin, chaperones [e. g., heat shock protein (HSP) 27 kDa, RB-crystallin] and regulator proteins (e.g., glucose-regulated protein 58 kDa). However, in the lighter muscle group, glycolytic enzymes were overexpressed and showed elevated levels for glutathione S-transferase. Another study aimed at differentiating

the proteomes of colour stable and colour labile beef muscles in aerobically packaged and assigned to nine days period in refrigerated retail display (Joseph et al., 2012). This study demonstrated that certain proteins in colour stable LL muscle presented a relatively positive correlation with meat redness (e.g., β -enolase, aldose reductase, and creatine kinase) and stability of colour (e.g., peptide methionine sulfoxide reductase, peroxiredoxin-2, and HSP 27 kDa), whereas in the colour labile PM, a specific protein (mitochondrial aconitase) content demonstrated negative correlation with redness. In addition, both antioxidants and chaperones showed increased expression patterns in LL muscle compared to PM. Furthermore, in the colour stable LL muscle, the overabundant peptide methionine sulfoxide reductase showed positive correlation with MRA, which ultimately contributes to the stability of meat colour. In addition, nine proteins from this study showed correlation with colour stability parameters of meat and, among those, eight proteins were from LL muscle.

Moreover, in the LL steaks the higher abundance of glycolytic enzymes (e.g., phosphoglucosmutase-1) probably contributed to improve meat colour stability in postmortem muscles by regenerating NADH as a reducing agent (Canto et al., 2015). Furthermore, the proposed mechanisms of lactate produced in postmortem muscle include NADH regeneration that facilitates MMb reduction and consequently minimizes discolouration (Kim et al., 2006). One of the important chaperones, HSP 27 kDa, protects actin filaments and cytoskeletal proteins against disintegration (Pivovarova et al., 2005). Moreover, chaperones prevent denaturation and aggregation of proteins and contribute to the stability of Mb and meat colour. Nonetheless, the exact functions of chaperones in meat colour stability are not yet completely established (Joseph et al., 2012).

Wu et al. (2016) conducted a study on Chinese *luxi* yellow cattle and described that the glycolytic enzymes were found predominantly in LL muscles and consequently responsible for the colour stability in LL compared with PM. Additionally, at different ageing times, identified proteins were glycerol-3-phosphate dehydrogenase, glycogen phosphorylase, phosphoglucosmutase-1, aldolase A, peroxiredoxin-2, superoxide dismutase and HSP 71 kDa, and these proteins could be used as potential biomarkers to assess meat colour stability during ageing.

In another study on beef muscles, Nair et al. (2018) reported that sarcoplasmic proteins could span from proteins involved in glycolysis, energy metabolism, antioxidant activity,

chaperone functions, and transportation, whereas in colour stable muscles, glycolytic enzymes exhibited an increase in expression patterns. During the comparison of LL vs PM at different ageing periods, the identified differential proteins at 2 d postmortem were mainly related to transport and energy metabolism and showed overabundance in LL. At the 7 d ageing period, the differential overabundant proteins were associated with transport, energy metabolism, chaperone, glycolytic enzymes and in this case, almost all proteins were dominantly identified in LL muscles. Furthermore, a 14 d ageing period exhibited similar protein groups and expression patterns to 7 d, however, the number of identified proteins was higher at 14 d. The glycolytic enzymes were found to retain the colour stability in LL muscles with ageing times, indicating that these enzymes could be utilized as potential biomarkers for measuring the stability of beef colour.

2. 5 Overview of bison

In North America, bison is the biggest land animal commercially raised for meat production (Galbraith et al., 2014). Although there were around 70 million bison reported in 1800, there was a dramatic fall in the number of bison in the late nineteenth century (e.g., only 1500 in 1880) due to the careless and unregulated slaughtering (NBA/CBA, 2010). However, the bison farming industry has seen tremendous growth over the past few decades. As per the CBA (2021b), the total number of commercially produced bison population was estimated over 400,000 in 2017. In recent years, bison meat products from North American farms have emerged as an alternative to the traditional red meats in the premium red meat marketplace (Galbraith et al., 2006; Marchello & Driskell, 2001). In 2016, the total international export of Canadian fresh bison meat was 728,613 kg in total (CBA, 2021c). The total market share contributed by bison meat is < 1% (Carter, 2017; Steiner et al., 2010). However, bison meat is gaining popularity in the red meat marketplace (Steiner et al., 2010), and production is expanded with 13.8% increase from 2018 to 2019 (CBA, 2019). Furthermore, because of the low farming costs and high demand in the market, bison has attracted immense interest amongst livestock producers as an alternative red meat product (Galbraith et al., 2014).

It is well accepted that North Americans are becoming more health-conscious, particularly regarding the types of fat and fatty acids consumed, as well as the cholesterol content of meats. As a result, the composition of nutrients, particularly lipids in meats, has become critical. Bison meat was reported to have lower energy and fat content when compared to beef (Mcclenahan & Driskell,

2002), and therefore, bison meat consumption has been considered as a healthier alternative (Rule et al., 2002). Bison meat could be a nutritious and tasty option for health-conscious consumers without impairing their eating experience (Galbraith et al., 2014). According to Health Canada (2007), bison meat is higher in protein and iron contents and lower in total fat and calorie contents than other red meats.

The presence of high levels of saturated fatty acids and elevated cholesterol in the traditional beef, pork, and lamb meats has been linked to several health problems such as the risk of cardiovascular disease (McDaniel et al., 2013). As a result of bison meat's high usefulness and potential, there is a growing necessity for maintaining strict quality control of the meat products.

2.5.1 Possible reasons for darker and unstable colour in bison meat

One of the major quality control attributes is the colour of the meats, which has been used as a crucial indicator of the freshness of meat products. However, fresh bison meat colour is darker (Koch et al., 1995) and discolouration under retail aerobic packaging conditions occurs faster compared with beef (Pietrasik et al., 2006), which remains a major challenge for the bison industry.

Discolouration in bison could be due to the inherent variations in the muscles' biochemical properties. Generally, bison differs in muscle-fibre (Koch et al., 1995), contains more red-fibre resulting in greater Mb (pigment) (Galbraith et al., 2016) and iron contents (Galbraith et al., 2006; Marchello & Driskell, 2001) when compared with beef. High Mb and iron concentrations in bison can subsequently cause oxidative instability (Galbraith et al., 2016), resulting in reduction in colour stability. Therefore, the rapid pigment oxidation in bison meat makes it highly vulnerable to early browning or discolouration under aerobically packaged retail conditions (Janz et al., 2001). Mb oxidation leads to the formation and accumulation of MMb, responsible for the surface discolouration in bison meat (Roberts et al., 2017). Furthermore, those species-specific variations in muscle composition can influence the light scattering properties, leading to differences in visual colour (Swatland, 2004).

Dietary factors and production systems can also affect the chemical composition of bison meat and its quality traits including colour (Galbraith et al., 2016). Recently, Janssen et al. (2021) reported that in bison finishing systems (grain- and grass-) have significant influences on the characteristics of carcass, meat quality parameters and nutritional components especially fatty acid

contents. In retail meat, oxidative stability is influenced by the fatty acid contents of meat and the fatty acid concentration in bison meat is influenced by the diet (Roberts et al., 2017). In Canada, most commercial bison are raised as grass-fed. Both grass-fed and grain-fed bison have higher levels of PUFA on the phospholipid compositions of their cell membrane structure compared to beef (Rule et al., 2002). Membrane PUFA content is one of the potential detrimental factors for the oxidative damage and consequent changes in meat's smell, taste and colour (Wood et al., 2008). The combined influences of both high PUFA and iron concentrations make bison meat more prone to lipid oxidation (Rule et al., 2002) and rapid colour deterioration. Moreover, in raw meat, heme iron has been shown to initiate and promote lipid oxidation (Decker et al., 2000). The oxidative instability of PUFA can further affect Mb's redox states, resulting in prompt meat discolouration (Faustman et al., 2010; Wood et al., 2004).

Furthermore, in bison meat, due to the oxidation of PUFA (Pietrasik et al., 2006), secondary lipid oxidation compounds, such as MDA and HNE, are produced (Hasan et al., 2021). These highly reactive oxidation products can subsequently initiate and accelerate Mb oxidation (MMb formation) resulting in the deterioration of meat colour (Joseph et al., 2010; Suman et al., 2006). Also, HNE can decrease MRA, and discolouration of meat may partly be attributed by the interactions of HNE with mitochondria (Ramanathan et al., 2012). Additionally, sarcoplasmic proteins and their prooxidant contents are responsible for initiating lipid oxidation in meat, leading to discolouration (Joseph et al., 2010; Ramanathan et al., 2009).

Among the other influential factors, the tocopherol or vitamin E content in bison meat may have effects on lipid oxidation and discolouration (Roberts et al., 2017). Generally, vitamin E has antioxidant properties and can maintain colour stability (Galbraith et al., 2016). In commercially raised bison, vitamin E content was reported as 1.13 $\mu\text{g/g}$ (Roberts et al., 2017), however, another study (Galbraith et al., 2016) found 2.2 $\mu\text{g/g}$ and 3.47 $\mu\text{g/g}$ in grain-fed and grass-fed bison meat, respectively. Furthermore, it has been demonstrated that in lamb, the vitamin E content $< 3.0 \mu\text{g/g}$ is linked to increased lipid oxidation rates (Ponnampalam et al., 2014).

Therefore, all the above-mentioned discolouration-induced factors need to be taken into consideration for the production and marketing of bison meat with desirable cherry-red colour.

2.5.2 Postharvest techniques to improve colour in bison

There are several postharvest techniques, which have already been studied for the mitigation of postmortem meat discolouration. However, only few postharvest techniques are currently available to improve bison meat colour. Therefore, this literature review section included the most important postharvest strategies practiced on bison meat for the improvement of its colour stability.

It is necessary to practice some suitable post-harvest intervention strategies to mitigate the discolouration problems in bison meat industry. In bison industry, some postharvest techniques have already been practiced for minimizing the discolouration issues such as elevated temperature conditioning (ETC) (Janz et al., 2000), blast and spray chilling (Janz, Aalhus, Price, and Greer, 2001), injection enhancement (Dhanda et al., 2002), low and high-voltage electrical stimulation (ES) (Ding et al., 2016; Janz et al., 2001), nitrite film packaging (NFP) (López-Campos et al., 2018; Narváez-Bravo et al., 2017; Roberts et al., 2017; Rodas-González et al., 2013), and rinse and chill (RC) method (Mickelson & Claus, 2020). However, most of the applied technologies were not fully successful in preventing colour deterioration in bison meat. Still, there is a need of technological improvements or new technologies for mitigating of discolouration problems in the bison industry. The postharvest techniques examined by various researchers over the last two decades (2000-2020) to improve bison meat colour are summarized below.

2.5.2.1 Carcass chilling techniques

Carcass chilling is a very important postharvest factor that can affect meat quality, attributes, including colour. There are different types of carcass chilling techniques practiced in meat industry such as conventional chilling (CC), ETC, blast chilling (BC), and spray chilling (SC).

Elevated temperature conditioning is a carcass cooling technique where carcasses are kept at 10 °C during the initial postmortem period of 10 h. This method was practiced for bison carcass chilling to avoid or minimize the cold-induced meat quality problems due to the application of CC (Janz et al., 2000). Generally, CC bison carcasses are placed in a cooler for 24 h at 0-2 °C. Janz et al. (2000) conducted one study on bison LL and SM muscles using ETC and reported that temperature/time conditioning resulted in samples with lighter colour and improved red colour

intensity, compared with samples chilled under the CC. ETC was able to improve the initial and after ageing tenderness significantly. Furthermore, there was no significant evaporative loss observed with ETC.

In another study, researchers (Janz, Aalhus, Price, and Greer, 2001) applied SC and BC techniques to bison carcasses to evaluate meat quality parameters, including colour. The SC method was applied on one side of the bison carcass by maintaining a cooler temperature at 2 °C employing a 60 s spray cycle for 8 hours (4 times/h), followed by CC at 2 °C for 24 h. The other side of the carcass was conventionally chilled and, after completing both chilling processes, LL muscles were stored for 6 weeks and then displayed for 7 days in vacuum packaging conditions. The surface discolouration pattern was similar for both conventionally and spray chilled steaks. Furthermore, for BC or very fast chilling technique, one side of the bison carcass was kept in a cooler at -35 °C for 2, 4, or 6 h, and then CC was applied for remainder of time. At the end of the chilling process, the samples were stored, displayed, and meat quality was evaluated in LL muscles, and compared with CC. BC resulted in drip and package loss, and the meat colour was slightly darker.

Therefore, it can be concluded that only significant improvement in colour parameters were observed when applying ETC alone. Further investigations are needed to manipulate other chilling processes for achieving desirable bison meat colour.

2.5.2.2 Injection enhancement combined with carcass chilling

Injection enhancement is a commonly used technique used in pork industry to improve quality parameters of meat such as tenderness and juiciness. This method is practised by injecting different types of salt and phosphate solutions into meat cuts. In general, this is a marination technique used to improve meat palatability including colour attributes.

In a previous study, Dhanda et al. (2002) demonstrated the use of injection enhancement technique combined with carcass chilling techniques in bison SM muscles to examine the meat palatability and colour parameters. The researchers applied both the chilling techniques (i.e. conventional and blast chilling) to bison carcasses and then collected the SM muscle from each carcass, vacuum packaged the meat and kept it at 4 °C for 6 days of postmortem ageing. Each SM muscle portion was equally divided into two portions where one part was injected with brine

solution and other part was non-injected. For injection, the brine solution was prepared as to gain 0.5% of sodium chloride (NaCl) and 0.3% of sodium tripolyphosphate in the final products with 10% weight increase relative to the original weight of each muscle sample. All injected and non-injected samples were vacuum packaged, stored for 24 h at -1 °C, and then steaks were prepared for 5 days in retail display. There were no differences observed in instrumental a^* (redness) and b^* (yellowness) values and injected steaks exhibited darker (lower L^* values) appearances than controls. Therefore, this injection and carcass chilling combined technique was not successful in improving bison meat colour.

2.5.2.3 Injection combined with packaging and storage temperature

The combined application of different postharvest techniques can be sometimes helpful to mitigate meat discolouration problems. Pietrasik et al. (2006) conducted a study on bison and beef LL steaks to examine the combined application effects of injection, packaging and storage temperatures in meat colour and other quality traits. For this experiment, muscles were first kept at 4 °C for 14 d postmortem, each muscle was cut into two equal portions, where one part was injected with brine solution (0.5% NaCl and 0.3% Na tripolyphosphate in finished product) to gain 20% relative to the original weight of muscles, and the other part was kept as control (non-injected). Then steaks were prepared, randomly packaged with both vacuum packaging (VP) and modified atmosphere packaging (MAP; 70% O₂ + 30% CO₂) and stored at two different temperatures (-1 °C and 4 °C) for 2 weeks (MAP) and 3 weeks (VP) in a dark room.

MAP contributed more to retain a bright red colour in beef LL compared with bison steaks. Storage of MAP samples at -1 °C exhibited greater colour stability in both beef and bison. Injection of brine also provided better colour stability, most prominently in bison steaks compared to beef. The overnight storage of steaks under MAP demonstrated the highest a^* values in retail display till d 5, relative to those stored under VP. Furthermore, MAP steaks maintained greater OMB contents up to 5 d in retail display compared with VP. Injection and storage at -1 °C showed significantly greater OMB amounts in comparison with non-injected steaks and storage at 4 °C. It was suggested that MAP can be used as a suitable technique for short-time storage, and keeping meat in MAP before placing in retail display could be another strategy to improve shelf life.

In general, MAP is a process by which the surrounding atmosphere of the meat product is replaced and/or removed before enclosing in a gas-barrier material (McMillin, 2008, 2017). The

gas mixtures are flushed in a rigid O₂ barrier tray by sealing with a transparent barrier film. Gases present in MAP have an influence on Mb redox biochemistry and thus meat colour; therefore, MAP systems are applied for the improvement of colour stability (Suman et al., 2014; Suman & Nair, 2017). Generally, this type of packaging includes various combinations of gases, O₂, CO, CO₂, and N₂ and has been proved to ensure prolonged microbiological and colour shelf life of meat and meat products in the retail display (Luño et al., 1998).

2.5.2.4 Electrical stimulation

Electrical stimulation is a technique used in meat industry for the acceleration of pH decline rate resulting in beneficial effects on meat quality parameters, including tenderness and colour (Ramanathan et al., 2020). Electrical stimulation has been applied to lamb, beef and goat carcasses and reported to improve the meat quality parameters (Smith, 1985). The main role of ES is the passing of a current flow through the muscle tissues resulting in reduced pH by increasing the postmortem glycolysis process and the acceleration of rigor mortis onset. It also prevents cold shortening, decreases the microbial load partially and improves the meat quality parameters such as tenderness, colour, and flavour. Generally, two types of ES processes are available in meat industry namely, low-voltage ES (LVES) and high-voltage ES (HVES). If the applied voltage for ES is lower than 100 volts, the process is known as LVES, whereas the treatment with higher than 100 volts is termed HVES. When compared to HVES, the LVES was shown to be less effective in improving tenderness. Moreover, HVES can cause higher muscle stimulation and contraction, which are sufficient for physical disruption of muscle tissue (Savell et al., 1978). However, LVES is safer for industry applications. LVES is the most effective practice with a simpler mechanism, by which cold shortening can be prevented at low chilling temperature of early postmortem stage (Marsh et al., 1987) and where the carcasses are lean enough for rapid dissipation of heat. The risk of cold shortening is high in bison carcasses because of leanness (Hawley, 1986; Koch et al., 1995) and thus LVES is considered to be a good practice.

In a previous study (Janz et al., 2001) on bison LL muscle, LVES (21 V, 0.25 A, 60 Hz; 20 s during exsanguination via nose clamp) was applied separately and in combination with blast chilling (BC; -20 °C, 3 ms⁻¹ air velocity, 2 h), and different meat quality parameters, including colour were investigated. Both LVES and BC treatments showed significantly higher effects on the measurement of objective colour attributes at 24 h postmortem compared with untreated

control bison meat samples. Additionally, LVES treatment exhibited significant effect on L^* (lightness) persistence until 6 d postmortem and, compared with control, samples were lighter and redder (greater cherry-red colour). The combined effect of LVES and BC treatments resulted in lactate accumulation and consequently upH declined to 5.6. As a result, LVES combined with BC can be used for the improvement of bison meat quality, including colour parameters.

Ding et al. (2016), conducted another study to investigate the effect of HVES (400 V; 5 ms pulses, 15 pulses s^{-1} for 30 s on one side of carcasses) on bison striploins steaks and ground patties. Except for lactate, they found no influence of HVES on the meat quality parameters of bison, including sensory qualities, retail display properties, and glycolysis metabolites. Electrical stimulation can be practiced in carcasses for the improvement of post-rigour meat colour as bison meat is generally darker compared with beef due to the presence of higher myoglobin contents.

2.5.2.5 Rinse and chill method

Rinse and chill is process applied at early postmortem (immediately after exsanguination), consisting of a vascular rinse system is practiced in meat industry for rinsing out the residual blood and delivering specific substrates, which have impact on meat quality attributes. Generally, in the RC process, a chilled (3 °C) isotonic substrate solution containing 98.5% water balanced with glucose, polyphosphates, and maltose is used, and a catheter is inserted into the carotid artery to rinse out vascular residual blood from the circulatory system at early postmortem exsanguination time with the application rate of 8% on the basis of carcass weight.

A recent study (Mickelson & Claus, 2020) was conducted on bison LL and *triceps brachii* (TB) to study the effect of the RC method on bison colour parameters and tenderness by using the using vascular RC technology (MPSC Inc., Hudson, WI, USA). They reported that the PVC wrapped bison steaks with RC showed lighter colour compared with conventionally chilled (CC), but a^* and b^* values were not affected at all. However, bison steaks with RC vacuum packaging exhibited lighter (L^*) and redder (a^*) properties, compared with CC. The OMB and DMb contents in RC steaks were found in greater amounts than CC, whereas significant difference in b^* value was observed among those process. In PVC and vacuum packaged ground bison samples, RC yielded lighter and redder product than CC. Additionally, yellower samples resulted from RC ground bison compared with CC under vacuum packaged conditions. The main purposes of using phosphates in meat products is to stabilize pH, increase WHC and shelf life, and improve the

texture and sensory attributes, including colour. The RC solution, including polyphosphates, may improve the colour and anti-microbial properties in RC bison samples.

In conclusion, apart from the higher cooking loss, RC technique can improve meat tenderness, and colour attributes, especially the increase in lightness and redness. As a result, the RC method could be used for large-scale commercial production of bison meat.

2.5.2.6 Nitrite film packaging

Packaging techniques are one of the most important postmortem strategies which have crucial influence on meat colour stability and therefore, these can effectively be used for improving meat colour in retail display and storage. Among packaging techniques, NFP can be an excellent strategy to maintain cherry-red colour of fresh meats in vacuum packages (López-Campos et al., 2018; Narváez-Bravo et al., 2017; Roberts et al., 2017; Suman et al., 2014).

For NFP use, packaging film is manufactured (FreshCase®, Bemis) with embedded sodium nitrite (NaNO_2), containing 113 mg NaNO_2/m^2 . When NaNO_2 is exposed to fresh meat, nitrite gets reduced to nitric oxide (NO). NO consequently binds to the 6th coordinate of the porphyrin ring iron (deoxygenated Fe^{2+} state) in Mb structure resulting in bright red pigment (Suman et al., 2014) nitrosomyoglobin (NOMb). The biochemical process for the formation of NOMb is known as nitrosylation (Roberts et al., 2017).

Roberts et al. (2017) conducted study on bison LL steaks and burger patties prepared from ground *rhomboideus* (RH) muscles to examine the effect of NFP on retail colour and oxidative stability. After completing the ageing periods of 6, 13, and 20 d for LL, and 6 d for RH muscles, the NFP samples were displayed in a retail cabinet for 5 d. NFP meat samples did not exhibit higher discolouration or MMb formation at the end of the retail display time as did aerobically packaged (AP) samples. Both NFP steaks and burger patties showed higher L^* values (lighter colour) and a^* values (redness) over the period in retail display than AP samples. Furthermore, in NFP burger patties TBARS (lipid oxidation) did not increase significantly under retail conditions compared with AP burger patties. Likewise, in a previous study in bison steaks and burger patties, (Rodas-González et al., 2013) reported that the use of NFP can improve the colour stability significantly.

Narváez-Bravo et al. (2017) reported similar improvements in colour stability using NFP under retail display conditions when compared with other packaging techniques and suggested the application of NFP in bison industry to maintain desirable colour. Recently, the use of NFP in bison meat (López-Campos et al., 2018) has been shown to reduce the discolouration process in comparison with meat samples overwrapped under control PVC, but blooming time was longer. Researchers suggested that NFP can be used as a useful technique for the mitigation of discolouration problems in bison meat. Therefore, the application of NFP has the potential to improve bison meat colour and can be practised by the industry as a valuable postharvest technique.

To fulfill the first objective of the present research work, experiments were conducted to analyze the products of lipid and protein oxidation and their influence on fresh bison LL and PM muscles with their inherent colour stability, and the results are presented on the following chapter.

CHAPTER 3: MANUSCRIPT NO. 1

Principal component analysis of lipid and protein oxidation products and their impact on colour stability in bison *longissimus lumborum* and *psoas major* muscles

This chapter was prepared in manuscript format for the *Meat Science* journal and has been published as: Hasan, M. M., Sood, V., Erkinbaev, C., Paliwal, J., Suman, S., & Rodas-Gonzalez, A. (2021). *Meat Science*, 178: 108523. <https://doi.org/10.1016/j.meatsci.2021.108523>

3.1 Abstract

The study aims were to compare lipid (malondialdehyde [MDA], 4-hydroxy-2-nonenal [HNE]) and protein (carbonyl content [CAR]) oxidation products between two bison muscles (*longissimus lumborum* [LL] and *psoas major* [PM]) at different ageing and retail display time and determine their influence on muscle colour stability. Regardless of the ageing and retail display time, LL showed greater redness (a^* value; $P = 0.04$) and lower surface discolouration ($P < 0.01$) than PM as well as LL exhibited lower MDA, HNE, and CAR content compared to PM ($P < 0.05$). In both muscles, MDA showed the highest correlation to a^* ($r = -0.78$; $P < 0.01$) and discolouration ($r_s = 0.82$; $P < 0.01$) scores, particularly in PM muscle compared to LL muscle. In conclusion, principal component analysis revealed 4 distinct colour deterioration clusters within steaks displayed at d 4 according to the muscle and ageing time, and MDA critically influences colour deterioration patterns in bison muscles.

Keywords: colour stability, discolouration mechanisms, oxidation, malondialdehyde, 4-hydroxy-2-nonenal, carbonyl content.

3.2 Introduction

In Canada, bison meat is a niche product that attracts health-conscious consumers who are looking for alternatives to traditional red meats (i.e. grass-fed and low-fat meat products) without sacrificing an excellent eating experience (SMA, 2012) and contributes $< 1\%$ of the market share (Steiner et al., 2010). Also, it is gradually taking its position in the red-meat market (Steiner et al., 2010) and its production is increasing (13.8 % in 2019 compared to 2018) (CBA, 2019).

Stability of colour is a drawback to the expansion of fresh bison meat marketing because its colour deteriorates more rapidly than beef under retail aerobically packaged conditions (Narváez-Bravo et al., 2017; Pietrasik et al., 2006) resulting loss in revenue. Structurally, beef and bison have identical myoglobin (Mb) that displays no difference in amino acid sequences, oxidation kinetics, and thermostability (Joseph et al., 2010). However, both range and feedlot bison have been shown a higher level of polyunsaturated fatty acids (PUFA) of phospholipid membranes compared to beef (Rule et al., 2002) which are prone to oxidative damage (Pietrasik et al., 2006; Wood et al., 2008) and produces secondary lipid oxidation products, malondialdehyde (MDA) and 4-hydroxy-2-nonenal (HNE). Furthermore, HNE can enhance oxidation of Mb to metmyoglobin (MMb) and produce subsequent meat discolouration (Alderton et al., 2003; Joseph et al., 2010; Lee et al., 2003; Schneider et al., 2001; Suman et al., 2006). HNE decreases both electron transport-mediated MMb reduction and NADH-dependent MMb reductase activity. In addition to covalent binding of HNE to Mb, the effect of HNE on colour stability also can be partially attributed to interactions between HNE and mitochondria (Ramanathan et al., 2012). However, the role of HNE in bison meat colour stability has not yet been evaluated.

Additionally, few studies have evaluated the effect of protein oxidation in muscle foods, although it has been reported that such oxidative damage leads to alterations in different functional properties of protein for example gelation, emulsification, viscosity, solubility, and hydration (Wang et al., 1997; Wang & Xiong, 1998). At the same time, the development of lipid and protein oxidation during refrigerated storage of beef and lamb is associated with the breakdown of the heme molecule and the subsequent release of free (non-heme) iron from the porphyrin ring which might also increase oxidative instability of the meat system (Estévez et al., 2006; Estévez & Cava, 2004). Lipid, Mb and oxymyoglobin (OMb) oxidation reactions can exacerbate each other (Faustman et al., 2010). Among other effects, the oxidative degradation of muscle proteins involves modification of amino acid side chains, leading mainly to the formation of carbonyl compounds (CAR) (Stadtman & Levine, 2003; Xiong et al., 2000). Furthermore, the oxidation of OMb to MMb generates reactive intermediates capable of enhancing further oxidation of OMb and/or unsaturated fatty acids (i.e. superoxide anion) in meat from ruminants, especially in beef. Thus, protein oxidation products in bison meat could have adverse effects on meat colour.

Muscle source and postmortem ageing are other factors influence colour stability (Guelker et al., 2013; Mancini & Hunt, 2005; Nair et al., 2018; Neethling et al., 2017; Suman & Joseph,

2014). Muscles in a beef carcass vary in their physicochemical and biochemical characteristics due to specific anatomical locations, physiological functions, energy metabolism, and fibre type (Hunt & Hedrick, 1977b). Also, postmortem ageing can influence cellular mechanisms (such as reducing enzymes, oxygen scavenging enzymes, and mitochondria) responsible for meat colour stability, resulting in lower colour stability during subsequent retail display (English et al., 2016; King et al., 2012; Ramanathan et al., 2020). However, the role of muscle source and ageing in bison meat colour stability has not yet been evaluated.

The role of different oxidation products in the colour stability in bison *longissimus lumborum* (LL) and *psoas major* (PM) muscles have not been evaluated yet. There is a need for a better understanding of the influence of those biochemical components in a muscle that changes meat myoglobin chemistry during storage and retail display of fresh bison meat in order to eliminate retail losses due to poor colour stability and early browning. As a result, we hypothesized that high levels of MDA, HNE and CAR vary among bison two major muscles (LL and PM), and HNE and CAR may have greater influence compared to MDA in increasing the discolouration of bison meat. Therefore, the objective of the current study was to compare lipid (MDA and HNE) and protein (CAR) oxidation products and determine their influence on colour stability in two bison muscles (LL = colour stable; PM = colour labile) during storage and retail display.

3.3 Material and methods

3.3.1 Sample collection and processing

A total of ten (n = 10) striploins (LL) and ten (n = 10) tenderloins (PM) from grade A1 (Canada Gazette, 1992) bison carcasses were obtained from a federally certified slaughter plant and shipped to the University of Manitoba Food Science Pilot plant (Winnipeg MB, Canada) within 48 h postmortem. Upon arrival, the sub-primals were unpackaged and each muscle was trimmed practically free of subcutaneous fat. From each muscle, a 10-cm thick section was removed and sub-sampled to evaluate the pH, MDA, HNE, CAR, myoglobin and fat contents which was immediately vacuum packaged and frozen (-40 °C) for subsequent analysis. These measurements allowed the establishment of a baseline for the different oxidation products. The remaining muscle was cut into two equal portions, and individual portions were assigned randomly to an ageing period of 7 or 14 d postmortem in vacuum packaging at 2 °C. At the end of each ageing period, each muscle portion was removed from its package and two 2.5 cm steaks were

obtained aseptically, using sterile cutting boards and knives without touching the fresh cut surface for colour evaluation (AMSA, 2012). The first steak was for estimation of MDA, HNE and CAR at d 0 of the retail display, which was immediately vacuum packaged and frozen (-40 °C). The second steak was for pH and sensory (muscle and discolouration scores) and instrumental colour measurements [L^* (lightness), a^* (redness) and b^* (yellowness)] over 5 days of retail display. The pH of each steak was recorded before placing it on a white polystyrene foam tray with a soaking pad (Ultra zap pad, Paper Pak Industries, Washington, GA, USA) and overwrapping with polyvinyl chloride film (PVC; 037242 PUR Value Polyvinylchloride Standard Meat Films, AGL, Richmond Hill, Ontario, Canada.). Once the trays were prepared, 20 trays (10 LL x 10 PM) were placed in the coffin-style retail display cabinets (Model M1, Hussmann) at 3 °C under LED lighting (light-emitting diodes; Acuity Brands Dimmable Rigid 30-LED Light Strip Board HTG S7 - 94v-0 – 4000k) with intensity 1240 lx. After 1 h in the retail display cabinet (d 0), the steaks bloomed, and colour evaluation was carried out by trained panelists and Minolta colorimeter (CR-410, Minolta Canada Inc., Mississauga, ON). The position of the trays was rotated within the retail display cabinet every 24 hours to ensure similar light and temperature exposure for all steaks as well as to avoid biased evaluation by the trained panel (AMSA, 2012). At the last day of retail display, colour and pH measures were taken, and then steaks were removed from the retail display cabinet, vacuum packaged and frozen (-40 °C) for subsequent MDA, HNE and CAR analysis.

3.3.2 pH

The pH was measured using a non-glass probe meat pH meter (HI 99163 Meat pH meter, Hanna instruments, Carrollton, TX; calibrated using two buffers pH 4.0 and 7.0). The measurements were done by inserting the pH meter probe directly into the muscles (Samuel & Trabelsi, 2012). Duplicate measurements per steak were performed at the beginning (d 0) and the end (d 4) of days retail display for each ageing period (7 and 14 d). Results were averaged prior to statistical analysis.

3.3.3 Instrumental colour measurement

The instrumental colour of the steaks was measured using Konica Minolta Chroma Meter (CR-410, Minolta Canada Inc., Mississauga, ON) using illuminant D65 with 2° standard observer angle, and 2.54 cm aperture (Commission Internationale de l'eclairage, 1978). The meter was

calibrated by scanning standard white tile covered with the polyvinyl chloride film (PVC; 037242 PUR Value Polyvinylchloride Standard Meat Films, AGL, Richmond Hill, Ontario, Canada) as the sample readings were taken with the film on the meat. CIE L^* (lightness), a^* (redness) and b^* (yellowness) values were measured at three randomly selected locations on each sample on d 0 and d 4 in the retail display AMSA (2012). The values from the three scans were averaged and used for statistical analysis.

3.3.4 Sensory evaluation of colour

A trained sensory panel was used for assessment of colour and discolouration of the bison steaks. The panel was screened and trained according to the method described in American Meat Science Association meat colour measurement guidelines based on their ability to discriminate colour differences by scoring 50 or less in Farnsworth-Munsell 100-Hue Test. Ten panelists who passed the screening test were selected from the department of Food and Human Nutritional Sciences and the department of Animal Science at University of Manitoba and provided training sessions and mock sensory trials. The sensory colour evaluation of meat surface (muscle colour and discolouration score) was conducted on d 0 (1 h post-bloom) and d 4 of retail display based on the meat colour measurement guidelines set by AMSA (2012). Muscle colour score was evaluated on an 8 point descriptive scale (1 = pale red or pale pinkish red; 2 = slight pale or pale pinkish red; 3 = moderately light red or light pinkish red; 4 = bright red or pinkish red; 5 = slightly dark red or pinkish red; 6 = moderately dark red or dark reddish tan; 7 = dark red or dark reddish tan or brownish; 8 = very dark red or tannish red or brown) and the surface discolouration score was evaluated on a 6 point descriptive scale (surface % MMb; 1 = no discolouration, 0%; 2 = slight discolouration, 1-20%; 3 = small discolouration, 21-40%; 4 = modest discolouration, 41-60%; 5 = moderate discolouration, 61-80%; 6 = extensive discolouration, 81-100%). The average scores obtained from the 10 sensory colour panelists were used for the statistical analysis.

3.3.5 Myoglobin concentration

Myoglobin concentrations of bison meat samples were measured according to the method mentioned by Faustman and Phillips (2001). Five grams of grinded meat samples were weighed in duplicate and placed in 50 ml polypropylene tubes. After that, 45 ml of ice-cold sodium phosphate buffer (pH 6.8, 40 mM) was added to each tube containing 5 g sample (Trout, 1989;

Warris, 1979) and homogenized for 40-45 s at low speed. Sample tubes were then placed in ice at 0-4 °C for 1 h and subsequent centrifugation in a Sorvall RC 6+ centrifuge (Thermo Fisher Scientific, Asheville, NC, USA) in rotor F13-14 x 50cy (FIBERLITE, Thermo Scientific, NC, USA) at 29,000 x g for 30 min at 5 °C. The supernatants were collected by filtration through Whatman grade1 filter paper and absorbances were measured at 525 nm wavelength with an UV/Visible spectrophotometer (Ultrospec 1100 pro, Biochrom Ltd, Cambridge, England) using sodium phosphate buffer as blank. Finally, myoglobin concentration was expressed as milligram of myoglobin per gram of meat (mg/g).

3.3.6 Fat content determination

Samples were analyzed for fat content using acid hydrolysis filter bag technique (ANKOM^{HCl} Hydrolysis System and ANKOMXT15 Extractor; ANKOM Technology, Macedon NY, USA) (Method Am 5-04; AOCS, 2004; Seenger et al., 2008). Minced samples (0.5 g) were placed in a pre-weighed filter bag and closed individually. Bags were placed in the chamber of the ANKOM Hydrolysis Instrument. The samples were then hydrolyzed in 3N HCL for 60 min at 90 °C, and then rinsed for 4-6 times depending on the fat content. After the hydrolysis, the automatic extraction was carried out for 60 min at 60 °C with petroleum ether as an extraction solvent. Lipids were extracted from triplicate samples. After extraction, the samples were dried for 1 h 30 min at 102 °C, cooled in a desiccant pouch to room temperature and weighed. The results were expressed as a percentage of sample weight. The analysis was conducted by Central Testing Laboratory Ltd. (Winnipeg, MB, Canada), which is accredited by the Standard Council of Canada.

3.3.7 Lipid oxidation analyses

3.3.7.1 MDA measurement

Lipid oxidation in the bison meat samples was evaluated by measuring thiobarbituric acid reactive substances (TBARS) using the modified extraction method described by Buege and Aust (1978). Samples were prepared by blending and homogenizing 10 g of meat sample with 30 ml of distilled water for approximately 60 s followed by centrifugation in a Sorvall RC 6+ centrifuge (Thermo Fisher Scientific, Asheville, NC, USA) in rotor F13-14 x 50cy (FIBERLITE, Thermo Scientific, Asheville, NC, USA) at 3000 rpm (1850 x g) for 10 min at 4 °C. 2 ml supernatant was carefully removed from each sample tube and 4 ml TCA/TBA and 100 µL BHA reagent were

added to each tube and mixed well by vortexing. All the tubes were heated in a boiling water bath (100 °C) for 15 minutes, then placed in ice-cold water bath for 10 min and centrifuged again at 1850 x g (3000 rpm; the rotor F14-6 x 250y, FIBERLite, Piramoon Technologies Inc. USA) for 10 min at 4 °C. The optical density of the resulting supernatant was measured using a visible spectrophotometer (GENESYS 30, Thermo Fisher Scientific, MA, USA) at a wavelength of 531 nm. All the samples were analyzed in duplicate and results were averaged prior to statistical analysis. The TBARS values were expressed as milligram of MDA produced per kilogram (mg of MDA/kg) of meat sample (Luqué et al., 2011).

3.3.7.2 HNE determination

HNE content of the meat samples was determined using Bovine 4-hydroxy-2-nonenal ELISA Kit (4-HNE ELISA kit, catalog number: MBS035690; MyBiosource, Inc., CA, USA) following the procedure provided by the manufacturer. 10 g of meat sample was weighed, chopped to small pieces, and mixed well by blender and finally 500 mg of minced meat sample was weighed and homogenized in 5 ml phosphate buffer saline (PBS) for 60 s. The resulting homogenates were centrifuged at 1500 × g (or 5000 rpm; rotor F14-6 x 250y, FIBERLite, Piramoon Technologies Inc. USA) for 15 min at 4 °C and supernatants were carefully collected and assayed immediately using bovine 4-HNE ELISA kit. The final absorbance was measured at 450 nm wavelength by using a multi-plate reader (ELX 800, BioTek Instruments Inc., VT, USA) and the concentration of HNE was expressed as µM per gram (µM/g) of the meat sample.

3.3.8 Protein oxidation

3.3.8.1 Muscle extraction, isolation of myofibrils and protein determination

Muscle extraction and isolation of myofibrils were done according to the protocol described by Martinaud et al. (1997). Ten grams of muscle was homogenized with a blender in 100 ml of a homogenizing buffer containing 150 mM NaCl, 25 mM KCl, 3 mM MgCl₂, 4 mM EDTA, to which 1 mM PMSF protease inhibitor (dissolved in isopropanol) was added just prior to analysis. Homogenate was rendered collagen free by filtration on gauze, followed by stirring in ice for 30 min and centrifugation at 2000 x g (rotor F14-6 x 250y, FIBERLite, Piramoon Technologies Inc. USA) for 15 min at 4 °C. The supernatant was discarded, and the protein pellets were washed twice with 100 ml of a 50 mM KCl and 5 mM mercaptoethanol solution at pH 6.4,

and then with 100 ml of 200 mM sodium phosphate buffer at pH 7.4. Finally, the pellets were resuspended in the same phosphate buffer. The protein concentration of the samples was determined using BCA (Bicinchoninic Acid) protein assay method (BCA protein assay kit, catalog numbers: BCA1 and B9643, Sigma-Aldrich, MO, USA) and adjusted to 1 mg/ml prior to determination of protein carbonyl contents.

3.3.8.2 Determination of protein carbonyl contents

Protein oxidation was measured by assessing total carbonyl contents (CAR) following the 2, 4-dinitrophenylhydrazine (DNPH) method described by Colombo et al. (2016) with slight modification. Two milliliters of protein samples (1.0 mg/ml) were taken and poured into test tube in duplicate and 400 μ L of 10 mM DNPH solution was added to each tube. A blank sample was prepared by adding 400 μ L of 2 N HCl (without DNPH) to 2 ml of protein sample in another test tube. All the samples were vortex-mixed and left in the dark at room temperature for 60 min, with vortex-mixing every 10-15 min. Then 2.4 ml of 20% TCA solution was added to protein samples and incubated on ice for 15 min. The samples were then centrifuged at $10,000 \times g$ (rotor F14-6 x 250y, FIBERLite, Piramoon Technologies Inc. USA) for 5 min at 4 $^{\circ}$ C, and supernatants were discarded. The obtained protein pellets were washed once with 2 ml of 20% TCA and vortex-mixed, and collected pellets by centrifuging at $10,000 \times g$ for 5 min at 4 $^{\circ}$ C. After discarding supernatants, protein pellets were washed again with 2 ml of 1:1 (v/v) ethanol-ethyl acetate and mixed by vortexing well in order to remove any free DNPH. These immediately described two washing steps were repeated at least twice until supernatants were completely transparent. Then all the sample tubes were centrifuged at $10,000 \times g$ for 5 min at 4 $^{\circ}$ C, and pellets were collected after discarding the supernatants. Pellets containing tubes were then allowed to vacuum dry for about 5 min for the complete evaporation of solvent. Finally, pellets were resuspended in 2 ml of 6 M guanidine hydrochloride (dissolved in 50 mM phosphate buffer, pH 2.3) and incubated at 37 $^{\circ}$ C for 15-30 min with vortex mixing. The DNP hydrazones thus formed were quantified as a measure of carbonyl contents by measuring absorbance values at 366 nm by using a spectrophotometer (GENESYS 30, ThermoFisher Scientific, MA, USA). The carbonyl content was calculated by using a molar absorption coefficient of $22,000 \text{ M}^{-1} \text{ cm}^{-1}$ and expressed as nmoles carbonyl/mg protein.

3.3.9 Statistical analysis

Data collected were analyzed using SAS, Version 9.4, SAS Institute INC., Cary, NC (SAS, 2012). The data were analyzed (PROC MIXED) as a 2 x 3 x 2 factorial structure, in a completely randomized design with a split-split plot arrangement. Muscle source (LL and PM) was considered as whole plot, ageing time (0, 7 and 14 d) was served as sub-plot, and display day (d 0 and d 4) was set as a sub-sub plot. Muscle source, ageing, retail display periods and their interactions were analyzed as fixed effects and individual muscle cuts were considered as random effect. The differences among means were detected using the least significant difference (LSD) at 5% level.

In the present study myoglobin (Mb; LL = 6.95 vs PM = 8.12 mg/g) and fat content (LL = 1.55 vs PM = 2.27 %) were significantly different between muscles ($P < 0.05$). Therefore, in order to determine whether colour traits and oxidation compounds differences could be due to Mb and fat content difference rather than to any muscle, ageing time, or retail display time effects, data were submitted to a simple regression test to determine if either Mb or fat content were correlated with colour traits and oxidation compounds; respectively. Thus, Mb or fat content was included as a covariate in the model when a significant correlation with any individual dependent variables was detected. In the data, Mb and fat content were fitted between muscle, ageing and retail display days. The Mb adjusted L^* (Mb-adjusted L^*) and CAR (Mb-adjusted CAR) values, while both Mb and fat content adjusted MDA (Mb/fat-adjusted MDA) values.

Additionally, correlation and regression analyses were performed to identify the influence of the measured chemical attributes on colour. For correlation analysis (PROC CORR), Pearson simple coefficient (r) and Spearman rank coefficient (r_s) were used to determining the relationship of oxidation compounds and pH to the objective and subjective colour attributes. For regression analysis, PROC REG RSQUARE was performed to determine how each oxidation compound interacts or contributed to the redness and subjective colour attributes.

Principal component (PC) analysis was performed on colour traits and biochemical components using PROC FACTOR of SAS (SAS, 2012). Three principal components were retained, and their correlation coefficients were plotted together to evaluate relationships.

3.4 Results

3.4.1 Effects on objective and subjective colour parameters

In terms of objective colour characteristics, both muscles did not differ in Mb-adjusted L^* (data not shown in tabular form; $P = 0.06$; PM = 42.75 vs LL = 40.73) and b^* values (data not shown in tabular form; LL = 6.00 vs PM = 6.30; $P = 0.23$). Muscle x retail display interactions affected a^* ($P < 0.05$); where no differences a^* values were observed at d 0 of retail display period between muscles ($P < 0.05$; **Figure 3.1**); however, at d 4, a^* values decreased in both LL and PM steaks, being more pronounced on PM steaks ($P < 0.05$). Regarding ageing time x retail display interaction (**Figure 3.2**), aged steaks for 7 and 14 d presented similar Mb-adjusted L^* values at d 0 of the retail display ($P > 0.05$); but, at d 4 of retail display, Mb-adjusted L^* values were higher on steaks aged for 7 d (being more bright at the surface) than steaks aged for 14 d ($P < 0.05$). On the other hand, steaks aged for 14 d presented higher a^* and b^* values at d 0 than steaks aged for 7 d ($P < 0.05$); nevertheless, a^* and b^* values decreased and got similar values at d 4 of retail display in both aged steaks ($P > 0.05$).

Muscle x ageing time x retail display interaction affected colour score ($P < 0.05$; **Figure 3.3**). At d 0 of the retail display, LL and PM steaks aged for 7 d were described by trained panelists as “slightly dark red or pinkish-red”; while LL and PM steaks aged for 14 d were “bright red or pinkish” (**Figure 3.3**). It was evident that LL and PM steaks aged for 14 d presented improved colour scores than their less-aged counterparts ($P < 0.05$). However, all aged steaks showed a progressive colour deterioration at d 4 of retail display; but LL steaks aged for 7 d presented the lowest score (“moderately dark red or dark reddish tan”). Discolouration score was affected by the interaction muscle x retail display ($P < 0.05$; **Figure 3.1**); thus, the results previously mentioned were in accordance with the discolouration score given by trained panelist where extensive discolouration area on PM samples was indicated as days of the display were increased (from 0 to > 60 %).

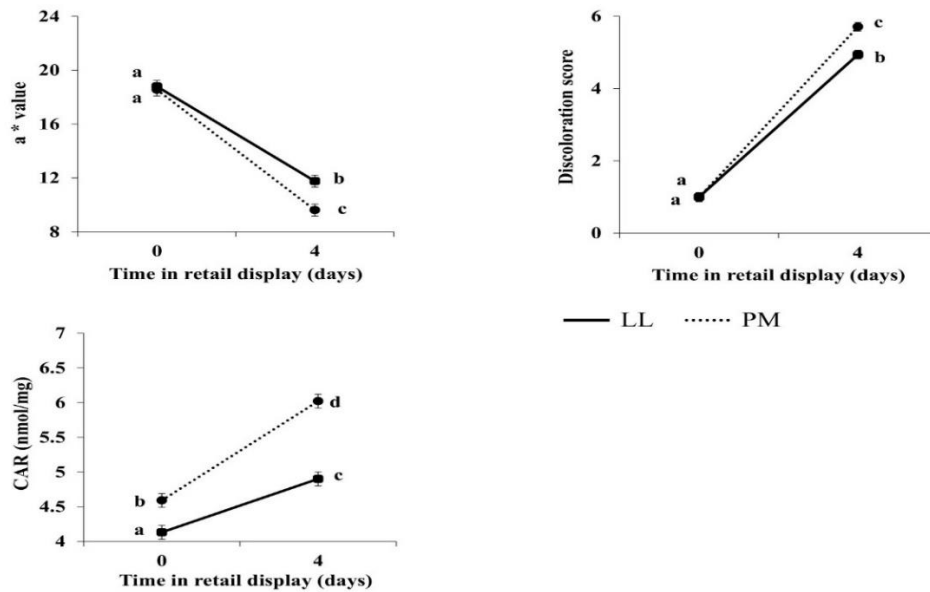


Figure 3.1. Effects of interaction of muscle \times retail display on redness (a^*), discoloration score and on carbonyl content¹.

LL = *longissimus lumborum*, PM = *psaos major*. ¹Adjusted by myoglobin content. CAR = carbonyl contents. Discoloration score: surface discoloration on a scale of 1-6 (1 = none, 0%; 6 = extensive discoloration, 81-100%). ^{a-d}: means with no-common superscript letter differ ($P < 0.05$).

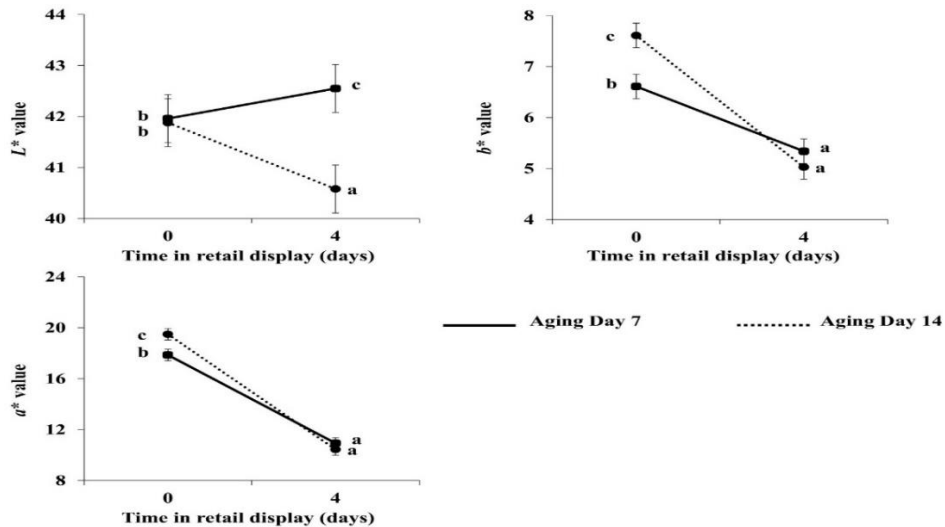


Figure 3.2. Effects of interaction of ageing \times retail display on objective colour evaluation.

L^* = Mb-adjusted lightness; a^* = redness; b^* = yellowness. ^{a-c}: means with no-common superscript letter differ ($P < 0.05$).

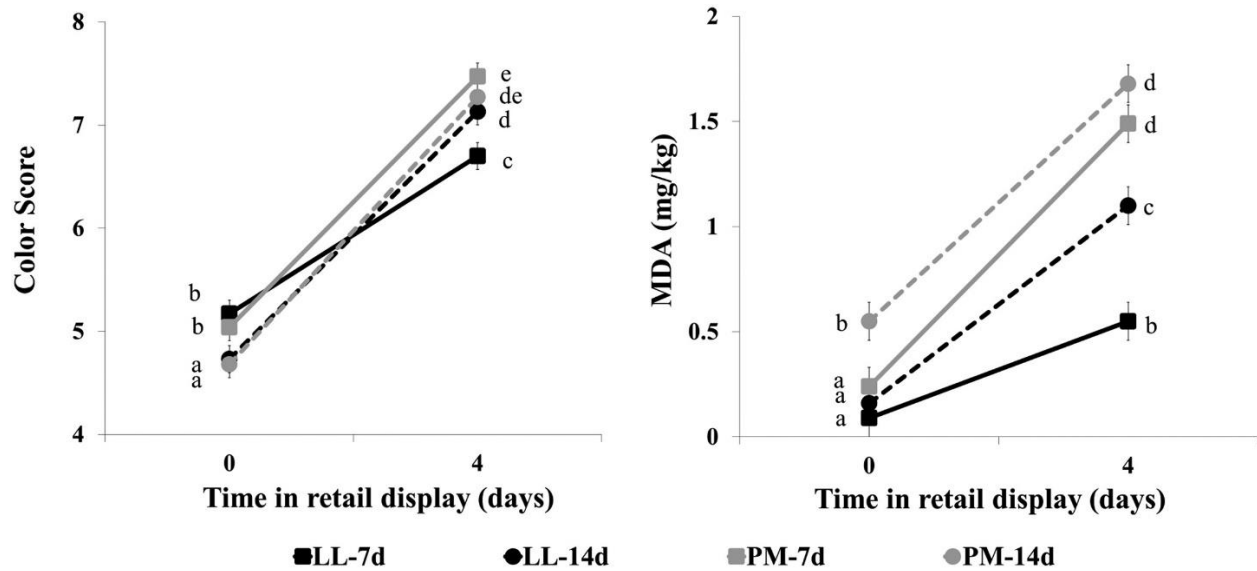


Figure 3.3. Effects of interaction of muscle \times postmortem ageing \times days of retail display on colour score and malondialdehyde¹.

MDA = malondialdehyde. ¹Adjusted by myoglobin and fat content. Colour score: descriptive scale for colour from 1 to 8 (1 = pale red or pale pinkish red; 8 = very dark red or tannish red or brown).
^{a-e}: means with no-common superscript letter differ ($P < 0.05$).

3.4.2 Effects on biochemical parameters

The pH was not affected by muscle type, retail display or interactions ($P > 0.05$); only steaks aged for 14 d were more acidic than steaks aged for 7 d (data not shown in tabular form; d 7 = 5.79 vs d 14 = 5.65; $P < 0.04$). The main effects of muscle type, ageing and retail display time affected HNE content ($P < 0.05$), where higher amount was observed either in PM muscle (data not shown in tabular form; LL = 8.51 vs PM = 9.66 $\mu\text{M/g}$), or steaks aged for 14 d (data not shown in tabular form; 7 d = 8.37 vs 14 d = 9.79 $\mu\text{M/g}$) or at the end of retail display period (data not shown in tabular form; d 0 = 6.88 vs d 4 = 11.29 $\mu\text{M/g}$).

Muscle \times ageing time \times retail display interaction affected Mb/fat-adjusted MDA ($P < 0.02$), where PM steaks aged for 14 d presented the highest Mb/fat-adjusted MDA values at d 0 of the retail display (**Figure 3.3**; $P < 0.05$). In contrast, no differences in Mb/fat-adjusted MDA values were detected between steaks from PM aged for 7 d, and LL aged 7 and 14 d at d 0 of the retail display ($P > 0.05$). The Mb/fat-adjusted MDA values increased in all steaks at d 4 of retail display;

but the MDA values were higher in PM steaks aged for 7 and 14 d ($P < 0.05$), followed by LL steaks aged for 14, and then LL steaks aged for 7 d.

Ageing days affected the CAR content (data not shown in tabular form; $P < 0.01$; 7 d = 4.59 vs 14 d = 5.24 nmol/mg). Also, an interaction was detected, where muscle x retail display affected Mb-adjusted CAR content ($P < 0.05$). In both muscles, the protein oxidation increased significantly at the end of the retail display period (**Figure 3.1**; $P < 0.05$). However, PM steaks showed higher Mb-adjusted CAR values than LL muscles at d 0 and d 4 of retail display ($P < 0.05$).

3.4.3 Correlation and regression between oxidation products and colour evaluation traits

Simple correlation coefficients associating oxidation products with colour evaluation traits in LL and PM steaks are presented in **Table 3.1**. In both muscles, MDA was the biochemical trait showing high correlation to a^* , colour and discolouration scores ($r > -0.7$; $P < 0.01$), and moderate association with b^* ($r = 0.5-0.7$; $P < 0.01$); indicating that greater MDA values would be associated with higher colour deterioration (less red colour and more brown areas). In contrast, HNE and CAR presented moderate association with the variables mentioned previously ($r = 0.5-0.7$; $P < 0.01$); except for b^* which showed low association with them ($r < 0.5$; $P < 0.01$). No correlation was observed between biochemical traits and L^* ($P > 0.05$). The pH was not correlated with colour traits in LL steaks; but had weak correlation with L^* in PM steaks ($P < 0.01$; $r < 0.5$).

For the stepwise regression analysis, the main variable entered into the equation for predicting a^* , colour and discolouration score in LL muscle was MDA with an R^2 of 0.62, 0.68, and 0.66, respectively (**Table 3.2**); while for PM muscle, MDA presented an R^2 of 0.72, 0.75 and 0.78 respectively (**Table 3.3**). The MDA resulted as the main contributor of redness changes in both muscles but explained more in PM ($R^2 > 0.72$) muscle than LL ($R^2 > 0.62$). The pH, HNE and CAR only explained until a maximum 6 % of the variation of those attributes in LL steaks, while contributed by 1% in PM. These results show that MDA (as measured by TBARS assay) could be an important oxidation product responsible for deterioration of the red colour in steaks during refrigerated storage and retail display.

Table 3.1: Correlation between oxidation products and colour evaluation traits from *longissimus lumborum* and *psoas major* steaks.

Parameters	Mb	Fat	pH	MDA	HNE	CAR
<i>Longissimus lumborum</i>						
Lightness	0.04 ns	0.26 ns	0.01 ns	-0.22 ns	0.22 ns	-0.15 ns
Redness	-0.07 ns	0.05 ns	-0.03 ns	-0.78 **	-0.60 **	-0.59 **
Yellowness	-0.07 ns	0.30 ns	-0.01 ns	-0.65 **	-0.42 **	-0.48 **
Colour score	0.02 ns	-0.01 ns	-0.01 ns	0.83 **	0.62 **	0.70 **
Discolouration score	-0.01 ns	0.03 ns	-0.01 ns	0.82 **	0.69 **	0.63 **
<i>Psoas major</i>						
Lightness	0.01 ns	-0.36 *	0.49 **	-0.17 ns	-0.17 ns	-0.04 ns
Redness	-0.04 ns	-0.06 ns	0.06 ns	-0.85 **	-0.69 **	-0.69 **
Yellowness	-0.15 ns	0.02 ns	0.24 ns	-0.53 **	-0.48 **	-0.39 **
Colour score	-0.01 ns	0.12 ns	0.01 ns	0.86 **	0.71 **	0.68 **
Discolouration score	-0.01 ns	0.05 ns	0.08 ns	0.89 **	0.74 **	0.74 **

Mb = myoglobin; MDA = malondialdehyde; HNE = 4-hydroxy-2-nonenal; CAR = carbonyl content. ns = no significant, $P > 0.05$; * = $P < 0.05$; ** = $P < 0.01$.

Table 3.2. Regression analysis for predicting colour traits with oxidation products for *longissimus lumborum* steaks.

Equation	R ²	Cp	Intercept	MDA	pH	Fat	CAR	HNE
<i>Redness</i>								
1	0.62	6.40	18.60	-6.98	-	-	-	-
2	0.67	2.00	50.32	-7.53	-5.52	-	-	-
3	0.71	2.18	54.37	-7.78	-6.45	0.91	-	-
3	0.68	3.00	52.60	-6.81	-5.32	-	-0.81	-
4	0.68	5.00	52.65	-6.85	-5.33	-	-0.83	0.01
<i>Colour score</i>								
1	0.68	5.75	5.03	1.89	-	-	-	-
2	0.73	1.79	-2.16	2.02	1.25	-	-	-
3	0.79	2.30	-3.49	2.10	1.56	-0.30	-	-

3	0.74	3.00	-2.63	1.87	1.21		0.17	-
4	0.74	5.00	-2.64	1.88	1.21		0.18	0.01
Discolouration score								
1	0.66	7.30	1.23	3.66	-		-	-
2	0.71	4.34	-11.70	3.88	2.25	-	-	-
3	0.72	3.98	-13.31	3.37	2.11	-	0.58	-
4	0.73	5.00	-12.77	3.04	2.00		0.46	0.09

R² (R-squared) is coefficient of determination. MDA = malondialdehyde; CAR = carbonyl contents; HNE = 4-hydroxy-2-nonenal.

Table 3.3. Regression analysis for predicting colour traits with oxidation products for *psoas major* steaks. (No other variable met the 0.1500 significance level for entry into the model).

Equation	R ²	Cp	Intercept	MDA	CAR	pH	HNE
Redness							
1	0.72	-1.34	19.86	-6.94	-	-	-
2	0.73	1.11	23.27	-5.12	-0.80	-	-
3	0.73	3.06	19.65	-5.16	-0.76	0.60	-
4	0.73	5.00	19.47	-5.01	-0.72	0.66	-0.05
Colour score							
1	0.75	-0.79	4.50	1.66	-	-	-
2	0.75	1.42	3.87	1.51	0.15	-	-
3	0.76	3.12	1.71	1.78	0.17	0.36	-
4	0.76	5.00	1.77	1.45	0.16	0.34	0.02
Discolouration score							
1	0.78	6.48	0.26	3.13	-	-	-
2	0.81	4.29	-1.99	3.58	0.53	-	-
3	0.83	2.70	-13.75	2.45	0.66	0.66	-
4	0.83	5.00	-13.56	2.30	1.89	0.61	0.05

R² (R-squared) is the coefficient of determination. MDA = malondialdehyde; CAR = carbonyl content; HNE = 4-hydroxy-2-nonenal.

3.4.4 Principal component analysis

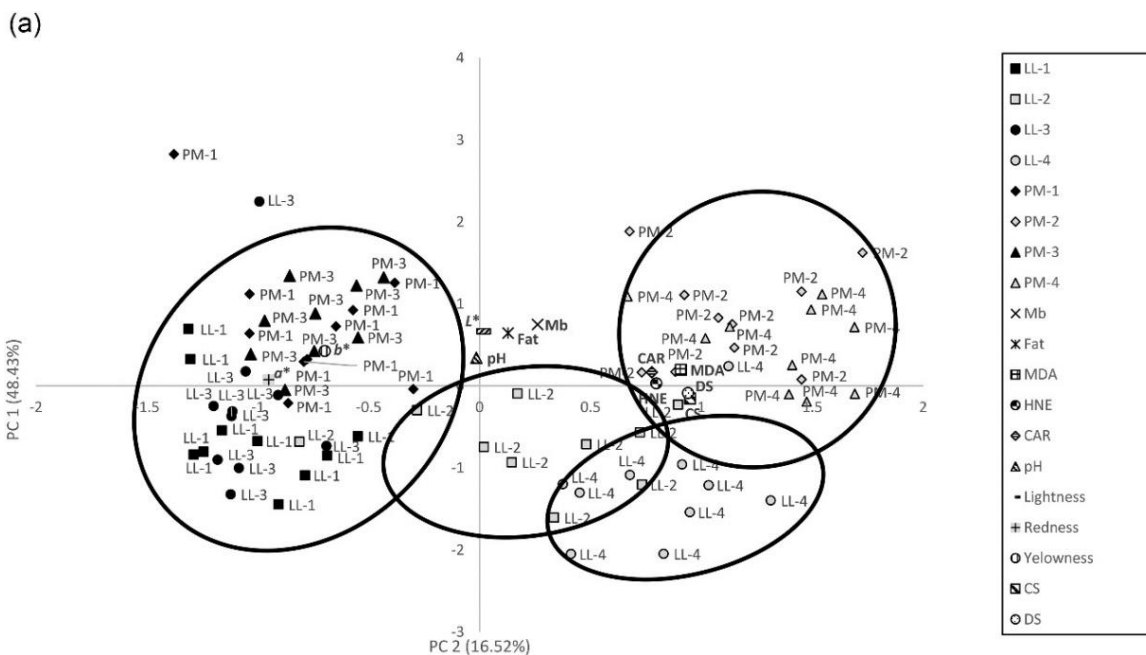
The factor analysis showed that the first three principal components (PC) with eigenvalues greater than 1.0 explained 74.85% of the standardized variance (PC1 explained 48.43%, PC2 16.52% and PC3 9.90%). The set of variables for the first PC included mainly MDA, HNE, CAR, a^* , b^* , and colour and discolouration scores (based on the largest loading values; **Table 3.4**), the PC2 was related to Mb, fat, pH, L^* and b^* ; while PC3 included fat, pH and L^* . Plotting PC1 x PC2 (**Figure 3.4a**) showed clear segregation between steaks displayed d 0 and d 4 (regardless of the muscle and ageing time); where PM and LL steaks aged for 7 and 14 d at d 0 of retail display were closely associated with redness and yellowness traits, and located far away of oxidation compounds and scores, indicating more red colour stability and less oxidation. In contrast, steaks at d 4 of the retail display were closely associated with oxidation compounds and scores. Noticeably, three distinct groups within steaks displayed at d 4 were identified according to the muscle and ageing time. The first group was represented by PM steaks aged for 7 and 14 d with more oxidation compounds and high scores (representing high oxidation level and less red colour). The second (close to the central axis) and third group (negative side of PC2) of steaks displayed at d 4 were represented by LL steaks aged for 7 and 14 d, respectively, showing different levels of colour deterioration based on ageing period. Plotting PC1 x PC3 (**Figure 3.4b**), PM steaks aged for 14 d and displayed at d 4, which were located previously in the positive side of the first plotting (PC1 x PC2) along with PM steaks aged for 7 d and displayed at d 4, were segregated to the negative side PC2 creating a fourth distinct group.

Table 3.4. Principal component loadings (74.85%).

Variables	PC1	PC2	PC3
Eigenvalue	5.327	1.817	1.089
Proportion	48.430	16.520	9.900
Mb	0.262	0.748	-0.175
Fat	0.129	0.643	-0.423
MDA	0.908	0.195	-0.149
HNE	0.797	0.031	-0.124
CAR	0.777	0.167	-0.105
pH	-0.014	0.342	0.778

L*	-0.012	0.664	0.408
a*	-0.095	0.075	-0.145
b*	-0.698	0.426	-0.106
CS	0.950	-0.154	0.106
DS	0.940	-0.088	0.126

Mb = total myoglobin; MDA = malondialdehyde; HNE = 4-hydroxy-2-nonenal, CAR = carbonyl contents; L^* = lightness; a^* = redness; b^* = yellowness; CS = colour score; DS = discolouration score. PC1, 2, 3 = principal component 1, 2 and 3 respectively.



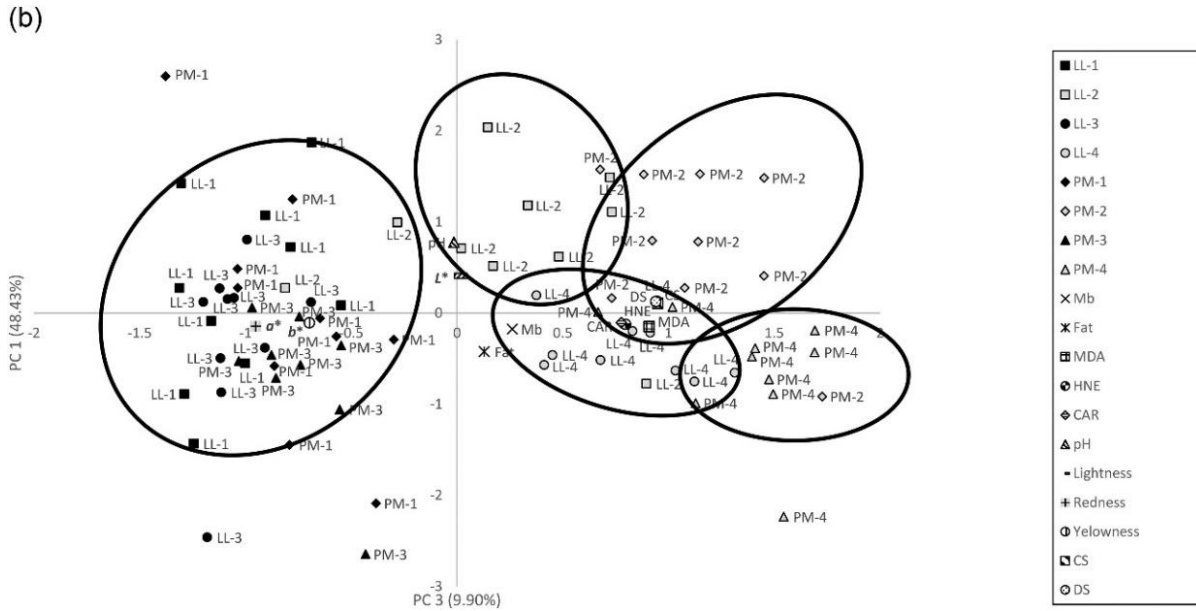


Figure 3.4. (a) Plotting principal component (PC1 × PC2) analysis for bison muscles under ageing and retail display conditions. (b) Plotting principal component (PC1 × PC3) analysis for bison muscles under ageing and retail display conditions.

LL = *longissimus lumborum*, PM = *psaos major*. LL-1 = LL-7D-0D; LL-2 = LL-7D-4D; LL-3 = LL-14D-0D; LL-4 = LL-14D-4D; PM-1 = PM-7D-0D; PM-2 = PM-7D-4D; PM-3 = PM-14D-0D; PM-4 = PM-14D-4D. 7D = 7-day ageing period, 14D = 14-day ageing period; 0D = retail display day 0, 4D = retail display day 4.

Mb = myoglobin; MDA = malondialdehyde; HNE = 4-hydroxy-2-nonenal; CAR = carbonyl contents. L^* = lightness, a^* = redness, b^* = yellowness; CS = colour score, DS = discolouration score.

3.5 Discussion

3.5.1 Objective and subjective colour evaluation

In the current study, lightness (L^*) and yellowness (b^*) values were not affected by muscle type, which is in agreement with previous studies reported in beef (Hwang et al., 2010; Joseph et al., 2012; Nair et al., 2018). Also in a^* values (redness), similar pattern has been reported in beef muscles by several authors (Canto et al., 2016; Kim et al., 2009; Mancini et al., 2009; Mancini et al., 2018; McKenna et al., 2005; Nair et al., 2018; Suman et al., 2004; Suman et al., 2009), where

LL maintained a redder (highest a^* value) surface colour than PM at the end of the retail display or dark storage.

Ageing time has been shown to reduce the ability to bloom and subsequent colour stability of meat (Robertson et al., 2007). In the present study, LL and PM steaks aged for 14 d presented improved red colour than LL and PM steaks aged for 7 d at d 0 of the retail display, but 14 d aged steaks showed an evident colour deterioration at d 4 of the retail display along with high discolouration score than counterparts; being more colour stable LL steaks aged for 7 d. Aged steaks for 15 or more days have shown an improved red colour on blooming compared with no-aged or < 15 d of ageing steaks, but it was not maintained during the subsequent retail display (Lindahl, 2011; O’Keeffe & Hood, 1981). The development of a normal cherry-red colour in meat depends on oxygen availability, oxygen diffusion into the meat and oxygen consumption rate (OCR), with this last factor decreasing as vacuum packaging time increases. Blooms occur more rapidly (Ledward, 1992), because increased penetration of oxygen creates a deeper layer of oxymyoglobin providing a redder and more desirable colour (MacDougall, 1972).

As in beef, differences between bison LL and PM muscles may be due to the differences in muscle fibre type. Beef PM muscles contain a high amount of type I fibre and oxidative metabolism than in LL muscles, which are mainly glycolytic in nature (Hwang et al., 2010; Seyfert et al., 2006; Totland & Kryvi, 1991) due to the high concentration of mitochondria and myoglobin (Hwang et al., 2010; Jeong et al., 2009; King et al., 2010; King et al., 2011; Mohan et al., 2010). This is ultimately responsible for the greater accumulation of metmyoglobin and surface discolouration in PM muscles (Jeong et al., 2009; Joseph et al., 2012; Seyfert et al., 2006). Overall, in the current study, bison LL and PM muscles can be classified based on their colour stability as beef (McKenna et al., 2005), where LL is considered a colour-stable muscle, and PM as an unstable colour muscle.

3.5.2 Biochemical parameters

The pH was not affected by bison muscle type ($P > 0.05$). In beef, the results have been inconsistent. Canto et al. (2016) and Joseph et al. (2012) indicated higher pH in PM muscles compared to LL counterparts at 14 d of ageing. In contrast, Hwang et al. (2010) found greater pH for LL than PM muscles, which is also in disagreement with our results. The main effect on pH

was due to ageing time. This is due to the changes in postmortem metabolism and accumulation of lactic acid during storage (Lawrie & Ledward, 2006; Neethling et al., 2017).

Regardless of different storage or retail display conditions, many researchers (Hwang et al., 2010; Jeong et al., 2009; Joseph et al., 2012; McKenna et al., 2005; O’Keeffe & Hood, 1982; Renerre & Labas, 1987; Seyfert et al., 2006) have documented that PM muscles presented greater MDA amount (TBARS) than LL muscles, which induce myoglobin oxidation and resulting on surface discolouration (Faustman et al., 2010; O’Grady et al., 2001; Suman et al., 2007). These reports were in agreement with our results. At the same time, it is well-documented increased storage or retail display time led to an increase in MDA content (Legako et al., 2018; Mancini et al., 2018; Wang et al., 2018; Wang et al., 2021).

In addition, in our study PM muscles presented greater HNE content than LL muscles. Bison meat presents higher PUFA content could mean greater vulnerability to oxidation (Pietrasik et al., 2006); particularly in PM muscle, and generate reactive secondary oxidation products such as HNE (α , β -unsaturated aldehydes), which can accelerate Mb oxidation and subsequent meat discolouration (Alderton et al., 2003; Joseph et al., 2010; Lee et al., 2003; Schneider et al., 2001; Suman et al., 2006). The HNE decreases both electron transport-mediated MMb reduction and NADH-dependent MMb reductase activity (Ramanathan et al., 2014). In addition to covalent binding of HNE to Mb, the effect of HNE on colour stability also can be partially attributed to interactions between HNE and mitochondria (Ramanathan et al., 2012). In vitro studies, where oxymyoglobin was incubated with HNE, have been demonstrated that MMb formation was greater in the presence of HNE than controls (Alderton et al., 2003; Ramanathan et al., 2012; Suman et al., 2006; Zanardi et al., 2002). However, our present study detected HNE concentrations directly in fresh bison samples by using ELISA. Also, in the current study, ageing and retail display time increase HNE content. These results were supported by Sakai et al. (1998) who reported an increase in HNE levels in pork samples after 7 d of storage at 0 °C.

In our study, the protein oxidation (CAR) increased during the retail display period and it was more evident on PM steaks. In agreement, Estévez et al. (2011) reported a higher concentration of protein oxidation products in PM muscles from fresh pork compared to LL muscles. The PM muscle is higher in lipid, myoglobin, and possess oxidative metabolism which makes the muscle very vulnerable to protein oxidation (deamination of threonine, lysine, proline and arginine) and

forms protein carbonyl products (Estévez et al., 2011). Also, storage time can lead to an increase in CAR content (Cho et al., 2015; Popova et al., 2009). The development of lipid and protein oxidation during refrigerated storage of beef and lamb is associated with the breakdown of the heme molecule and the subsequent release of free (non-heme) iron from the porphyrin ring which might also increase oxidative instability of the meat system (Estévez et al., 2006; Estévez & Cava, 2004).

3.5.3 Relationship between oxidation products and colour evaluation traits

Not all studies have been able to demonstrate the link between lipid oxidation and myoglobin oxidation in meat. These two processes depend on the species, animal age, diet and postmortem interventions (e.g., antioxidant additives), but the oxidation of those components is strongly related to the concentration of oxygen present in the meat (Faustman et al., 2010). However, several researchers have indicated lipid oxidation products such as α - and β -aldehydes decrease oxymyoglobin redox stability (Alderton et al., 2003; Faustman et al., 1999; Lee et al., 2003; Lynch & Faustman, 2000; Mancini & Hunt, 2005; Ramanathan et al., 2020). A study has suggested that HNE content in beef and pork might be an important index of food quality (Sakai et al., 1995). However, from a colour perspective, the current study demonstrated that lipid oxidation products were correlated to the colour stability of both bison muscles; but their impact on meat colour was not equally, where MDA resulted in the main contributor of redness changes in both muscles. Thus, HNE cannot be considered a reliable marker as a predictor of bison meat colour stability.

On the other hand, few studies have evaluated the effect of protein oxidation in muscle food, although it has been reported that such oxidative damage leads to alterations in functional properties of protein such as gelation, emulsification, viscosity, solubility and hydration (Wang et al., 1997; Wang & Xiong, 1998). Estévez et al. (2006) and Estévez & Cava (2004) suggested protein oxidation is associated with the breakdown of the heme molecule and the subsequent release of free (non-heme) iron from the porphyrin ring but it seemed not to be directly related to processed meat discolouration. Based on author's knowledge, this link has not been established on fresh meat previously.

Finally, each muscle showed different levels of colour deterioration based on the ageing period at 4 d of the retail display. Furthermore, LL is a colour-stable muscle due to the lower level

of protein and lipid oxidation products developed during storage and retail displays compared to PM muscle.

3.6 Conclusions

In bison muscle, MDA (as measured by TBARS assay) seemed to have remarkable importance in the colour deterioration than HNE and CAR, particularly in bison PM muscle. The relationships between colour stability and oxidation compounds produce distinctive muscle-specific pattern of colour deterioration in bison muscles; where LL is a colour-stable muscle due to the lower level of protein and lipid oxidation products developed during storage and retail displays compared to PM muscle.

The implications of this research on the bison meat industry can be summarized as - (i) consider MDA as a convenient biomarker for lipid peroxidation in meat product, (ii) facilitate the development of different muscle specific strategies and packaging technologies, (iii) expand the fresh bison meat marketing (national and international level) without fear of retail loss due to retail colour instability (early browning), and (iv) offer a more consistent, acceptable and desirable product (in colour) to consumers.

To achieve the second goal of the current thesis work, experimental work was carried out to investigate the potential application of NIRS for the segregation of bison LL and PM muscles based on muscle types, ageing and retail display times with their inherent colour stability, and the results are provided in the next chapter.

CHAPTER 4: MANUSCRIPT NO. 2

Application of Vis-NIR and SWIR spectroscopy for the segregation of bison muscles based on their colour stability

This chapter was prepared as a manuscript, formatted, and submitted as per the guidelines of *Meat Science* journal and has been published as: Hasan, M. M., Chaudhry, M. M. A., Erkinbaev, C., Paliwal, J., Suman, S. P., & Rodas-Gonzalez, A. (2022). *Meat Science*, 188: 108774. <https://doi.org/10.1016/j.meatsci.2022.108774>

4.1 Abstract

The study objective was to examine the potential for using visible-near infrared (Vis-NIR) and short-wave infrared (SWIR) spectroscopy to segregate bison portions based on muscle types and storage periods. In the Vis-NIR range, principal component analysis showed clear segregation of the muscles based on storage at retail display d 4 whereas discrimination based on muscle type was better portrayed in the SWIR region. Furthermore, partial least squares discriminant analysis (PLS-DA) models classified muscles based on muscle type and storage in the Vis-NIR range with the classification accuracy of 97% for calibration and 86% for cross-validation. Finally, PLS-regression models were developed for the successful prediction of a^* value with an R^2 of 0.88 (RMSEC: 1.57), 0.84 (RMSECV: 1.88), and 0.90 (RMSEP: 1.41), colour score with an R^2 of 0.96 (0.25), 0.95 (0.27), and 0.92 (0.32), and discolouration score with an R^2 of 0.96 (0.47), 0.93 (0.63), and 0.93 (0.56) for calibration, cross-validation, and prediction, respectively. Therefore, NIRS was successful for the classification of muscles based on muscle type, retail display and ageing periods, as well as the prediction of a^* value, colour and, discolouration score.

Keywords: meat colour, visible near infrared, short wave infrared, principal component analysis, classification, partial least squares discriminant analysis.

4.2 Introduction

Bison (*Bison bison*) is a North American native species, which is raised commercially for meat and meat products (Galbraith et al., 2016). Bison meat is marketed most of them as frozen products due to its faster colour deterioration under aerobic packaged retail conditions (Hasan et al., 2021; Narváez-Bravo et al., 2017; Pietrasik et al., 2006), which limits its expansion in the retail market

(Sood et al., 2020) and put it in disadvantage before other meat commodities that are sold fresh (i.e., pork, beef, lamb, and ground beef). In this sense, excessive inherent variation in colour stability and shelf life of bison meat makes it difficult to provide a consistent and stable product at the retail level to attract consumers' eyes.

Muscle colour stability is determined by the particular anatomical locations as well as the physiological roles of muscles, resulting in variations on postmortem biochemistry and colour stability among and within each muscle (King et al., 2011; Suman et al., 2014). Thus, assorting meat portions based on colour stability would make it possible to designate muscle-specific technology or management (e.g., nitrite film packaging) to mitigate colour deterioration and supply bison meat with desirable and stable colour, but it could be a challenge at purveyors, and retail levels apply a rapid and reliable sorting technique. In this context, it is necessary to explore a contactless and fast evaluation to sort the meat portion on a large scale at those processing and packaging facilities. Therefore, near-infrared (NIR) spectroscopy (NIRS) could be an alternative.

Colorimeters are used to assess the colour of fresh meat or trained panelists are used in laboratory environments for small-scale investigation and are time-consuming, being not feasible to be applied on the industrial scale for sorting meat portions (Pathare et al., 2013). Colorimeters are contact-based methods and provide limited information of non-uniform surfaces (averaging three points of reading on the sample without taking into account the entire area) particularly if the viewing port is small (Balaban, 2008). On the other hand, trained panelists require a proper panelist selection and training in order to minimize human error (AMSA, 2012; Hasan et al., 2021; Hutchings, 1994). Consequently, NIRS eliminates many restrictions of those methods by mapping each pixel of the whole view area providing spatial information and colour attributes distribution on the entire surface area (Brosnan & Sun, 2004; Chaudhry et al., 2021; Du & Sun, 2004). Moreover, NIRS is a rapid, objective and non-destructive technique that can be performed without reagent requirements and minimal sample preparation, which provides cost-effective and valuable qualitative and quantitative information of a scanned sample tissue (Downey & Hildrum, 2004; Prieto et al., 2009; Prieto et al., 2017).

The NIRS has been implemented successfully for the prediction of muscle composition including chemical and colour attributes (Prieto et al., 2011; 2014; Damez & Clerjon, 2008; Hildrum et al., 1994; Prieto et al., 2008). Thus, NIR spectral features possess the potential to

segregate meat muscles and predict ageing periods based on colour changes (Moran et al., 2018). Recently, Chaudhry et al. (2021) used the NIR hyperspectral imaging (HSI) pixel-based approach for the discrimination of bison *longissimus lumborum* (LL) and *psoas major* (PM) muscles at different ageing and retail display times. In that study, spectral information from selected pixels of few NIR hyperspectral images was used to build the models. Even though the method was accurate, it was considered an exploratory technique that could only be used in a lab setup as a proof of concept. The technique has a slow acquisition rate, is very expensive (requires a fast computer, sensitive detector, large data storage, and complex data analysis), and is not suitable for commercial applications where high throughput is required (Manley, 2014). In consequence, apply spectra-based classification and prediction models could be conveniently implemented in the industry by further translating these results into development of micro-NIR instruments and other hand-held devices, which can be easily interpreted by personnel that are not experts in spectroscopy; moreover, they are cheaper as compared to hyperspectral imaging systems (Patel, Toledo-Alvarado, & Bittante, 2021; Savoia et al., 2020). Consequently, the NIR spectral based analysis could have potential and be utilized in the meat industry as a user-friendly, economically viable, and reliable technique. Therefore, it was hypothesized that NIRS predicts colour parameters, and segregate stable vs. unstable colour bison muscles. In this context, the objective of this research work was to test the potential of visible near-infrared (Vis-NIR) and short wave infrared (SWIR) spectroscopy for segregating bison portions, based on muscle type (LL and PM), aging and retail display periods, as well as to predict both instrumental and sensory color parameters. The study was conducted on muscle portions supplied by the studies reported by Hasan et al. (2021).

4.3 Material and methods

4.3.1 Sample collection and processing

For the experiment, two major bison muscles LL and PM were chosen as two most suitable candidates for investigating the colour stability-based discrimination of bison portions. Those bison muscles were differentiated as colour-stable and colour-labile, respectively, based on meat colour parameters, lipid and protein oxidation products (Hasan et al., 2021). The details of sample collection and processing during the experiment were described in a previous article by Chaudhry et al. (2021) and Hasan et al. (2021). Ten LL (striploin) and ten PM (tenderloin) muscles from

bison A1 grade (Canada Gazette, 1992) carcasses were collected within 48 h postmortem from a government-inspected slaughter plant and transported to the Food Science Pilot plant of the University of Manitoba (Winnipeg, MB, Canada). Upon arrival at the pilot plant, 4 cm² of muscle samples were aseptically separated from two muscle types for the acquisition of a first scan at 2 d postmortem from both Vis-NIR and SWIR regions of the spectra. After dividing the remaining LL and PM muscles into two equal parts, each portion was immediately vacuum packaged, and randomly assigned for 7 and 14 d (day) of postmortem ageing period at 2 °C.

After the fulfillment of each ageing period and immediately after removing the muscle portions from the previously packaged condition, again a 4 cm² of sample was taken from each muscle for the spectral acquisition after blooming for 30 min at 2 °C, considered as retail display d 0. Each sample was obtained aseptically by working with a sterilized cutting board and knife without any touch on the freshly cut muscle surface in order to colour evaluation (AMSA, 2012). After the acquisition of scans, muscle samples were overwrapped with polyvinyl chloride (PVC) films (PVC Standard Meat Films, AGL, Richmond Hill, Ontario, Canada) immediately after placing those individually over a soaking pad on a polystyrene foam tray (White, Paper Pak Industries, Washington, GA, USA). Once prepared, the sample containing trays were then placed in a retail display cabinet (Coffin-style, Model M1, Hussmann) at 3 °C under the light-emitting diodes (LED) lighting (Fixed 30-LED Light Strip Board HTG S7 - 94v-0 – 4000k, 1240 lx intensity). After 60 min blooming of muscle samples in the retail display cabinet (d 0), the instrumental [L^* (lightness), a^* (redness) and b^* (yellowness)] and sensory (muscle colour and discolouration score) colour evaluations were performed by using Minolta colorimeter CR-410 (Minolta Canada Inc., Mississauga, ON) and the trained sensory panelists, respectively (AMSA, 2012). The trays in the display cabinet were rotated every 24 h to equalize exposure to light and temperature for all experimental samples and to minimize bias in the evaluations by the trained sensory colour panelists or colorimeter. Evaluations of both sensory and instrumental colour were conducted at d 0 (beginning) and at d 4 (end) of the 5 day period on retail display. Followed by the evaluation of colour parameters at d 4 of the period on retail display, the muscle samples were taken out from the display cabinet and scans were acquired again (d 4).

4.3.2 Vis-NIR and SWIR spectral collection

Bison muscle samples from three different ageing periods (2 d, 7 d and 14 d) and two different retail display periods (d 0 and d 4) were scanned using a bench top HSI system at two wavelengths ranges. One of which covered the 400-1000 nm known as Vis-NIR whereas other range covered 1000-2500 nm region known as SWIR by following the methods mentioned by Erkinbaev et al. (2017).

This first system for HSI acquisition was carried out by using a Vis-NIR line scan sensor (400-1000 nm) from SPECIM (Spectral Imaging Ltd., Oulu, Finland). A charge coupled device camera with a spatial resolution of 1024 x 896 pixels, a V10E spectrograph (SPECIM, 397.66–1003.81 nm, spectral resolution of 2.6 nm), and a focusing lens (OLET 15) were equipped with this imaging system. Moreover, two 150 W 3900-ER tungsten lamps (Illumination Technology Inc., USA) were positioned at 45° to the sample stage in the illumination unit. On the other hand, the SWIR HSI acquisition system was equipped with a camera and a mercury-cadmium-tellurium detector combined with N25E spectrograph (SPECIM Spectral Imaging Ltd., Oulu, Finland) and focusing lens (OLES30) from the same company and possessed a spatial resolution of 384×288 pixels. The imaging unit consisted of a translation stage with sample tray, a lighting setup similar to the Vis-NIR system, and a desktop computer (Tower 3620, Dell, Round Rock, TX) with Lumo software for the acquisition of HSIs and motor control.

4.3.3 Acquisition and correction of images

Prior to the image acquisition, the spectral imaging systems were switched on for 30 min to reach stability in both temporal and thermal (Erkinbaev et al., 2017; Babellahi et al., 2020). The exposure time was 20 ms and the frame rate used was 20 frames per second (fps). The sample stage speed of 7 mm/s was utilized to obtain the optimal aspect ratio for the given frame rate and exposure period (Erkinbaev et al., 2019). Black and white reference image acquisitions were performed in addition to raw HSIs of bison muscle samples. The camera shutter was fully closed and an image for acquired as black reference where for acquiring the white reference image, reference standard with a 99% Spectralon (Labsphere, North Sutton, NH) was used. Image colour correction was done using the following equation:

$$\text{Corrected HSI} = \frac{\text{Raw HSI} - \text{Black reference image}}{\text{White reference image} - \text{Black reference image}}$$

4.3.4 Segmentation of images, spectral data extraction and preprocessing

Image segmentation was done using the Otsu method, during the process, binary images were developed where the pixels of the background were set to zero and only nonzero elements were used for the extraction of the bison muscle sample pixels. For each image, the spectra of the pixels of the bison muscle sample were averaged to develop a representative spectrum.

For the spectral extraction purposes, two binary masks were developed for each image, the first one for the removal of saturated pixels and the second mask for the removal of background hence segregating the pixels of the bison muscle sample. In case of the Vis-NIR region, images at 460 nm were used for the saturated pixel removal while images at 715 nm were used for the segregation of pixels of interest from the background. In the SWIR region, the saturated part of the image was removed by creating a mask at 1174 nm whereas the most contrast between the pixels of bison muscle sample and their background was attained at 2073 nm. The regions with the lowest signal-to-noise ratio were eliminated. The two binary masks were generated, and merged into one using a logical AND operator, resulting in the removal of background and saturated pixels, hence only providing the muscle sample pixels. In the case of Vis-NIR HSIs, this final binary image was applied to all 224 waveband images, whereas in the case of SWIR HSIs, it was applied to all 288 waveband images.

The spectral data extracted from each sample was organized in an excel file for further processing. The image segmentation and spectral data extraction was done by using MATLAB software (version R2020a, MathWorks Inc., Natick, MA, USA). The spectral profiles were preprocessed using various preprocessing methods individually as well in combination with each other. The most common preprocessing techniques used were mean centering, in combination of first derivative with mean centering, and combined second derivative and mean centering using MATLAB (version R2020a, MathWorks Inc., Natick, MA, USA).

4.3.5 Measurement of colour parameters and sensory evaluation

The details of objective and subjective colour evaluation were described by Chaudhry et al. (2021) and Hasan et al. (2021). On retail display d 0 and d 4, the colour was measured by using

a Minolta colorimeter (Chroma Meter CR-410, Konica Minolta, Inc., Japan), calibrated each daily by scanning a standard white tile. CIE L^* (lightness), a^* (redness) and b^* (yellowness) values were measured (illuminant D65, diameter aperture A 2.54, 2° standard observer) through the PVC package film at three randomly selected locations on each sample (AMSA, 2012). Furthermore, the three values from random scans were then averaged and subsequently utilized for the statistical analysis.

Ten panelists were selected for sensory colour evaluation from student of the University of Manitoba Food Sciences and Animal Science Department. The selection process of colour panelists was based on the screen results obtained from Farnsworth-Munsell 100 Hue Test. Group training sessions for the evaluation of bison muscle sample colour were arranged for the selected sensory panelists according to the AMSA meat colour guidelines (AMSA, 2012). Sensory colour (muscle colour and discolouration score) of surface of the bison muscle samples was recorded on d 0 and d 4 of the retail display period (AMSA, 2012). For the muscle colour score, a scale of 1 to 8 was established with score 1 being pale red and pale pinkish red while score 8 representing bison muscle samples that is very dark red in colour or tannish red or brown. For the evaluation of colour and discolouration scores, a scale of 1 to 6 was set where score 1 was allocated to the bison muscle samples with 0% discolouration (no discolouration) while score 6 was allocated to the muscle samples with 81-100% discolouration (extensive discolouration). The averaged data from the scores recorded by ten panelists were used for further analysis.

4.3.6 Statistical analysis

Principal component analysis (PCA) was conducted as an unsupervised classification method for the discrimination of bison muscle samples based on muscle type and storage time. Initially, PCA was performed for visualizing the spectral data by using the PCA toolbox (Ballabio, 2015) in MATLAB (version R2020a, MathWorks Inc., Natick, MA, USA). The main purpose was to investigate the spectral features of experimental bison muscle samples and to examine for possible groups based on spectral data from two different bison muscle types, ageing periods (2 d, 7 d and 14 d) and retail display time (d 0 and d 4). The spectral data obtained from the Vis-NIR and SWIR regions were mean centered prior to the application of PCA.

Prior to the application of supervised classification, the spectral datasets in the Vis-NIR and SWIR ranges were divided into calibration and prediction/external validation sets using

supervised method known as Kennard-stone algorithm. The calibration dataset comprised on 70 samples while the prediction/external validation set contained 30 samples both in the case of Vis-NIR and SWIR datasets. After the splitting of the spectral datasets into calibration and external validation sets, the partial least squares discriminant analysis (PLS-DA) method was applied for developing calibration models to discriminate the different classes of bison muscle on the basis of muscle type, ageing and retail display periods and this method is a commonly used chemometric technique for the classification of spectra obtained from NIRS. PLS-DA is used widely for the classification of hyperspectral data (Chevallier et al., 2006), and both the response and dependent variables are categorical (Barker & Rayens, 2003). Furthermore, a target matrix (Y) was developed and a PLS model was constructed between the spectral data matrix (X) and the target matrix (Y) to generate a group of predicted class memberships and finally prediction values resulted from PLS analysis were used for comparing with the original class membership. For the development of every calibration model, contiguous block cross-validation with 7 data splits was used. The sensitivity and specificity values from various classes were used to evaluate the performance of PLS-DA models. The capacity of a PLS-DA model to accurately categorize muscle samples associated with a particular class is referred to as sensitivity, whereas specificity refers to the misclassification of samples from other classes into the class in consideration.

For the prediction of instrumental (L^* , a^* and b^*) and sensory (colour and discolouration score) colour parameters, PLSR modeling approach was implemented for the Vis-NIR spectral profiles using the PLS toolbox. The principle of PLSR relies on the finding of the predictor values that have a higher covariance with the response. To pretreat or preprocess the spectra, mean centering, a combination of first derivative and mean centering, as well as second derivative and mean centering were used, and finally mean centering was selected as it was best preprocessing method. For the development of calibration and prediction models, the dataset was divided into calibration and prediction models using Kennard stone algorithm. Calibration models were developed using 56 samples. Contiguous block cross-validation was used with 6 data splits. Based on the highest R^2 in calibration and cross-validation, as well as the lowest root mean square errors (RMSE) in calibration (RMSEC) and cross-validation (RMSECV), the best calibration model was chosen. The prediction/external validation set of 24 samples was utilized for the evaluation of the calibration model in external prediction. Different PLSR models were developed to investigate which model works best for the prediction of colour attributes. Firstly, the models were developed

using the whole wavelength Vis-NIR (400-1000 nm) range. Secondly, interval based PLS (iPLS) was used by setting particular intervals in Vis-NIR region for wavelength selection purposes. The third strategy used for wavelength selection was variable importance in projection (VIP) score. After the development of models, the performance of each model was compared and the best model was selected based on calibration and prediction statistics.

4.4 Results and discussion

4.4.1 Overview of the spectra

The reflectance spectra of the bison muscle samples were extracted from the images both in the Vis-NIR and SWIR range and are plotted in **Figure 4.1** and **Figure 4.2**, respectively. The **Figure 4.1a** represents the overall spectra and **Figure 4.1b** depicts the averaged spectra from the muscle samples based on muscle types in the Vis-NIR range. **Figure 4.1c** and **Fig 4.1d** represent the overall and averaged spectra based on storage periods within the same spectral region. On the other hand, **Figure 4.2a** and **Figure 4.2b** depict the overall and averaged spectra based on muscle types, and **Figure 4.2c** and **Figure 4.2d** portray the spectra based on storage periods, respectively, in the SWIR region. In Vis-NIR spectra, a major peak was found between 500 and 660 nm representing the redness (a^* value) of meat (Andrés et al., 2008; Kamruzzaman et al., 2016). On the other hand, spectra from SWIR range portrayed a major peak between 1100 and 1500 nm, presenting the O-H bond of water (Prieto et al., 2008).

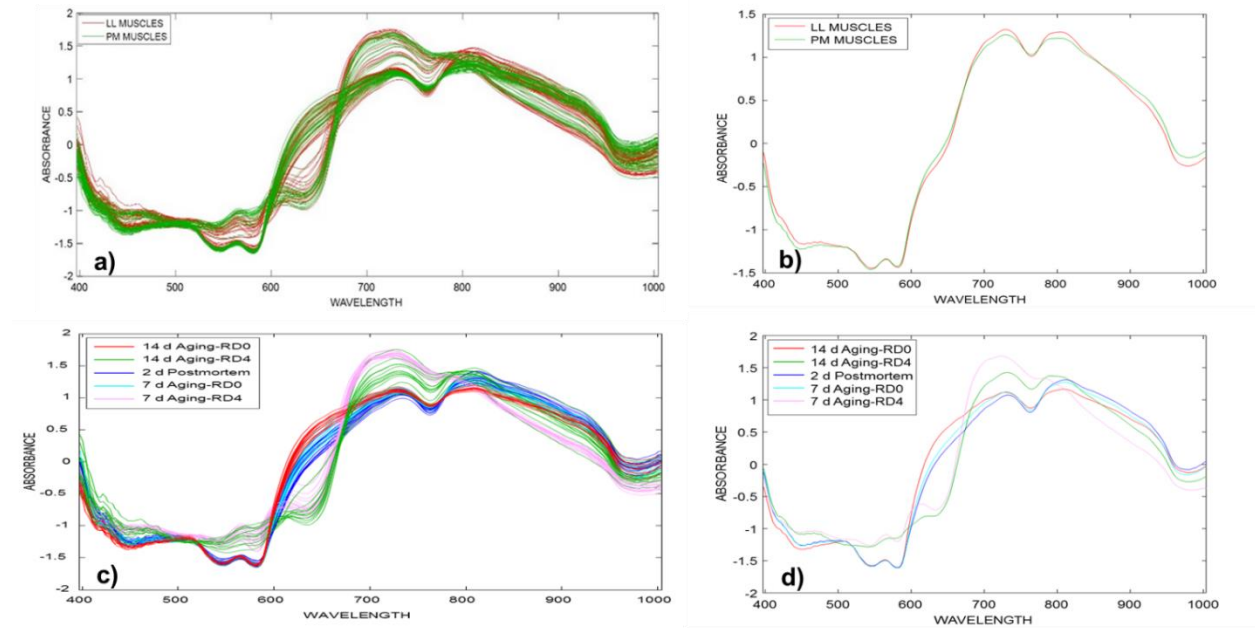


Figure 4.1. Overview of spectra in the Vis-NIR range. a) Spectra based on muscles types (LL and PM), b) Averaged spectra based on muscles types (LL and PM), c) Spectra based on ageing periods, and d) Averaged spectra based on ageing periods.

LL = *longissimus lumborum*; PM = *psoas major*.

Vis-NIR = visible near infrared.

2 d postmortem = 2-day postmortem; 7 d ageing-RD0 = 7-day ageing-retail display d 0; 7 d ageing-RD4 = 7-day ageing-retail display d 4; 14 d ageing-RD0 = 14-day ageing-retail display d 0 and 14 d ageing-RD4 = 14-day ageing-retail display d 4.

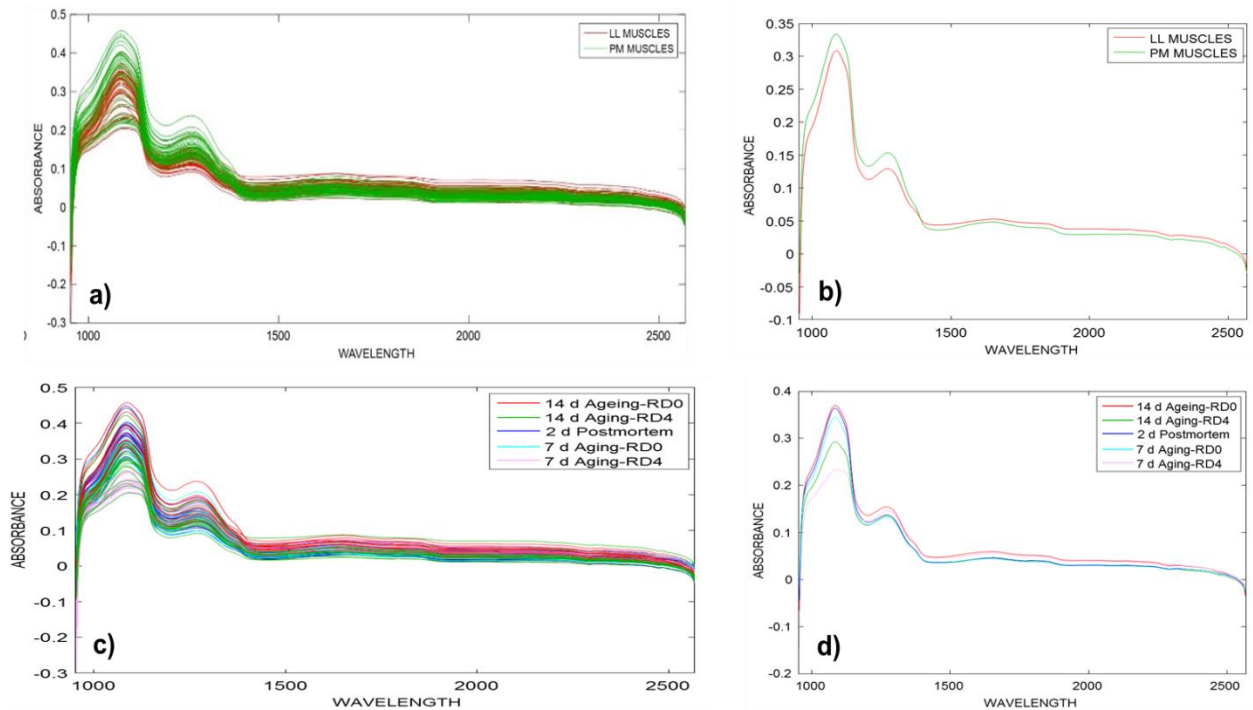


Figure 4.2. Overview of spectra in the SWIR range. a) Spectra based on muscles types (LL and PM), b) Averaged spectra based on muscles types (LL and PM), c) Spectra based on ageing periods, and d) Averaged spectra based on ageing periods.

LL = *longissimus lumborum*; PM = *psoas major*.

SWIR = short wave infrared.

2 d postmortem = 2-day postmortem; 7 d ageing-RD0 = 7-day ageing-retail display d 0; 7 d ageing-RD4 = 7-day ageing-retail display d 4; 14 d ageing-RD0 = 14-day ageing-retail display d 0 and 14 d ageing-RD4 = 14-day ageing-retail display d 4.

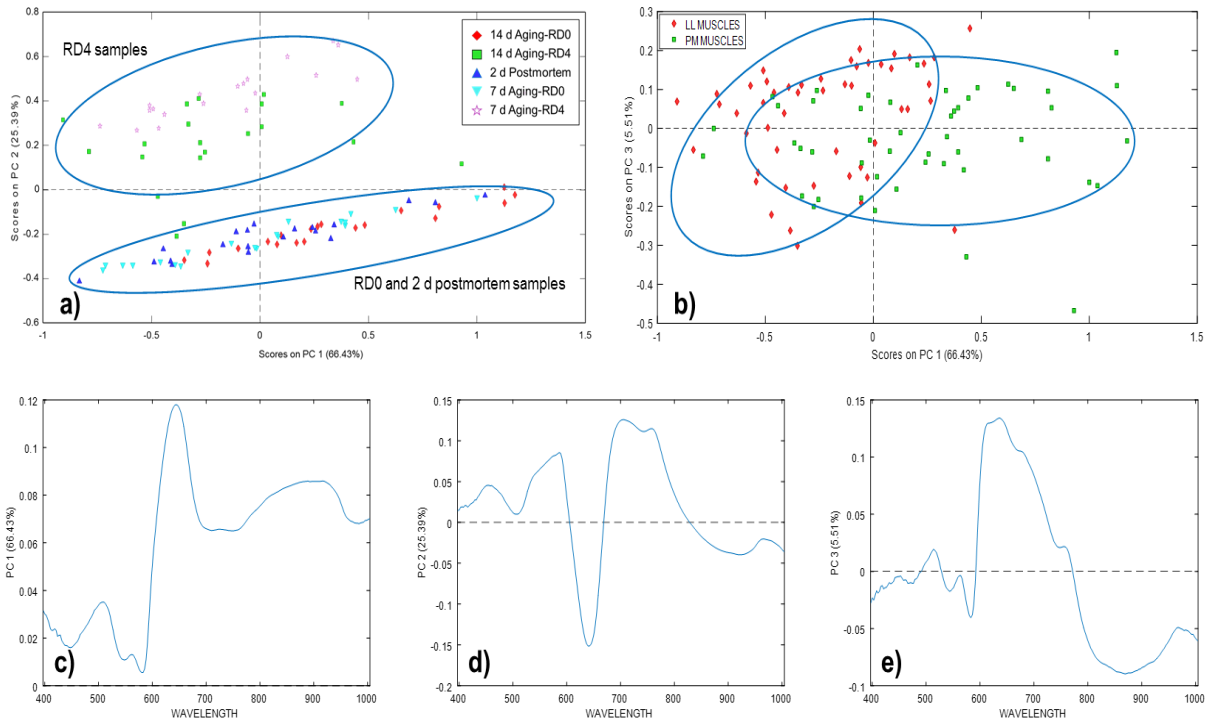


Figure 4.3. PCA based classification in the Vis-NIR range. a) Scores plot for PC1 and PC2 (coloured by ageing and retail display period), b) Scores plot for PC1 and PC3 (coloured by muscle type), c) Loadings plot for PC1, d) Loadings plot for PC2 and e) Loadings plot for PC3.

LL = *longissimus lumborum*; PM = *psoas major*. Vis-NIR = visible near infrared.

2 d postmortem = 2-day postmortem; 7 d ageing-RD0 = 7-day ageing-retail display d 0; 7 d ageing-RD4 = 7-day ageing-retail display d 4; 14 d ageing-RD0 = 14-day ageing-retail display d 0 and 14 d ageing-RD4 = 14-day ageing-retail display d 4.

PC 1, 2 and 3 = principal component 1, 2 and 3.

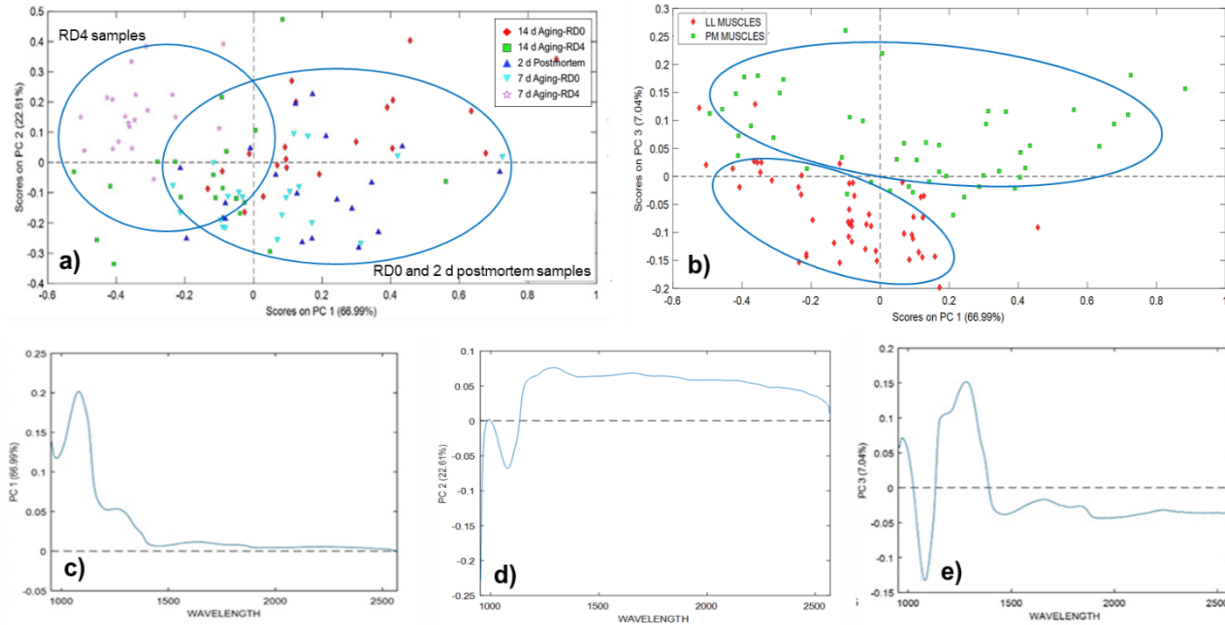


Figure 4.4. PCA based classification in the SWIR range. a) Scores plot of PC1 and PC2 (coloured by ageing and retail display period), b) Scores plot of PC1 and PC3 (coloured by muscle type), c) Loadings plot of PC1, d) Loadings plot of PC2, and d) Loadings plot of PC3.

LL = *longissimus lumborum*; PM = *psoas major*. SWIR = short wave infrared.

2 d postmortem = 2-day postmortem; 7 d ageing-RD0 = 7-day ageing-retail display d 0; 7 d ageing-RD4 = 7-day ageing-retail display d 4; 14 d ageing-RD0 = 14-day ageing-retail display d 0 and 14 d ageing-RD4 = 14-day ageing-retail display d 4.

PC 1, 2 and 3 = principal component 1, 2 and 3.

4.4.2 PCA based unsupervised classification in the Vis-NIR range

The PCA model was developed after mean centering the spectral profiles in the Vis-NIR range to classify the LL and PM bison muscle samples based on spectral features. The first four principal components (PCs) covered almost 98.90% of the total variance in the data where the PC1, PC2 and PC3 explained 66.43%, 25.39% and 5.51% of variance, respectively. The PCA model was developed using 224 wavelengths at 3 nm interval within the Vis-NIR region from each muscle sample. In PC1 x PC2 plotting (**Figure 4.3a**), PC2 provided a very good discrimination based on the storage period in retail display by totally segregating the scores of the bison muscle samples at the end (d 4) of the retail display time. No groupings were observed between the samples based on the ageing period itself. However, the second plotting (PC1 x PC3) presented a

slight grouping pattern based on the muscle types (LL or PM) on the PC1 axis (**Figure 4.3b**). The reason behind that could be the muscle-specific (LL or PM muscle) changes on colour deterioration pattern due to the differences in fibre type (Hunt & Hedrick, 1977b) and accumulation of lipid and protein oxidation products overtime. In fact, Hasan et al. (2021) reported that during retail display period (from d 0 to d 4) colour deterioration occurs in both bison LL and PM muscles due to the production of malondialdehyde (MDA) and 4-hydroxy-2-nonenal (HNE) as secondary lipid oxidation, and carbonyl compounds as protein oxidation products; but they produced remarkable changes in redness in PM. Among those oxidation products, MDA was found to be the most notorious factor for the discolouration in bison meat. Therefore, these biochemical factors may also inherently contribute for the classification of bison muscles based on storage in retail display.

Moreover, the loadings plot for PC1 showed that the slight classification between the muscle type was observed due to the contribution of wavelengths from 500 to 660 nm (**Figure 4.3c**) because the wavelengths in this distinct region are closely attributed to the colour values, especially the redness of muscle samples (Liu et al., 2003). The observed peaks in the wavelength range between 500 to 600 nm are usually related to oxymyoglobin (OMb) content in muscle samples which is actually responsible for the redness of the meat (De Marchi, 2013). The present study results are also in agreement with the spectral plot investigated by several researchers (Tang et al., 2004; Mamani-Linares et al., 2012; Kamruzzaman et al., 2016) who reported the absorption bands at 560 and 595 nm which were associated with meat pigment myoglobin, especially deoxymyoglobin or OMb responsible for the red colour or a^* values of meat (Andrés et al., 2008). The absorbance values in the wavelength range of 520-590 nm usually decrease with the passage of storage period since the OMb content decreases hence inversely affecting the muscle sample freshness (Peyvasteh, Popov, Bykov, & Meglinski, 2020) resulting discolouration for the MMb accumulation (Roberts et al., 2017) in meat surface with the progression of ageing and retail display times. Generally, in freshly cut meat, DMb is the main Mb form with representative purplish-red colour. With the oxygenation reaction, DMb is converted to OMb (cherry-red colour). This OMb is then oxidized to MMb at low oxygen pressure (1% to 2%) and accumulated in between outer OMb and inner DMb layer in meat surface and this MMb (brownish red) progressively thickens and covers the meat outer surface resulting meat discolouration (AMSA, 2012). Loadings plot on PC1, PC2 and PC3 are showing on the **Figure 4.3c**, **4.3d** and **4.3e**

respectively. Similar peaks were observed in the loadings plot for both PC1 (**Figure 4.3c**) and PC3 (**Figure 4.3e**) loadings and attributed by the presence of Omb. In the **Figure 4.3b**, slight misclassification based on muscle type was detected for a dataset of 100 samples of bison muscles. The reason behind that misclassification could be due to the major contribution of PC scores (**Figure 4.3c and Figure 4.3e**) from the Omb content of 2 d postmortem bison samples.

4.4.3 PCA based unsupervised classification in the SWIR range

PCA model was also developed to classify the muscle type, and storage and retail display period over the entire SWIR wavelength range. PCA model was developed using 288 wavelengths at 5 nm interval within SWIR region from each muscle sample. The data was mean centered prior to the application of PCA. In this case, the first four PCs accounted for 99.52% of the total variance in the data including 66.99%, 22.61% and 7.04% of explained variance for PC1, PC2 and PC3 respectively. In PC1 x PC2 plotting (**Figure 4.4a**), slight grouping based on the stored and retail displayed samples was observed on the PC1 axis as portrayed in the loadings plot (**Figure 4.4c**). In contrast, the plotting of PC1 x PC3 (**Figure 4.4b**) showing the clear discrimination based on muscle types on the PC3 axis and loadings on PC3 in **Figure 4.4e**. It was observed that PC1 and PC3 were of significant importance to segregate the bison muscle samples based on storage and retail display periods, and muscle types respectively. As a result, no sample discrimination based on storage period was detected in this case. However, the discrimination between the ageing and retail display samples was not clear as in this case as compared to the Vis-NIR results. Only, the segregation between retail display d 0 and d 4 samples from 7 d ageing was clearly visible. The loadings plot for PC1, PC2 and PC3 are presented in the **Figure 4.4c, 4.4d and 4.4e** respectively. The loadings plot for PC3 showed that significant peaks were observed between 1100-1500 nm which can be attributed to the O-H sensitive region and can indicate differences between the moisture content of the samples (**Figure 4.4e**). These results are supported by the other researchers who observed the water absorption bands associated with the overtones for O-H stretching (Prieto et al., 2008; Barlocco, Vadell, Ballesteros, Galiotta, & Cozzolino, 2006) which is an indicator of moisture domination in the spectral features. In addition, the region from 1100-1300 nm can be linked with a combination of absorption bands for water and protein. In agreement with this information, Kamruzzaman et al. (2012) reported that the spectral peaks detected in the SWIR region are linked to the O-H, C-H and N-H bonds of water, fat, and protein, respectively.

Accordingly, the differences in the water content or the protein content can also be a factor for the clear groupings observed based on the muscle type. Similar peaks as those of PC3 (**Figure 4.4e**) were observed in the loadings plot in case of PC1 (**Figure 4.4c**), but the groupings based on ageing and retail display period were not as encouraging enough as those in case of Vis-NIR region. The reason for this can be the lack of the ability of the SWIR region to depict or assess the colour-based changes. Since colour is a significant parameter and highly influences the meat quality based on storage periods. Since, the SWIR range covers 1000-2500 nm, the meat colour a^* (redness) portraying pigment Mb and its redox forms show reflectance peaks within the Vis-NIR region (400-1000 nm wavelength) of the spectra (Kamruzzaman et al., 2016; Liu et al., 2003). As a result, colour-based variations were not detected by SWIR spectral region.

However, there are some no-pigment or achromatic aspects that could alter the meat colour, in particular lightness/darkness of meat (Hughes et al., 2020; Purslow et al., 2020) and can be explained with the mechanisms of light scattering from the microstructure of meat tissues. Generally, meat surface moisture contents may affect the reflection and scattering properties which are ultimately related to the pH and water holding capacity. According to Purslow et al. (2020), when light is passed into the meat, one part is absorbed by the pigment, and some part may be scattered by the microstructures, particles present, or muscle fiber and myofibril interfaces. Muscle appears lighter if the surface light scattering and reflection is high. However, when the light absorption by pigment is higher, the light scattering is low resulting darker appearance of meat. The lightness in meat may be due to the light refraction through myofibrils affected by type and shape of muscle fibers. The light transmittance of fibers with larger diameter is higher compared to small diameter counterpart because the higher mitochondrial density in small fibers can scatter more light. Moreover, at low pH, the refraction of light through the lattice structure of myofilaments is high due to the shrinkage of lattice and higher refractive index resulting lighter appearance (Hughes et al., 2019). The surface of A-band and the junctions between A-band and I-band, are two very important locations within the myofibrils where the intensity of observed light scattering is very high (Offer et al., 1989). Furthermore, the adjacent gaps between the myofibrils are the best possible location for the scattered light (Hughes et al., 2017). The main reason for that light scattering is the differences of refractive index between A-bands (protein dense) and the fluid containing lateral gaps within the myofibrils. Hughes et al. (2017) also reported that the low muscle

pH is strong positively related to the muscle lightness. Because, with the decrease in pH, muscle fiber shrinkage occurs progressively resulting longer sarcomere length.

Furthermore, there is a possibility on the presence of few glycolytic enzymes or proteins in sarcomere which could affect light scattering behaviors. Among those enzymes, aldolase and glyceraldehyde-3-phosphate dehydrogenase have been identified and found to have significant effects on the light scattering properties of myofibrils (Hughes et al., 2019; Hughes et al., 2020; Purslow et al., 2020). The darker muscles have higher mass centered to the actin filaments within the I-band due to the active bindings of these enzymes at higher pH compared to medium and lighter muscles. However, at lower pH, those proteins were less active and denatured and ultimately scattered more light showing more lightness. Therefore, the myofibril diameter, and consequently muscle fibre diameter changing with the ultimate pH changes and the binding of specific proteins with actin filaments are the major factors for the variations in lightness/darkness of meat. Even within the same muscle group such as white muscles, *biceps femoris* (BF) and LL, the light scattering properties differs for the variations in collagen contents, and BF exhibits more light scattering due to the greater collagen contents compared to LL (Van Beers et al., 2018). As a result, the achromatic factors mentioned above may have active contributions for the NIRS based discrimination of bison muscles according to muscle type, ageing and retail display periods.

4.4.4 PLS-DA based supervised classification in the Vis-NIR range

To discriminate between the bison muscle samples based on the type of muscles i.e., LL and PM muscles, PLS-DA based supervised models were developed utilizing the spectral data acquired in the Vis-NIR region. Models developed with different pretreatment methods and their combinations were examined, and it was exhibited that mean centering process provided the highest sample misclassification in both wavelength ranges. Though the combinations of first and second derivatives with mean centering provided reliable results. The best calibration models were achieved using the combination of first derivative and mean centering as a preprocessing method. In addition, the confusion matrix in **Table 4.1** contains further statistical features of the PLS-DA calibration models in details based on the best preprocessing (first derivative and mean centering). The PLS-DA calibration models were generated after dividing the dataset of 100 samples into two sets namely, calibration set with 70 samples and prediction/external validation set with 30 samples

using Kennard-stone algorithm. The dataset for calibration was used for both calibration and cross-validation and rest of the sample's dataset was utilized for the prediction.

Firstly, for the classification of the bison muscle samples based on the muscle type, the developed PLS-DA model included the entire wavelength range from 400-1000 nm. The model resulted in 94% classification accuracy in terms of calibration and 83% accuracy in terms of cross-validation (data not shown in table). The loadings plot of the PLS-DA model depicted that the wavelength range from 470-750 nm highly contributed towards the classification of muscles based on the muscle type. Secondly, this wavelength range (470-750 nm) was selected for the development of the final calibration model. In this finally achieved model, the classification accuracy in calibration was observed to be 97% and for cross-validation the classification accuracy was 86% (data not shown in table). After the development of the calibration model the prediction/external validation was done which resulted in the classification accuracy of 82% (data not shown in table). The detailed classification results for this calibration model can be seen in the confusion matrix given in **Table 4.1**. The PLS-DA scores plot for the classification of bison muscle samples based on muscle type shown in **Figure 4.5a** and a distinct/clear segregation between two muscles (LL and PM) with prominent groupings was observed. Moreover, **Figure 4.5b** represented the loadings plots of the 3 latent variables (LV1, LV2 and LV3) which accounted for 99.14% of the covariance in the data.

Additionally, for the classification of muscle samples based on the periods in ageing and retail display, reliable results were obtained. The spectral dataset in this case was divided into 5 different classes namely, 2 d postmortem, 7 d ageing-retail display d 0 (7 d ageing-RD0), 7 d ageing-RD4, 14 d ageing-RD0, and 14 d ageing-RD4. In this case, 7 d ageing-RD4 and 14 d ageing-RD4 represent the muscle samples belonging to the d 4 (fourth day) of retail display. Moreover, the confusion matrix for the best calibration model in this case can be observed in **Table 4.2**.

The loadings plots for both classification models for ageing periods revealed significantly noticeable peaks at 590 nm, which is related with meat redness. As a result, this could be concluded that ageing causes prominently observable alterations in the a^* value of meat. It was reported that the a^* value of bison meat declines overtime during ageing and retail display period causing discolouration for the accumulation of brown metmyoglobin in meat surface (Hasan et al., 2021).

The highest misclassification was observed in case of 7 d ageing-RD0 samples where the samples were either misclassified as 2 d postmortem or 14 d ageing-RD0, which can be due to the fact that at this stage the a^* value of the muscle samples were not very different from both classes. But in case of 2 d postmortem and 14 d ageing-RD0 and retail display day 4 (7 d ageing-RD4 and 14 d ageing-RD4) muscle samples the classification accuracies were higher indicating significant differences in the a^* value.

Table 4.1. Confusion matrix for the classification of *longissimus lumborum* and *psoas major* muscle samples in the Vis-NIR range

Real/Predicted in calibration	Pre-processing	# of LVs	LL muscle	PM muscle	Specificity	Sensitivity
LL muscle class			35	0	1.00	0.97
PM muscle class			1	34	0.97	1.00
Real/Predicted in cross-validation	1 st derivative and mean centering	4	LL muscle	PM muscle	Specificity	Sensitivity
LL muscle class			35	4	0.88	0.97
PM muscle class			1	30	0.97	0.88
Real/Predicted in prediction			LL muscle	PM muscle	Specificity	Sensitivity
LL muscle class			14	3	0.81	1.00
PM muscle class			0	13	1.00	0.81

LL = *longissimus lumborum*; PM = *psoas major*.

Vis-NIR = visible near infrared. LV = latent variable.

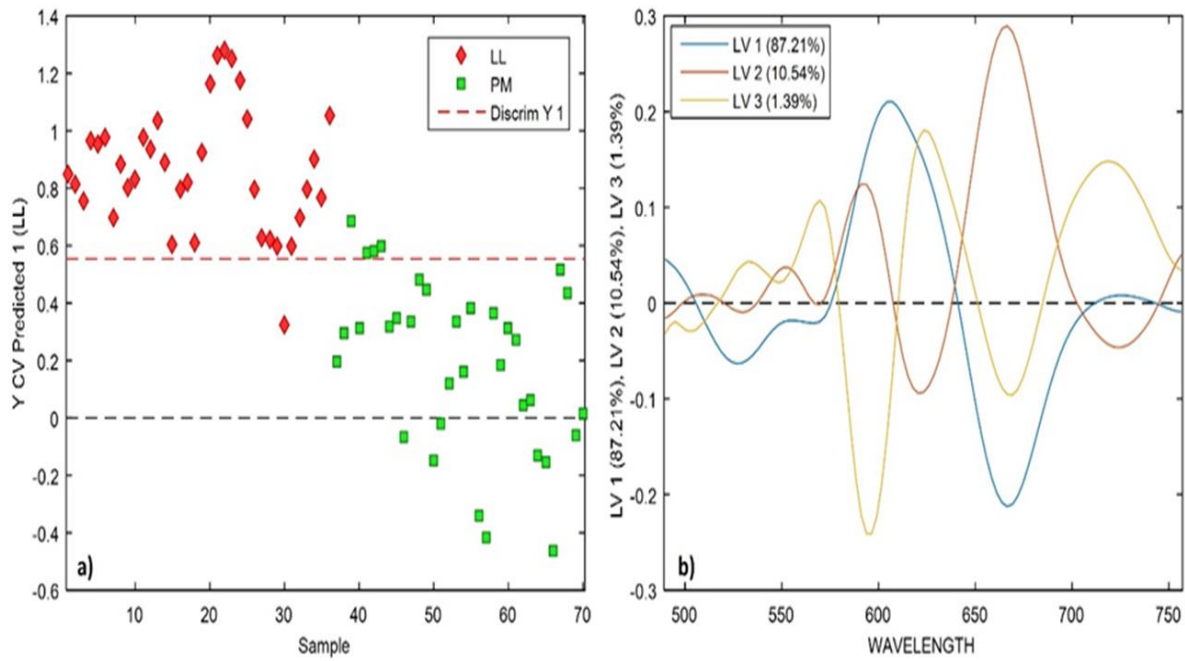


Figure 4.5. a) PLS-DA scores plot for the classification of *longissimus lumborum* and *psoas major* muscle samples, and b) Loadings plots for LV1, LV2 and LV3.

LL = *longissimus lumborum*; PM = *psoas major*.

LV 1, 2 and 3 = latent variables 1, 2 and 3. PLS-DA = partial least squares discriminant analysis.

Table 4.2. Confusion matrix with best calibration model for the classification of *longissimus lumborum* and *psoas major* muscle samples based on ageing and retail display periods

Real/Predicted in calibration	Pre-processing	# of LVs	14 d Ageing-RD0	14 d Ageing-RD4	2 d Postmortem	7 d Ageing-RD0	7 d Ageing-RD4	Specificity	Sensitivity
14 d Ageing-RD0	1 st derivative and mean centering	4	11	0	0	1	0	0.98	0.84
14 d Ageing-RD4	1 st derivative and mean centering	4	0	12	0	0	0	1.00	0.92
2 d Postmortem	1 st derivative and mean centering	4	0	0	8	1	0	0.98	0.53
7 d Ageing-RD0	1 st derivative and mean centering	4	2	0	7	11	0	0.84	0.85

7 d Ageing-RD4	0	1	0	0	16	0.98	1.00
Real/Predicted in cross- validation	14 d Agein g- RD0	14 d Agein g- RD4	2 d Postmorte m	7 d Agein g- RD0	7 d Agein g- RD4	Specificit y	Sensitivit y
14 d Ageing- RD0	9	0	4	2	0	0.90	0.69
14 d Ageing- RD4	0	3	0	0	3	0.95	0.23
2 d Postmortem	3	5	6	9	0	0.69	0.40
7 d Ageing-RD0	1	1	5	2	0	0.88	0.15
7 d Ageing-RD4	0	4	0	0	13	0.93	0.81
Real/Predicted in prediction	14 d Agein g- RD0	14 d Agein g- RD4	2 d Postmorte m	7 d Agein g- RD0	7 d Agein g- RD4	Specificit y	Sensitivit y
14 d Ageing- RD0	3	0	0	1	0	0.96	0.43
14 d Ageing- RD4	0	6	0	0	1	0.96	0.86
2 d Postmortem	0	0	1	1	0	0.96	0.20
7 d Ageing-RD0	4	0	4	5	0	0.65	0.71
7 d Ageing-RD4	0	1	0	0	3	0.96	0.75

LL = *longissimus lumborum*; PM = *psoas major*. LV = latent variable. 2 d postmortem = 2-day postmortem; 7 d ageing-RD0 = 7-day ageing-retail display d 0; 7 d ageing-RD4 = 7-day ageing-retail display d 4; 14 d ageing-RD0 = 14-day ageing-retail display d 0; and 14 d ageing-RD4 = 14-day ageing-retail display d 4.

Table 4.3. Calibration and prediction statistics for a^* value, and colour and discolouration score

Parameters	Pre-processing	# of LVs	Wavelength range (nm)	R^2_C	RMSE C	R^2_{CV}	RMSEC V	R^2_P	RMSE P
a^* value		3	Full wavelength h range [400-1000]	0.89	1.56	0.83	1.96	0.91	1.34
		2	VIP score based [580-670]	0.88	1.57	0.84	1.88	0.90	1.41
		3	iPLS based [434-437 599-601]	0.92	1.32	0.90	1.50	0.87	1.76
Colour score		3	Full wavelength h range [400-1000]	0.96	0.26	0.94	0.30	0.92	0.32
		3	VIP score based [580-672]	0.96	0.25	0.95	0.27	0.92	0.32
		3	iPLS based [572, 574, 604, 607]	0.96	0.26	0.95	0.28	0.93	0.32
Discolouration score	Mean centering	3	Full wavelength h range [400-1000]	0.96	0.47	0.93	0.63	0.93	0.56
		3	VIP scores based [599-601 789-792]	0.94	0.54	0.93	0.62	0.91	0.69
		2	iPLS based [572-588 610-667]	0.94	0.54	0.92	0.64	0.93	0.58

a^* = redness. LV = latent variable. VIP = variable importance in the projection. iPLS = interval partial least-squares regression. R^2_C , R^2_{CV} , and R^2_P = coefficient of determinant (R) of calibration (C), cross-validation (CV), and prediction (P), respectively. RMSEC, RMSECV, and RMSEP = root mean square error (RMSE) of calibration (C), cross-validation (CV), and prediction (P), respectively.

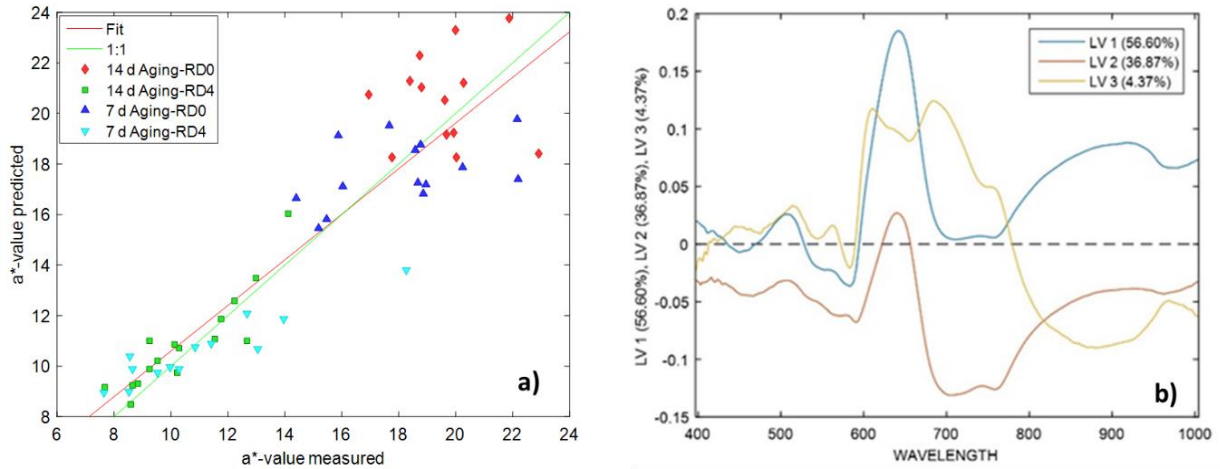


Figure 4.6. a) Calibration plot for the prediction of a^* value, and b) loadings plot for first 3 LVs. a^* = redness. LV 1, 2 and 3 = latent variables 1, 2 and 3. 7 d ageing-RD0 = 7-day ageing-retail display d 0; 7 d ageing-RD4 = 7-day ageing-retail display d 4; 14 d ageing-RD0 = 14-day ageing-retail display d 0 and 14 d ageing-RD4 = 14-day ageing-retail display d 4.

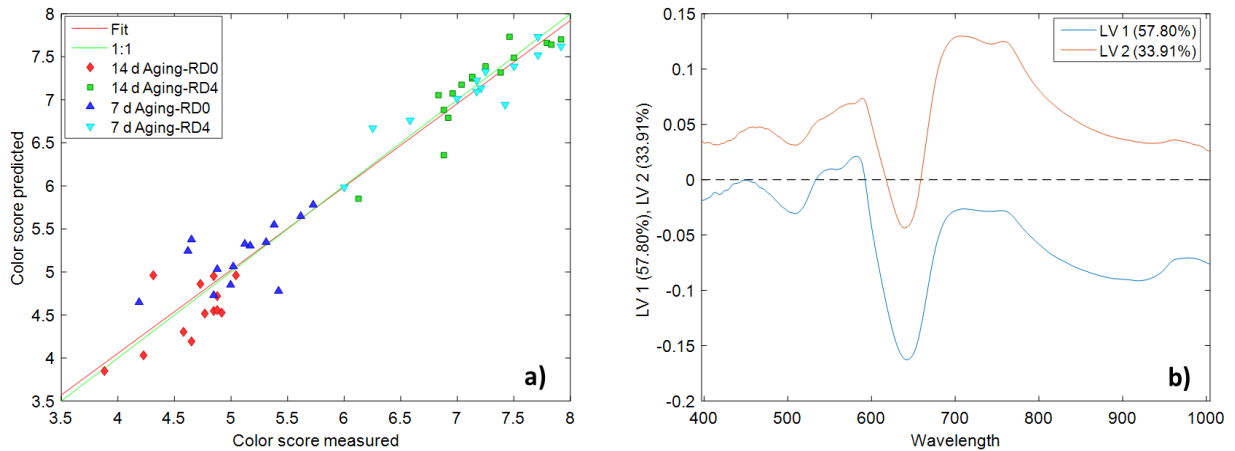


Figure 4.7. a) Calibration plot for the prediction of colour score, and b) loadings plot for first 2 LVs.

Colour score: descriptive scale for colour from 1 to 8 (1= pale red or pale pinkish red; 8= very dark red or tannish red or brown). 7 d ageing-RD0 = 7-day ageing-retail display d 0; 7 d ageing-RD4 = 7-day ageing-retail display d 4; 14 d ageing-RD0 = 14-day ageing-retail display d 0 and 14 d ageing-RD4 = 14-day ageing-retail display d 4. LV 1 and 2 = latent variables 1, and 2.

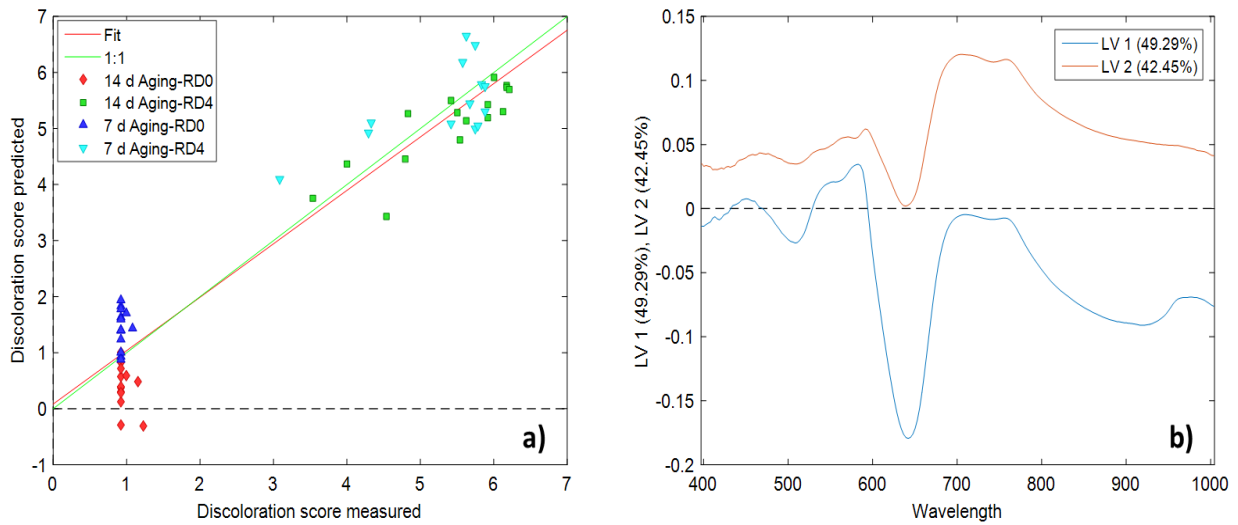


Figure 4.8. a) Calibration plot for the prediction of discoloration score, and b) loadings plot for first 2 LVs.

Discoloration score: surface discoloration on a scale of 1-6 (1 = none, 0%; 6 = extensive discoloration, 81-100%). 7 d ageing-RD0 = 7-day ageing-retail display d 0; 7 d ageing-RD4 = 7-day ageing-retail display d 4; 14 d ageing-RD0 = 14-day ageing-retail display d 0 and 14 d ageing-RD4 = 14-day ageing-retail display d 4.

LV 1 and 2 = latent variables 1, and 2.

4.4.4.1 Prediction of a^* value

For the prediction of L^* (lightness), a^* (redness) and b^* (yellowness) values, prediction model was developed using PLSR analysis. Only successful prediction results were obtained for a^* value. Bison muscle classification based on the periods in ageing and retail display was observed due to the degradation of bright cherry-red colour (as OMb) during storage. The distinctive peaks of LVs observed in the PLSR classification models, particularly in the wavelength range of 500-690 nm indicated the underlying fact that the specific pigments (Mb and OMb) representing the redness of meat are primarily responsible for the classification of muscles. As a result, this could be noted that the a^* value is one of the most noticeable influential factors for the classification of bison muscles at crucial time periods. Therefore, by utilizing a spectral dataset of 80 muscle samples (40 LL and 40 PM) in total, PLSR models were created to correlate spectral properties with redness values. The dataset of 80 samples when divided using the Kennard stone algorithm resulted in 56 samples for the calibration set and 24 samples for the

prediction/external validation set. In this scenario, PLSR models development were performed utilizing raw unprocessed data as well as and data that had been preprocessed with mean centering, and the combination of the first derivative and mean centering. As a preprocessing method, mean centering provided the best suitable PLSR model with an R^2 for calibration and cross-validation values of 0.89, and 0.86 with RMSEC and RMSECV of 1.58 and 1.72, respectively (data not shown in table). The developed PLSR model was constructed with total first three LVs where LV1, LV2 and LV3 explained 56.60%, 36.87% and 4.37% of the total covariance, respectively. A plot was constructed utilizing regression coefficients and used that to examine the variables which had maximum contributions to the developed model and it was noticed that the variables within 503-850 nm wavelength range played the most significant role. Therefore, the variables other than within this region (503-850 nm) were excluded from the PLSR model and final model was constructed with only total 129 variables. The overall findings of this model were not distinctively different considering R^2 of calibration (0.89) and R^2 of cross-validation (0.86) whereas RMSEC value decreased to 1.57 which was not significantly different from the RMSEC obtained using full wavelength range. At the same time another two models, iPLS and VIP score based models were also developed. Finally, VIP score based PLS model was selected as best model with an R^2 of 0.88 (RMSEC: 1.57) for calibration and R^2 of 0.84 (RMSECV: 1.88) for cross-validation (**Table 4.3**). This model showed best results for a specific wavelength (580-670) range containing only 34 variables. After the development of the calibration model, the 24 prediction/external validation muscle samples were tested resulting in R^2 of prediction of 0.90 and RMSE of prediction (RMSEP) of 1.41. Furthermore, **Figure 4.6** showing the calibration plot (**Figure 4.6a**) and loadings plot (**Figure 4.6b**) for the prediction of a^* value.

A significant amount of data covariance was explained by the three first LVs of PLSR model, which showed prominent peaks near 592, 645, and 692 nm, all of which are associated with the pigments of meat (Cozzolino et al., 2003; Aït-Kaddour et al., 2017). The current study findings showed that the PLSR calibration model revealed more accurate results for the prediction of a^* values in comparison with Cozzolino et al. (2003) who reported the R^2 for calibration as approximately 0.60 for pork samples. This might be because there are major differences between a^* values of pork and bison muscle samples. Differing results for the prediction of a^* values in the samples of red meats have been presented by various research works. The authors Su et al. (2018) found that the prediction of a^* values of beef samples weren't very reliable since the

spectrophotometer used for their investigation lacked the visible range. In another study, Prieto et al. (2008) examined beef muscles and presented unsatisfactory prediction results for a^* values. In contrast, Cozzolino et al. (2003) obtained satisfactory results in predicting colorimetric parameters based on spectral profiles in the Vis-NIR range. As a result, it can be summarized that the spectral information obtained from the Vis-NIR region of the electromagnetic spectrum, coupled with the techniques associated with the multivariate pattern recognition, might be considered as a potential solution to classify bison muscle samples on the basis of muscle type and ageing, as well as retail display periods. Therefore, the redness value prediction in bison muscle samples could also be satisfactorily achieved by using NIRS.

4.4.4.2 Prediction of colour and discolouration score

PLSR models were developed for the prediction of colour and discolouration scores using iPLS and VIP scores as wavelength selection methods. For the prediction of colour score, the VIP score based PLSR demonstrated the best prediction results within a particular wavelength (580-672 nm) range of the Vis-NIR spectra using mean centering as a preprocessing method. Colour score prediction was successful with an R^2 of 0.96 (RMSEC: 0.25), 0.95 (RMSECV: 0.27), and 0.92 (RMSEP: 0.32) for calibration, cross-validation, and prediction, respectively (**Table 4.3**). The overall prediction results are presented in **Figure 4.7** where **Figure 4.7a** and **Figure 4.7b** exhibited the calibration plot and loadings plot for the prediction of colour score. Total 91.71% of covariance was explained by the first two LVs (LV1 = 57.80% and LV2 = 33.91%).

Furthermore, for discolouration score prediction, PLSR models were developed and model performance revealed that the whole Vis-NIR (400-1000 nm) range provided the best model. The PLSR model was successful for the prediction of discolouration score with an R^2 of 0.96 (RMSEC: 0.47) for calibration, 0.93 (RMSECV: 0.63) for cross-validation, and 0.93 (RMSEP: 0.56) for prediction (**Table 4.3**). Furthermore, **Figure 4.8** represents the calibration results with calibration plot (**Figure 4.8a**) and loadings plot (**Figure 4.8b**) for the prediction of discolouration score. The total explained covariance (91.74%) for first two LVs was also significant where LV1 and LV2 explained 49.29% and 42.45% of covariance respectively.

4.5 Conclusions

There is an increasing interest in the meat industry for developing and applying online techniques like NIRS to discriminate meat samples and predict instrumental and sensory colour attributes. In the current study, Vis-NIR and SWIR spectral ranges were highly effective for classifying bison portions based on storage period in retail display and muscle type, respectively. In addition, PLS-DA based classification using spectral information from the Vis-NIR region can achieve an accurate segregation pattern according to muscle type and storage periods. The PLSR calibration model can be used to predict the instrumental (redness) and sensory (colour and discolouration scores) colour of bison meat successfully. Therefore, the study findings may result in adopting this technology to expand bison fresh meat sales as the bison industry grows, as it is a fast and sensitive technique for large-scale application. Based on this experience, additional research should be conducted to detect other colors' labile and defects portions from different muscles.

To achieve the third goal of present thesis work, a proteomic research was conducted to investigate the muscle-specific proteome changes during postmortem ageing of bison LL and PM muscles, and the results are reported in the next chapter.

CHAPTER 5: MANUSCRIPT NO. 3

Tandem mass tag labeling-based analysis to characterize muscle-specific proteome changes during postmortem ageing of bison *longissimus lumborum* and *psoas major* muscles

This chapter was written as a manuscript and submitted in accordance with the *Meat and Muscle Biology* journal format and has been published as: Hasan, M. M., Rashid, M., Suman, S. P., Perreault, H., Paliwal, J. & Rodas-Gonzalez, A. (2022). *Meat and Muscle Biology*, 6(1): 13055, 1-23. <https://doi.org/10.22175/mmb.13055>

5.1 Abstract

The objective of the study was to examine the variations in sarcoplasmic proteomes of bison *longissimus lumborum* (LL) and *psoas major* (PM) muscles during postmortem ageing utilizing tandem mass tag (TMT) isobaric labeling coupled with liquid chromatography mass-spectrometry (LC-MS/MS) for the categorization of muscles with muscle-specific inherent colour stability. A total of 576 proteins were identified in both bison LL and PM muscles, where 97 proteins were identified as differentially abundant (fold change > 1.5, $P < 0.05$) from the three comparisons between muscles during postmortem ageing periods (PM vs LL at 2 d, 7 d and 14 d). Between muscles, the most abundant protein groups were based on functions such as electron transport chain (ETC) or oxidative phosphorylation, tricarboxylic acid cycle (TCA), ATP transport, carbohydrate metabolism, fatty acid oxidation, chaperones, oxygen transport, muscle contraction, calcium signaling, and protein synthesis. In PM, most of the proteins from ETC, TCA cycle, fatty acid oxidation, ATP and oxygen transport, and muscle contraction were more abundant or exhibited increased expression during ageing compared to LL. On the other hand, the proteins involved in carbohydrate metabolism, chaperone function and protein synthesis mostly exhibited decreased expression in PM muscles relative to LL. These results clearly demonstrate that the proteins associated with oxidative metabolism showed increased expression in PM muscles. This indicates that oxidative damage and subsequent colour deterioration resulted in bison PM muscles being attacked by the reactive oxygen species produced during those metabolic processes. In contrast, proteins involved in glycolysis and chaperone activity exhibited a decrease in expression in bison PM muscles, resulting decline in colour stability compared with LL. Because glycolytic enzymes and chaperones maintain oxidative and/or colour stability by producing reducing

equivalents in glycolytic pathway and with the protein folding ability of chaperones, respectively in LL muscles.

Keywords: colour stability, proteomics, sarcoplasmic proteins, isobaric tags, liquid chromatography mass-spectrometry

5.2 Introduction

Fresh meat colour is one of the most important characteristics influencing purchase intention (Mancini & Hunt, 2005; Suman et al., 2014). Generally, consumers are more likely to buy bright cherry-red colour meat because it represents meat's freshness and wholesomeness. However, bison meat exhibits a darker appearance, and its colour deterioration rate is rapid in aerobically packaged conditions compared with beef; therefore, colour stability has been marked as a critical drawback for the growth of bison meat marketing (Narváez-Bravo et al., 2017; Pietrasik et al., 2006). Moreover, during ageing and retail display periods, meat colour deterioration leads to product rejection and economic loss (Canto et al., 2015; Nair et al., 2018; Smith et al., 2000).

The rapid discolouration of bison meat could not be attributed to a difference in the biochemistry of bison myoglobin (Mb) per se (identical amino acid sequences, similar oxidation kinetics and thermostability) (Joseph et al., 2010). However, compared to beef, bison have a different muscle fibre type (Aalhus et al., 2009; Koch et al., 1995), resulting in higher amount of pigment (Galbraith et al., 2016) and iron levels (Galbraith et al., 2006; Marchello & Driskell, 2001). In addition, polyunsaturated fatty acid (PUFA) levels (weight %) were found to be higher in range-fed and feedlot-fed bison than in range-fed or feedlot-fed cattle. (Rule et al., 2002). Also, malondialdehyde critically influences colour deterioration patterns in bison muscles and not 4-hydroxy-2-nonenal (Hasan et al., 2021), which is contrary to what observed in beef (Alderton et al., 2003; Suman et al., 2006). Those elements can accelerate Mb oxidation and subsequent meat discolouration. In beef, cellular biochemical mechanisms that govern the colour change during postmortem ageing affect the muscle-specific sarcoplasmic proteomes (Matarneh et al., 2017; Nair et al., 2018; Xiong, 2018). Furthermore, variations in the balance between antioxidants and pro-oxidants proteins within the sarcoplasm can cause lipid oxidation, lead to Mb oxidation, and cause discolouration in meat (Joseph et al., 2010; Ramanathan et al., 2009). Thus, we hypothesized that the protein profile in bison could differ from beef and explain its inherent rapid colour deterioration.

The sarcoplasmic proteins found in beef muscles have been investigated using gel-based proteomic analyses focusing on two-dimensional (2D) gel electrophoresis with label-free approach (Canto et al., 2015; Joseph et al., 2012; Nair et al., 2018; Salim et al., 2020; Suman et al., 2014; Yu et al., 2018). In meat science studies, tandem mass tags (TMT) proteomics is a very recent gel-free approach that has been used for exploring postmortem biochemical and cellular processes in bovine (Zhai et al., 2020), ovine (Li et al., 2018), and porcine (Liu et al., 2018) muscles. The TMT allows a high throughput approach for the accurate quantification and identification of cellular macromolecules, which help establish interactions and cellular pathways for complex proteomic analysis (Churchman et al., 2015; Mertz et al., 2015; Wang et al., 2016). Therefore, this study objective was to examine the changes in sarcoplasmic proteomes in bison LL and PM muscles during postmortem ageing periods using TMT labeling coupled with liquid chromatography mass-spectrometry (LC-MS/MS) for the segregation of muscles based on muscle-specific inherent colour stability. The study was conducted on muscles supplied by the studies reported by Hasan et al. (2021).

5.3 Material and methods

5.3.1 Sample collection and processing

Experiment was conducted using bison meat samples described by Hasan et al. (2021). Briefly, ten (n = 10) LL (striploin) and ten (n = 10) PM (tenderloin) muscles from bison A1 grade (< 50% ossification on the 9th - 11th thoracic vertebrae cartilaginous caps) (Canada Gazette, 1992) carcasses were purchased from a government inspected slaughter plant (True North Foods, Carman, MB, Canada) within 48 h postmortem and transported to the University of Manitoba Food Science Pilot plant (Winnipeg, MB, Canada). Immediately after arrival, muscles were trimmed practically free of subcutaneous fat. A 10-cm thick portion from each muscle was collected to evaluate biochemistry parameters baseline (Hasan et al., 2021), and then 15-20 g of sample were obtained and instantly vacuum packaged (very low oxygen permeable, FlairPak Vacuum Pouch, Flair Flexible Packaging Corporation, Canada/USA) using Vac Master (VAC545, Overland Park, KS, USA) with high vacuum and stored at -80 °C for the analysis of sarcoplasmic proteomes. The remaining muscle samples were cut into two equal portions, immediately vacuum packed individually and assigned for an ageing period of 7 and 14 d (days) at 2 °C. At the end of each assigned ageing period, steaks (2.5 cm thick) were obtained for colour and biochemistry

evaluations, and 15-20 g of muscle samples from each muscle portion were collected and stored as described above. Samples for colour, biochemistry and proteomic evaluation were obtained randomly starting from the anterior end of the cut alternating anatomical position. Details about methods applied to evaluate colour and biochemical parameters were described by Hasan et al. (2021).

5.3.2 Extraction of sarcoplasmic proteins

A subsamples from six LL (n = 6) and six PM (n = 6) frozen (-80 °C) muscle samples from each ageing group (2-, 7- and 14 d) were used (total 36 samples; LL-01-2D – LL-06-2D, LL-01-7D – LL-06-7D, LL-01-14D – LL-06-14D, PM-01-2D – PM-06-2D, PM-01-7D – PM-06-7D, PM-01-14D – PM-06-14D) for the extraction and isolation of sarcoplasmic proteomes. The extraction and other necessary procedures were optimized in the laboratory of the Manitoba Centre for Proteomics and System Biology (Winnipeg, MB, Canada). Briefly, 50-60 mg of iced-thawed muscle tissue sample devoid of any subcutaneous fat and connective tissue was cut using 70% ethanol cleaned blades and weighed on an electronic balance. Each sample was homogenized four times in 500 µl of lysis buffer solution (50 mM HEPES, 5 mM EDTA, pH 7.5; 150 mM NaCl, 1% Triton X100, 1X Protease inhibitor) for 20 sec/cycle with 60 s cooling period on ice each time by using a tissue homogenizer (THP115, 115-V, 144-W, 5000-35000 rpm, OMNI International Inc., USA). The homogenate was then centrifuged at 13,000 g for 10 min at 4 °C (SORVALL LEGEND Micro 21R centrifuge, Thermo Fisher Scientific, Germany) and the supernatant was transferred to another microcentrifuge tube and the final volume obtained was recorded. The supernatant was kept in ice for 5 min and then stored at -80 °C for subsequent analysis. From each muscle sample extract, the protein concentration of the sarcoplasmic proteome was measured in duplicate by the Bradford assay method (Bradford, 1976), using a protein assay kit (Thermo Fisher Scientific, USA).

5.3.3 Preparation, purification, and digestion of protein samples

The preprocessing of protein samples was performed in three steps namely reduction, alkylation and quenching. Firstly, for reduction, a 200 µl aliquot from protein stock was taken in a microcentrifuge tube and 20.0 µl of 20% sodium dodecyl sulphate (SDS) were added to each tube to increase the solubility, reaching a final 2% SDS concentration. Then, 20.0 µl of 100 mM

dithiothreitol (DTT) was added to the tubes (final concentration of DTT 10 mM) and after vortex mixing, the sample tubes were incubated at 57 °C for 30 min. Secondly, after cooling down the reduced incubated sample, alkylation was done by adding 20.0 µl of 500 mM iodoacetamide (IAA) to get a final IAA concentration of 50 mM. After mixing well, the sample tubes were placed in a dark place at room temperature for 45 min. Lastly, quenching was done to minimize the excess IAA in the sample mixture by adding 34.0 µl of 100 mM DTT to each tube and then all sample tubes were vortexed for 10 min.

For purification and digestion, 21.1 µl of sample (containing 100 µg protein) was pipetted in each microcentrifuge tube and 10 µl SP3 beads (from 20 µg/µl preparation) were added. To adjust the pH at 7.0, 21.1 µl of 200 mM HEPES was added. After adding 121.9 µl of acetonitrile (70% of final concentration) to each tube, incubated samples were placed in an agitator at room temperature for 18 min and checked for clumping. Then, the sample tubes were put on a magnetic stand and the supernatant was removed. The SP3 beads were then washed twice with 70% ethanol and one time with 100% acetonitrile. Trypsin was first dissolved in 250 µl of 50 mM digestion buffer (HEPES at pH 8.0) and 50 µl of trypsin solution were added to each tube to maintain the final protein concentration of 2.0 µg/µl. Samples were then sonicated for 20 s to disperse the beads and incubated for 16 h at 37 °C. After removing the sample tubes from the incubator, samples were sonicated for 20 s, put on the magnetic stand after spinning the tubes quickly and the supernatant was transferred to another micro-centrifuge tube. Finally, the SP3 beads were washed with 50 µl digestion buffer, sample tubes were sonicated again for 20 s, put on the magnetic stand prior to quick spin and the supernatant was transferred to the previously collected peptide sample tubes. The samples were then stored at -80 °C for further analysis.

5.3.4 Tandem mass tag peptide labelling

Prior to peptide labelling by TMT10Plex isobaric label [Thermo Scientific, Rockford, IL, USA; Coleman et al. (2020)] peptides from digested protein samples were measured using a quantitative fluorometric peptide assay kit according to the manufacturer's (Thermo Scientific, Rockford, IL, USA) procedure. TMT label reagents were first equilibrated at room temperature. For each vial containing 0.80 mg of label, 41 µl of anhydrous acetonitrile was added to each tube, the reagent was dissolved by vortexing for 5 min and the tube was centrifuged briefly to solubilize the label. At first, 41 µl of the prepared TMT label reagent was added to 100 µl of sample

(containing 25-100 µg protein digest) in a microcentrifuge tube and the labelling reaction was incubated for 60 min at room temperature. Then, 8.0 µL of 5% hydroxylamine were added to the sample followed by incubation for 15 min to quench the reaction. After that, equal amounts of each sample were combined in another microcentrifuge tube, which was subjected to Speedvac vacuum concentration (Thermo Fisher Scientific, USA) for drying. Finally, samples were cleaned-up on peptide desalting spin columns (Thermo Fisher Scientific, USA). Additionally, a reference TMT-peptide pool was prepared for TMT LC-MS/MS analysis. The pool was prepared by combining equal volumes of samples LL-01-2D, LL-01-7D, and LL-01-14D, and treated in a similar fashion as the individual samples. An aliquot of the pool was added to every set of TMT sample to account for any instrumental variations across the LC-MS/MS runs.

5.3.5 Liquid chromatography-mass spectrometry analysis

The analysis of TMT labeled protein digests (peptides) was carried out (Fakankun et al., 2021) on an Orbitrap Exploris 480 instrument (Thermo Fisher Scientific, Bremen, Germany). Samples were introduced into the Orbitrap instrument at 2.0 µg per injection, using an Easy-nLC 1000 system (Thermo Fisher Scientific). The mobile phase A and B were 0.1% (v/v) formic acid, and 0.1% (v/v) formic acid in LC-MS grade 80% acetonitrile, respectively. The gradient separation of peptides was accomplished on a C18 column [Luna C18(2), 3 µm particle size, Phenomenex, Torrance, CA] packed in-house in Pico-Frit (100 µm X 30 cm) capillaries (New Objective, Woburn, MA). The separation of peptide was done using the gradients as follow: increase of phase B 3-7% over 5 min, 7-28% over 204 min, 28-48% over 15 min, 48-95 % over 1 min, with the final 95% phase B elution for 15 min at a flow rate of 300 nL/min.

Data acquisition redundant was used for the data-dependent (DD) analysis configuring the full MS/DD-MS/MS setup in the positive mode. The spray voltage was fixed to 2.3 kV with funnel RF level at 40, and then the capillary was heated at 275 °C. Then, the survey scans were acquired at a resolution of 120,000 (at m/z 200), covering the mass range of 375-1575 m/z, with a 50 ms time for maximum ion injection, and a normalized automatic gain control (AGC) target of 300%. For the triggering of MS2 scan, likely 20 most sufficient ions were selected for fragmentation at 36% normalized collision energy, with the intensity threshold at 2×10^4 . A normalized AGC target value for fragment spectra was set at 200%, and acquired at a resolution of 45,000, with a 100 ms maximum ion injection time, and an isolation width fixed at 0.7 m/z. At the end, the dynamic

exclusion of previously selected masses was enabled for 45 s, while the charge state filtering was limited to 2-6, the peptide match was set to preferred, as well as isotope exclusion was on.

5.3.6 MS/MS protein identification and data processing

Each LC-MS/MS run was searched for tryptic peptides against the bison protein database using X! Tandem software (cyclone 2012.10.01.1) with standard Orbitrap settings: 20 ppm each for parent and fragment ions (Coleman et al., 2020). The TMT intensities of peptide were integrated over a window of ± 3 mDa and the isotopic overlap was corrected/adjusted utilizing the batch-specific matrix supplied with the TMT label kit. Labels were assigned sequentially as TMT0 to TMT9. Standard variable post-translational modification (PTMS) including oxidation, phosphorylation, cyclization and deamidation were permitted. Overall, identification efficiency was highly stable: ~ 30 k peptides from ~ 104 k spectra per run. Protein level quantification needed at least two distinct peptides with $\log(e)=-1.5$ expectation values, resulting in extremely confident protein assignments of $\log(e)=-3$. $\log(e)$ can be defined as the estimation of likelihood based on the expected number of random matches among two peptides. Peptide to protein assignment was handled by X! Tandem. The intensity of each protein for each TMT channel was computed as the sum of the intensities of the member peptides, then converted into \log_2 for differential analysis. These \log_2 expression matrices were normalized (mean = 0, standard deviation = 1) for simplified differential analysis. Total matrix assembly relied on a common pool sample occupying the last TMT channel in every run. On a protein-by-protein basis, the nine TMT individual sample channels were corrected by subtracting out the reference pool value encoded in the last TMT channel.

5.3.7 Statistical analysis

Data were analyzed by using the Perl 6 programming language (Perl Inc.). The standard deviation pre-normalization for all runs and channels was 2.38; this was used as a scaling factor between (corrected) normalized values back up to the \log_2 scale. These values were also all offset by a constant of 21.35, the pre-normalization average for all runs and channels. Then the pairwise t-test was conducted, using six ($n = 6$) replicates, to investigate the comparisons between different ageing periods (time points) and muscle types (LL and PM). Multiple-testing corrections were not applied to P scores, and any difference with $P < 0.05$ were considered as a possibility for biological

expedition. The proteins were considered as significantly more or less abundant with the fold change value of > 1.5 and $P < 0.05$.

5.3.8 Bioinformatics analysis

To investigate the overall expression pattern of differentially abundant proteins in LL and PM muscles at different ageing times, a Heatmap was generated by Morpheus (<https://software.broadinstitute.org/morpheus/>) and the output is presented in **Figure 5.1**. Additionally, the distribution of differential proteins (**Figure 5.2**) was prepared with the aid of another online tool called InteractiVenn (<http://www.interactivenn.net>; Heberle et al. 2015). Then, the protein-protein interaction networks between identified proteins (**Figure 5.3**) were examined using String v11 (<https://string-db.org/>; Szklarczyk et al. 2019) with the inflation parameter of 3.4 in Markov clustering (MCL; Zhai et al., 2020). The proteins are presented as network nodes, and the predicted functional interactions are represented as edges. The proteins were mainly grouped according to their function enlisted in the KEGG Pathway database (<https://www.genome.jp/kegg/pathway.html>) and the Reactome Pathway database (<https://reactome.org>; Fabregat et al. 2018) and literature search was done to investigate the proteins with limited function. The functional clusters of identified proteins were generated with results obtained from the Panther database (<http://pantherdb.org/>) and presented in **Figure 5.4**. Finally, the Ingenuity pathway analysis (IPA, QIAGEN, USA) was performed to examine the most important pathway involved (**Figure 5.5**) and the most important protein-protein interaction networks (**Figure 5.6**).

5.4 Results

5.4.1 Colour and biochemical characteristics

Details about colour and biochemical parameter results were described by Hasan et al. (2021). Briefly, myoglobin (Mb; LL = 6.95 vs PM = 8.12 mg/g) and fat content (LL = 1.55 vs PM = 2.27 %) were included as a covariate in the model due to difference among muscles ($P < 0.05$). LL showed greater colour stability (higher a^* value and lower surface discolouration; $P < 0.05$) compared to PM, as well as LL presented lower malondialdehyde (MDA), 4-hydroxy-2-nonenal (HNE) and carbonyl content (CAR) content compared to PM ($P < 0.05$). The pH in bison samples was not influenced by muscle type, retail display periods or their interaction effects ($P > 0.05$);

however, only 14 d (5.65) aged steaks exhibited lower pH values than steaks aged for 7 d (5.79). In both LL and PM muscles, MDA exhibited the highest correlation to a^* ($r = -0.78$; $P < 0.01$) and discolouration score ($r_s = 0.82$; $P < 0.01$), and in both muscles, MDA contributed as the main factor for changes in redness, being more remarkable in PM ($R^2 > 0.72$) than in LL ($R^2 > 0.62$). However, the pH, HNE and CAR explained up to 6 % maximum variation of the colour traits in LL steaks, while only affected by 1% in PM. On the other hand, the principal component analysis indicated that 7 and 14 d aged PM and LL steaks displayed at d 0 were showed a close association with redness and located distantly from oxidation compounds, indicating the stability of more red colour and less oxidation; however, 7 and 14 d aged PM steaks displayed at d 4 segregated away from LL, and PM was closely related to oxidation compounds and located far away of redness (representing high oxidation level and less red colour).

5.4.2 Comparison of proteomic profiles between LL and PM muscles at each postmortem ageing period

A total of 576 proteins were identified by TMT based proteomic analysis in both LL and PM muscles and among those, 97 proteins were found as differentially abundant (fold change > 1.5 , $P < 0.05$) from the three comparisons between muscles during postmortem storage periods (PM vs LL at 2 d, 7 d and 14 d; **Table 5.1**). Among these proteins, the major protein groups identified in muscles (PM vs LL) are related to electron transport chain (ETC), tricarboxylic acid cycle (TCA), ATP production and transport, carbohydrate metabolism, lipid or fatty acids oxidation, chaperones, oxygen transport, calcium signaling, muscle contraction, and protein synthesis.

In **Figure 5.1**, the Heatmap presents the overall expression of all differentially abundant proteins in LL and PM muscles from three different ageing periods. By careful investigation of the Heatmap, protein expression changing patterns are quite visible from LL to PM muscles, from LL-D2 to LL-D7, and from PM-D2 to PM-D7 samples. The blue and red colours indicated decreased and increased protein expression levels, respectively (**Figure 5.1**). The Venn diagram (**Figure 5.2**) represents the overall distribution of 97 differentially abundant proteins identified in LL and PM muscles from 2, 7, and 14 ageing periods and 31 differential proteins were found regardless of postmortem ageing times. Most of the differential proteins were identified at 2 d postmortem (87 proteins), whereas 7 d (45 proteins) and 14 d (43 proteins) exhibited almost similar number of proteins between them. This indicates that changes in protein expression occur mainly at the early

postmortem stage (2 d) compared to the later periods (7 d and 14 d). **Figure 5.3** exhibits the protein-protein interactions patterns among the differentially abundant proteins identified at 2-, 7- and 14 d postmortem. In **Figure 5.3a**, three visible clusters of proteins were found with proteins involved in ETC, fatty acid oxidation, and muscle contraction at 2 d postmortem. The only protein-protein interactions cluster at 7 d postmortem (**Figure 5.3b**) included muscle contraction proteins, whereas **Figure 5.3c** shows a slightly different clustering pattern including carbohydrate metabolism, fatty acid oxidation, and muscle contraction proteins at 14 d postmortem.

The overall distribution of differentially abundant protein in LL and PM muscles from three ageing periods based on their functional clusters is presented in **Figure 5.4**. The identified proteins were related to cytoskeleton (involved both in structure and muscle contraction), metabolic enzymes, chaperones, and cellular transportation. They were distributed differently at three ageing periods. The overall changes in muscles' biochemical and colour attributes could be due to the metabolic enzymes (ETC, TCA cycle, fatty acid oxidation and carbohydrate metabolism) at 14 d (31%), cytoskeletal proteins at 2 d (24%), 7 d (32%) and 14 d (30%) and transporter proteins (ATP and oxygen transport) at 2 d (17%) postmortem periods (**Figure 5.4**). The most important differentially abundant proteins during comparisons of PM and LL at 2, 7 and 14 d postmortem and their expression patterns in ETC complexes are illustrated in **Figure 5.5**. It is clear from the figure that at 2 d postmortem, proteins from complexes II and V of ETC were upregulated. In contrast, the upregulation of proteins from complexes II, IV and V is found at 7 d and from complexes II, III, IV and V were noticed at 14 d postmortem. Moreover, a gradual involvement of number of ETC complexes were also evident in the progression of 2 d (2), 7 d (3), and 14 d (4) ageing periods. These findings suggest that at 14 d postmortem, the maximum number of ETC complexes and their associated proteins were activated and contributed to muscles' oxidative changes. By investigating the protein-protein interaction networks at different ageing periods when comparing PM and LL, some critical networks were explored using the Ingenuity pathway analysis (IPA) software and are presented in **Figure 5.6**. IPA is a very efficient tool for in-depth investigation of protein-protein interaction networks analysis.

In PM muscles at 2 d postmortem (**Table 5.1**), most of the identified differential proteins involved in ETC, fatty acid oxidation, TCA cycle, ATP and oxygen transport, and muscle contraction (50% proteins) exhibits increased expression when compared to LL. Similarly, in PM muscles at 7 d postmortem, fatty acid oxidation, ATP and oxygen transport, and muscle contraction

proteins shows increased expression level than LL (**Table 5.1**). Furthermore, in PM muscles at 14 d postmortem, most of the proteins from fatty acid oxidation and oxygen transport, almost 50% of the muscle contraction proteins, few ETC proteins (2) and one ATP transport protein appears with increased expression levels related to LL (**Table 5.1**). However, the other protein groups exhibited different identification patterns. The differentially identified proteins presented in **Table 5.1** are described below in detail.

Table 5.1. Differentially abundant proteins between bison *longissimus lumborum* and *psoas major* muscles at 2 d, 7 d and 14 d postmortem (fold change >1.5; $P < 0.05$) ageing periods

Protein Description	Specific Function	Accession Number	Abbreviations (String Code)	Fold Change		
				PM vs. LL at 2 d	PM vs. LL at 7 d	PM vs. LL at 14 d
Electron Transport Chain (ETC)/ Oxidative Phosphorylation						
Succinate dehydrogenase [ubiquinone] cytochrome b small subunit, mitochondrial isoform X1	Complex II component and blocks generation of excess reactive O ₂	XP_010828629.1	SDHD	1.61		1.55
Succinate dehydrogenase [ubiquinone] flavoprotein subunit, mitochondrial	Complex II component and metal ion binding	XP_010830641.1	SDHA	1.53		
Cytochrome c	Complex III and IV component, heme and metal ion binding	XP_010853678.1	TACO1 (LOC104999778)	1.58		
ATP synthase subunit gamma, mitochondrial isoform X1	Complex V component and ATP synthesis	XP_010851442.1	ATP5C1	1.79		
ATP synthase subunit delta, mitochondrial	Proton transportation and ATP synthase activity	XP_010842883.1	ATP5D	1.55		
ATP synthase subunit epsilon, mitochondrial	Complex V component, hydrogen ion transport, and ATP synthesis	XP_010837454.1	ATP5E	1.67		
ATP synthase F(0) complex subunit B1, mitochondrial	Complex V component and ATP synthesis	XP_010829138.1	ATP5F1	1.52		
ATP synthase F(0) complex subunit C2, mitochondrial	Complex V component and ATP synthesis	XP_010831422.1	ATP5G2			1.53
ATP synthase-coupling factor 6, mitochondrial	ATP synthesis coupled proton transport	XP_010836757.1	ATP5J	1.55		
ATP synthase subunit f, mitochondrial	Complex V component, hydrogen ion transport, and ATP synthesis	XP_010844025.1	ATP5J2	1.58		
TCA Cycle						
Citrate synthase, mitochondrial isoform X1	Citric acid synthesis	XP_010837550.1	CS	1.58		
Malate dehydrogenase, mitochondrial	NADH production	XP_010852621.1	MDH2	1.53		
Succinyl-CoA ligase, subunit beta, mitochondrial	GTP production	XP_010852852.1	SUCLG2	1.82	1.52	
Mitochondrial pyruvate carrier 2	Mitochondrial uptake of pyruvate, pyruvate transport	XP_010844313.1	MPC2	1.74		
2-oxoglutarate dehydrogenase, mitochondrial isoform X1	TPP binding and oxidoreductase activity	XP_010827341.1	OGDH		-1.51	

ATP Transport Related

Phosphate carrier protein, mitochondrial isoform X1	Transmembrane phosphate carrier	XP_010829873.1	SLC25A3	1.71	1.52	1.59
ADP/ATP translocase 1	Catalyzes the exchange of ADP and ATP across the membrane	XP_010834070.1	SLC25A4	1.84	1.61	

Transporter/carrier Proteins

Potassium channel subfamily K member 10	Transporter or carrier proteins (K ion channel binding)	XP_010843536.1	KCNK10	1.99	1.95	
Thiosulfate sulfurtransferase	Cellular transport, detoxification, and transferase activity	XP_010858855.1	TSTD3	1.95		
Putative sodium-coupled neutral amino acid transporter 10 isoform X1	Membrane component and neutral amino acid transport	XP_010854613.1	SLC38A10			-1.67

Carbohydrate Metabolism

Glycogen phosphorylase, muscle form	Glycogen catabolism	XP_010836307.1	PYGM	-1.79	-1.77	-2.19
Glycogen phosphorylase, brain form	Glycogen catabolism	XP_010834913.1	PYGB	-1.53		-1.62
Phosphoglycerate kinase 2	ATP utilization	XP_010861335.1	PGK2	-1.53		
Phosphoglucomutase-1 isoform X2	Magnesium binding	XP_010832195.1	PGM1	-1.56		
ATP-dependent 6-phosphofructokinase, muscle type	ATP binding and utilization	XP_010835801.1	PFKM			-1.75
L-lactate dehydrogenase	Lactate to pyruvate conversion and NADH production	XP_010854247.1	LDHB	1.73		1.54

Lipid Metabolism/Fatty Acid Oxidation

Fatty acid-binding protein, heart	Fatty acid binding and inhibit cell growth	XP_010835191.1	FABP3	2.33	1.93	1.82
Fatty acid-binding protein, epidermal	Fatty acid binding and transport	XP_010861708.1	FABP5	1.74	1.57	1.60
Acetyl-CoA acetyltransferase, mitochondrial isoform X1	Beta oxidation	XP_010861136.1	ACAT1	2.10	1.69	1.65
Succinyl-CoA:3-ketoacid coenzyme A transferase 1, mitochondrial	Ketone body metabolism	XP_010852017.1	OXCT1	2.07	1.82	1.80
Very long-chain specific acyl-CoA dehydrogenase, mitochondrial isoform X1	Beta oxidation, FAD binding and dehydrogenase	XP_010845646.1	ACADVL	1.56		
Medium-chain specific acyl-CoA dehydrogenase, mitochondrial	Beta oxidation, FAD binding and dehydrogenase	XP_010856422.1	ACADM (LOC105001724)	1.97	1.67	1.67
Short-chain specific acyl-CoA dehydrogenase, mitochondrial isoform X1	Beta oxidation, FAD binding and oxidoreductase activity	XP_010826938.1	ACADS	1.93	1.65	1.64
Hydroxyacyl-coenzyme A dehydrogenase, mitochondrial	NAD/NADP binding and oxidoreductase activity	XP_010856864.1	HADH	1.82	1.59	1.56
Enoyl-CoA hydratase	Beta oxidation, NADH production	XP_010838888.1	HADHA	1.57		

Muscle Contraction

Myosin regulatory light chain 2	Calcium ion binding	XP_010839683.1	MYL2	1.88	1.93	1.85
Myosin light chain 3	Calcium ion binding	XP_010860678.1	MYL3	3.73	2.83	2.33
Myosin-7	Calcium ion binding	XP_010829714.1	MYH7	2.73	2.50	2.62

Tropomyosin alpha-1 chain isoform X2	Actin binding	XP_010831764.1	TPM1	1.66	1.55	
Tropomyosin alpha-3 chain isoform X1	Actin binding	XP_010836667.1	TPM3	1.95	1.72	1.85
Tropomyosin beta chain isoform X1	Actin binding	XP_010844389.1	TPM2	1.79	1.80	1.79
Tropomodulin-2 isoform X1	Tropomyosin binding	XP_010837785.1	TMOD2	1.75	2.22	1.80
Troponin C, slow skeletal muscle	Calcium ion binding	XP_010850036.1	TNNC1	1.62		1.67
Troponin I, slow skeletal muscle	Prevents muscle contraction	XP_010829410.1	TNNI1	1.62		1.54
Thymosin beta-4	Actin binding	XP_010828621.1	TMSB4X	1.56		
Up-regulated during skeletal muscle growth protein 5	Transmembrane protein	XP_010857721.1	USMG5	1.56		
Troponin C, skeletal muscle	Calcium ion binding	XP_010833333.1	TNNC2	-1.68		
coiled-coil domain-containing protein 25	Receptor protein and cytoskeleton rearranges during cell motility	XP_010837897.1	CCDC25	-1.87	-1.74	
myosin-binding protein H	Myosin binding	XP_010852420.1	MYBPH	-1.51		
Alpha-actinin-1 isoform X1	Actin and Calcium binding	XP_010845002.1	ACTN1			-1.53
Alpha-actinin-3	Actin and Calcium binding	XP_010836049.1	ACTN3 (LOC104986993)	-2.45	-1.96	-1.79
Alpha-actinin-3-like	Actin binding	XP_010836047.1	SSX2IP (LOC104986992)	-2.19	-1.85	-1.62
Alpha-actinin-4	Actin and Calcium binding	XP_010847616.1	ACTN4	-1.56		
Obscurin	Muscle structure, cell adhesion and ATP binding	XP_010845591.1	OBSL1	-1.58		
14-3-3 protein beta/alpha	Muscle structure, signal transduction	XP_010839277.1	YWHAB	-1.59		
14-3-3 protein gamma	Muscle structure	XP_010852658.1	YWHAG	-1.62		
Myozenin-1	Actin and Z disc binding	XP_010850615.1	MYOZ1	-1.95	-1.66	
Myomesin-2	Actin and kinase binding	XP_010833576.1	MYOM2			-1.52
Myopalladin isoform X1	Actin binding and sarcomere organization	XP_010850458.1	MYPN	-2.85	-2.25	
LOW QUALITY PROTEIN: immunoglobulin-like and fibronectin type III domain-containing protein 1	Serine protease inhibitor (Metalloendopeptidase inhibitor)	XP_010829429.1	IGFN1 (WFIIKN2)	-1.67	-1.58	
Calcium Signaling						
Calsequestrin-1	Calcium storage and binding	XP_010845176.1	CASQ1	-2.14	-1.82	-1.58
Protein S100-A1	Calcium binding	XP_010836708.1	S100A1		-1.53	
Muscle Structure Component						
Leucine zipper putative tumor suppressor 3 isoform X1	Cell cycle (cell growth prevention)	XP_010834798.1	LZTS3 (LOC104986066)	5.82	6.19	4.82
Collagen alpha-2(VI) chain	Muscle structure, connective tissue	XP_010833290.1	COL6A2	1.59	1.66	1.52
PDZ and LIM domain protein 7 isoform X3	protein-protein interaction	XP_010844848.1	PDLIM7	-1.72		
Protein CFAP46, partial	Muscle structure and motility	XP_010857855.1	CFAP46			-1.69
CAP-Gly domain-containing linker protein 1 isoform X1	Muscle Structure	XP_010839621.1	CLIP1	-2.68	-2.41	-1.99

LOW QUALITY PROTEIN: filamin-C	Muscle structure	XP_010830065.1	FLNC	-1.59		
LOW QUALITY PROTEIN: keratin, type I cytoskeletal 14-like	Muscle structure	XP_010840848.1	KRT14 (LOC104990465)	-1.59		
LOW QUALITY PROTEIN: titin	Muscle structure and ATP binding	XP_010858056.1	TTN	-1.93	-1.79	-1.67
Chaperones						
Peptidyl-prolyl cis-trans isomerase A	Protein folding and MAPK/ERK activation	XP_010829539.1	PPIA (LOC104981978)	-1.83	-1.87	-2.10
Heat shock protein 27 kDa	Protein folding, actin organization and stress resistance	XP_010852626.1	HSPB1	-1.79	-1.52	
Alpha-crystallin B chain	Chaperone-like activity in stress condition	XP_010861174.1	CRYAB	-1.58		
10 kDa heat shock protein, mitochondrial	Protein folding, ATP binding and, ATPase activity	XP_010859205.1	HSPE1	1.73	1.55	
Oxygen Transport						
Hemoglobin subunit alpha-I/II	Heme and O ₂ binding, and H ₂ O ₂ detoxification	XP_010855734.1	HBA1 (LOC105001245)	1.82	1.88	1.79
Hemoglobin subunit beta	Heme, metal ion and O ₂ binding	XP_010830570.1	HBB	1.82	1.95	1.74
Protein Synthesis						
Transcription						
CCR4-NOT transcription complex subunit 3-like	Transcription repression	XP_010834567.1	CNOT8 (LOC104985867)	-3.07	-2.66	-2.13
Zinc finger protein 606 isoform X2	Transcription regulation by binding RNA Polymerase II	XP_010855944.1	ZNF606 (LOC105001395)	-1.75	-1.59	
Heterogeneous nuclear ribonucleoprotein K isoform X1	Transcription regulation, DNA and RNA binding, repressor	XP_010838359.1	HNRNPK	-1.52		
Cysteine and glycine-rich protein 3	Positive modulator/cofactor for myogenic transcription factor MYOD1	XP_010856729.1	CSRP3	-1.92		
Transcription elongation factor B polypeptide 1	Ubiquitin dependent catabolic protein, protein synthesis, translation	XP_010845244.1	TCEB1	-1.71		
Heterogeneous nuclear ribonucleoprotein A/B	RNA binding and transcription termination	XP_010844805.1	HNRNPAB	1.65		1.69
Translation						
Elongation factor 1-alpha 2	Protein biosynthesis, GTP binding, Translation	XP_010834950.1	EEF1A2	-1.52		
Eukaryotic translation initiation factor 5A-1	Translation initiation, elongation, protein synthesis and transport	XP_010845638.1	EIF5AL1	-1.56		
Other Functions						
Antioxidant						
Glutathione S-transferase Mu 1-like	Neutralizes reactive oxygen species	XP_010829201.1	GSTM7 (LOC104981668)	-1.61		
Hydrolases						
14 kDa phosphohistidine phosphatase, partial	Histidine phosphatase	XP_010852119.1	PHPT1	-1.83	-1.54	-1.51
Carboxymethylenebutenolidase homolog	Cysteine hydrolase	XP_010845828.1	CMBL	-1.51		
Aspartyl aminopeptidase isoform X1	Aminopeptidase, metallopeptidase, Zinc binding	XP_010859551.1	DNPEP	-3.18		

Purine Metabolism

GTP:AMP phosphotransferase AK3, mitochondrial isoform X1	ATP and GTP binding, and adenylate kinase activity	XP_010859018.1	AK3	1.62	1.51	1.51
Adenylate kinase isoenzyme 1	ATP binding and utilization	XP_010855189.1	AK1			-1.53
Bifunctional purine biosynthesis protein PURH	Purine biosynthesis, transferase, and IMP synthase activity	XP_010859447.1	ATIC		-1.53	

Demethylation

Protein phosphatase methyl esterase 1 isoform X1	Protein demethylation	XP_010847156.1	PPME1	1.60		
--	-----------------------	----------------	-------	------	--	--

DNA Binding

Non-histone chromosomal protein HMG-17	Nucleosomal DNA binding	XP_010828409.1	HMGN2	1.59	1.60	1.56
--	-------------------------	----------------	-------	------	------	------

Protein Ubiquitination

E3 ubiquitin-protein ligase HERC2 isoform X1/ HECT-type E3 ubiquitin transferase	Protein ubiquitination and modification	XP_010851284.1	HERC2 (LOC104997998)	1.59		
Ubiquitin carboxyl-terminal hydrolase isozyme L3	Ubiquitin dependent protein catabolism, peptidase, esterase, and amidase activity	XP_010837967.1	UCHL3	-1.55		

Signal Transduction

Kelch-like protein 41	Regulation of Rac protein signal transduction and cell motility	XP_010847693.1	RABEPK	-2.23	-1.96	-1.64
Platelet glycoprotein 4/Glycoprotein IIIB	Cell signalling, immune response, and lipid utilization	XP_010846409.1	CD36 (LOC104994511)	1.56		
LOW QUALITY PROTEIN: ras-specific guanine nucleotide-releasing factor 1	small GTPase mediated signal transduction and regulation of Rho protein	XP_010841694.1	RASGRF1	1.85		

ADP = adenosine diphosphate; AMP = adenosine monophosphate; ATP = adenosine triphosphate; CS = citrate synthase; ETC = electron transport chain; FABP3 = Fatty acid-binding protein, heart; FABP5 = Fatty acid-binding protein, epidermal; GTP = guanosine triphosphate; HMGN2 = non-histone chromosomal protein HMG-17; LDHB = L-lactate dehydrogenase; MPC2 = mitochondrial pyruvate carrier 2; NADH = nicotinamide adenine dinucleotide; OGDH = 2-oxoglutarate dehydrogenase mitochondrial isoform X1; PPME1 = protein phosphatase methyl esterase 1 isoform X1; TCA = tricarboxylic acid cycle; LL = longissimus lumborum; PM = psoas major.

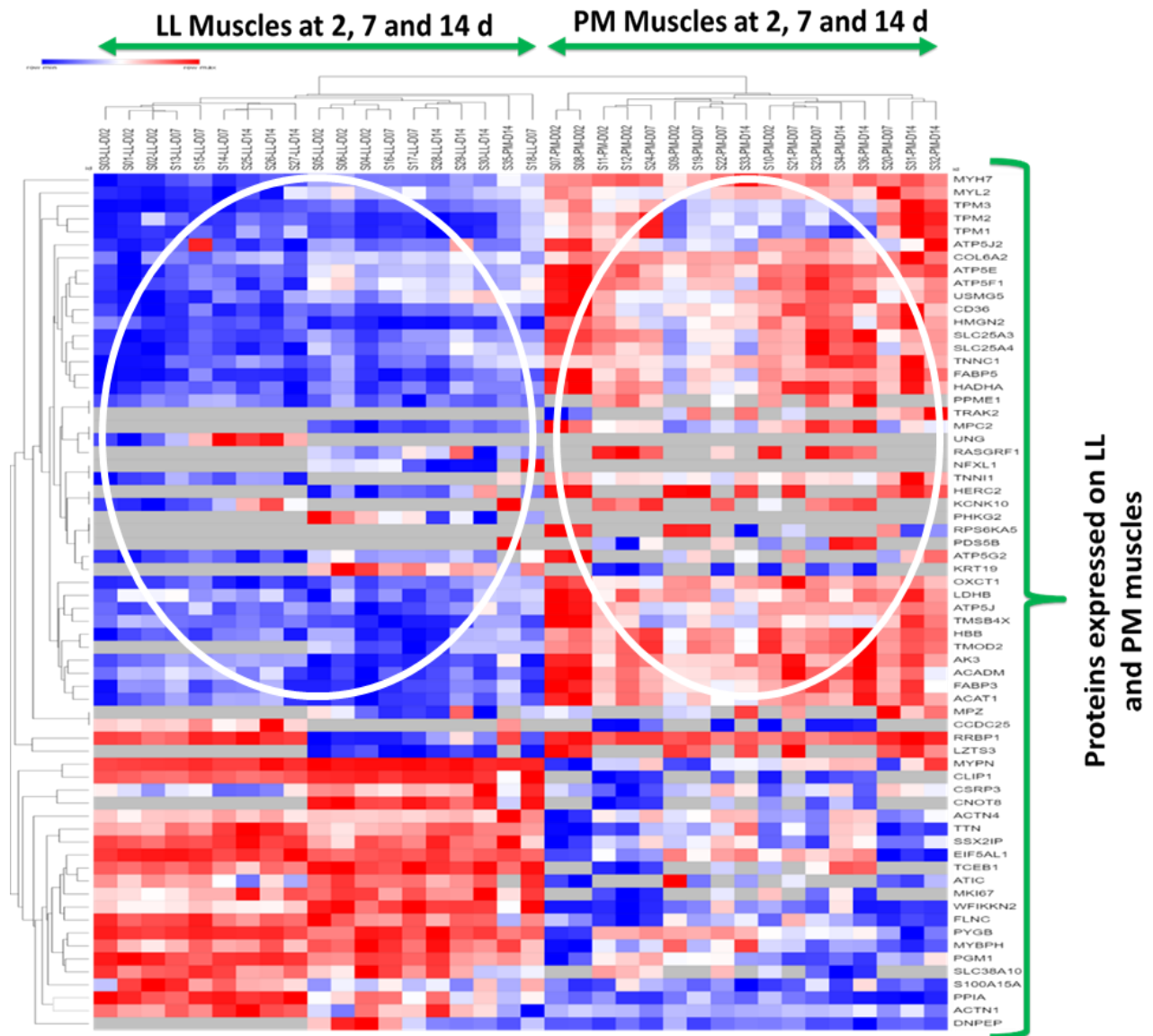


Figure 5.1. Heatmap showing overall expression of differential proteins ($P < 0.05$, > 1.5 -fold change) in bison *longissimus lumborum* and *psoas major* muscles from different ageing periods. (The left and right circles indicates the expression patterns of different proteins at 2, 7 and 14 d postmortem in LL and PM muscles, respectively.)

LL = *longissimus lumborum*; PM = *psoas major*

2, 7 and 14 d = 2 day, 7 day and 14 day postmortem

Blue colour: decreased expression of proteins; **Red colour:** increased expression of proteins



Figure 5.2. Distribution of differentially abundant proteins between bison *longissimus lumborum* and *psoas major* muscles at 2 d, 7 d and 14 d postmortem ageing.
 2-day, 7-day and 14-day = 2 d, 7 d and 14 d postmortem ageing

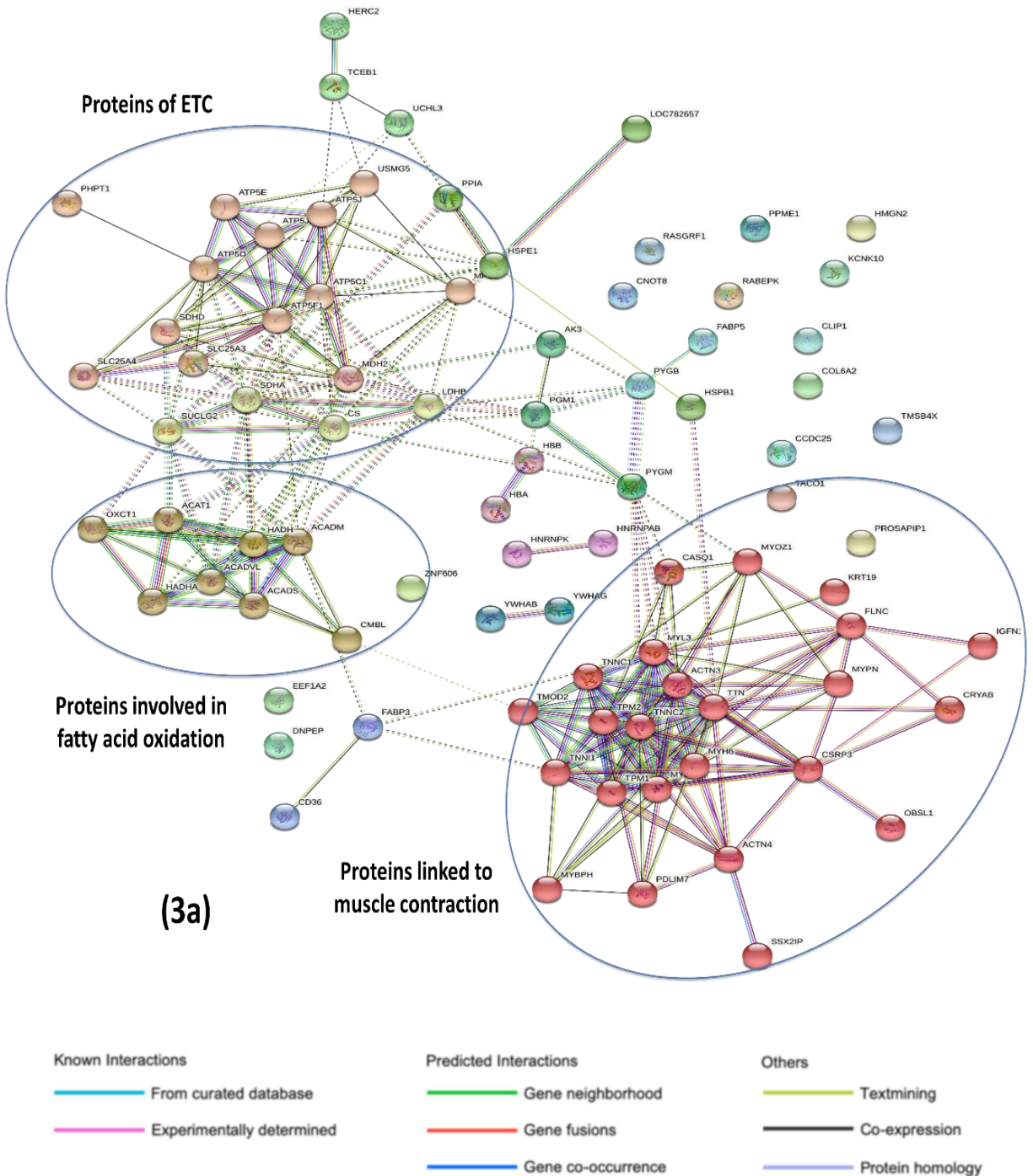
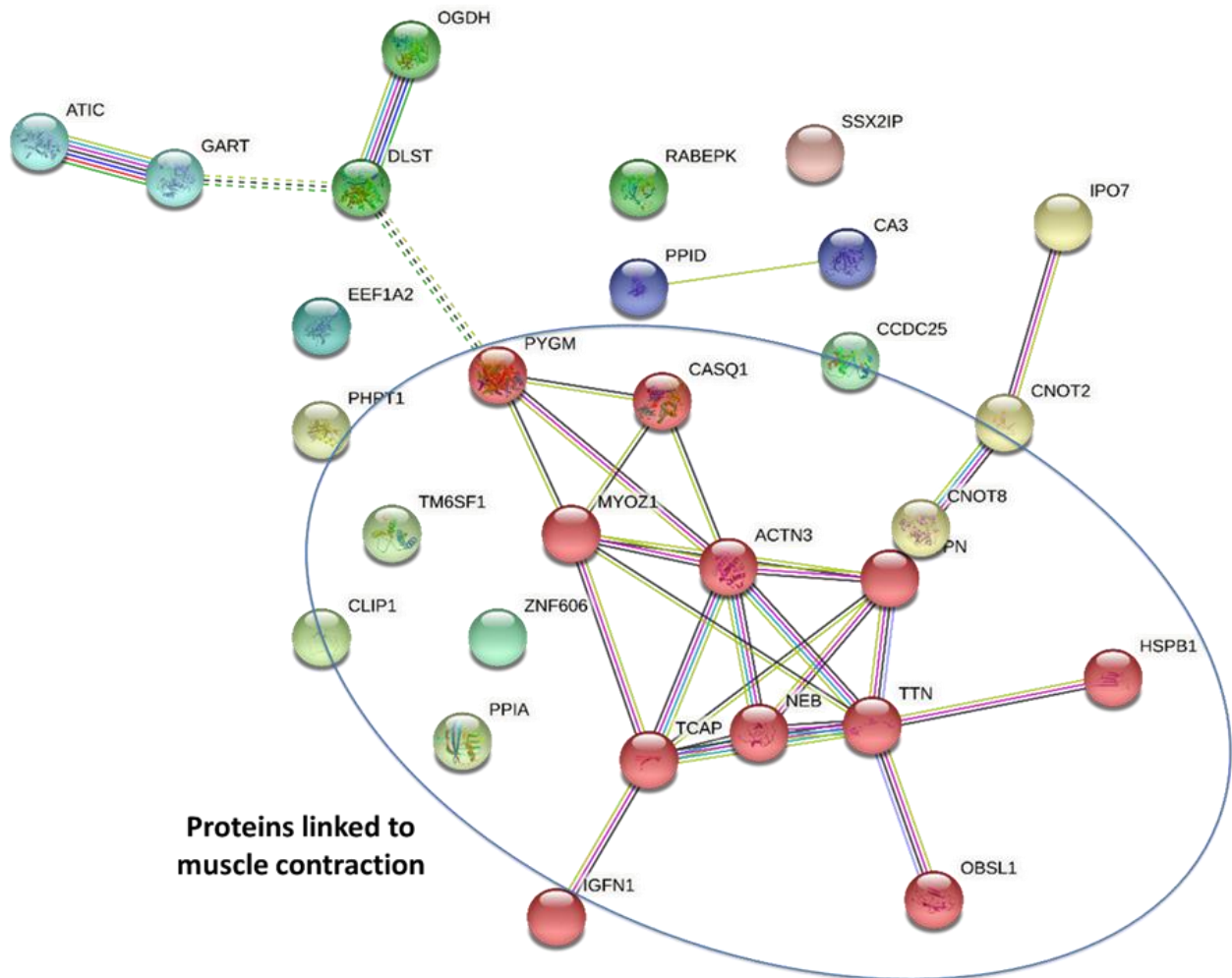


Figure 5.3. Protein-protein interaction networks of differential proteins between bison *longissimus lumborum* and *psoas major* muscles at (3a) 2 d postmortem, (3b) 7 d postmortem and (3c) 14 d postmortem ageing. (For more details on each protein and its function, please see the differentially abundant proteins listed on Table 5.1).

LL = *longissimus lumborum*; PM = *psoas major*. ETC = electron transport chain



Proteins linked to muscle contraction

(3b)

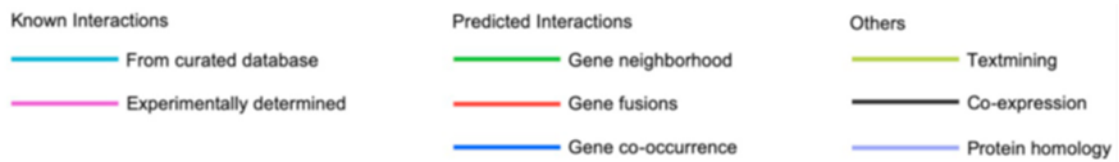


Figure 5.3. (Continued)

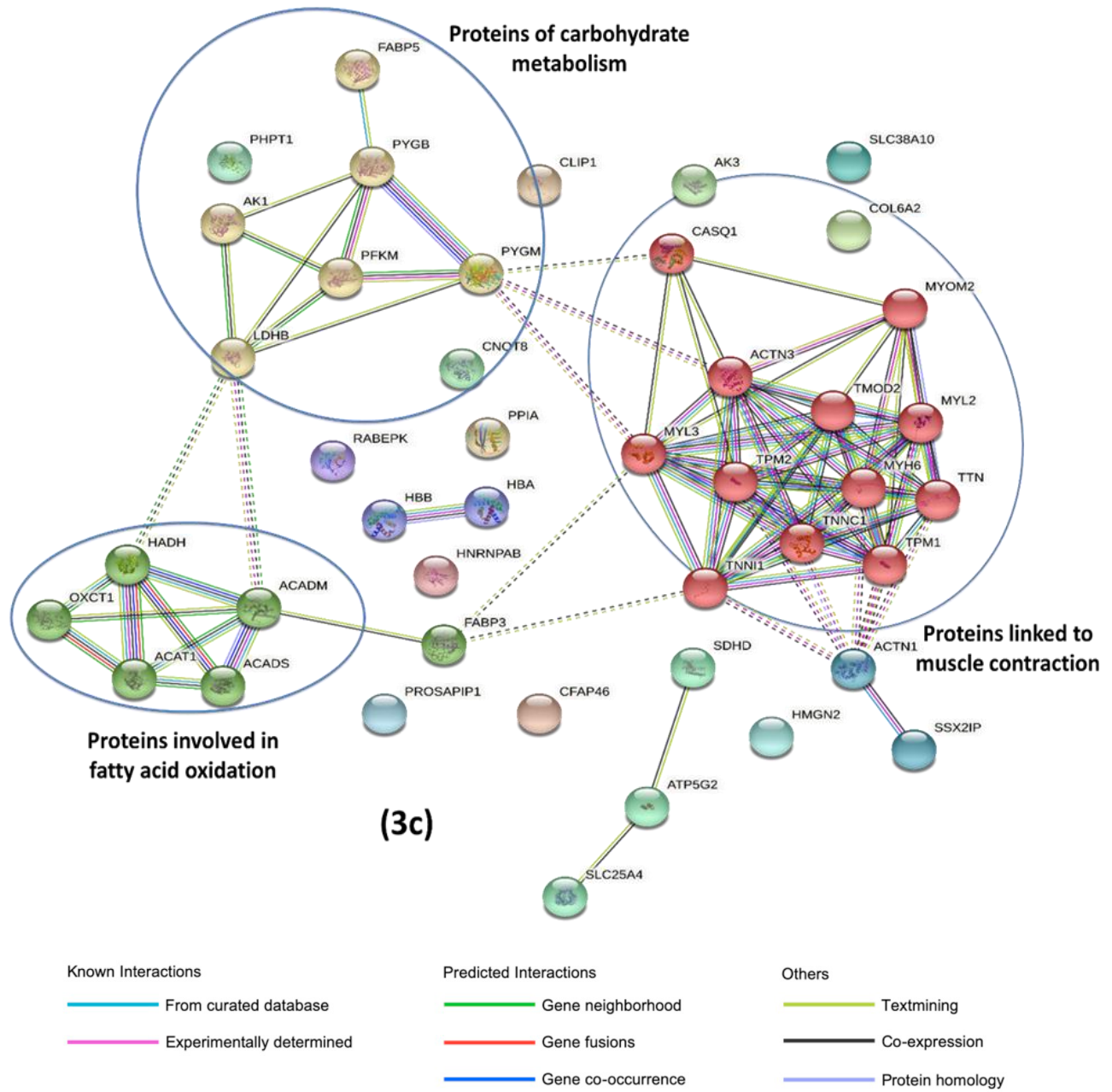


Figure 5.3. (Continued)

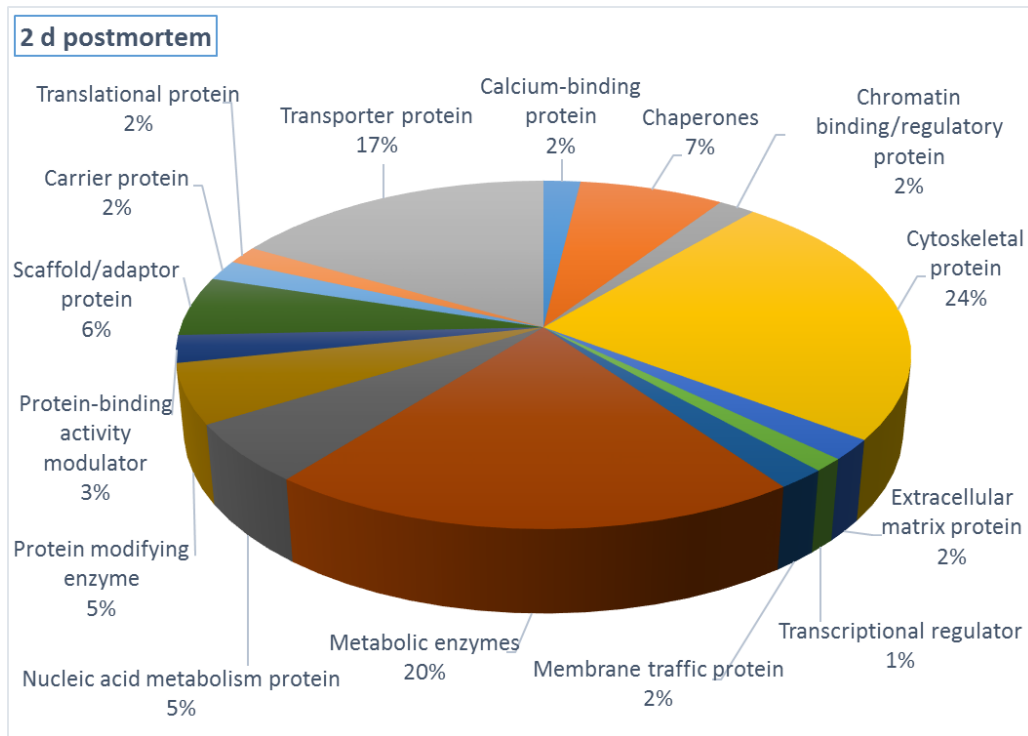


Figure 5.4. Distribution of the functional clusters of differential proteins between bison *longissimus lumborum* and *psaos major* muscles at 2 d, 7 d and 14 d postmortem ageing.

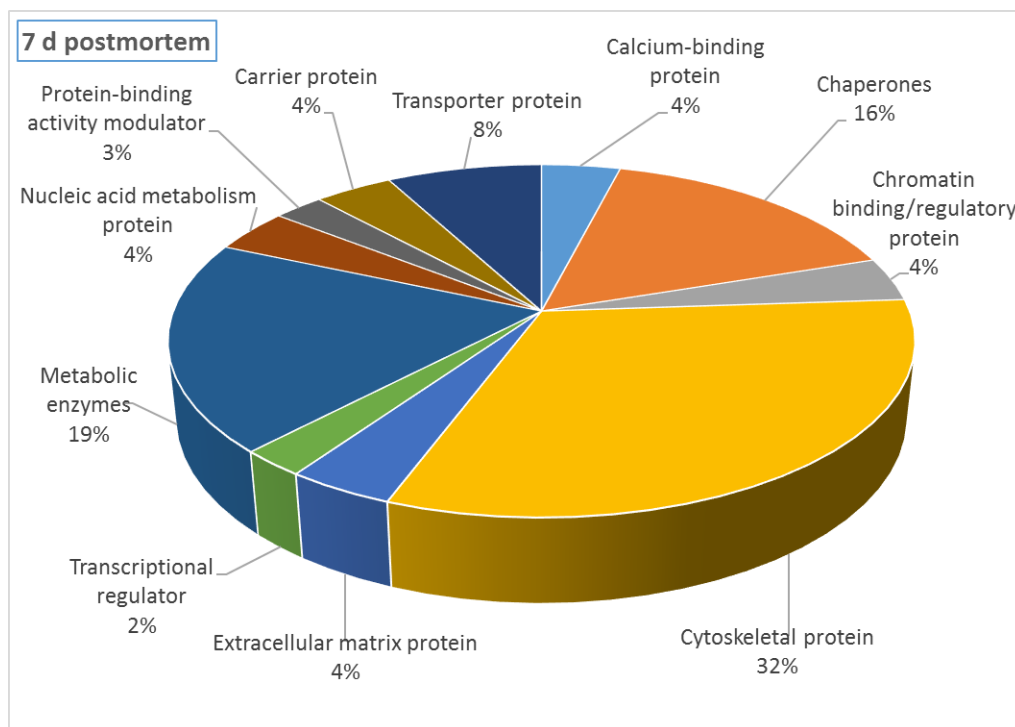


Figure 5.4. (Continued)

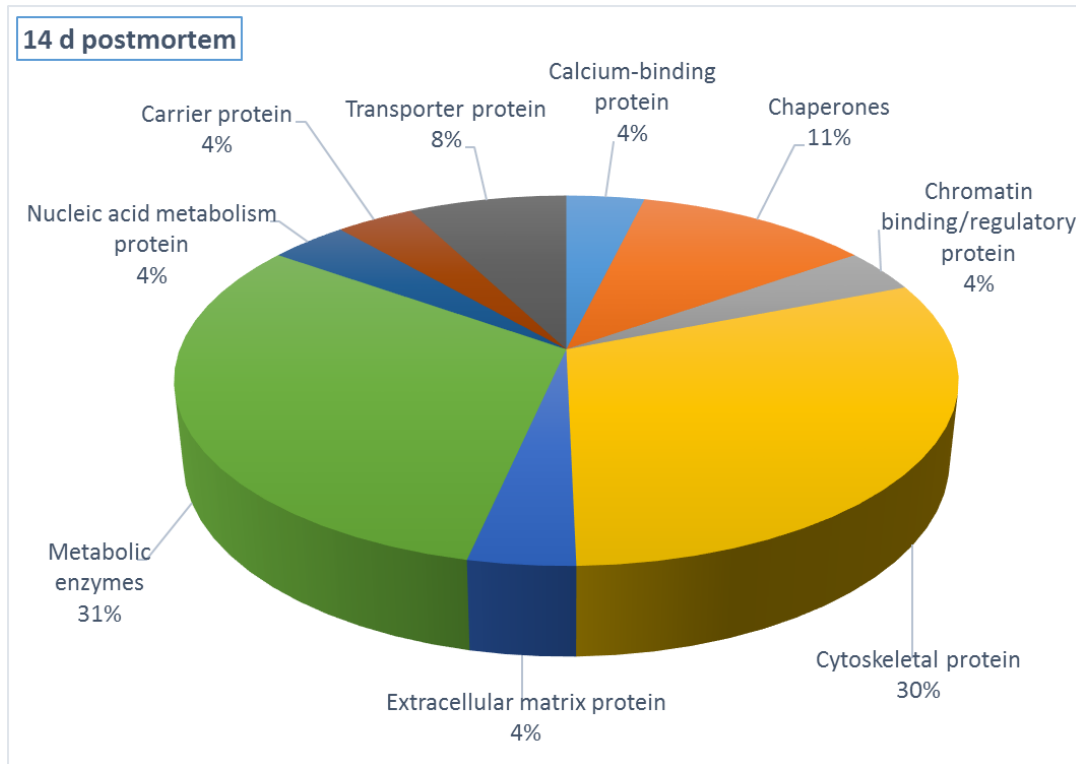


Figure 5.4. (Continued)

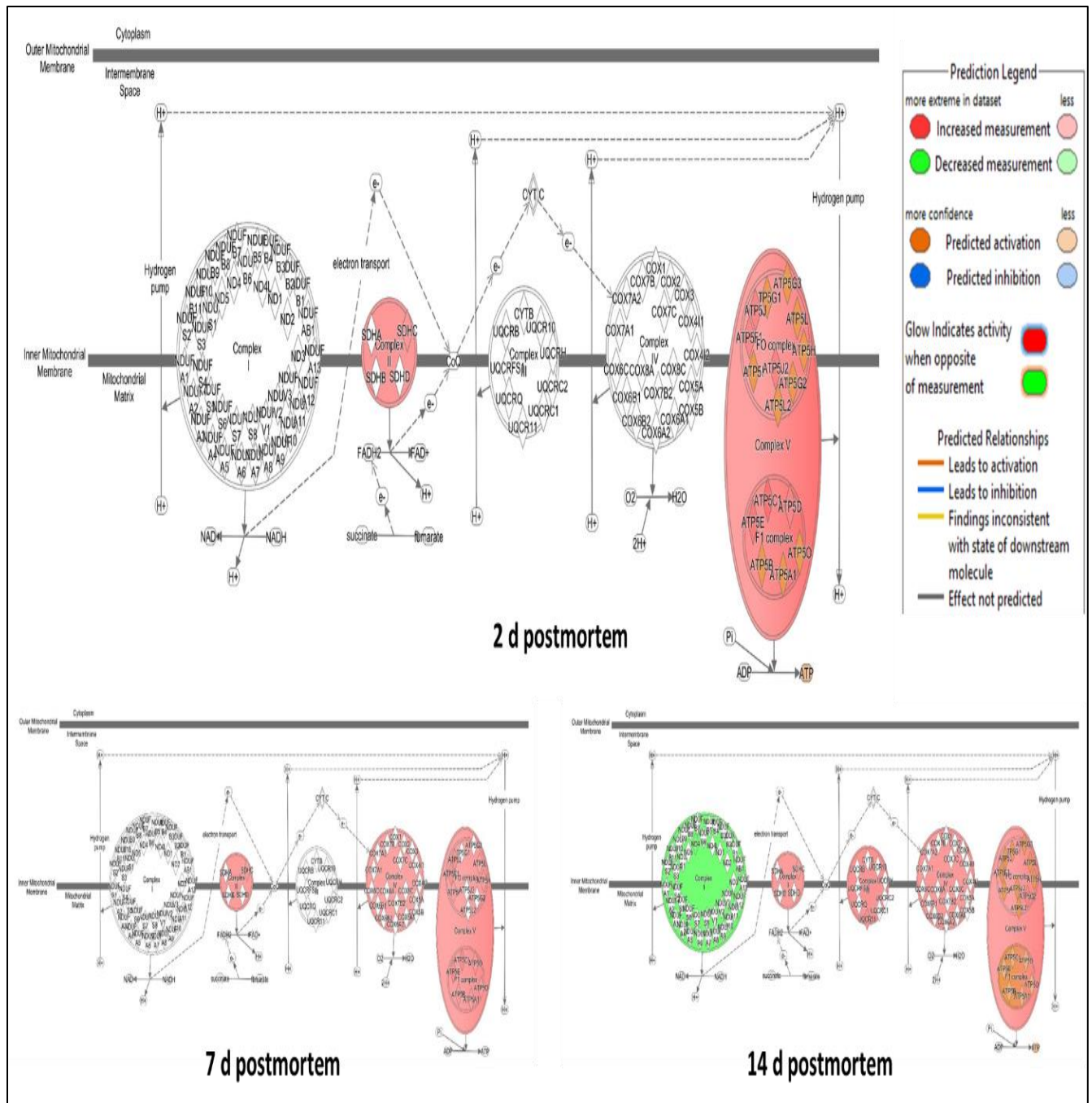
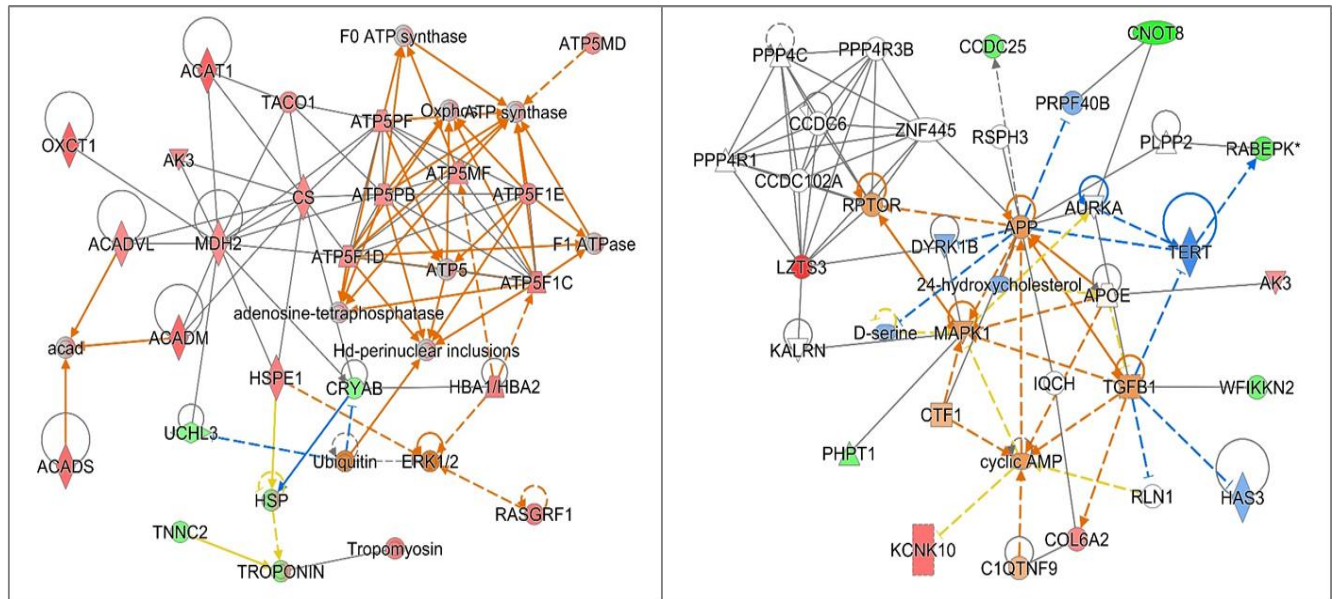


Figure 5.5. Complexes of ETC pathway affected during comparisons of bison *psaos major* vs *longissimus lumborum* muscle at 2 d, 7 d and 14 d postmortem ageing. (For more details on each protein and its function, please see the differentially abundant proteins listed on Table 5.1).

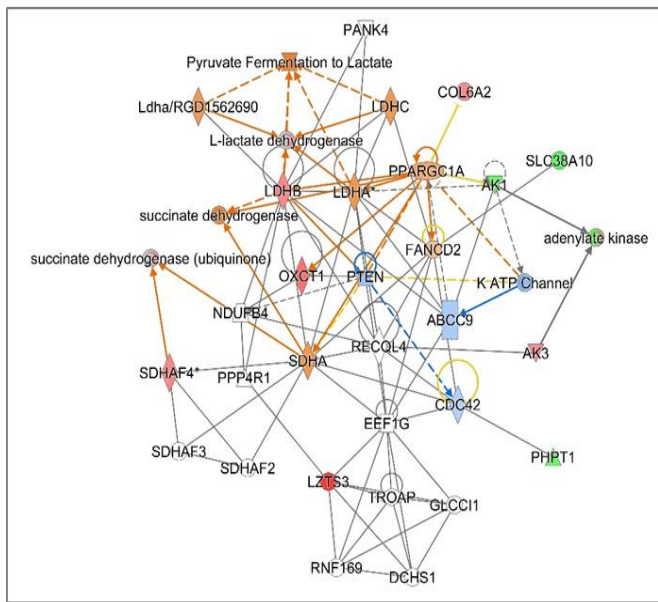
LL = *longissimus lumborum*; PM = *psaos major*

ETC = electron transport chain



2 d postmortem

7 d postmortem



14 d postmortem

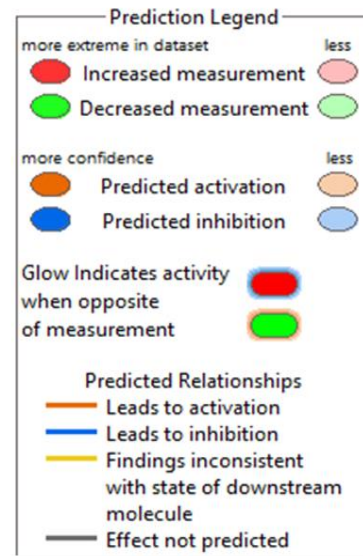


Figure 5.6. Major protein-protein interaction networks during comparisons of bison *psaos major* vs *longissimus lumborum* muscle at 2 d, 7 d and 14 d postmortem identified using Ingenuity pathway analysis. (For more details on each protein and its function, please see the differentially abundant proteins listed on Table 5.1).

LL = *longissimus lumborum*; PM = *psaos major*

5.4.3. Enzymes involved in oxidative phosphorylation and ATP-transport proteins

In oxidative phosphorylation or ETC, 10 differential proteins were identified (**Table 5.1**) during comparisons of LL and PM muscles from three ageing periods. Among those proteins, succinate dehydrogenase cytochrome b small subunit (SDHD), and succinate dehydrogenase flavoprotein subunit (SDHA) were the component of mitochondrial complex II. Only one protein (cytochrome c) was part of mitochondrial complex IV that transfers electrons from cytochrome c molecules to dioxygen, resulting in the conversion of molecular oxygen into two water molecules (Li et al., 2006; Zhai et al., 2020). Other the seven differentially abundant proteins were the structural components of complex V (ATP synthase) and eventually involved in the ATP synthesis process. Among those, ATP synthase subunit gamma (ATP5C1), ATP synthase subunit delta (ATP5D), ATP synthase subunit epsilon (ATP5E), ATP synthase subunit f (ATP5J2) and ATP synthesis-coupling factor 6 (ATP5J) were components of the F₁ part of complex V. ATP synthase subunit B1 (ATP5F) and ATP synthase subunit C2 (ATP5G2) were part of the F₀ portion of complex V. All these above-mentioned proteins were found more abundant in PM muscles than in LL in each postmortem ageing period. Also, two ATP-related transport proteins (**Table 5.1**) such as phosphate carrier protein (SLC25A3) and ADP/ATP translocase 1 (SLC25A4) were identified as more abundant in PM muscles in almost all the ageing periods compared with LL.

5.4.4 TCA cycle and carbohydrate metabolism enzymes

Among the differential proteins in TCA cycle (**Table 5.1**), citrate synthase (CS), malate dehydrogenase (MDH2) and succinyl-CoA ligase (SUCLG2) were identified as more abundant in PM muscles than in LL mainly at 2 d postmortem. Related to carbohydrate metabolism enzymes, five proteins were reported less abundant in PM muscles than LL, which were glycogen phosphorylase M (PYGM), glycogen phosphorylase B (PYGB), phosphoglycerate kinase 2 (PGK2), phosphoglucomutase-1 (PGM1) and ATP-dependent 6-phosphofructokinase (PFKM), at 2 and 14 d ageing periods (**Table 5.1**).

5.4.5 Fatty acid oxidation enzymes

A total of nine differential proteins (**Table 5.1**) linked to fatty acid degradation or β -oxidation were identified as more abundant in PM muscles at different ageing periods compared with LL. Among those, two fatty acid-binding proteins (FABP5 and FABP3) are actively involved in fatty

acid catabolism, and binding and transporting fatty acids through cell membranes to mitochondria for oxidation (Zhai et al., 2020). Acetyl-CoA acetyltransferase mitochondrial isoform X1 (ACAT1) is involved in the reversible conversion of two acetyl-CoA to acetoacetyl-CoA and was reported more abundant in PM muscles (Zhai et al., 2020). Three proteins also overexpressed in PM muscles compared with LL, such as long-chain specific acyl-CoA dehydrogenase (ACADVL), medium-chain specific acyl-CoA dehydrogenase (ACADM) and short-chain specific acyl-CoA dehydrogenase (ACADS) catalyze the first step of very long-chain, medium-chain, and short-chain fatty acids in β -oxidation pathway, respectively (<http://www.uniprot.org/>; Zhai et al., 2020). Moreover, another enzyme, succinyl-CoA:3-ketoacid coenzyme A transferase 1 (OXCT1), involved in the extrahepatic ketone body catabolism and energy supply (El Midaoui et al., 2005; Yu, Wu, Tian, Hou, et al., 2017), was overexpressed in PM muscles compared with LL. Almost all of the above mentioned β -oxidation proteins were identified at all three ageing periods.

5.4.6 Chaperone and oxygen transport related proteins

Among the four differentially identified chaperones (**Table 5.1**), three proteins showed decreased expression levels in PM muscles such as peptidyl-prolyl cis-trans isomerase A (PPIA), heat shock 27 kDa protein (HSPB1), and alpha-crystallin B chain (CRYAB). In contrast, mitochondrial 10 kDa heat shock protein (HSPE1) exhibited increased expression in PM compared with LL at 2 and 7 d postmortem. On the other hand, two major oxygen transport proteins (**Table 5.1**), hemoglobin subunit alpha-I/II (HBA1) and hemoglobin subunit beta (HBB), were detected as more abundant in PM muscles compared with LL, at 2, 7 and 14 d postmortem.

5.4.7 Proteins with other functions

Among the other functions (**Table 5.1**), only antioxidant protein, namely Glutathione S-transferase Mu 1-like (GSTM7) showed lower expression pattern, in PM muscles compared with LL. Moreover, the proteins involved in hydrolase activity such as 14 kDa phosphohistidine phosphatase (PHPT1), carboxymethylenebutenolidase (CMBL) and aspartyl aminopeptidase isoform X1 (DNPEP) also exhibited lower expression in PM than in LL. However, the proteins associated with demethylation (PPME1) and DNA binding (HMGN2) showed upregulation patterns in PM muscles compared with LL. Almost all of the proteins described above were detected only at 2 d postmortem, except for HMGN2 which was identified on each ageing period.

The downregulation of glutathione S-transferase (GSTM7) antioxidant protein in PM muscles indicates that this muscle is more prone to oxidative damage resulting in less stability in colour. A protein involved in purine metabolism, namely GTP:AMP phosphotransferase AK3 (AK3), exhibited more expression in PM muscles than in LL at all three ageing periods; whereas adenylate kinase 1 (AK1) showed less expression in PM only at 14 d ageing time.

Proteins related to signal transduction such as kelch-like protein 41 (RABEPK↓), platelet glycoprotein 4/glycoprotein IIIB (CD36↑) and ras-specific guanine nucleotide-releasing factor 1 (RASGRF1↑), protein ubiquitination E3 ubiquitin-protein ligase HERC2 isoform X1/ HECT-type E3 ubiquitin transferase (HERC2↑), and ubiquitin carboxyl-terminal hydrolase isozyme L3 (UCHL3↓) proteins showed different (↓ = decreased and ↑ = increased) expression levels. Among these proteins, CD36 showed more expression in PM muscles at 2 d postmortem.

5.4.8 Proteins involved in muscle contraction and calcium signaling

Among muscle contraction related proteins (**Table 5.1**), myosin regulatory light chain 2 (MYL2), myosin light chain 3 (MYL3), myosin-7 (MYH7), tropomyosin alpha-1 chain isoform X2 (TPM1), tropomyosin beta chain isoform X1 (TPM2), tropomyosin alpha-3 chain isoform X1 (TPM3), tropomodulin-2 isoform X1 (TMOD2), troponin C (slow skeletal muscle; TNNC1), troponin I (slow skeletal muscle; TNNI1), thymosin beta-4 (TMSB4X), up-regulated during skeletal muscle growth protein 5 (USMG5) showed increase expression in PM muscles compared with LL at almost all three ageing periods.

On the other hand, troponin C (TNNC2), coiled-coil domain-containing protein 25 (CCDC25), myosin-binding protein H (MYBPH), alpha-actinin-1 (ACTN1), alpha-actinin-3 (ACTN3), alpha-actinin-3-like (SSX2IP), alpha-actinin-4 (ACTN4), obscurin (OBSL1), 14-3-3 protein beta/alpha (YWHAB), 14-3-3 protein gamma (YWHAG), myozenin-1 (MYOZ1), myomesin-2 (MYOM2), myopalladin isoform X1 (MYPN), immunoglobulin-like and fibronectin type III domain-containing protein 1 (IGFN1) were identified less abundances in PM muscles than in LL (Table 1) at 2 d postmortem. Two proteins from the calcium signaling pathway such as calsequestrin-1 (CASQ1) and protein S100-A1 (S100A1) were found down regulated in PM muscles in comparison with LL (**Table 5.1**). CASQ1 was detected at all three ageing times whereas S100-A1 was identified only at 7 d postmortem.

5.4.9 Muscle structure components

Eight proteins associated with muscle structure showed different abundance levels in LL and PM muscles (**Table 5.1**). Among those, leucine zipper putative tumor suppressor 3 (LZTS3) and collagen alpha-2(VI) chain (COL6A2) are components of the cell cycle and connective tissue. They exhibited increased expression in PM compared with LL at all three ageing times. On the other hand, PDZ and LIM domain protein 7 (PDLIM7), protein CFAP46 (CFAP46), CAP-Gly domain-containing linker protein 1 (CLIP1), filamin-C (FLNC), keratin type I cytoskeletal 14-like (KRT14) and titin (TTN) were expressed in decreased levels in PM relative LL with different identification pattern at three ageing periods.

5.4.10 Proteins involved in protein synthesis

Most differential proteins identified from the transcription (**Table 5.1**) process such as CCR4-NOT transcription complex subunit 3-like (CNOT8), zinc finger protein 606 (ZNF606), heterogeneous nuclear ribonucleoprotein K (HNRNPK), cysteine and glycine-rich protein 3 (CSR3) and transcription elongation factor B polypeptide 1 (TCEB1) were downregulated in PM muscles than in LL. However, only heterogeneous nuclear ribonucleoprotein A/B (HNRNPAB) from the above-mentioned group showed upregulation pattern in PM compared with LL muscles (**Table 5.1**). Two translation process-associated proteins (elongation factor 1-alpha 2; EEF1A2 and eukaryotic translation initiation factor 5A-1; EIF5AL1) showed decreased expression in PM muscles compared with LL. Almost all above described proteins were detected at 2 d postmortem.

5.5 Discussion

5.5.1 Enzymes involved in oxidative phosphorylation and ATP-transport proteins

Ten differential oxidative phosphorylation or ETC proteins were found more abundant in PM muscles than in LL in each postmortem ageing period. Those proteins increase the rates of oxygen consumption in mitochondria (McKenna et al., 2005; O'Keeffe & Hood, 1982; Yu et al., 2018; Yu et al., 2017; Zhai et al., 2020). These studies support our presented results. On the other hand, ATP related transport proteins such as SLC25A3 and SLC25A4 are responsible for transmembrane phosphate transport and exchange of ADP/ATP across the membrane respectively, which could contribute to the higher production of ATP (Zhai et al., 2020) and regulate the permeability of mitochondria (Yu et al., 2018). In the current study, these proteins were abundant

in PM muscles, which could enhance oxidative phosphorylation enzymes function (Yu et al., 2017; Yu et al., 2018; Zhai et al., 2020). Furthermore, the ETC and ATP transport occur in mitochondria and related proteins are connected within the same protein-protein interaction cluster (**Figure 5.3a**) at 2 d postmortem and thus participate in oxidative phosphorylation reactions together.

Generally in ETC, complex-I (Genova et al., 2001; Kushnareva et al., 2002; Turrens and Boveris, 1980), complex-II (Quinlan et al., 2012) and complex-III (Dröse and Brandt, 2008) can generate reactive oxygen species (ROS) in the course of oxidative phosphorylation reactions. These ROS can directly damage complex I-IV (Brown, 1999) and SLC25A4 (Yan & Sohal, 1998) which can consequently initiate signal transduction, resulting in cell death (Vakifahmetoglu-Norberg et al., 2017). Therefore, ROS producing proteins found overabundant in PM muscles relative LL indicate more oxidative stress, release of cytochrome c and quick degradation of mitochondria in PM, confirm this muscle as colour labile compared with LL in early display periods (Ke et al., 2017; Mancini et al., 2018).

5.5.2 TCA cycle and carbohydrate metabolism enzymes

Among the differential proteins in TCA cycle, CS, MDH2 and SUCLG2 were more abundant in PM muscles compared with LL (Yu et al., 2018; Yu et al., 2017; Ramanathan et al., 2021). These proteins contribute on the production of ATP by oxidative phosphorylation in PM muscles, resulting in production of ROS and consequently, oxidative and colour instability. Another protein, MPC2, is responsible for the uptake of pyruvate in mitochondria which ultimately enters into TCA cycle after converting to acetyl-coA and contributes to the production of NADH and other reducing equivalents, also fed into ETC for ATP production. On the other hand, PM muscle contains greater amounts of Mb and mitochondria, resulting in more oxygen utilization in PM compared with LL (Canto et al., 2016; Hwang et al., 2010). Therefore, these TCA cycle enzymes (Yu et al., 2018; Yu et al., 2017; Zhai et al., 2020) could contribute to the higher consumption of oxygen in oxidative metabolism (McKenna et al., 2005; O’Keeffe & Hood, 1982) and ROS generation, inducing stress in postmortem PM muscles; which consequently may lead to lower metmyoglobin reducing activity (MRA) and increase discolouration in PM (Ramanathan et al., 2019).

NADH is a crucial component of enzymatic and non-enzymatic MRA (Echevarne et al., 1990; Kim et al., 2006; Mancini and Hunt, 2005; Ramanathan et al., 2021) and MPC2 protein

could contribute to the production of reducing equivalents including NADH. At the same time, OGDH plays a role in catalytic conversion of 2-oxoglutarate to succinyl-CoA, CO₂ and NADH (Qi et al., 2011; Zhai et al., 2019). The less abundance of OGDH in PM muscles may lead to less MRA, resulting lower colour stability (Ramanathan et al., 2020a; Ramanathan et al., 2020b).

Previous studies were also confirmed the lower abundance of glycolytic enzymes in PM muscles than LL, resulting negative effects on colour attributes (Hunt & Hedrick, 1977; Joseph et al., 2012; Kirchofer et al., 2002; Mancini et al., 2018; Ramanathan & Mancini, 2018; Yu et al., 2018). However, LDHB, which converts lactate to pyruvate in the anaerobic glycolysis process and generates NADH, was identified as more abundant in PM muscles compared with LL. Nevertheless, as oxidative phosphorylation was dominant in PM muscles, this NADH could be mainly utilized by the electron transport chain for producing ATP rather than involved in other reduction processes like metmyoglobin reducing activity. As a result, the presence LDHB may not be effective enough for maintaining the oxidative and colour stability in PM muscles.

5.5.3 Fatty acid oxidation enzymes

In PM muscles, more fatty acid oxidation enzymes than in LL could be the reflection of elevated lipid oxidation. In agreement with this view, previous studies reported more lipid oxidation in PM compared with LL (Canto et al., 2015; Hasan et al., 2021). Other studies also demonstrated more β -oxidation enzymes in PM than LL (Yu et al., 2018; Zhai et al., 2020) during postmortem ageing. One interaction cluster, including fatty acid oxidation proteins were detected both at 2 d (**Figure 5.3a**) and 14 d (**Figure 5.3c**), emphasizing the contributions of β -oxidation to the oxidative processes that may occur within the postmortem bison muscles. Therefore, the overabundance of fatty acid oxidation enzymes in PM muscles could be a reason of more oxidative stress, resulting in the production of ROS and deterioration of colour in PM (Zhai et al., 2020) in combination with overexpression of the TCA cycle and oxidative phosphorylation enzymes.

5.5.4 Chaperone and oxygen transport related proteins

In PM muscles, PPIA, HSPB1 and CRYAB showed decreased expression, whereas HSPE1 exhibited increased expression in PM compared with LL. PPIA plays a prominent role for the survival of cells (Cheng et al., 2016; Obchoei et al., 2009) by minimizing the cellular damage caused by ROS (Doyle et al., 1999; Kyu et al., 2007; Lee et al., 2001; Suzuki et al., 2006). HSPE1

is involved in mitochondrial protein import, macromolecular structure assembly, subsequently may contribute to protein folding in association with HSP60 (Maciel et al., 2020). Although, HSPE1 was more abundant in PM muscles, this protein may have functions other than chaperone activity. Generally, chaperones are involved in the covalent folding or unfolding of protein structures and consequently minimize the cellular stress (Zhai et al., 2020). The lower expression of most of the identified chaperones in PM muscles is a possible indication of higher stress levels, ROS production, and consequently accelerated colour deterioration relative to LL.

Oxygen transporters, HBA1 and HBB were detected as up regulated in PM muscles compared with LL; which are in agreement with previous studies (Yu et al., 2017; Zhai et al., 2020). The presence of more hemoglobin subunits in PM muscle could make it highly vulnerable to autoxidation, due to the oxidative stress induced lipid oxidation and consequently, lower stability of colour in PM muscles compared with LL (Canto et al., 2016; Misra & Fridovich, 1972; Moxness et al., 1996; Olsson et al., 2010; Sadrzadeh et al., 1984).

5.5.5 Proteins with other functions

Antioxidant proteins such as GSTM7, PHPT1, CMBL and DNPEP exhibited lower expression in PM than in LL. GSTM7 mainly belongs to the glutathione S-transferase (GST) superfamily and neutralizes the cellular ROS and protects cells from oxidative stress and damage (Oakley, 2011; Zhao et al., 2010). The down regulation of GSTM7 in PM muscles may indicate that this muscle is more prone to oxidative damage resulting in less stability in colour. Among other proteins, AK3 can generate AMP from ADP and AMP in turn is related to the signalling cascade linked to cellular damage (Dzeja & Terzic, 2009; Panayiotou et al., 2014; Zhai et al., 2020). In contrast, the overabundance of AK1 protein was found to be linked to the stability of colour in fresh beef (Canto et al., 2015). Signal transduction protein such as CD36 showed more expression in PM muscles and this protein is involved in the immune response, cell signalling and lipid oxidation (<http://www.uniprot.org/>) and thus could contribute to colour deterioration in PM muscles, especially by exerting its effect on lipid oxidation process.

5.5.6 Proteins involved in muscle contraction, calcium signaling, muscle structure components, and protein synthesis

Most of those proteins were more abundant in PM muscles compared with LL ($P > 0.05$). Among those groups, muscle contraction proteins showed protein-protein interaction networks at all three ageing times (**Figure 5.3**) and indicating that these proteins could have significant roles in the postmortem changes in bison muscles. However, their impact on colour stability has not been reported according to author's knowledge and needs to be investigated.

5.6 Conclusions

In summary, based on the overall results, the enzymes involved in oxidative metabolism may contributed to oxidative stress as well as colour instability in bison PM muscles by producing reactive oxygen species. ATP production and transport-related proteins increased its expression in PM muscles also may have contributions on oxidative instability, which could be reflected in meat colour instability. To the best of our knowledge, this study is the first to report most of the proteins involved in muscle contraction, calcium signaling, muscle structure components, protein synthesis, as well as antioxidant, hydrolase, demethylation, protein binding, and DNA ubiquitination in bison muscles compared to other proteome studies on cattle. However, their impact on colour stability needs to be investigated. Therefore, this isobaric tag-based TMT analysis was successful to uncover the variations in sarcoplasmic proteomes of bison two major muscles (LL and PM), resulting in discrimination of those muscles with inherent colour stability.

CHAPTER 6: GENERAL CONCLUSIONS

Fresh bison meat colour is the most important attribute influencing consumers' purchase intention and consequently has a substantial economic impact on the bison industry. It is well known that meat colour is muscle-specific (e.g., LL = colour stable, PM = colour labile), with each muscle's inherent colour stability significantly varying during retail display and ageing periods. Generally, biochemical parameters such as pH, Mb and total fat contents, lipid (MDA and HNE) and protein (CAR) oxidation products change during ageing and retail display. The changes in biochemical and colour parameters among muscles could also be examined and predicted using the NIRS technique. Furthermore, muscle-specific changes could occur in sarcoplasmic proteomes during ageing. However, the variations in colour stability in bison LL and PM muscles have not been examined yet. The overall goals of this thesis were to examine the rapid discolouration mechanisms in bison LL and PM muscles with their inherent muscle-specific colour stability during ageing and retail display periods. Therefore, the overall objectives of this thesis research were: ii) to compare the MDA, HNE and CAR and their impacts on colour stability; ii) to investigate the potential of NIRS systems (both Vis-NIR and SWIR) application to discriminate between those muscles and predict colour attributes; and iii) to characterize the proteome profile of bison LL and PM muscles during ageing.

The first experiment was designed and aimed at determining MDA, HNE and CAR and how these oxidation products affect the colour traits of bison LL and PM muscles during ageing and retail display periods. LL was found to be a colour-stable muscle for accumulating the lower levels of MDA, HNE and CAR generated during ageing retail display times compared with PM muscle. In both muscles, MDA demonstrated the highest impact and was the most critical oxidation compound for the deterioration of colour relative to both HNE and CAR. The relationships among colour stability and oxidation products exhibited a distinct muscle-specific colour deterioration pattern. This research finding has significant importance and could be implemented in the bison meat industry in various aspects. Firstly, MDA could be considered as the best suitable biomarker of lipid oxidation for the quality assessment of bison meat products. Secondly, the creation of various discolour mitigation strategies by muscle-specific colour stability type would be possible. Thirdly, the national and international fresh bison meat market could be

expanded without any risk of retail colour inconsistency. Finally, consumers can receive a more desirable meat product which is more consistent and acceptable visually.

The second experiment was aimed to investigate the application of NIRS techniques (Vis-NIR and SWIR) for the segregation of bison LL and PM muscles and prediction of colour traits. NIRS acquired HSI has been found as an attractive non-destructive method for the discrimination of bison meat samples based on muscle type and storage period. In Vis-NIR region, the PCA based unsupervised classification process was successful for the classification of bison muscles based on ageing periods, while SWIR successfully segregated samples based on muscle type. Additionally, for the supervised classification process, PLS-DA models were developed using the data in the Vis-NIR range and found to have a potential for the discrimination of bison muscles based on both muscle type and ageing period. Furthermore, the developed PLSR models were successful in predicting the redness, colour and discolouration scores. These research findings have significant importance in research and quality control process, as well as valuable asset for industrial application. Online NIRS techniques could facilitate the classification of bison muscles based on muscle type and ageing periods. As LL and PM muscles are two commercially valuable cuts having muscle-specific colour stability, the segregation of these muscles using NIRS could be a suitable, quick and non-destructive approach. Consequently, it would be also possible to apply special mitigation techniques, particularly for the processing and packaging of colour-stable LL and colour-labile PM muscles in bison industry.

The third experiment was aimed at examining the proteomic basis of bison LL and PM with inherent muscle-specific colour stability during ageing. The results indicated that in PM muscles, the proteins associated with oxidative metabolisms such as the enzymes from ETC, TCA cycle, ATP generation and transport, and oxygen transport exhibited an increase in expression patterns compared with LL during both ageing periods. The underlying mechanism for these protein expression levels may lie in the formation of reactive oxygen species. The reactive oxygen products are consequently responsible for the overall oxidative instability of the muscle system and colour deterioration during ageing. In contrast, most of the proteins associated with carbohydrate metabolism and chaperone activity demonstrated decreased expression in PM muscles relative to LL. As a result, PM muscles exhibited lower production of reducing equivalents in glycolysis and the protein folding ability was lower due to the decreased level of

chaperones than in LL. These findings also indicated that in PM muscles, both MMb reduction and protein folding/stability activities could be lower, resulting in colour deterioration than in LL.

In conclusion, to the best of our knowledge, this is the first research work attempted on bison LL and PM muscles to compare biochemical and oxidative parameters, and examine the potential of NIRS (both Vis-NIR and SWIR regions), and compare the changes in sarcoplasmic proteomes during ageing. Furthermore, this current study reported the first direct estimation of HNE using ELISA from meat samples directly and the use of Vis-NIR for the prediction of sensory colour attributes, colour and discolouration score. As the bison industry is still growing, these research findings could be valuable for their industrial application. Thus, they could contribute to the expansion and marketing of fresh bison meat.

LITERATURE CITED

- Aalhus, J., & Dugan, M. (2014). Oxidative and Enzymatic. In *Encyclopedia of Meat Sciences* (Second Ed, pp. 394–400). Elsevier Ltd. <https://doi.org/10.1016/B978-0-12-384731-7.00091-X>
- Aalhus, J. L., Robertson, W. M., & Ye, J. (2009). Muscle fiber characteristics and their relation to meat quality. In *Applied Muscle Biology and Meat Science* (pp. 97–114). <https://doi.org/10.1201/b15797-9>
- Abeni, F., & Bergoglio, G. (2001). Characterization of different strains of broiler chicken by carcass measurements, chemical and physical parameters and NIRS on breast muscle. *Meat Science*, 57(2), 133–137. [https://doi.org/10.1016/S0309-1740\(00\)00084-X](https://doi.org/10.1016/S0309-1740(00)00084-X)
- Aberle, E. D., Forrest, J. C., Gerrard, D. E., & Mills, E. W. (2001). Principles of meat science. 4th ed. *Kendall/Hunt Publishing Co., Dubuque, IA*.
- Abraham, A., Dillwith, J. W., Mafi, G. G., VanOverbeke, D. L., & Ramanathan, R. (2017). Metabolite Profile Differences between Beef Longissimus and Psoas Muscles during Display. *Meat and Muscle Biology*, 1(1), 18–27. <https://doi.org/10.22175/mmb2016.12.0007>
- Adzitey, F., & Nurul, H. (2011). Pale soft exudative (PSE) and dark firm dry (DFD) meats: Causes and measures to reduce these incidences - a mini review. *International Food Research Journal*, 18(1), 11–20.
- Aït-Kaddour, A., Jacquot, S., Micol, D., & Listrat, A. (2017). Discrimination of beef muscle based on visible-near infrared multi-spectral features: Textural and spectral analysis. *International Journal of Food Properties*, 20(6), 1391–1403. <https://doi.org/10.1080/10942912.2016.1210163>
- Alderton, A. L., Faustman, C., Liebler, D. C., & Hill, D. W. (2003). Induction of redox instability of bovine myoglobin by adduction with 4-hydroxy-2-nonenal. *Biochemistry*, 42(15), 4398–4405. <https://doi.org/10.1021/bi0271695>
- Alomar, D., Gallo, C., Castañeda, M., & Fuchslocher, R. (2003). Chemical and discriminant analysis of bovine meat by near infrared reflectance spectroscopy (NIRS). *Meat Science*, 63(4), 441–450. [https://doi.org/10.1016/S0309-1740\(02\)00101-8](https://doi.org/10.1016/S0309-1740(02)00101-8)
- AMSA. (2012). AMSA Meat Color Measurement Guidelines: AMSA. In *American Meat Science Association*. (Issue December).
- Andersen, J. R., Borggaard, C., Rasmussen, A. J., & Houmøller, L. P. (1999). Optical

- measurements of pH in meat. *Meat Science*, 53(2), 135–141. [https://doi.org/10.1016/S0309-1740\(99\)00045-5](https://doi.org/10.1016/S0309-1740(99)00045-5)
- Andrés, S., Murray, I., Navajas, E. A., Fisher, A. V., Lambe, N. R., & Bünger, L. (2007). Prediction of sensory characteristics of lamb meat samples by near infrared reflectance spectroscopy. *Meat Science*, 76(3), 509–516. <https://doi.org/10.1016/j.meatsci.2007.01.011>
- Andrés, S., Silva, A., Soares-Pereira, A. L., Martins, C., Bruno-Soares, A. M., & Murray, I. (2008). The use of visible and near infrared reflectance spectroscopy to predict beef *M. longissimus thoracis et lumborum* quality attributes. *Meat Science*, 78(3), 217–224. <https://doi.org/10.1016/j.meatsci.2007.06.019>
- AOCS. (2004). Rapid Determination of Oil / Fat Utilizing High Temperature Solvent Extraction. *Rapid Determination of Oil/Fat Utilizing High Temperature Solvent Extraction*, 1–3.
- Apple, J. K., Maxwell, C. V., DeRodas, B., Watson, H. B., & Johnson, Z. B. (2000). Effect of magnesium mica on performance and carcass quality of growing-finishing swine. *Journal of Animal Science*, 78(8), 2135–2143. <https://doi.org/10.2527/2000.7882135x>
- Apple, J. K., Roberts, W. J., Maxwell, C. V., Boger, C. B., Fakler, T. M., Friesen, K. G., & Johnson, Z. B. (2004). Effect of supplemental manganese on performance and carcass characteristics of growing-finishing swine. *Journal of Animal Science*, 82(11), 3267–3276. <https://doi.org/10.2527/2004.82113267x>
- Arihara, K., Cassens, R. G., Greaser, M. L., Luchansky, J. B., & Mozdziak, P. E. (1995). Localization of metmyoglobin-reducing enzyme (NADH-cytochrome b5 reductase) system components in bovine skeletal muscle. *Meat Science*, 39(2), 205–213. [https://doi.org/10.1016/0309-1740\(94\)P1821-C](https://doi.org/10.1016/0309-1740(94)P1821-C)
- Arihara, K., Itoh, M., & Kondo, Y. (1997). Quantification of NADH-Cytochrome b5 Reductase (Metmyoglobin-Reducing Enzyme) in Bovine Skeletal Muscle by an Immunoblotting Assay. *Nihon Chikusan Gakkaiho*, 68(1), 29–33. <https://doi.org/10.2508/chikusan.68.29>
- Arnold, R. N., Arp, S. C., Scheller, K. K., Williams, S. N., & Schaefer, D. M. (1993). Tissue equilibration and subcellular distribution of vitamin E relative to myoglobin and lipid oxidation in displayed beef. *Journal of Animal Science*, 71(1), 105–118. <https://doi.org/10.2527/1993.711105x>
- Atkinson, J. L., & Follett, M. J. (1973). Biochemical studies on the discoloration of fresh meat. *International Journal of Food Science & Technology*, 8(1), 51–58.

<https://doi.org/10.1111/j.1365-2621.1973.tb01688.x>

- Babellahi, F., Paliwal, J., Erkinbaev, C., Amodio, M. L., Chaudhry, M. M. A., & Colelli, G. (2020). Early detection of chilling injury in green bell peppers by hyperspectral imaging and chemometrics. *Postharvest Biology and Technology*, *162*, 111100. <https://doi.org/10.1016/j.postharvbio.2019.111100>
- Balaban, M. O. (2008). Quantifying nonhomogeneous colors in agricultural materials part I: Method development. *Journal of Food Science*, *73*(9). <https://doi.org/10.1111/j.1750-3841.2008.00807.x>
- Balage, J. M., da Luz e Silva, S., Gomide, C. A., Bonin, M. de N., & Figueira, A. C. (2015). Predicting pork quality using Vis/NIR spectroscopy. *Meat Science*, *108*, 37–43. <https://doi.org/10.1016/j.meatsci.2015.04.018>
- Ballabio, D. (2015). A MATLAB toolbox for Principal Component Analysis and unsupervised exploration of data structure. *Chemometrics and Intelligent Laboratory Systems*, *149*, 1–9. <https://doi.org/10.1016/j.chemolab.2015.10.003>
- Barker, M., & Rayens, W. (2003). Partial least squares for discrimination. *Journal of Chemometrics*, *17*(3), 166–173. <https://doi.org/10.1002/cem.785>
- Barlocco, N., Vadell, A., Ballesteros, F., Galietta, G., & Cozzolino, D. (2006). Predicting intramuscular fat, moisture and Warner-Bratzler shear force in pork muscle using near infrared reflectance spectroscopy. *Animal Science*, *82*(1), 111–116. <https://doi.org/10.1079/ASC20055>
- Baron, C. P., & Andersen, H. J. (2002). Myoglobin-induced lipid oxidation. A review. *Journal of Agricultural and Food Chemistry*, *50*(14), 3887–3897. <https://doi.org/10.1021/jf011394w>
- Bekhit, A. E. D., & Faustman, C. (2005). Metmyoglobin reducing activity. *Meat Science*, *71*(3), 407–439. <https://doi.org/10.1016/j.meatsci.2005.04.032>
- Bekhit, A. E. D., Geesink, G. H., Morton, J. D., & Bickerstaffe, R. (2001). Metmyoglobin reducing activity and colour stability of ovine longissimus muscle. *Meat Science*, *57*(4), 427–435. [https://doi.org/https://doi.org/10.1016/S0309-1740\(00\)00121-2](https://doi.org/https://doi.org/10.1016/S0309-1740(00)00121-2)
- Berg, J. M., Stryer, L., & Tymoczko, J. L. (2012). *Biochemistry* (pp. xxxii, 1054, [132] p.). W.H. Freeman. <file://catalog.hathitrust.org/Record/011192253>
- Bertram, H. C., Petersen, J. S., & Andersen, H. J. (2000). Relationship between RN- genotype and drip loss in meat from Danish pigs. *Meat Science*, *56*(1), 49–55.

[https://doi.org/10.1016/S0309-1740\(00\)00018-8](https://doi.org/10.1016/S0309-1740(00)00018-8)

- Berzaghi, P., Dalle Zotte, A., Jansson, L. M., & Andrighetto, I. (2005). Near-infrared reflectance spectroscopy as a method to predict chemical composition of breast meat and discriminate between different n-3 feeding sources. *Poultry Science*, *84*(1), 128–136. <https://doi.org/10.1093/ps/84.1.128>
- Bradford, M. M. (1976). A rapid and sensitive method for the quantitation of microgram quantities of protein utilizing the principle of protein-dye binding. *Analytical Biochemistry*, *72*, 248–254. <https://doi.org/10.1006/abio.1976.9999>
- Brøndum, J., Byrne, D. V, Bak, L. S., Bertelsen, G., & Engelsen, S. B. (2000). Warmed-over flavour in porcine meat — a combined spectroscopic, sensory and chemometric study. *Meat Science*, *54*(1), 83–95. [https://doi.org/10.1016/S0309-1740\(99\)00085-6](https://doi.org/10.1016/S0309-1740(99)00085-6)
- Brosnan, T., & Sun, D. W. (2004). Improving quality inspection of food products by computer vision—a review. *Journal of Food Engineering*, *61*(1), 3–16. [https://doi.org/10.1016/S0260-8774\(03\)00183-3](https://doi.org/10.1016/S0260-8774(03)00183-3)
- Brown, G. C. (1999). Nitric oxide and mitochondrial respiration. *Biochimica et Biophysica Acta - Bioenergetics*, *1411*(2–3), 351–369. [https://doi.org/10.1016/S0005-2728\(99\)00025-0](https://doi.org/10.1016/S0005-2728(99)00025-0)
- Bruce, H. L., Stark, J. L., & Beilken, S. L. (2004). The effects of finishing diet and postmortem ageing on the eating quality of the M. longissimus thoracis of electrically stimulated Brahman steer carcasses. *Meat Science*, *67*(2), 261–268. <https://doi.org/10.1016/j.meatsci.2003.10.014>
- Buege, J. A., & Aust, S. D. (1978). Biomembranes - Part C: Biological Oxidations. *Methods in Enzymology*, *52*, 302–310. [https://doi.org/10.1016/S0076-6879\(78\)52032-6](https://doi.org/10.1016/S0076-6879(78)52032-6)
- Butterfield, D. A., Reed, T., Perluigi, M., De Marco, C., Coccia, R., Cini, C., & Sultana, R. (2006). Elevated protein-bound levels of the lipid peroxidation product, 4-hydroxy-2-nonenal, in brain from persons with mild cognitive impairment. *Neuroscience Letters*, *397*(3), 170–173. <https://doi.org/10.1016/j.neulet.2005.12.017>
- Byrne, C. E., Downey, G., Troy, D. J., & Buckley, D. J. (1998). Non-destructive prediction of selected quality attributes of beef by near-infrared reflectance spectroscopy between 750 and 1098 nm. *Meat Science*, *49*(4), 399–409. [https://doi.org/10.1016/S0309-1740\(98\)00005-9](https://doi.org/10.1016/S0309-1740(98)00005-9)
- Canada Gazette. (1992). Part II: Livestock and poultry carcass grading regulations. Part III. Grade names and grade standards for beef carcasses. <https://laws-lois.justice.gc.ca/eng/regulations/SOR-92-541/20070503/P1TT3xt3.html>.

- Čandek-Potokar, M., Prevolnik, M., & Škrlep, M. (2006). Ability of near Infrared Spectroscopy to Predict Pork Technological Traits. *Journal of near Infrared Spectroscopy (United Kingdom)*, *14*(4), 269–277. <https://doi.org/10.1255/jnirs.644>
- Canto, A. C. V. C. S., Costa-Lima, B. R. C., Suman, S. P., Monteiro, M. L. G., Viana, F. M., Salim, A. P. A. A., Nair, M. N., Silva, T. J. P., & Conte-Junior, C. A. (2016). Color attributes and oxidative stability of longissimus lumborum and psoas major muscles from Nellore bulls. *Meat Science*, *121*, 19–26. <https://doi.org/10.1016/j.meatsci.2016.05.015>
- Canto, A. C. V. C. S., Suman, S. P., Nair, M. N., Li, S., Rentfrow, G., Beach, C. M., Silva, T. J. P., Wheeler, T. L., Shackelford, S. D., Grayson, A., McKeith, R. O., & King, D. A. (2015). Differential abundance of sarcoplasmic proteome explains animal effect on beef Longissimus lumborum color stability. *Meat Science*, *102*, 90–98. <https://doi.org/10.1016/j.meatsci.2014.11.011>
- Carpenter, C. E., Cornforth, D. P., & Whittier, D. (2001). Consumer preferences for beef color and packaging did not affect eating satisfaction. *Meat Science*, *57*(4), 359–363. [https://doi.org/10.1016/S0309-1740\(00\)00111-X](https://doi.org/10.1016/S0309-1740(00)00111-X)
- Carter, D. (2017). Take a look at the bison industry. *Research Strategies*, 1–4.
- CBA. (2019). Bison market and supply update. Regina, Saskatchewan: Canadian Bison Association. January 25, 2019. Accessed on February 25, 2021. https://www.canadianbison.ca/application/files/2015/7807/4563/BISON_market_December_20_2019_-_English.pdf
- CBA. (2021a). Canadian Bison Association. Why Bison? Nutritional Value. Retrieved July 01, 2021 from <https://www.canadianbison.ca/consumers/why-bison/nutritional-value>
- CBA. (2021b). Canadian Bison Association. Bison History. Retrieved September 01, 2021 from <https://www.canadianbison.ca/producers/about-bison/bison-history>
- CBA. (2021c). Canadian Bison Association. Present Trends. Bison industry continues to evolve. Canadian Fresh Meat Exports. Retrieved September 01, 2021 from <https://www.canadianbison.ca/producers/about-bison/present-trends>
- Chan, D. E., Walker, P. N., & Mills, E. W. (2002). PREDICTION OF PORK QUALITY CHARACTERISTICS USING VISIBLE AND NEAR-INFRARED SPECTROSCOPY. *Transactions of the ASAE*, *45*(5), 1519–1527. <https://doi.org/10.13031/2013.11044>
- Chaudhry, M. M. A., Hasan, M. M., Erkinbaev, C., Paliwal, J., Suman, S., & Rodas-Gonzalez, A.

- (2021). Bison muscle discrimination and color stability prediction using near-infrared hyperspectral imaging. *Biosystems Engineering*, 209, 1–13. <https://doi.org/10.1016/j.biosystemseng.2021.06.010>
- Cheng, S., Luo, M., Ding, C., Peng, C., Lv, Z., Tong, R., Xiao, H., Xie, H., Zhou, L., Wu, J., & Zheng, S. (2016). Downregulation of Peptidylprolyl isomerase A promotes cell death and enhances doxorubicin-induced apoptosis in hepatocellular carcinoma. *Gene*, 592(1), 236–244. <https://doi.org/10.1016/j.gene.2016.07.020>
- Chevallier, S., Bertrand, D., Kohler, A., & Courcoux, P. (2006). Application of PLS-DA in multivariate image analysis. *Journal of Chemometrics*, 20(5), 221–229. <https://doi.org/10.1002/cem.994>
- Cho, S., Kang, G., Seong, P. N., Park, B., & Kang, S. M. (2015). Effect of slaughter age on the antioxidant enzyme activity, color, and oxidative stability of Korean Hanwoo (*Bos taurus coreanae*) cow beef. *Meat Science*, 108, 44–49. <https://doi.org/10.1016/j.meatsci.2015.05.018>
- Churchman, M. L., Low, J., Qu, C., Paietta, E. M., Kasper, L. H., Chang, Y., Payne-Turner, D., Althoff, M. J., Song, G., Chen, S. C., Ma, J., Rusch, M., McGoldrick, D., Edmonson, M., Gupta, P., Wang, Y. D., Caufield, W., Freeman, B., Li, L., ... Mullighan, C. G. (2015). Efficacy of Retinoids in IKZF1-Mutated BCR-ABL1 Acute Lymphoblastic Leukemia. *Cancer Cell*, 28(3), 343–356. <https://doi.org/10.1016/j.ccell.2015.07.016>
- Coleman, S. R., Smith, M. L., Spicer, V., Lao, Y., & Mookherjee, N. (2020). *crossm and Proteins*, *Resulting in Altered Motility*, *Cytotoxicity*, *and Tobramycin Resistance*. 5(3), 1–18.
- Colombo, G., Clerici, M., Garavaglia, M. E., Giustarini, D., Rossi, R., Milzani, A., & Dalle-Donne, I. (2016). A step-by-step protocol for assaying protein carbonylation in biological samples. *Journal of Chromatography B: Analytical Technologies in the Biomedical and Life Sciences*, 1019, 178–190. <https://doi.org/10.1016/j.jchromb.2015.11.052>
- Commission Internationale de l'éclairage. (1978). Recommendations on uniform colour spaces-colour difference equations, psychometric colour terms. Paris: CIE.
- Cornforth, D. P., & Jayasingh, P. (2004). CHEMICAL AND PHYSICAL CHARACTERISTICS OF MEAT | Colour and Pigment. In *Encyclopedia of Meat Sciences* (pp. 249–256). Elsevier. <https://doi.org/10.1016/b0-12-464970-x/00115-x>
- Cozzolino, D., Barlocco, N., Vadell, A., Ballesteros, F., & Gallieta, G. (2003). The use of visible and near-infrared reflectance spectroscopy to predict colour on both intact and homogenised

- pork muscle. *LWT - Food Science and Technology*, 36(2), 195–202. [https://doi.org/10.1016/S0023-6438\(02\)00199-8](https://doi.org/10.1016/S0023-6438(02)00199-8)
- Cozzolino, D., & Murray, I. (2002). Effect of Sample Presentation and Animal Muscle Species on the Analysis of Meat by near Infrared Reflectance Spectroscopy. *Journal of near Infrared Spectroscopy (United Kingdom)*, 10(1), 37–44. <https://doi.org/10.1255/jnirs.319>
- Cozzolino, Daniel, Murray, I., Scaife, J. R., & Paterson, R. (2000). Study of dissected lamb muscles by visible and near infrared reflectance spectroscopy for composition assessment. *Animal Science*, 70, 417–423. <https://doi.org/10.1017/S1357729800051766>
- Curzio, M., Esterbauer, H., Di Mauro, C., & Dianzani, M. U. (1990). Influence of the lipid peroxidation product 4-hydroxynonenal on human neutrophil migration. *International Journal of Immunotherapy*, 6(1), 13–18.
- Dalle-Donne, I., Rossi, R., Giustarini, D., Milzani, A., & Colombo, R. (2003). Protein carbonyl groups as biomarkers of oxidative stress. *Clinica Chimica Acta*, 329(1), 23–38. [https://doi.org/10.1016/S0009-8981\(03\)00003-2](https://doi.org/10.1016/S0009-8981(03)00003-2)
- Damez, J. L., & Clerjon, S. (2008). Meat quality assessment using biophysical methods related to meat structure. *Meat Science*, 80(1), 132–149. <https://doi.org/10.1016/j.meatsci.2008.05.039>
- De Marchi, M., Penasa, M., Battagin, M., Zanetti, E., Pulici, C., & Cassandro, M. (2011). Feasibility of the direct application of near-infrared reflectance spectroscopy on intact chicken breasts to predict meat color and physical traits. *Poultry Science*, 90(7), 1594–1599. <https://doi.org/10.3382/ps.2010-01239>
- De Marchi, M., Penasa, M., Cecchinato, A., & Bittante, G. (2013). The relevance of different near infrared technologies and sample treatments for predicting meat quality traits in commercial beef cuts. *Meat Science*, 93(2), 329–335. <https://doi.org/10.1016/j.meatsci.2012.09.013>
- De Marchi, Massimo. (2013). On-line prediction of beef quality traits using near infrared spectroscopy. *Meat Science*, 94(4), 455–460. <https://doi.org/10.1016/j.meatsci.2013.03.003>
- De Marchi, Massimo, Berzaghi, P., Boukha, A., Mirisola, M., & Gallo, L. (2007). Use of near infrared spectroscopy for assessment of beef quality traits. *Italian Journal of Animal Science*, 6(SUPPL. 1), 421–423. <https://doi.org/10.4081/ijas.2007.1s.421>
- Decker, E., Faustman, C., & Lopez-bote, C. (2000). Antioxidants in Muscle Foods : Nutritional Strategies to Improve Quality / Ed. de E. Decker, C. Faustman, C.J. López-Bote. *Chapter 4*.
- Decker, E.A., Faustman, C., & Lopez-Bote, C. J. (2000). Antioxidants in muscle foods. *Protein*

Oxidation and Implications for Muscle Food Quality., 85–112.

- Decker, Eric A., & Xu, Z. (1998). Minimizing rancidity in muscle foods. *Food Technology*, 52(10), 54–59.
- Dhanda, J. S., Pegg, R. B., Janz, J. A. M., Aalhus, J. L., & Shand, P. J. (2002). Palatability of bison semimembranosus and effects of marination. *Meat Science*, 62(1), 19–26. [https://doi.org/10.1016/S0309-1740\(01\)00222-4](https://doi.org/10.1016/S0309-1740(01)00222-4)
- Dianzani, M. U., Paradisi, L., Barrera, G., Rossi, M. A., & Parola, M. (1989). *The action of 4-hydroxynonenal on the plasma membrane enzymes from rat hepatocytes.*
- Ding, C., Rodas-González, A. R., López-Campos, Galbraith, J., Juárez, M., Larsen, I. L., Jin, Y., & Aalhus, J. L. (2016). Effects of electrical stimulation on meat quality of bison striploin steaks and ground patties. *Canadian Journal of Animal Science*, 96(1), 79–89. <https://doi.org/10.1139/cjas-2015-0001>
- Djenane, D., Sánchez-Escalante, A., Beltrán, J. A., & Roncalés, P. (2001). Extension of the retail display life of fresh beef packaged in modified atmosphere by varying lighting conditions. *Journal of Food Science*, 66(1), 181–186. <https://doi.org/10.1111/j.1365-2621.2001.tb15603.x>
- Domínguez, R., Pateiro, M., Gagaoua, M., Barba, F. J., Zhang, W., & Lorenzo, J. M. (2019). A Comprehensive Review on Lipid Oxidation in Meat and Meat Products. *Antioxidants*, 8(10), 429. <https://doi.org/10.3390/antiox8100429>
- Downey, G., & Hildrum, K. I. (2004). Analysis of Meats. In *Near-Infrared Spectroscopy in Agriculture* (pp. 599–632). <https://doi.org/10.2134/agronmonogr44.c21>
- Downey, G., & Hildrum, K. I. (2015). Analysis of Meats. In *Near-Infrared Spectroscopy in Agriculture* (pp. 599–632). <https://doi.org/10.2134/agronmonogr44.c21>
- Doyle, V., Virji, S., & Crompton, M. (1999). Evidence that cyclophilin-A protects cells against oxidative stress. *Biochemical Journal*, 341(1), 127–132. <https://doi.org/10.1042/bj3410127>
- Dröse, S., & Brandt, U. (2008). The mechanism of mitochondrial superoxide production by the cytochrome bc1 Complex. *Journal of Biological Chemistry*, 283(31), 21649–21654. <https://doi.org/10.1074/jbc.M803236200>
- Du, C.-J., & Sun, D.-W. (2004). Recent developments in the applications of image processing techniques for food quality evaluation. *Trends in Food Science & Technology*, 15(5), 230–249. <https://doi.org/10.1016/j.tifs.2003.10.006>

- Dzeja, P., & Terzic, A. (2009). Adenylate kinase and AMP signaling networks: metabolic monitoring, signal communication and body energy sensing. *International Journal of Molecular Sciences*, *10*(4), 1729–1772. <https://doi.org/10.3390/ijms10041729>
- Echevarne, C., Renerre, M., & Labas, R. (1990a). Metmyoglobin reductase activity in bovine muscles. *Meat Science*, *27*(2), 161–172. [https://doi.org/10.1016/0309-1740\(90\)90063-C](https://doi.org/10.1016/0309-1740(90)90063-C)
- Echevarne, C., Renerre, M., & Labas, R. (1990b). Metmyoglobin reductase activity in bovine muscles. *Meat Science*, *27*(2), 161–172. [https://doi.org/10.1016/0309-1740\(90\)90063-C](https://doi.org/10.1016/0309-1740(90)90063-C)
- El Midaoui, A., Chiasson, J. L., Tancrede, G., & Nadeau, A. (2005). Physical training reverses defect in 3-ketoacid CoA-transferase activity in skeletal muscle of diabetic rats. *American Journal of Physiology - Endocrinology and Metabolism*, *288*(4 51-4), 748–752. <https://doi.org/10.1152/ajpendo.00515.2004>
- English, A. R., Mafi, G. G., Vanoverbeke, D. L., & Ramanathan, R. (2016). Effects of extended aging and modified atmospheric packaging on beef top loin steak color. *Journal of Animal Science*, *94*(4), 1727–1737. <https://doi.org/10.2527/jas.2015-0149>
- Enoch, H. G., Fleming, P. J., & Strittmatter, P. (1977). Cytochrome b5 and cytochrome b5 reductase-phospholipid vesicles. Intervesicle protein transfer and orientation factors in protein-protein interactions. *The Journal of Biological Chemistry*, *252*(16), 5656–5660. [https://doi.org/10.1016/S0021-9258\(17\)40072-X](https://doi.org/10.1016/S0021-9258(17)40072-X)
- Enser, M., Hallett, K., Hewitt, B., Fursey, G. A. J., & Wood, J. D. (1996). Fatty acid content and composition of English beef, lamb and pork at retail. *Meat Science*, *42*(4), 443–456. [https://doi.org/10.1016/0309-1740\(95\)00037-2](https://doi.org/10.1016/0309-1740(95)00037-2)
- Erkinbaev, C., Derksen, K., & Paliwal, J. (2019). Single kernel wheat hardness estimation using near infrared hyperspectral imaging. *Infrared Physics and Technology*, *98*, 250–255. <https://doi.org/10.1016/j.infrared.2019.03.033>
- Erkinbaev, C., Henderson, K., & Paliwal, J. (2017). Discrimination of gluten-free oats from contaminants using near infrared hyperspectral imaging technique. *Food Control*, *80*, 197–203. <https://doi.org/10.1016/j.foodcont.2017.04.036>
- Estévez, M., & Cava, R. (2004). Lipid and protein oxidation, release of iron from heme molecule and colour deterioration during refrigerated storage of liver pâté. *Meat Science*, *68*(4), 551–558. <https://doi.org/10.1016/j.meatsci.2004.05.007>
- Estévez, M., Díaz-Velasco, S., & Martínez, R. (2021). Protein carbonylation in food and nutrition:

- a concise update. *Amino Acids*, 1–15. <https://doi.org/10.1007/s00726-021-03085-6>
- Estévez, M., Ventanas, S., & Cava, R. (2006). Effect of natural and synthetic antioxidants on protein oxidation and colour and texture changes in refrigerated stored porcine liver pâté. *Meat Science*, *74*(2), 396–403. <https://doi.org/10.1016/j.meatsci.2006.04.010>
- Estévez, M., Ventanas, S., Heinonen, M., & Puolanne, E. (2011). Protein carbonylation and water-holding capacity of pork subjected to frozen storage: Effect of muscle type, premincing, and packaging. *Journal of Agricultural and Food Chemistry*, *59*(10), 5435–5443. <https://doi.org/10.1021/jf104995j>
- Estévez, M., & Xiong, Y. (2021). Protein Oxidation in Foods: Mechanisms, Consequences, and Antioxidant Solutions. *Foods*, *10*, 2346. <https://doi.org/10.3390/foods10102346>
- Fàbrega, E., Manteca, X., Font, J., Gispert, M., Carrión, D., Velarde, A., Ruiz-de-la-Torre, J. L., & Diestre, A. (2002). Effects of halothane gene and pre-slaughter treatment on meat quality and welfare from two pig crosses. *Meat Science*, *62*(4), 463–472. [https://doi.org/10.1016/S0309-1740\(02\)00040-2](https://doi.org/10.1016/S0309-1740(02)00040-2)
- Fabregat, A., Sidiropoulos, K., Viteri, G., Marin-Garcia, P., Ping, P., Stein, L., D'Eustachio, P., & Hermjakob, H. (2018). Reactome diagram viewer: Data structures and strategies to boost performance. *Bioinformatics*, *34*(7), 1208–1214. <https://doi.org/10.1093/bioinformatics/btx752>
- Fakankun, I., Spicer, V., & Levin, D. B. (2021). Proteomic analyses of the oleaginous and carotenogenic yeast *Rhodotorula diobovata* across growth phases under nitrogen- and oxygen-limited conditions. *Journal of Biotechnology*, *332*, 11–19. <https://doi.org/https://doi.org/10.1016/j.jbiotec.2021.03.016>
- Faustman, C., & Cassens, R. G. (1990). the Biochemical Basis for Discoloration in Fresh Meat: a Review. *Journal of Muscle Foods*, *1*(3), 217–243. <https://doi.org/10.1111/j.1745-4573.1990.tb00366.x>
- Faustman, C., & Cassens, R. G. (1991). The effect of cattle breed and muscle type on discoloration and various biochemical parameters in fresh beef. *Journal of Animal Science*, *69*(1), 184–193. <https://doi.org/10.2527/1991.691184x>
- Faustman, C., Cassens, R. G., Schaefer, D. M., Buege, D. R., & Scheller, K. K. (1989). Vitamin E Supplementation of Holstein Steer Diets Improves Sirloin Steak Color. *Journal of Food Science*, *54*(2), 485–486. <https://doi.org/10.1111/j.1365-2621.1989.tb03114.x>

- Faustman, C., Cassens, R. G., Schaefer, D. M., Buege, D. R., Williams, S. N., & Scheller, K. K. (1989). Improvement of Pigment and Lipid Stability in Holstein Steer Beef by Dietary Supplementation with Vitamin E. *Journal of Food Science*, 54(4), 858–862. <https://doi.org/10.1111/j.1365-2621.1989.tb07899.x>
- Faustman, C., Liebler, D. C., McClure, T. D., & Sun, Q. (1999). α,β -Unsaturated aldehydes accelerate oxymyoglobin oxidation. *Journal of Agricultural and Food Chemistry*, 47(8), 3140–3144. <https://doi.org/10.1021/jf990016c>
- Faustman, C., & Suman, S. P. (2017). The Eating Quality of Meat: I-Color. In *Lawrie's Meat Science: Eighth Edition* (pp. 329–356). <https://doi.org/10.1016/B978-0-08-100694-8.00011-X>
- Faustman, C., Yin, S., Tatiyaborworntham, N., & Naveena, B. M. (2010). Oxidation and protection of red meat. In *Oxidation in Foods and Beverages and Antioxidant Applications* (pp. 3–49). Elsevier. <https://doi.org/10.1533/9780857090331.1.3>
- Faustman, Cameron. (2007). Food from Supplement-Fed Animals. In *Technology of Reduced Additive Foods* (pp. 162–190). Blackwell Publishing Ltd. <https://doi.org/10.1002/9780470995044.ch8>
- Faustman, Cameron, & Phillips, A. (2001). Measurement of Discoloration in Fresh Meat. *Current Protocols in Food Analytical Chemistry*, 00(1), F3.3.1-F3.3.13. <https://doi.org/10.1002/0471142913.faf0303s00>
- Faustman, Cameron, Sun, Q., Mancini, R., & Suman, S. P. (2010). Myoglobin and lipid oxidation interactions: Mechanistic bases and control. *Meat Science*, 86(1), 86–94. <https://doi.org/10.1016/j.meatsci.2010.04.025>
- Feiner, G. (2006). Meat products Handbook: Practical Science and Technology. In *Journal of Chemical Information and Modeling* (Vol. 53, Issue 9). Elsevier Science & Technology.
- Feldhusen, F., Warnatz, A., Erdmann, R., & Wenzel, S. (1995). Influence of storage time on parameters of colour stability of beef. *Meat Science*, 40(2), 235–243. [https://doi.org/https://doi.org/10.1016/0309-1740\(94\)00048-C](https://doi.org/https://doi.org/10.1016/0309-1740(94)00048-C)
- Fisher, P., Mellett, F. D., & Hoffman, L. C. (2000). Halothane genotype and pork quality. 1. Carcass and meat quality characteristics of three halothane genotypes. *Meat Science*, 54(2), 97–105. [https://doi.org/10.1016/S0309-1740\(99\)00077-7](https://doi.org/10.1016/S0309-1740(99)00077-7)
- Font, R., del Río-Celestino, M., & de Haro-Bailón, A. (2007). *Near-Infrared Reflectance*

- Spectroscopy*, 23(1), 205–217. https://doi.org/10.1007/978-1-59745-098-0_17
- Gaitán-Jurado, A. J., Ortiz-Somovilla, V., España-España, F., Pérez-Aparicio, J., & De Pedro-Sanz, E. J. (2008). Quantitative analysis of pork dry-cured sausages to quality control by NIR spectroscopy. *Meat Science*, 78(4), 391–399. <https://doi.org/10.1016/j.meatsci.2007.07.005>
- Galbraith, J. K., Aalhus, J. L., Juárez, M., Dugan, M. E. R., Larsen, I. L., Aldai, N., Goonewardene, L. A., & Okine, E. K. (2016). Meat Colour Stability and Fatty Acid Profile in Commercial Bison and Beef. *Journal of Food Research*, 5(3), 92. <https://doi.org/10.5539/jfr.v5n3p92>
- Galbraith, J. K., Hauer, G., Helbig, L., Wang, Z., Marchello, M. J., & Goonewardene, L. A. (2006). Nutrient profiles in retail cuts of bison meat. *Meat Science*, 74(4), 648–654. <https://doi.org/10.1016/j.meatsci.2006.05.015>
- Galbraith, J., Rodas-González, A., López-Campos, Ó., Juárez, M., & Aalhus, J. (2014). Bison meat: Characteristics, challenges, and opportunities. *Animal Frontiers*, 4(4), 68–73. <https://doi.org/10.2527/af.2014-0036>
- Ganhão, R., Estévez, M., & Morcuende, D. (2011). Suitability of the TBA method for assessing lipid oxidation in a meat system with added phenolic-rich materials. *Food Chemistry*, 126(2), 772–778. <https://doi.org/10.1016/j.foodchem.2010.11.064>
- Genova, M. L., Ventura, B., Giuliano, G., Bovina, C., Formiggini, G., Parenti Castelli, G., & Lenaz, G. (2001). The site of production of superoxide radical in mitochondrial Complex I is not a bound ubiquinone but presumably iron-sulfur cluster N2. *FEBS Letters*, 505(3), 364–368. [https://doi.org/10.1016/S0014-5793\(01\)02850-2](https://doi.org/10.1016/S0014-5793(01)02850-2)
- Goi, A., Hocquette, J. F., Pellattiero, E., & De Marchi, M. (2021). Handheld near-infrared spectrometer allows on-line prediction of beef quality traits. *Meat Science*, 184(October), 108694. <https://doi.org/10.1016/j.meatsci.2021.108694>
- Gotoh, T., & Shikama, K. (1976). Generation of the Superoxide Radical during Autoxidation of Oxymyoglobin. *Journal of Biochemistry (Tokyo)*, 80(2), 397–399. <https://doi.org/10.1093/oxfordjournals.jbchem.a131289>
- Govari, M., & Pexara, A. (2015). Nitrates and nitrites in meat products. *Journal of the Hellenic Veterinary Medical Society*, 66(3), 127–140. <https://doi.org/10.12681/jhvms.15856>
- Gray, J. I., Goma, E. A., & Buckley, D. J. (1996). Oxidative quality and shelf life of meats. *Meat Science*, 43(SUPPL. 1), 111–123. [https://doi.org/10.1016/0309-1740\(96\)00059-9](https://doi.org/10.1016/0309-1740(96)00059-9)
- Guelker, M. R., Haneklaus, A. N., Brooks, J. C., Carr, C. C., Delmore, R. J., Griffin, D. B., Hale,

- D. S., Harris, K. B., Mafi, G. G., Johnson, D. D., Lorenzen, C. L., Maddock, R. J., Martin, J. N., Miller, R. K., Raines, C. R., Vanoverbeke, D. L., Vedral, L. L., Wasser, B. E., & Savell, J. W. (2013). National beef tenderness survey-2010: Warner-Bratzler shear force values and sensory panel ratings for beef steaks from United States retail and food service establishments. *Journal of Animal Science*, *91*(2), 1005–1014. <https://doi.org/10.2527/jas.2012-5785>
- Hagler, L., Coppes, R. I., & Herman, R. H. (1979). Metmyoglobin reductase. Identification and purification of a reduced nicotinamide adenine dinucleotide-dependent enzyme from bovine heart which reduces metmyoglobin. *The Journal of Biological Chemistry*, *254*(14), 6505–6514. [https://doi.org/10.1016/S0021-9258\(18\)50397-5](https://doi.org/10.1016/S0021-9258(18)50397-5)
- Halliwell, B., & Gutteridge, J. M. C. (1986). Oxygen free radicals and iron in relation to biology and medicine: Some problems and concepts. *Archives of Biochemistry and Biophysics*, *246*(2), 501–514. [https://doi.org/10.1016/0003-9861\(86\)90305-X](https://doi.org/10.1016/0003-9861(86)90305-X)
- Harel, S., & Kanner, J. (1985). Muscle membranal lipid peroxidation initiated by H₂O₂-activated metmyoglobin. *Journal of Agricultural and Food Chemistry*, *33*(6), 1188–1192. <https://doi.org/10.1021/jf00066a042>
- Hasan, M. M., Sood, V., Erkinbaev, C., Paliwal, J., Suman, S., & Rodas-Gonzalez, A. (2021). Principal component analysis of lipid and protein oxidation products and their impact on color stability in bison longissimus lumborum and psoas major muscles. *Meat Science*, *178*(April), 108523. <https://doi.org/10.1016/j.meatsci.2021.108523>
- Hawley, A. W. L. (1986). CARCASS CHARACTERISTICS OF BISON (*Bison bison*) STEERS. *Canadian Journal of Animal Science*, *66*(1), 293–295. <https://doi.org/10.4141/cjas86-030>
- Heberle, H., Meirelles, V. G., da Silva, F. R., Telles, G. P., & Minghim, R. (2015). InteractiVenn: A web-based tool for the analysis of sets through Venn diagrams. *BMC Bioinformatics*, *16*(1), 1–7. <https://doi.org/10.1186/s12859-015-0611-3>
- Hildrum, K. I., Nilsen, B. N., Mielnik, M., & Næs, T. (1994). Prediction of sensory characteristics of beef by near-infrared spectroscopy. *Meat Science*, *38*(1), 67–80. [https://doi.org/10.1016/0309-1740\(94\)90096-5](https://doi.org/10.1016/0309-1740(94)90096-5)
- Hood, D. E. (1980). Factors affecting the rate of metmyoglobin accumulation in pre-packaged beef. *Meat Science*, *4*(4), 247–265. [https://doi.org/10.1016/0309-1740\(80\)90026-1](https://doi.org/10.1016/0309-1740(80)90026-1)
- Hood, D. E., & Riordan, E. B. (1973). Discolouration in pre-packaged beef: measurement by

- reflectance spectrophotometry and shopper discrimination. *International Journal of Food Science & Technology*, 8(3), 333–343. <https://doi.org/10.1111/j.1365-2621.1973.tb01721.x>
- Hoving-Bolink, A. H., Vedder, H. W., Merks, J. W. M., de Klein, W. J. H., Reimert, H. G. M., Frankhuizen, R., van den Broek, W. H. A. ., & Lambooij, en E. (2005). Perspective of NIRS measurements early post mortem for prediction of pork quality. *Meat Science*, 69(3), 417–423. <https://doi.org/10.1016/j.meatsci.2004.08.012>
- Hughes, J., Clarke, F., Li, Y., Purslow, P., & Warner, R. (2019). Differences in light scattering between pale and dark beef longissimus thoracis muscles are primarily caused by differences in the myofilament lattice, myofibril and muscle fibre transverse spacings. *Meat Science*, 149(November 2018), 96–106. <https://doi.org/10.1016/j.meatsci.2018.11.006>
- Hughes, J., Clarke, F., Purslow, P., & Warner, R. (2017). High pH in beef longissimus thoracis reduces muscle fibre transverse shrinkage and light scattering which contributes to the dark colour. *Food Research International*, 101(September), 228–238. <https://doi.org/10.1016/j.foodres.2017.09.003>
- Hughes, J. M., Clarke, F. M., Purslow, P. P., & Warner, R. D. (2020). Meat color is determined not only by chromatic heme pigments but also by the physical structure and achromatic light scattering properties of the muscle. *Comprehensive Reviews in Food Science and Food Safety*, 19(1), 44–63. <https://doi.org/10.1111/1541-4337.12509>
- Hunt, M. C., & Hedrick, H. B. (1977a). CHEMICAL, PHYSICAL AND SENSORY CHARACTERISTICS OF BOVINE MUSCLE FROM FOUR QUALITY GROUPS. *Journal of Food Science*, 42(3), 716–720. <https://doi.org/10.1111/j.1365-2621.1977.tb12586.x>
- Hunt, M. C., & Hedrick, H. B. (1977b). Fiber Types and Related Properties Materials & Methods. *Journal of Food Science*, 42(2), 513–517.
- Hutchings, J. B. (1994). *Sensory Assessment of Appearance—Methodology BT - Food Colour and Appearance* (J. B. Hutchings (ed.); pp. 104–141). Springer US. https://doi.org/10.1007/978-1-4615-2123-5_5
- Hwang, Y. H., Kim, G. D., Jeong, J. Y., Hur, S. J., & Joo, S. T. (2010). The relationship between muscle fiber characteristics and meat quality traits of highly marbled Hanwoo (Korean native cattle) steers. *Meat Science*, 86(2), 456–461. <https://doi.org/10.1016/j.meatsci.2010.05.034>
- Igene, J. O., King, J. A., Pearson, A. M., & Gray, J. I. (1979). Influence of Heme Pigments, Nitrite, and Non-Heme Iron on Development of Warmed-over Flavor (WOF) in Cooked Meat.

- Journal of Agricultural and Food Chemistry*, 27(4), 838–842.
<https://doi.org/10.1021/jf60224a052>
- Janssen, J., Cammack, K., Legako, J., Cox, R., Grubbs, J. K., Underwood, K., Hansen, J., Kruse, C., & Blair, A. (2021). Influence of grain-and grass-finishing systems on carcass characteristics, meat quality, nutritional composition, and consumer sensory attributes of bison. *Foods*, 10(5), 1–23. <https://doi.org/10.3390/foods10051060>
- Janz, J. A. M., Aalhus, J. L., Price, M. A. and Greer, G. G. (2001). *Bison meat quality research: and investigation of spray chilling, very fast chilling, and the relationship of grade factors to meat quality*.
- Janz, J. A. M., Aalhus, J. L., & Price, M. A. (2001). Blast chilling and low voltage electrical stimulation influences on bison (*Bison bison bison*) meat quality. *Meat Science*, 57(4), 403–411. [https://doi.org/10.1016/S0309-1740\(00\)00118-2](https://doi.org/10.1016/S0309-1740(00)00118-2)
- Janz, J. A. M., Aalhus, J. L., Price, M. A., & Schaefer, A. L. (2000). The influence of elevated temperature conditioning on bison (*Bison bison bison*) meat quality. *Meat Science*, 56(3), 279–284. [https://doi.org/10.1016/S0309-1740\(00\)00054-1](https://doi.org/10.1016/S0309-1740(00)00054-1)
- Jeong, J. Y., Hur, S. J., Yang, H. S., Moon, S. H., Hwang, Y. H., Park, G. B., & Joo, S. T. (2009). Discoloration characteristics of 3 major muscles from cattle during cold storage. *Journal of Food Science*, 74(1), 3–7. <https://doi.org/10.1111/j.1750-3841.2008.00983.x>
- Jimenez-Villarreal, J. R., Pohlman, F. W., Johnson, Z. B., Brown, A. H., & Baublits, R. T. (2003). The impact of single antimicrobial intervention treatment with cetylpyridinium chloride, trisodium phosphate, chlorine dioxide or lactic acid on ground beef lipid, instrumental color and sensory characteristics. *Meat Science*, 65(3), 977–984. [https://doi.org/10.1016/S0309-1740\(02\)00315-7](https://doi.org/10.1016/S0309-1740(02)00315-7)
- Joseph, P., Suman, S. P., Li, S., Beach, C. M., Steinke, L., & Fontaine, M. (2010). Characterization of bison (*Bison bison*) myoglobin. *Meat Science*, 84(1), 71–78. <https://doi.org/10.1016/j.meatsci.2009.08.014>
- Joseph, P., Suman, S. P., Rentfrow, G., Li, S., & Beach, C. M. (2012). Proteomics of muscle-specific beef color stability. *Journal of Agricultural and Food Chemistry*, 60(12), 3196–3203. <https://doi.org/10.1021/jf204188v>
- Joseph, P., Poulson, Suman, S. P., Rentfrow, G., Li, S., & Beach, C. M. (2012). Proteomics of muscle-specific beef color stability. *Journal of Agricultural and Food Chemistry*, 60(12), 3196–3203.

<https://doi.org/10.1021/jf204188v>

- Kamruzzaman, M., ElMasry, G., Sun, D. W., & Allen, P. (2012). Prediction of some quality attributes of lamb meat using near-infrared hyperspectral imaging and multivariate analysis. *Analytica Chimica Acta*, *714*, 57–67. <https://doi.org/10.1016/j.aca.2011.11.037>
- Kamruzzaman, M., Makino, Y., & Oshita, S. (2016). Online monitoring of red meat color using hyperspectral imaging. *Meat Science*, *116*, 110–117. <https://doi.org/10.1016/j.meatsci.2016.02.004>
- Kanner, J., & Doll, L. (1991). Ferritin in Turkey Muscle Tissue: A Source of Catalytic Iron Ions for Lipid Peroxidation. *Journal of Agricultural and Food Chemistry*, *39*(2), 247–249. <https://doi.org/10.1021/jf00002a004>
- Kanner, J., & Harel, S. (1985). Lipid peroxidation and oxidation of several compounds by H₂O₂ activated metmyoglobin. *Lipids*, *20*(9), 625–628. <https://doi.org/10.1007/BF02534290>
- Kanner, J., Hazan, B., & Doll, L. (1988). Catalytic “free” iron ions in muscle foods. *Journal of Agricultural and Food Chemistry*, *36*(3), 412–415. <https://doi.org/10.1021/jf00081a002>
- Kapper, C., Klont, R. E., Verdonk, J. M. A. ., & Urlings, H. A. P. (2012). Prediction of pork quality with near infrared spectroscopy (NIRS). *Meat Science*, *91*(3), 294–299. <https://doi.org/10.1016/j.meatsci.2012.02.005>
- Ke, Y., Mitacek, R. M., Abraham, A., Mafi, G. G., VanOverbeke, D. L., Desilva, U., & Ramanathan, R. (2017). Effects of Muscle-Specific Oxidative Stress on Cytochrome c Release and Oxidation-Reduction Potential Properties. *Journal of Agricultural and Food Chemistry*, *65*(35), 7749–7755. <https://doi.org/10.1021/acs.jafc.7b01735>
- Kendrick, J. L., & Watts, B. M. (1969). Nicotinamide and Nicotinic Acid in Color Preservation of Fresh Meat. *Journal of Food Science*, *34*(3), 292–292. <https://doi.org/10.1111/j.1365-2621.1969.tb10346.x>
- Kim, Y. H., Keeton, J. T., Smith, S. B., Berghman, L. R., & Savell, J. W. (2009). Role of lactate dehydrogenase in metmyoglobin reduction and color stability of different bovine muscles. *Meat Science*, *83*(3), 376–382. <https://doi.org/10.1016/j.meatsci.2009.06.009>
- Kim, Yuan H., Hunt, M. C., Mancini, R. A., Seyfert, M., Loughin, T. M., Kropf, D. H., & Smith, J. S. (2006). Mechanism for lactate-color stabilization in injection-enhanced beef. *Journal of Agricultural and Food Chemistry*, *54*(20), 7856–7862. <https://doi.org/10.1021/jf061225h>
- King, D. A., Shackelford, S. D., Kalchayanand, N., & Wheeler, T. L. (2012). Sampling and aging

- effects on beef longissimus color stability measurements. *Journal of Animal Science*, 90(10), 3596–3605. <https://doi.org/10.2527/jas.2011-4871>
- King, D. A., Shackelford, S. D., Kuehn, L. A., Kemp, C. M., Rodriguez, A. B., Thallman, R. M., & Wheeler, T. L. (2010). Contribution of genetic influences to animal-to-animal variation in myoglobin content and beef lean color stability. *Journal of Animal Science*, 88(3), 1160–1167. <https://doi.org/10.2527/jas.2009-2544>
- King, D. A., Shackelford, S. D., & Wheeler, T. L. (2011). Relative contributions of animal and muscle effects to variation in beef lean color stability. *Journal of Animal Science*, 89(5), 1434–1451. <https://doi.org/10.2527/jas.2010-3595>
- Kirchofer, K. S., Calkins, C. R., & Gwartney, B. L. (2002). Fiber-type composition of muscles of the beef chuck and round. *Journal of Animal Science*, 80(11), 2872–2878. <https://doi.org/10.2527/2002.80112872x>
- Koch, R. M., Jung, H. G., Crouse, J. D., Varel, V. H., & Cundiff, L. V. (1995). Growth, digestive capability, carcass, and meat characteristics of Bison bison, Bos taurus, and Bos x Bison. *Journal of Animal Science*, 73(5), 1271–1281. <https://doi.org/10.2527/1995.7351271x>
- Kushnareva, Y., Murphy, A. N., & Andreyev, A. (2002). Complex I-mediated reactive oxygen species generation: Modulation by cytochrome c and NAD(P)⁺ oxidation-reduction state. *Biochemical Journal*, 368(2), 545–553. <https://doi.org/10.1042/BJ20021121>
- Kyu, J. C., Yu, J. P., Min, J. L., Jin, H. K., Ha, J., Choe, W., & Sung, S. K. (2007). Overexpressed cyclophilin A in cancer cells renders resistance to hypoxia- and cisplatin-induced cell death. *Cancer Research*, 67(8), 3654–3662. <https://doi.org/10.1158/0008-5472.CAN-06-1759>
- Lametsch, R., & Bendixen, E. (2001). Proteome analysis applied to meat science: Characterizing post mortem changes in porcine muscle. *Journal of Agricultural and Food Chemistry*, 49(10), 4531–4537. <https://doi.org/10.1021/jf010103g>
- Lanari, M. C., & Cassens, R. G. (1991). Mitochondrial Activity and Beef Muscle Color Stability. *Journal of Food Science*, 56(6), 1476–1479. <https://doi.org/10.1111/j.1365-2621.1991.tb08619.x>
- Larsson, K., Harrysson, H., Havenaar, R., Alminger, M., & Undeland, I. (2016). Formation of malondialdehyde (MDA), 4-hydroxy-2-hexenal (HHE) and 4-hydroxy-2-nonenal (HNE) in fish and fish oil during dynamic gastrointestinal in vitro digestion. *Food and Function*, 7(2), 1176–1187. <https://doi.org/10.1039/c5fo01401h>

- Lawrie, R. A., & Ledward, D. (2006). Lawrie's Meat Science: Seventh Edition. In *Lawrie's Meat Science: Seventh Edition*. <https://doi.org/10.1533/9781845691615>
- Ledward, D. A. (1970). Metmyoglobin Formation in Beef Stored in Carbon Dioxide Enriched and Oxygen Depleted Atmospheres. *Journal of Food Science*, 35(1), 33–37. <https://doi.org/10.1111/j.1365-2621.1970.tb12362.x>
- Ledward, D. A., Johnston, D. E., & Knight, M. K. (1992). *The chemistry of muscle-based foods*. Royal Society of Chemistry.
- Lee, S. P., Hwang, Y. S., Kim, Y. J., Kwon, K. S., Kim, H. J., Kim, K., & Chae, H. Z. (2001). Cyclophilin A Binds to Peroxiredoxins and Activates Its Peroxidase Activity. *Journal of Biological Chemistry*, 276(32), 29826–29832. <https://doi.org/10.1074/jbc.M101822200>
- Lee, S., Phillips, A. L., Liebler, D. C., & Faustman, C. (2003). Porcine oxymyoglobin and lipid oxidation in vitro. *Meat Science*, 63(2), 241–247. [https://doi.org/10.1016/S0309-1740\(02\)00076-1](https://doi.org/10.1016/S0309-1740(02)00076-1)
- Legako, J. F., Cramer, T., Yardley, K., Murphy, T. J., Gardner, T., Chail, A., Pitcher, L. R., & Macadam, J. W. (2018). Retail stability of three beef muscles from grass-, legume-, and feedlot-finished cattle. *Journal of Animal Science*, 96(6), 2238–2248. <https://doi.org/10.1093/jas/sky125>
- Leroy, B., Lambotte, S., Dotreppe, O., Lecocq, H., Istasse, L., & Clinquart, A. (2004). Prediction of technological and organoleptic properties of beef Longissimus thoracis from near-infrared reflectance and transmission spectra. *Meat Science*, 66(1), 45–54. [https://doi.org/10.1016/S0309-1740\(03\)00002-0](https://doi.org/10.1016/S0309-1740(03)00002-0)
- Li, Y., Park, J.-S., Deng, J.-H., & Bai, Y. (2006). Cytochrome c oxidase subunit IV is essential for assembly and respiratory function of the enzyme complex. *Journal of Bioenergetics and Biomembranes*, 38(5), 283–291. <https://doi.org/10.1007/s10863-006-9052-z>
- Li, Z., Li, M., Li, X., Xin, J., Wang, Y., Shen, Q. W., & Zhang, D. (2018). Quantitative phosphoproteomic analysis among muscles of different color stability using tandem mass tag labeling. *Food Chemistry*, 249(1), 8–15. <https://doi.org/10.1016/j.foodchem.2017.12.047>
- Lindhahl, G. (2005). Colour characteristics of fresh pork. *Uppsala, 2005*. <http://pub.epsilon.slu.se/827/>
- Lindhahl, G. (2011). Colour stability of steaks from large beef cuts aged under vacuum or high oxygen modified atmosphere. *Meat Science*, 87(4), 428–435.

<https://doi.org/10.1016/j.meatsci.2010.10.023>

- Liu, H.-P., & Watts, B. M. (1970). CATALYSTS OF LIPID PEROXIDATION IN MEATS. 3. Catalysts of Oxidative Rancidity in Meats. *Journal of Food Science*, 35(5), 596–598. <https://doi.org/10.1111/j.1365-2621.1970.tb04819.x>
- Liu, R., Fu, Q., Lonergan, S., Huff-Lonergan, E., Xing, L., Zhang, L., Bai, Y., Zhou, G., & Zhang, W. (2018). Identification of S-nitrosylated proteins in postmortem pork muscle using modified biotin switch method coupled with isobaric tags. *Meat Science*, 145(March), 431–439. <https://doi.org/10.1016/j.meatsci.2018.07.027>
- Liu, Y, Lyon, B. G., Windham, W. R., Lyon, C. E., & Savage, E. M. (2004). Prediction of physical, color, and sensory characteristics of broiler breasts by visible/near infrared reflectance spectroscopy. *Poultry Science*, 83(8), 1467–1474. <https://doi.org/10.1093/ps/83.8.1467>
- Liu, Yongliang, Lyon, B. G., Windham, W. R., Realini, C. E., Pringle, T. D. D., & Duckett, S. (2003). Prediction of color, texture, and sensory characteristics of beef steaks by visible and near infrared reflectance spectroscopy. A feasibility study. *Meat Science*, 65(3), 1107–1115. [https://doi.org/10.1016/S0309-1740\(02\)00328-5](https://doi.org/10.1016/S0309-1740(02)00328-5)
- López-Campos, Ó., Roberts, J. C., , Argenis Rodas-González, C., , Jayson Galbraith, C., Nuria Prieto, B., , Michael E.R. Dugana, B., , Ivy L. Larsena, B., & Aalhusa, J. L. (2018). Nitrite embedded vacuum packaging improves retail characteristics of bison steaks. *Meat Science*, 137, 280. <https://doi.org/10.1016/j.meatsci.2017.08.018>
- Lund, M. N., Heinonen, M., Baron, C. P., & Estévez, M. (2011). Protein oxidation in muscle foods: A review. *Molecular Nutrition and Food Research*, 55(1), 83–95. <https://doi.org/10.1002/mnfr.201000453>
- Luño, M., Beltrán, J. A., & Roncalés, P. (1998). Shelf-life extension and colour stabilisation of beef packaged in a low O₂ atmosphere containing CO: Loin steaks and ground meat. *Meat Science*, 48(1–2), 75–84. [https://doi.org/10.1016/S0309-1740\(97\)00078-8](https://doi.org/10.1016/S0309-1740(97)00078-8)
- Luqué, L. D., Johnson, B. J., Martin, J. N., Miller, M. F., Hodgen, J. M., Hutcheson, J. P., Nichols, W. T., Streeter, M. N., Yates, D. A., Allen, D. M., & Brooks, J. C. (2011). Zilpaterol hydrochloride supplementation has no effect on the shelf life of ground beef. *Journal of Animal Science*, 89(3), 817–825. <https://doi.org/10.2527/jas.2010-3317>
- Lynch, A., Buckley, D. J., Galvin, K., Mullen, A. M., Troy, D. J., & Kerry, J. P. (2002). Evaluation of rib steak colour from Friesian, Hereford and Charolais heifers pastured or overwintered

- prior to slaughter. *Meat Science*, 61(3), 227–232. [https://doi.org/10.1016/S0309-1740\(01\)00177-2](https://doi.org/10.1016/S0309-1740(01)00177-2)
- Lynch, M. P., & Faustman, C. (2000). Effect of aldehyde lipid oxidation products on myoglobin. *Journal of Agricultural and Food Chemistry*, 48(3), 600–604. <https://doi.org/10.1021/jf990732e>
- MacDougall, D. B. (1972). The effect of time and storage temperature on consumer quality. *Meat Chilling: Why and How*, 8–11.
- Maciel, L., de Oliveira, D. F., Monnerat, G., Campos de Carvalho, A. C., & Nascimento, J. H. M. (2020). Exogenous 10 kDa-Heat Shock Protein Preserves Mitochondrial Function After Hypoxia/Reoxygenation. *Frontiers in Pharmacology*, 11(May), 1–15. <https://doi.org/10.3389/fphar.2020.00545>
- Madhavi, D. L., & Carpenter, C. E. (1993). Aging and Processing Affect Color, Metmyoglobin Reductase and Oxygen Consumption of Beef Muscles. *Journal of Food Science*, 58(5), 939–942. <https://doi.org/10.1111/j.1365-2621.1993.tb06083.x>
- Maheswarappa, N. B., Faustman, C., Tatiyaborworntham, N., Yin, S., Ramanathan, R., & Mancini, R. A. (2009). Mass Spectrometric Characterization and Redox Instability of Turkey and Chicken Myoglobins As Induced by Unsaturated Aldehydes. *Journal of Agricultural and Food Chemistry*, 57(18), 8668–8676. <https://doi.org/10.1021/jf902705q>
- Mamani-Linares, L. W., Gallo, C., & Alomar, D. (2012). Identification of cattle, llama and horse meat by near infrared reflectance or transreflectance spectroscopy. *Meat Science*, 90(2), 378–385. <https://doi.org/10.1016/j.meatsci.2011.08.002>
- Mancini, R. A., & Hunt, M. C. (2005). Current research in meat color. *Meat Science*, 71(1), 100–121. <https://doi.org/10.1016/j.meatsci.2005.03.003>
- Mancini, R. A., & Ramanathan, R. (2014). Effects of postmortem storage time on color and mitochondria in beef. *Meat Science*, 98(1), 65–70. <https://doi.org/10.1016/j.meatsci.2014.04.007>
- Mancini, R. A., Suman, S. P., Konda, M. K. R., & Ramanathan, R. (2009). Effect of carbon monoxide packaging and lactate enhancement on the color stability of beef steaks stored at 1 °C for 9 days. *Meat Science*, 81(1), 71–76. <https://doi.org/10.1016/j.meatsci.2008.06.021>
- Mancini, Richard A., Belskie, K., Suman, S. P., & Ramanathan, R. (2018). Muscle-Specific Mitochondrial Functionality and Its Influence on Fresh Beef Color Stability. *Journal of Food*

- Science*, 83(8), 2077–2082. <https://doi.org/10.1111/1750-3841.14219>
- Manley, M. (2014). Near-infrared spectroscopy and hyperspectral imaging: Non-destructive analysis of biological materials. *Chemical Society Reviews*, 43(24), 8200–8214. <https://doi.org/10.1039/c4cs00062e>
- Marchello, M. J., & Driskell, J. A. (2001). NUTRIENT COMPOSITION OF GRASS- AND GRAIN-FINISHED BISON. *Great Plains Research*, 11(1), 65–82. <http://www.jstor.org/stable/23775641>
- Marchello, M. J., Slinger, W. D., Hadley, M., Milne, D. B., & Driskell, J. A. (1998). Nutrient Composition of Bison Fed Concentrate Diets. *Journal of Food Composition and Analysis*, 11(3), 231–239. <https://doi.org/10.1006/jfca.1998.0583>
- Marsh, B. B., Ringkob, T. P., Russell, R. L., Swartz, D. R., & Pagel, L. A. (1987). Effects of early-postmortem glycolytic rate on beef tenderness. *Meat Science*, 21(4), 241–248. [https://doi.org/10.1016/0309-1740\(87\)90061-1](https://doi.org/10.1016/0309-1740(87)90061-1)
- Martinaud, A., Mercier, Y., Marinova, P., Tassy, C., Gatellier, P., & Renerre, M. (1997). Comparison of Oxidative Processes on Myofibrillar Proteins from Beef during Maturation and by Different Model Oxidation Systems. *Journal of Agricultural and Food Chemistry*, 45(7), 2481–2487. <https://doi.org/10.1021/jf960977g>
- McClenahan, J., & Driskell, J. (2002). *Nutrient Content and Sensory Characteristics of Bison Meat. McClenahan.*
- McDaniel, J., Askew, W., Bennett, D., Mihalopoulos, J., Anantharaman, S., Fjeldstad, A. S., Rule, D. C., Nanjee, N. M., Harris, R. A., & Richardson, R. S. (2013). Bison meat has a lower atherogenic risk than beef in healthy men. *Nutrition Research*, 33(4), 293–302. <https://doi.org/10.1016/j.nutres.2013.01.007>
- McDevitt, R. M., Gavin, A. J., Andrés, S., & Murray, I. (2005). The Ability of Visible and near Infrared Reflectance Spectroscopy to Predict the Chemical Composition of Ground Chicken Carcasses and to Discriminate between Carcasses from Different Genotypes. *Journal of near Infrared Spectroscopy (United Kingdom)*, 13(3), 109–117. <https://doi.org/10.1255/jnirs.463>
- McKenna, D. R., Mies, P. D., Baird, B. E., Pfeiffer, K. D., Ellebracht, J. W., & Savell, J. W. (2005). Biochemical and physical factors affecting discoloration characteristics of 19 bovine muscles. *Meat Science*, 70(4), 665–682. <https://doi.org/10.1016/j.meatsci.2005.02.016>
- McMillin, K. W. (2008). Where is MAP Going? A review and future potential of modified

- atmosphere packaging for meat. *Meat Science*, 80(1), 43–65.
<https://doi.org/10.1016/j.meatsci.2008.05.028>
- McMillin, K. W. (2017). Advancements in meat packaging. *Meat Science*, 132, 153–162.
<https://doi.org/10.1016/J.MEATSCI.2017.04.015>
- Mertz, J., Tan, H., Pagala, V., Bai, B., Chen, P. C., Li, Y., Cho, J. H., Shaw, T., Wang, X., & Peng, J. (2015). Sequential elution interactome analysis of the mind bomb 1 ubiquitin ligase reveals a novel role in dendritic spine outgrowth. *Molecular and Cellular Proteomics*, 14(7), 1898–1910. <https://doi.org/10.1074/mcp.M114.045898>
- Meulemans, A., Dotreppe, O., Leroy, B., Istasse, L., & Clinquart, A. (2003). Prediction of organoleptic and technological characteristics of pork meat by near infrared spectroscopy. *Sciences Des Aliments - SCIALIMENT*, 23, 159–162. <https://doi.org/10.3166/sda.23.159-162>
- Mickelson, M. A., & Claus, J. R. (2020). Carcass chilling method effects on color and tenderness of bison meat. *Meat Science*, 161, 108002. <https://doi.org/10.1016/j.meatsci.2019.108002>
- Mikkelsen, A., Juncher, D., & Skibsted, L. H. (1999). Metmyoglobin reductase activity in porcine m. longissimus dorsi muscle. *Meat Science*, 51(2), 155–161. [https://doi.org/10.1016/S0309-1740\(98\)00114-4](https://doi.org/10.1016/S0309-1740(98)00114-4)
- Mikkelsen, A., & Skibsted, L. H. (1992). Kinetics of enzymatic reduction of metmyoglobin in relation to oxygen activation in meat products. *Zeitschrift Für Lebensmittel-Untersuchung Und -Forschung*, 194(1), 9–16. <https://doi.org/10.1007/BF01191032>
- Miller, D. K., Smith, V. L., Kanner, J., Miller, D. D., & Lawless, H. T. (1994). Lipid Oxidation and Warmed-Over Aroma in Cooked Ground Pork from Swine Fed Increasing Levels of Iron. *Journal of Food Science*, 59(4), 751–756. <https://doi.org/10.1111/j.1365-2621.1994.tb08119.x>
- Misra, H. P., & Fridovich, I. (1972). The generation of superoxide radical during the autoxidation of hemoglobin. *Journal of Biological Chemistry*, 247(21), 6960–6962. [https://doi.org/10.1016/s0021-9258\(19\)44679-6](https://doi.org/10.1016/s0021-9258(19)44679-6)
- Moelich, E. I., Hoffman, L. C., & Conradie, P. J. (2003). Sensory and functional meat quality characteristics of pork derived from three halothane genotypes. *Meat Science*, 63(3), 333–338. [https://doi.org/10.1016/S0309-1740\(02\)00090-6](https://doi.org/10.1016/S0309-1740(02)00090-6)
- Mohan, A., Hunt, M. C., Muthukrishnan, S., Barstow, T. J., & Houser, T. A. (2010). Myoglobin redox form stabilization by compartmentalized lactate and malate dehydrogenases. *Journal*

- of *Agricultural and Food Chemistry*, 58(11), 7021–7029. <https://doi.org/10.1021/jf100714g>
- Monahan, F. J. (2000). Oxidation of lipids in muscle foods: Fundamental and applied concerns. *Antioxidants in Muscle Foods: Nutritional Strategies to Improve Quality*, 1, 499. [https://books.google.co.za/books?hl=en&lr=&id=SoTso4ucfcsC&oi=fnd&pg=PA3&dq=Oxidation+of+lipids+in+muscle+foods:+Fundamental+and+applied+concerns&ots=BtFB7yZv5q&sig=bR2cVdDCyhVPkSY7yxJUsOUj16I#v=onepage&q=Oxidation of lipids in muscle foods%3A](https://books.google.co.za/books?hl=en&lr=&id=SoTso4ucfcsC&oi=fnd&pg=PA3&dq=Oxidation+of+lipids+in+muscle+foods:+Fundamental+and+applied+concerns&ots=BtFB7yZv5q&sig=bR2cVdDCyhVPkSY7yxJUsOUj16I#v=onepage&q=Oxidation%20of%20lipids%20in%20muscle%20foods%3A)
- Moran, L., Andres, S., Allen, P., & Moloney, A. P. (2018). Visible and near infrared spectroscopy as an authentication tool: Preliminary investigation of the prediction of the ageing time of beef steaks. *Meat Science*, 142(December 2017), 52–58. <https://doi.org/10.1016/j.meatsci.2018.04.007>
- Moxness, M. S., Brunauer, L. S., & Huestis, W. H. (1996). Hemoglobin oxidation products extract phospholipids from the membrane of human erythrocytes. *Biochemistry*, 35(22), 7181–7187. <https://doi.org/10.1021/bi952167o>
- Nair, M. N., Li, S., Beach, C. M., Rentfrow, G., & Suman, S. P. (2018). Changes in the Sarcoplasmic Proteome of Beef Muscles with Differential Color Stability during Postmortem Aging. *Meat and Muscle Biology*, 2(1), 1. <https://doi.org/10.22175/mmb2017.07.0037>
- Nair, M.N., Ramanathan, R., Rentfrow, G., & Suman, S. P. (2017). Intramuscular variation in mitochondrial functionality of beef semimembranosus. *South African Journal of Animal Sciences*, 47(5), 635–639. <https://doi.org/10.4314/sajas.v47i5.6>
- Nair, Mahesh N., Li, S., Beach, C. M., Rentfrow, G., & Suman, S. P. (2018). Changes in the Sarcoplasmic Proteome of Beef Muscles with Differential Color Stability during Postmortem Aging. *Meat and Muscle Biology*, 2(1). <https://doi.org/10.22175/mmb2017.07.0037>
- Nair, V., O’Neil, C. L., & Wang, P. G. (2008). Malondialdehyde. In *Encyclopedia of Reagents for Organic Synthesis*. <https://doi.org/https://doi.org/10.1002/047084289X.rm013.pub2>
- Narváez-Bravo, C., Rodas-González, A., Ding, C., López-Campos, O., Galbraith, J., Larsen, I. L., Ye, J., Siegel, D., & Aalhus, J. L. (2017). Effects of novel nitrite packaging film on the bacterial growth of bison strip-loin steaks. *Journal of Food Processing and Preservation*, 41(6), 1–7. <https://doi.org/10.1111/jfpp.13311>
- Naveena, B. M., Faustman, C., Tatiyaborworntham, N., Yin, S., Ramanathan, R., & Mancini, R. A. (2010). Detection of 4-hydroxy-2-nonenal adducts of turkey and chicken myoglobins

- using mass spectrometry. *Food Chemistry*, 122(3).
<https://doi.org/10.1016/j.foodchem.2010.02.062>
- NBA/CBA. (2010). *The bison producer's handbook*.
- NCBI. (2021a). National Center for Biotechnology Information. PubChem Compound Summary for CID 10964, Malonaldehyde. Retrieved October 29, 2021 from <https://pubchem.ncbi.nlm.nih.gov/compound/Malonaldehyde>.
- NCBI. (2021b). National Center for Biotechnology Information. PubChem Compound Summary for CID 5283344, 4-Hydroxynonenal. Retrieved October 29, 2021 from <https://pubchem.ncbi.nlm.nih.gov/compound/4-Hydroxynonenal>.
- Neethling, N. E., Suman, S. P., Sigge, G. O., Hoffman, L. C., & Hunt, M. C. (2017). Exogenous and Endogenous Factors Influencing Color of Fresh Meat from Ungulates. *Meat and Muscle Biology*, 1(1), 253. <https://doi.org/10.22175/mmb2017.06.0032>
- O'Grady, M. N., Monahan, F. J., & Brunton, N. P. (2001). Oxymyoglobin oxidation and lipid oxidation in bovine muscle - Mechanistic studies. *Journal of Food Science*, 66(3), 386–392. <https://doi.org/10.1111/j.1365-2621.2001.tb16115.x>
- O'Keeffe, M., & Hood, D. E. (1981). Anoxic storage of fresh beef. 2: Colour stability and weight loss. *Meat Science*, 5(4), 267–281. [https://doi.org/10.1016/0309-1740\(81\)90017-6](https://doi.org/10.1016/0309-1740(81)90017-6)
- O'Keeffe, M., & Hood, D. E. (1982). Biochemical factors influencing metmyoglobin formation on beef from muscles of differing colour stability. *Meat Science*, 7(3), 209–228. [https://doi.org/10.1016/0309-1740\(82\)90087-0](https://doi.org/10.1016/0309-1740(82)90087-0)
- Oakley, A. (2011). Glutathione transferases: a structural perspective. *Drug Metabolism Reviews*, 43(2), 138–151. <https://doi.org/10.3109/03602532.2011.558093>
- Obchoei, S., Wongkhan, S., Wongkham, C., Li, M., Yao, Q., & Chen, C. (2009). Cyclophilin A: Potential functions and therapeutic target for human cancer. *Medical Science Monitor*, 15(11), RA221-32.
- Offer, G., Knight, P., Jeacocke, R., Almond, R., Cousins, T., Elsey, J., Parsons, N., Sharp, A., Starr, R., & Purslow, P. (1989). The structural basis of the water-holding, appearance and toughness of meat and meat products. *Food Microstructure*, 8(1), 151–170.
- Okolie, N. P., & Okugbo, O. T. (2013). a Comparative Study of Malondialdehyde Contents of Some Meat and Fish Samples Processed By Different Methods. *Journal of Pharmaceutical and Scientific Innovation*, 2(4), 26–29. <https://doi.org/10.7897/2277-4572.02448>

- Olsson, M. G., Centlow, M., Rutardóttir, S., Stenfors, I., Larsson, J., Hosseini-Maaf, B., Olsson, M. L., Hansson, S. R., & Åkerström, B. (2010). Increased levels of cell-free hemoglobin, oxidation markers, and the antioxidative heme scavenger α 1-microglobulin in preeclampsia. *Free Radical Biology and Medicine*, 48(2), 284–291. <https://doi.org/10.1016/j.freeradbiomed.2009.10.052>
- Osborne, B. G., Fearn, T., & Hindle, P. T. (1993). *Practical NIR spectroscopy : with applications in food and beverage analysis* (2nd ed.). Longman Scientific & Technical.
- Panayiotou, C., Solaroli, N., & Karlsson, A. (2014). The many isoforms of human adenylate kinases. *The International Journal of Biochemistry & Cell Biology*, 49, 75–83. <https://doi.org/https://doi.org/10.1016/j.biocel.2014.01.014>
- Patel, N., Toledo-Alvarado, H., & Bittante, G. (2021). Performance of different portable and hand-held near-infrared spectrometers for predicting beef composition and quality characteristics in the abattoir without meat sampling. *Meat Science*, 178, 108518. <https://doi.org/10.1016/j.meatsci.2021.108518>
- Pathare, P. B., Opara, U. L., & Al-Said, F. A. J. (2013). Colour Measurement and Analysis in Fresh and Processed Foods: A Review. *Food and Bioprocess Technology*, 6(1), 36–60. <https://doi.org/10.1007/s11947-012-0867-9>
- Peyvasteh, M., Popov, A., Bykov, A., & Meglinski, I. (2020). Meat freshness revealed by visible to near-infrared spectroscopy and principal component analysis. *Journal of Physics Communications*, 4(9), 1–11. <https://doi.org/10.1088/2399-6528/abb322>
- Phung, V. T., Sælid, E., Egelanddal, B., Volden, J., & Slinde, E. (2011). Oxygen Consumption Rate of Permeabilized Cells and Isolated Mitochondria from Pork M. Masseter and Liver Examined Fresh and after Freeze-Thawing at Different pH Values. *Journal of Food Science*, 76(6), C929–C936. <https://doi.org/10.1111/j.1750-3841.2011.02275.x>
- Pietrasik, Z., Dhanda, J. S., Shand, P. J., & Pegg, R. B. (2006). Influence of injection, packaging, and storage conditions on the quality of beef and bison steaks. *Journal of Food Science*, 71(2), S110–S118. <https://doi.org/10.1111/j.1365-2621.2006.tb08913.x>
- Pivovarova, A. V., Mikhailova, V. V., Chernik, I. S., Chebotareva, N. A., Levitsky, D. I., & Gusev, N. B. (2005). Effects of small heat shock proteins on the thermal denaturation and aggregation of F-actin. *Biochemical and Biophysical Research Communications*, 331(4), 1548–1553. <https://doi.org/10.1016/j.bbrc.2005.04.077>

- Ponnampalam, E. N., Norng, S., Burnett, V. F., Dunshea, F. R., Jacobs, J. L., & Hopkins, D. L. (2014). The Synergism of Biochemical Components Controlling Lipid Oxidation in Lamb Muscle. *Lipids*, *49*(8), 757–766. <https://doi.org/10.1007/s11745-014-3916-5>
- Popova, T., Marinova, P., Vasileva, V., Gorinov, Y., & Lidji, K. (2009). Oxidative changes in lipids and proteins in beef during storage. *Archiva Zootechnica*, *12*(3), 30–38.
- Prieto, N., Andrés, S., Giráldez, F. J., Mantecón, A. R., & Lavín, P. (2008). Ability of near infrared reflectance spectroscopy (NIRS) to estimate physical parameters of adult steers (oxen) and young cattle meat samples. *Meat Science*, *79*(4), 692–699. <https://doi.org/10.1016/j.meatsci.2007.10.035>
- Prieto, N., López-Campos, Ó., Aalhus, J. L., Dugan, M. E. R., Juárez, M., & Uttaro, B. (2014). Use of near infrared spectroscopy for estimating meat chemical composition, quality traits and fatty acid content from cattle fed sunflower or flaxseed. *Meat Science*, *98*(2), 279–288. <https://doi.org/10.1016/j.meatsci.2014.06.005>
- Prieto, N., Roehe, R., Lavín, P., Batten, G., & Andrés, S. (2009). Application of near infrared reflectance spectroscopy to predict meat and meat products quality: A review. *Meat Science*, *83*(2), 175–186. <https://doi.org/10.1016/j.meatsci.2009.04.016>
- Prieto, N., Ross, D. W., Navajas, E. A., Richardson, R. I., Hyslop, J. J., Simm, G., & Roehe, R. (2011). Online prediction of fatty acid profiles in crossbred Limousin and Aberdeen Angus beef cattle using near infrared reflectance spectroscopy. *Animal*, *5*(1), 155–165. <https://doi.org/10.1017/S1751731110001618>
- Prieto, N., Andrés, S., Giráldez, F. J., Mantecón, A. R., & Lavín, P. (2006). Potential use of near infrared reflectance spectroscopy (NIRS) for the estimation of chemical composition of oxen meat samples. *Meat Science*, *74*(3), 487–496. <https://doi.org/10.1016/j.meatsci.2006.04.030>
- Prieto, Nuria, Pawluczyk, O., Dugan, M. E. R., & Aalhus, J. L. (2017). A Review of the Principles and Applications of Near-Infrared Spectroscopy to Characterize Meat, Fat, and Meat Products. *Applied Spectroscopy*, *71*(7), 1403–1426. <https://doi.org/10.1177/0003702817709299>
- Purslow, P. P., Warner, R. D., Clarke, F. M., & Hughes, J. M. (2020). Variations in meat colour due to factors other than myoglobin chemistry; a synthesis of recent findings (invited review). *Meat Science*, *159*(June 2019). <https://doi.org/10.1016/j.meatsci.2019.107941>
- Qi, F., Pradhan, R. K., Dash, R. K., & Beard, D. A. (2011). Detailed kinetics and regulation of

- mammalian 2-oxoglutarate dehydrogenase. *BMC Biochemistry*, 12(1).
<https://doi.org/10.1186/1471-2091-12-53>
- Quinlan, C. L., Orr, A. L., Perevoshchikova, I. V., Treberg, J. R., Ackrell, B. A., & Brand, M. D. (2012). Mitochondrial complex II can generate reactive oxygen species at high rates in both the forward and reverse reactions. *Journal of Biological Chemistry*, 287(32), 27255–27264.
<https://doi.org/10.1074/jbc.M112.374629>
- Ramanathan, R., Konda, M. K. R., Mancini, R. A., & Faustman, C. (2009). Species-specific effects of sarcoplasmic extracts on lipid oxidation in vitro. *Journal of Food Science*, 74(1).
<https://doi.org/10.1111/j.1750-3841.2008.01021.x>
- Ramanathan, R., Mancini, R. A., Suman, S. P., & Cantino, M. E. (2012). Effects of 4-hydroxy-2-nonenal on beef heart mitochondrial ultrastructure, oxygen consumption, and metmyoglobin reduction. *Meat Science*, 90(3), 564–571. <https://doi.org/10.1016/j.meatsci.2011.09.017>
- Ramanathan, R., Nair, M. N., Hunt, M. C., & Suman, S. P. (2019). Mitochondrial functionality and beef colour: A review of recent research. *South African Journal of Animal Sciences*, 49(1), 9–19. <https://doi.org/10.4314/sajas.v49i1.2>
- Ramanathan, Ranjith, Hunt, M. C., Mancini, R. A., Nair, M. N., Denzer, M. L., Suman, S. P., & Mafi, G. G. (2020). Recent Updates in Meat Color Research: Integrating Traditional and High-Throughput Approaches. *Meat and Muscle Biology*, 4(2).
<https://doi.org/10.22175/mmb.9598>
- Ramanathan, Ranjith, & Mancini, R. A. (2018). Role of Mitochondria in Beef Color: A Review. *Meat and Muscle Biology*, 2(1). <https://doi.org/10.22175/mmb2018.05.0013>
- Ramanathan, Ranjith, Mancini, R. A., & Konda, M. R. (2009). Effects of lactate on beef heart mitochondrial oxygen consumption and muscle darkening. *Journal of Agricultural and Food Chemistry*, 57(4), 1550–1555. <https://doi.org/10.1021/jf802933p>
- Ramanathan, Ranjith, Mancini, R. A., Suman, S. P., & Beach, C. M. (2014). Covalent binding of 4-hydroxy-2-nonenal to lactate dehydrogenase decreases nadh formation and metmyoglobin reducing activity. *Journal of Agricultural and Food Chemistry*, 62(9), 2112–2117.
<https://doi.org/10.1021/jf404900y>
- Ramanathan, Ranjith, Nair, M. N., Wang, Y., Li, S., Beach, C. M., Mancini, R. A., Belskie, K., & Suman, S. P. (2021). Differential Abundance of Mitochondrial Proteome Influences the Color Stability of Beef *Longissimus Lumborum* and *Psoas Major* Muscles. *Meat and Muscle*

- Biology*, 5(1). <https://doi.org/10.22175/mmb.11705>
- Ramanathan, Ranjith, Suman, S. P., & Faustman, C. (2020). Biomolecular Interactions Governing Fresh Meat Color in Post-mortem Skeletal Muscle: A Review. *Journal of Agricultural and Food Chemistry*, 68(46), 12779–12787. <https://doi.org/10.1021/acs.jafc.9b08098>
- Realini, C. E., Duckett, S. K., Brito, G. W., Dalla Rizza, M., & De Mattos, D. (2004). Effect of pasture vs. concentrate feeding with or without antioxidants on carcass characteristics, fatty acid composition, and quality of Uruguayan beef. *Meat Science*, 66(3), 567–577. [https://doi.org/10.1016/S0309-1740\(03\)00160-8](https://doi.org/10.1016/S0309-1740(03)00160-8)
- Reddy, L. M., & Carpenter, C. E. (1991). Determination of Metmyoglobin Reductase Activity in Bovine Skeletal Muscles. *Journal of Food Science*, 56(5), 1161–1164. <https://doi.org/10.1111/j.1365-2621.1991.tb04724.x>
- Renner, M. (2000). Oxidative processes and myoglobin. *Antioxidants in Muscle Foods*, 2000, 113–133.
- Renner, M., & Labas, R. (1987). Biochemical factors influencing metmyoglobin formation in beef muscles. *Meat Science*, 19(2), 151–165. [https://doi.org/10.1016/0309-1740\(87\)90020-9](https://doi.org/10.1016/0309-1740(87)90020-9)
- Requena, J. R., Fu, M. X., Ahmed, M. U., Jenkins, A. J., Lyons, T. J., Baynes, J. W., & Thorpe, S. R. (1997). Quantification of malondialdehyde and 4-hydroxynonenal adducts to lysine residues in native and oxidized human low-density lipoprotein. *Biochemical Journal*, 322(1), 317–325. <https://doi.org/10.1042/bj3220317>
- Rhee, K. S., Ziprin, Y. A., & Ordonez, G. (1987). Catalysis of lipid oxidation in raw and cooked beef by metmyoglobin-H₂O₂, nonheme iron, and enzyme systems. *Journal of Agricultural and Food Chemistry*, 35(6), 1013–1017. <https://doi.org/10.1021/jf00078a037>
- Ripoll, G., Albertí, P., Panea, B., Olleta, J. L., & Sañudo, C. (2008). Near-infrared reflectance spectroscopy for predicting chemical, instrumental and sensory quality of beef. *Meat Science*, 80(3), 697–702. <https://doi.org/10.1016/j.meatsci.2008.03.009>
- Roberts, J. C., Rodas-González, A., Galbraith, J., Dugan, M. E. R., Larsen, I. L., Aalhus, J. L., & López-Campos, Ó. (2017). Nitrite Embedded Vacuum Packaging Improves Retail Color and Oxidative Stability of Bison Steaks and Patties. *Meat and Muscle Biology*, 1(1), 169–180. <https://doi.org/10.22175/mmb2017.03.0015>
- Robertson, W., Veale, T., Kirbyson, H., Landry, S., & Aalhus, J. (2007). Can ultimate pH of the longissimus muscle help differentiate borderline dark-cutting beef carcasses from slow

- blooming carcasses. *Canadian Meat Science Association*, 16–22.
- Rodas-González, A., López-Campos, O., Galbraith, J., Uttaro, B., Siegel, M., & Aalhus, J. L. (2013, June 18). *Effects of electrical stimulation and nitrite film packaging on colour stability of bison steaks and ground meat*.
- Rossi, M. A., Fidale, F., Garramone, A., Esterbauer, H., & Dianzani, M. U. (1990). Effect of 4-hydroxyalkenals on hepatic phosphatidylinositol-4,5-bisphosphate-phospholipase C. *Biochemical Pharmacology*, 39(11), 1715–1719. [https://doi.org/10.1016/0006-2952\(90\)90116-3](https://doi.org/10.1016/0006-2952(90)90116-3)
- Rule, D. C., Broughton, K. S., Shellito, S. M., & Maiorano, G. (2002). Comparison of muscle fatty acid profiles and cholesterol concentrations of bison, beef cattle, elk, and chicken. *Journal of Animal Science*, 80(5), 1202–1211. <https://doi.org/10.2527/2002.8051202x>
- Sadrzadeh, S. M. H., Graf, E., Panter, S. S., Hallaway, P. E., & Eaton, J. W. (1984). Hemoglobin. A biologic Fenton reagent. *Journal of Biological Chemistry*, 259(23), 14354–14356. [https://doi.org/10.1016/s0021-9258\(17\)42604-4](https://doi.org/10.1016/s0021-9258(17)42604-4)
- Sakai, T., & Kuwazuru, S. (1995). A lipid peroxidation-derived aldehyde, 4-hydroxy-2-nonenal, contents in several fish meats. *Fisheries Science*, 61(3), 527–528. <https://doi.org/10.2331/fishsci.61.527>
- Sakai, T., Kuwazuru, S., Yamauchi, K., & Uchida, K. (1995). A Lipid Peroxidation-Derived Aldehyde, 4-Hydroxy-2-Nonenal and ω 6 Fatty Acids Contents in Meats. *Bioscience, Biotechnology, and Biochemistry*, 59(7), 1379–1380. <https://doi.org/10.1271/bbb.59.1379>
- Sakai, T., Yamauchi, K., Kuwazuru, S., & Gotoh, N. (1998). Relationships between 4-hydroxy-2-nonenal, 2-thiobarbituric acid reactive substances and n-6 polyunsaturated fatty acids in refrigerated and frozen pork. *Bioscience, Biotechnology and Biochemistry*, 62(10), 2028–2029. <https://doi.org/10.1271/bbb.62.2028>
- Salim, A. P. A. A., Wang, Y., Li, S., Conte-Junior, C. A., Chen, J., Zhu, H., Rentfrow, G., & Suman, S. P. (2020). Sarcoplasmic Proteome Profile and Internal Color of Beef Longissimus Lumborum Steaks Cooked to Different Endpoint Temperatures. *Meat and Muscle Biology*, 4(1). <https://doi.org/10.22175/mmb.9470>
- Sammel, L. M., Hunt, M. C., Kropf, D. H., Hachmeister, K. A., & Johnson, D. E. (2002). Comparison of assays for metmyoglobin reducing ability in beef inside and outside semimembranosus muscle. *Journal of Food Science*, 67(3), 978–984.

<https://doi.org/10.1111/j.1365-2621.2002.tb09439.x>

- Samuel, D., & Trabelsi, S. (2012). Influence of color on dielectric properties of marinated poultry breast meat. *Poultry Science*, *91*(8), 2011–2016. <https://doi.org/10.3382/ps.2011-01837>
- Sanderson, R., Lister, S. J., Dhanoa, M. S., Barnes, R. J., & Thomas, C. (1997). Use of near infrared reflectance spectroscopy to predict and compare the composition of carcass samples from young steers. *Animal Science*, *65*(1), 45–54. <https://doi.org/DOI:10.1017/S1357729800016283>
- SAS. (2012). SAS institute incorporation. Cary, NC, USA.
- Savell, J. . W., Dutson, T. . R., Smith, G. C., & Carpenter, Z. L. (1978). STRUCTURAL CHANGES IN ELECTRICALLY STIMULATED BEEF MUSCLE. *Journal of Food Science*, *43*(5), 1606–1607. <https://doi.org/10.1111/j.1365-2621.1978.tb02553.x>
- Savenije, B., Geesink, G. H., van der Palen, J. G. P., & Hemke, G. (2006). Prediction of pork quality using visible/near-infrared reflectance spectroscopy. *Meat Science*, *73*(1), 181–184. <https://doi.org/10.1016/j.meatsci.2005.11.006>
- Savoia, S., Albera, A., Brugiapaglia, A., Di Stasio, L., Ferragina, A., Cecchinato, A., & Bittante, G. (2020). Prediction of meat quality traits in the abattoir using portable and hand-held near-infrared spectrometers. *Meat Science*, *161*(July 2019), 108017. <https://doi.org/10.1016/j.meatsci.2019.108017>
- Sayd, T., Morzel, M., Chambon, C., Franck, M., Figwer, P., Larzul, C., Le Roy, P., Monin, G., Chérel, P., & Laville, E. (2006). Proteome analysis of the sarcoplasmic fraction of pig Semimembranosus muscle: Implications on meat color development. *Journal of Agricultural and Food Chemistry*, *54*(7), 2732–2737. <https://doi.org/10.1021/jf052569v>
- Schneider, C., Tallman, K. A., Porter, N. A., & Brash, A. R. (2001). Two distinct pathways of formation of 4-hydroxynonenal. Mechanisms of nonenzymatic transformation of the 9- and 13-hydroperoxides of linoleic acid to 4-hydroxyalkenals. *Journal of Biological Chemistry*, *276*(24), 20831–20838. <https://doi.org/10.1074/jbc.M101821200>
- Seenger, J., Nuernberg, G., Hartung, M., Szucs, E., Ender, K., & Nuernberg, K. (2008). ANKOM - A new instrument for the determination of fat in muscle and meat cuts - A comparison. *Archives Animal Breeding*, *51*(5), 449–457. <https://doi.org/10.5194/aab-51-449-2008>
- Seideman, S. C., Cross, H. R., Smith, G. C., & Durland, P. R. (1984). Factors associated with fresh meat color: a review [Discusses the various color forms of myoglobin in muscle, species,

- atmospheric conditions, antemortem factors and storage characteristics]. *Journal of Food Quality*, 6(3), 211–237. <https://doi.org/10.1111/j.1745-4557.1984.tb00826.x>
- Seman, D. L., Decker, E. A., & Crum, A. D. (1991). Factors Affecting Catalysis of Lipid Oxidation by a Ferritin containing Extract of Beef Muscle. *Journal of Food Science*, 56(2), 356–358. <https://doi.org/10.1111/j.1365-2621.1991.tb05279.x>
- Seyfert, M., Mancini, R. A., Hunt, M. C., Tang, J., & Faustman, C. (2007). Influence of carbon monoxide in package atmospheres containing oxygen on colour, reducing activity, and oxygen consumption of five bovine muscles. *Meat Science*, 75(3), 432–442. <https://doi.org/10.1016/j.meatsci.2006.08.007>
- Seyfert, Mark, Mancini, R. A., Hunt, M. C., Tang, J., Faustman, C., & Garcia, M. (2006). Color stability, reducing activity, and cytochrome c oxidase activity of five bovine muscles. *Journal of Agricultural and Food Chemistry*, 54(23), 8919–8925. <https://doi.org/10.1021/jf061657s>
- Sharaf el Din, M., Dussing, G., Egger, G., Hofer, H. P., Schaur, R. J., & Schauenstein, E. (1989). Detection of 4-hydroxy-nonenal, a mediator of traumatic inflammation, in a patient with surgical trauma and in the Sephadex inflammation model. *Progress in Clinical and Biological Research*, 308, 351–356.
- Shirabe, K., Yubisui, T., Borgese, N., Tang, C., Hultquist, D. E., & Takeshita, M. (1993). Erratum: Enzymatic instability of NADH-cytochrome b5 reductase as a cause of hereditary methemoglobinemia type I (red cell type) (*Journal of Biological Chemistry* (1992) 267 (20416-20421)). *Journal of Biological Chemistry*, 268(6), 4567.
- Siu, G. M., & Draper, H. H. (1978). a Survey of the Malonaldehyde Content of Retail Meats and Fish. *Journal of Food Science*, 43(4), 1147–1149. <https://doi.org/10.1111/j.1365-2621.1978.tb15256.x>
- SMA. (2012). *Bison Feedlot Production Information*. 36.
- Smith, G., Belk, K., Sofos, J., Tatum, J., & Williams, S. N. (2000). Economic implications of improved color stability in beef. In *Antioxidants in Muscle Foods: Nutritional Strategies to Improve Quality*.
- Smith, G. C. (1985). Effects of electrical stimulation on meat quality, color, grade, heat ring, and palatability. In *Advances in meat research* (pp. 121–158). Springer.
- Soladoye, O. P., Juárez, M. L., Aalhus, J. L., Shand, P., & Estévez, M. (2015). Protein oxidation in processed meat: Mechanisms and potential implications on human health. *Comprehensive*

- Reviews in Food Science and Food Safety*, 14(2), 106–122. <https://doi.org/10.1111/1541-4337.12127>
- Sood, V., Tian, W., Narvaez-Bravo, C., Arntfield, S. D., & González, A. R. (2020). Plant extracts effectiveness to extend bison meat shelf life. *Journal of Food Science*, 85(4), 936–946. <https://doi.org/10.1111/1750-3841.15062>
- Stadtman, E. R., & Levine, R. L. (2003). Free radical-mediated oxidation of free amino acids and amino acid residues in proteins. *Amino Acids*, 25(3–4), 207–218. <https://doi.org/10.1007/s00726-003-0011-2>
- Steiner, B., Gao, F., & Unterschultz, J. (2010). Alberta Consumers' Valuation of extrinsic and intrinsic red meat attributes: A choice experimental approach. *Canadian Journal of Agricultural Economics*, 58(2), 171–189. <https://doi.org/10.1111/j.1744-7976.2009.01177.x>
- Stivarius, M. R., Pohlman, F. W., McElyea, K. S., & Waldroup, A. L. (2002). Effects of hot water and lactic acid treatment of beef trimmings prior to grinding on microbial, instrumental color and sensory properties of ground beef during display. *Meat Science*, 60(4), 327–334. [https://doi.org/10.1016/S0309-1740\(01\)00127-9](https://doi.org/10.1016/S0309-1740(01)00127-9)
- Su, H., Zhang, S., Li, H., Xie, P., & Sun, B. (2018). Using near-infrared reflectance spectroscopy to predict physical parameters of beef. *Spectroscopy Letters*, 51(4), 163–168. <https://doi.org/10.1080/00387010.2018.1442355>
- Suman, S. P., Faustman, C., Lee, S., Tang, J., Sepe, H. A., Vasudevan, P., Annamalai, T., Manojkumar, M., Marek, P., Decesare, M., & Venkitanarayanan, K. S. (2004). Effect of muscle source on premature browning in ground beef. *Meat Science*, 68(3), 457–461. <https://doi.org/10.1016/j.meatsci.2004.04.012>
- Suman, S. P., Faustman, C., Stamer, S. L., & Liebler, D. C. (2006). Redox instability induced by 4-hydroxy-2-nonenal in porcine and bovine myoglobins at pH 5.6 and 4°C. *Journal of Agricultural and Food Chemistry*, 54(9), 3402–3408. <https://doi.org/10.1021/jf052811y>
- Suman, S. P., & Joseph, P. (2013). Myoglobin chemistry and meat color. *Annual Review of Food Science and Technology*, 4(1), 79–99. <https://doi.org/10.1146/annurev-food-030212-182623>
- Suman, S. P., & Joseph, P. (2014). Color and Pigment. In *Encyclopedia of Meat Sciences* (Vol. 1, pp. 244–251). <https://doi.org/10.1016/B978-0-12-384731-7.00084-2>
- Suman, S. P., Mancini, R. A., Ramanathan, R., & Konda, M. R. (2009). Effect of lactate-enhancement, modified atmosphere packaging, and muscle source on the internal cooked

- colour of beef steaks. *Meat Science*, 81(4), 664–670. <https://doi.org/10.1016/j.meatsci.2008.11.007>
- Suman, S.P., Faustman, C., Stamer, S. L., & Liebler, D. C. (2006). Redox instability induced by 4-hydroxy-2-nonenal in porcine and bovine myoglobins at pH 5.6 and 4°C. *Journal of Agricultural and Food Chemistry*, 54(9), 3402–3408. <https://doi.org/10.1021/jf052811y>
- Suman, S.P., Hunt, M. C., Nair, M. N., & Rentfrow, G. (2014). Improving beef color stability: Practical strategies and underlying mechanisms. *Meat Science*, 98(3), 490–504. <https://doi.org/10.1016/j.meatsci.2014.06.032>
- Suman, S.P., & Nair, M. N. (2017). Current Developments in Fundamental and Applied Aspects of Meat Color. *New Aspects of Meat Quality*, 111–127. <https://doi.org/10.1016/b978-0-08-100593-4.00007-2>
- Suman, Surendranath P., Faustman, C., Stamer, S. L., & Liebler, D. C. (2007). Proteomics of lipid oxidation-induced oxidation of porcine and bovine oxymyoglobins. *Proteomics*, 7(4), 628–640. <https://doi.org/10.1002/pmic.200600313>
- Suzuki, J., Jin, Z. G., Meoli, D. F., Matoba, T., & Berk, B. C. (2006). Cyclophilin A is secreted by a vesicular pathway in vascular smooth muscle cells. *Circulation Research*, 98(6), 811–817. <https://doi.org/10.1161/01.RES.0000216405.85080.a6>
- Swatland, H. J. (2004). Progress in understanding the paleness of meat with a low pH. *South African Journal of Animal Sciences*, 34(6SUPPL.2), 1–7. <https://doi.org/10.4314/sajas.v34i6.3816>
- Szklarczyk, D., Gable, A. L., Lyon, D., Junge, A., Wyder, S., Huerta-Cepas, J., Simonovic, M., Doncheva, N. T., Morris, J. H., Bork, P., Jensen, L. J., & Von Mering, C. (2019). STRING v11: Protein-protein association networks with increased coverage, supporting functional discovery in genome-wide experimental datasets. *Nucleic Acids Research*, 47(D1), D607–D613. <https://doi.org/10.1093/nar/gky1131>
- Tang, J., Faustman, C., & Hoagland, T. A. (2004). Krzywicki revisited: Equations for spectrophotometric determination of myoglobin redox forms in aqueous meat extracts. *Journal of Food Science*, 69(9), C717–C720. <https://doi.org/10.1111/j.1365-2621.2004.tb09922.x>
- Tang, Jiali, Faustman, C., Hoagland, T. A., Mancini, R. A., Seyfert, M., & Hunt, M. C. (2005a). Interactions between mitochondrial lipid oxidation and oxymyoglobin oxidation and the

- effects of vitamin E. *Journal of Agricultural and Food Chemistry*, 53(15), 6073–6079. <https://doi.org/10.1021/jf0501037>
- Tang, Jiali, Faustman, C., Hoagland, T. A., Mancini, R. A., Seyfert, M., & Hunt, M. C. (2005b). Postmortem oxygen consumption by mitochondria and its effects on myoglobin form and stability. *Journal of Agricultural and Food Chemistry*, 53(4), 1223–1230. <https://doi.org/10.1021/jf048646o>
- Tang, Jiali, Faustman, C., Mancini, R. A., Seyfert, M., & Hunt, M. C. (2006). The effects of freeze-thaw and sonication on mitochondrial oxygen consumption, electron transport chain-linked metmyoglobin reduction, lipid oxidation, and oxymyoglobin oxidation. *Meat Science*, 74(3), 510–515. <https://doi.org/10.1016/j.meatsci.2006.04.021>
- Tichivangana, J. Z., & Morrissey, P. A. (1985). Metmyoglobin and inorganic metals as pro-oxidants in raw and cooked muscle systems. *Meat Science*, 15(2), 107–116. [https://doi.org/10.1016/0309-1740\(85\)90051-8](https://doi.org/10.1016/0309-1740(85)90051-8)
- Tøgersen, G., Arnesen, J. F., Nilsen, B. N., & Hildrum, K. I. (2003). On-line prediction of chemical composition of semi-frozen ground beef by non-invasive NIR spectroscopy. *Meat Science*, 63(4), 515–523. [https://doi.org/10.1016/S0309-1740\(02\)00113-4](https://doi.org/10.1016/S0309-1740(02)00113-4)
- Tøgersen, G., Isaksson, T., Nilsen, B. N., Bakker, E. A., & Hildrum, K. I. (1999). On-line NIR analysis of fat, water and protein in industrial scale ground meat batches. *Meat Science*, 51(1), 97–102. [https://doi.org/10.1016/S0309-1740\(98\)00106-5](https://doi.org/10.1016/S0309-1740(98)00106-5)
- Totland, G. K., & Kryvi, H. (1991). Distribution patterns of muscle fibre types in major muscles of the bull (*Bos taurus*). *Anatomy and Embryology*, 184(5), 441–450. <https://doi.org/10.1007/BF01236050>
- TROUT, G. R. (1989). Variation in Myoglobin Denaturation and Color of Cooked Beef, Pork, and Turkey Meat as Influenced by pH, Sodium Chloride, Sodium Tripolyphosphate, and Cooking Temperature. *Journal of Food Science*, 54(3), 536–540. <https://doi.org/10.1111/j.1365-2621.1989.tb04644.x>
- Turrens, J. F., & Boveris, A. (1980). Generation of superoxide anion by the NADH dehydrogenase of bovine heart mitochondria. *The Biochemical Journal*, 191(2), 421–427. <https://doi.org/10.1042/bj1910421>
- Vakifahmetoglu-Norberg, H., Ouchida, A. T., & Norberg, E. (2017). The role of mitochondria in metabolism and cell death. *Biochemical and Biophysical Research Communications*, 482(3),

426–431. <https://doi.org/10.1016/j.bbrc.2016.11.088>

- Van Beers, R., Kokawa, M., Aernouts, B., Watté, R., De Smet, S., & Saeys, W. (2018). Evolution of the bulk optical properties of bovine muscles during wet aging. *Meat Science*, *136*(September 2017), 50–58. <https://doi.org/10.1016/j.meatsci.2017.10.010>
- Velarde, A., Gispert, M., Faucitano, L., Alonso, P., Manteca, X., & Diestre, A. (2001). Effects of the stunning procedure and the halothane genotype on meat quality and incidence of haemorrhages in pigs. *Meat Science*, *58*(3), 313–319. [https://doi.org/10.1016/S0309-1740\(01\)00035-3](https://doi.org/10.1016/S0309-1740(01)00035-3)
- Venel, C., Mullen, A. M., Downey, G., & Troy, D. J. (2001). Prediction of Tenderness and other Quality Attributes of Beef by near Infrared Reflectance Spectroscopy between 750 and 1100 nm; Further Studies. *Journal of near Infrared Spectroscopy (United Kingdom)*, *9*(3), 185–198. <https://doi.org/10.1255/jnirs.305>
- Vestergaard, M., Oksbjerg, N., & Henckel, P. (2000). Influence of feeding intensity, grazing and finishing feeding on muscle fibre characteristics and meat colour of semitendinosus, longissimus dorsi and supraspinatus muscles of young bulls. *Meat Science*, *54*(2), 177–185. [https://doi.org/10.1016/S0309-1740\(99\)00097-2](https://doi.org/10.1016/S0309-1740(99)00097-2)
- Wang, B., & Xiong, Y. L. (1998). Functional stability of antioxidant-washed, cryoprotectant-treated beef heart surimi during frozen storage. *Journal of Food Science*, *63*(2), 293–298. <https://doi.org/10.1111/j.1365-2621.1998.tb15729.x>
- Wang, B., Xiong, Y. L., & Srinivasan, S. (1997). Chemical stability of antioxidant-washed beef heart surimi during frozen storage. *Journal of Food Science*, *62*(5). <https://doi.org/10.1111/j.1365-2621.1997.tb15011.x>
- Wang, X., Pandey, A. K., Mulligan, M. K., Williams, E. G., Mozhui, K., Li, Z., Jovaisaite, V., Quarles, L. D., Xiao, Z., Huang, J., Capra, J. A., Chen, Z., Taylor, W. L., Bastarache, L., Niu, X., Pollard, K. S., Ciobanu, D. C., Reznik, A. O., Tishkov, A. V., ... Williams, R. W. (2016). Joint mouse-human phenome-wide association to test gene function and disease risk. *Nature Communications*, *7*. <https://doi.org/10.1038/ncomms10464>
- Wang, Z., He, Z., Gan, X., & Li, H. (2018). Interrelationship among ferrous myoglobin, lipid and protein oxidations in rabbit meat during refrigerated and superchilled storage. *Meat Science*, *146*(2), 131–139. <https://doi.org/10.1016/j.meatsci.2018.08.006>
- Wang, Z., Tu, J., Zhou, H., Lu, A., & Xu, B. (2021). A comprehensive insight into the effects of

- microbial spoilage, myoglobin autoxidation, lipid oxidation, and protein oxidation on the discoloration of rabbit meat during retail display. *Meat Science*, 172(September 2020), 108359. <https://doi.org/10.1016/j.meatsci.2020.108359>
- Warris, P. D. (1979). The extraction of haem pigments from fresh meat. *International Journal of Food Science & Technology*, 14(1), 75–80. <https://doi.org/https://doi.org/10.1111/j.1365-2621.1979.tb00849.x>
- Warriss, P. D. (2000). Meat science: an introductory text. In *Meat science: an introductory text*. <https://doi.org/10.1079/9780851994246.0000>
- Weeranantanaphan, J., Downey, G., Allen, P., & Sun, D. W. (2011). A review of near infrared spectroscopy in muscle food analysis: 2005-2010. *Journal of Near Infrared Spectroscopy*, 19(2), 61–104. <https://doi.org/10.1255/jnirs.924>
- Witz, G. (1989). Biological interactions of α,β -unsaturated aldehydes. *Free Radical Biology and Medicine*, 7(3), 333–349. [https://doi.org/https://doi.org/10.1016/0891-5849\(89\)90137-8](https://doi.org/https://doi.org/10.1016/0891-5849(89)90137-8)
- Wood, J. D. (1990). Muscle and meat biochemistry. In *Food Chemistry* (Vol. 38, Issue 3, pp. 236–237). Elsevier Ltd. [https://doi.org/10.1016/0308-8146\(90\)90198-d](https://doi.org/10.1016/0308-8146(90)90198-d)
- Wood, J. D., Enser, M., Fisher, A. V., Nute, G. R., Sheard, P. R., Richardson, R. I., Hughes, S. I., & Whittington, F. M. (2008). Fat deposition, fatty acid composition and meat quality: A review. *Meat Science*, 78(4), 343–358. <https://doi.org/10.1016/j.meatsci.2007.07.019>
- Wood, J. D., Nute, G. R., Richardson, R. I., Whittington, F. M., Southwood, O., Plastow, G., Mansbridge, R., Da Costa, N., & Chang, K. C. (2004). Effects of breed, diet and muscle on fat deposition and eating quality in pigs. *Meat Science*, 67(4), 651–667. <https://doi.org/10.1016/j.meatsci.2004.01.007>
- Wu, W., Yu, Q. Q., Fu, Y., Tian, X. J., Jia, F., Li, X. M., & Dai, R. T. (2016). Towards muscle-specific meat color stability of Chinese Luxi yellow cattle: A proteomic insight into post-mortem storage. *Journal of Proteomics*, 147, 108–118. <https://doi.org/10.1016/j.jprot.2015.10.027>
- Xiong, Y. L. (2018). Muscle proteins. In *Proteins in Food Processing: Second Edition* (Second Edi, pp. 127–148). Elsevier Ltd. <https://doi.org/10.1016/B978-0-08-100722-8.00006-1>
- Xiong, Youling L, & Guo, A. (2020). Animal and Plant Protein Oxidation: Chemical and Functional Property Significance. *Foods*, 10(1), 40. <https://doi.org/10.3390/foods10010040>
- Yan, L. J., & Sohal, R. S. (1998). Mitochondrial adenine nucleotide translocase is modified

- oxidatively during aging. *Proceedings of the National Academy of Sciences of the United States of America*, 95(22), 12896–12901. <https://doi.org/10.1073/pnas.95.22.12896>
- Yu, Q., Tian, X., Shao, L., Xu, L., Dai, R., & Li, X. (2018). Label-free proteomic strategy to compare the proteome differences between longissimus lumborum and psoas major muscles during early postmortem periods. *Food Chemistry*, 269(April), 427–435. <https://doi.org/10.1016/j.foodchem.2018.07.040>
- Yu, Q., Wu, W., Tian, X., Hou, M., Dai, R., & Li, X. (2017). Unraveling proteome changes of Holstein beef M. semitendinosus and its relationship to meat discoloration during post-mortem storage analyzed by label-free mass spectrometry. *Journal of Proteomics*, 154(December), 85–93. <https://doi.org/10.1016/j.jprot.2016.12.012>
- Yu, Q., Wu, W., Tian, X., Jia, F., Xu, L., Dai, R., & Li, X. (2017). Comparative proteomics to reveal muscle-specific beef color stability of Holstein cattle during post-mortem storage. *Food Chemistry*, 229, 769–778. <https://doi.org/10.1016/j.foodchem.2017.03.004>
- Zanardi, E., Jagersma, C. G., Ghidini, S., & Chizzolini, R. (2002). Solid phase extraction and liquid chromatography-tandem mass spectrometry for the evaluation of 4-hydroxy-2-nonenal in pork products. *Journal of Agricultural and Food Chemistry*, 50(19), 5268–5272. <https://doi.org/10.1021/jf020201h>
- Zhai, C., Suman, S. P., Nair, M. N., Li, S., Luo, X., Beach, C. M., Harsh, B. N., Boler, D. D., Dilger, A. C., & Shike, D. W. (2019). Supranutritional supplementation of vitamin E influences mitochondrial proteome profile of post-mortem longissimus lumborum from feedlot heifers. *South African Journal of Animal Sciences*, 48(6), 1140–1147. <https://doi.org/10.4314/sajas.v48i6.18>
- Zhai, Chaoyu, Djimsa, B. A., Prenni, J. E., Woerner, D. R., Belk, K. E., & Nair, M. N. (2020). Tandem mass tag labeling to characterize muscle-specific proteome changes in beef during early postmortem period. *Journal of Proteomics*, 222(April), 103794. <https://doi.org/10.1016/j.jprot.2020.103794>
- Zhang, W., Xiao, S., & Ahn, D. U. (2013). Protein Oxidation: Basic Principles and Implications for Meat Quality. *Critical Reviews in Food Science and Nutrition*, 53(11), 1191–1201. <https://doi.org/10.1080/10408398.2011.577540>
- Zhao, D., Chen, L., Qin, C., Zhang, H., Wu, P., & Zhang, F. (2010). A delta-class glutathione transferase from the Chinese mitten crab *Eriocheir sinensis*: cDNA cloning, characterization

and mRNA expression. *Fish & Shellfish Immunology*, 29(4), 698–703.
<https://doi.org/10.1016/j.fsi.2010.06.002>

Zhu, L. G., & Brewer, M. S. (1998). Metmyoglobin Reducing Capacity of Fresh Normal, PSE, and DFD Pork During Retail Display. *Journal of Food Science*, 63(3), 390–393.
<https://doi.org/https://doi.org/10.1111/j.1365-2621.1998.tb15749.x>

